

**HIGH GLUCOSE AND HUMAN ENDOTHELIAL
CELL AGEING.**

**by
LEANDRA-LOUISE BOWERS BSc (Hons)**

**This thesis is presented for the degree of Doctor of
Philosophy at the University of Leicester.**
2009

DEPARTMENT OF CARDIOVASCULAR SCIENCES
VASCULAR MEDICINE
UNIVERSITY OF LEICESTER
LEICESTER



ABSTRACT

Increased generation of reactive oxygen species (ROS) in hyperglycaemia is linked to endothelial cell DNA damage in diabetes. Nuclear and/or mitochondrial DNA (mtDNA) damage may accelerate ageing of endothelial cells and, in part, account for the endothelial dysfunction associated with the pathogenesis of many cardiovascular diseases. The aim of this thesis was to investigate cell ageing in human endothelial cells, by studying the role of ROS in telomere attrition after exposure to increased glucose levels. This thesis also analysed the effects of mtDNA depletion on the pro-inflammatory phenotype of endothelial cells.

Human umbilical vein endothelial cells (HUVECs) were treated with high glucose (HG; 22mM) or alternating 'normal' (5.5mM) /HG (AG; to mimic post-prandial fluctuations in glucose). Telomere attrition rate, measured globally across all chromosomes using Southern blotting and specifically on the XpYp chromosome using single telomere length analysis (STELA) were increased 3-6-fold in HUVECs cultured in HG or AG. This was preceded by increased ROS generation and largely blocked by an antioxidant and inhibition of mitochondrial electron transport. Moreover, mtDNA content was lower in HUVECs cultured in HG. It was hypothesised that changes in mtDNA mediated some of the effects of HG on accelerated vascular ageing in cardiovascular disease. This was supported by experiments showing that mtDNA depletion, using ethidium bromide or dideoxycytidine, resulted in a shift towards a pro-inflammatory phenotype; namely that levels of endothelial nitric oxide synthase protein were decreased and the expression of the adhesion molecule, ICAM-1, was increased.

The data confirmed that exposure to high glucose raised ROS production in HUVECs and resulted in increased telomere attrition. This thesis also highlighted the possible importance of mtDNA integrity as a determinant of endothelial cell function and showed that agents which affected mtDNA content/integrity accelerated the process of endothelial dysfunction through phenotypic modulation.

DEDICATION

I would like to dedicate my thesis to my mum and dad for all their love and support in the last 25 years.

ACKNOWLEDGEMENTS

I would like to say a huge thank you to all of my colleagues within Cardiovascular Sciences. I would like to say a special thanks to Jane Allen for helping with all the ordering and any problems that have arisen. Furthermore, I would like to very special thanks to Hash Patel for always being there for me in all circumstances over the past three years. Lastly, I would like to say a huge thank you to my supervisors Dr Karl Herbert and Professor Bryan Williams for directing me through the past three years and always being there when I need any support or guidance.

TABLE OF CONTENTS

LIST OF FIGURES.....	i
LIST OF TABLES.....	xv
ABBREVIATIONS.....	xvi
1 INTRODUCTION	1
1.1 HIGH GLUCOSE IN HUMANS	1
1.1.1 <i>Hyperglycaemia and diabetes</i>	1
1.1.2 <i>High glucose and the vascular endothelium</i>	2
1.1.2.1 Entry of glucose into endothelial cells	2
1.1.2.2 High glucose activates the polyol, protein kinase C, hexosamine and the AGE pathways	3
1.1.3 <i>Effect of high glucose and diabetes on ROS production</i>	7
1.1.4 <i>Effect of high glucose and diabetes on atherosclerosis</i>	8
1.2 REACTIVE OXYGEN AND NITROGEN SPECIES	9
1.2.1 <i>Definition</i>	9
1.2.2 <i>Origin of ROS and RNS</i>	9
1.2.3 <i>Protection against ROS and RNS – antioxidants</i>	12
1.2.4 <i>Effects of increased ROS/RNS</i>	13
1.2.4.1 Nuclear and mtDNA damage by ROS/RNS	13
1.2.4.2 Increased ROS and ageing	14
1.3 MITOCHONDRIA	15
1.3.1 <i>Structure</i>	15
1.3.2 <i>Dysfunction</i>	16
1.4 TELOMERES	17
1.4.1 <i>Structure</i>	17
1.4.2 <i>Telomeric proteins</i>	19
1.4.3 <i>Function</i>	21
1.4.4 <i>Telomeres in vascular disease</i>	21
1.4.5 <i>Result of telomere loss</i>	21
1.4.6 <i>Telomere loss leads to replicative senescence</i>	22
1.5 TELOMERASE	23
1.5.1 <i>Structure and Function</i>	23
1.5.2 <i>Differences in the expression of telomerase</i>	23
1.6 VASCULAR ENDOTHELIUM	24
1.6.1 <i>Structure and Function of blood vessels</i>	24
1.6.2 <i>Endothelial Ageing</i>	25
1.6.2.1 Changes in Structure and Function	25
1.6.2.2 Mechanisms Leading to Endothelial Dysfunction	26
1.6.3 <i>Diseases associated with endothelial dysfunction</i>	28
1.6.3.1 Diabetes	29
1.6.3.2 Atherosclerosis.....	29
1.7 HYPOTHESIS AND AIMS:	31
2 MATERIALS AND METHODS	33
2.1 MATERIALS AND EQUIPMENT	33
2.1.1 <i>Cell culture</i>	33
2.1.2 <i>Immunofluorescence</i>	34

2.1.3	<i>Measurement of glucose concentration</i>	34
2.1.4	<i>Assessment of telomere length and heterogeneity using Southern blotting and STELA</i>	35
2.1.4.1	Plugs	35
2.1.4.2	DNA extraction, quantification and digestion	35
2.1.4.3	Ligation and PCR for STELA	35
2.1.4.4	DNA electrophoresis	36
2.1.4.5	Southern blotting	36
2.1.4.6	Radioactive labelling of the membrane	36
2.1.5	<i>Measuring ROS using the Amplex Red assay</i>	37
2.1.6	<i>Treatment of cells to deplete mitochondria</i>	37
2.1.7	<i>Real time PCR</i>	37
2.1.8	<i>Protein extraction and quantification</i>	38
2.1.9	<i>Western blotting</i>	38
2.2	METHODS:	40
2.2.1	<i>Cell Culture</i>	40
2.2.1.1	Reviving frozen cells	40
2.2.1.2	Sub-culture/passaging of cells	40
2.2.1.3	Media changing of cells	41
2.2.2	<i>Phenotypic characterisation of HUVECs</i>	41
2.2.3	<i>Measurement of glucose concentration in media</i>	42
2.2.3.1	Cell and media preparation	42
2.2.3.2	Hexokinase assay	43
2.2.4	<i>Measuring telomere length and heterogeneity using Southern blotting</i>	44
2.2.4.1	DNA extraction from cells	44
2.2.4.2	DNA quantification	44
2.2.4.3	Plug formation	45
2.2.4.4	Digestion of plugs or extracted DNA	46
2.2.4.5	Gel Electrophoresis	47
2.2.4.6	Southern blotting	48
2.2.5	<i>Measuring telomere length and telomere length heterogeneity using STELA</i>	49
2.2.5.1	DNA preparation	49
2.2.5.2	Reconstitution of the primers for PCR	49
2.2.5.3	Ligation of teltail onto the end of DNA	49
2.2.5.4	PCR	49
2.2.6	<i>Radioactively labelling the membrane</i>	50
2.2.6.1	Preparing the membrane	50
2.2.6.2	Labelling the telomere probe	50
2.2.6.3	Labelling the marker probe	50
2.2.6.4	Labelling the telomere adjacent probe	51
2.2.6.5	Hybridisation of the membrane	53
2.2.6.6	Analysis of the blots using Telometric software	54
2.2.7	<i>Measuring extracellular H₂O₂ concentration using Amplex Red</i>	54
2.2.7.1	Performing the Amplex Red assay	54
2.2.7.2	Optimisation of the lysis of HUVECs in wells	55
2.2.7.3	Bradford Assay	56
2.2.8	<i>Measurement of the expression of pro-inflammatory markers in HUVECs</i>	57

2.2.8.1	Cell lysis and Western blotting	57
2.2.8.2	Stripping protocol	60
2.2.9	<i>Depletion of mitochondrial DNA</i>	60
2.2.9.1	Treatment with ethidium bromide (Rho0 HUVECs)	60
2.2.9.2	Treatment of HUVECs with chloramphenicol	61
2.2.9.3	Treatment of HUVECs with ddC	62
2.2.9.4	Analysis of eNOS and ICAM1 protein expression in Rho0 HUVECs, chloramphenicol treated HUVECs and ddC treated HUVECs	62
2.2.9.5	Statistical Analysis of the data	62
3	THE EFFECT OF HIGH GLUCOSE ON TELOMERE LENGTH AND ROS PRODUCTION IN HUVECS	63
3.1	INTRODUCTION	63
3.1.1	<i>Glucose in diabetes</i>	63
3.1.2	<i>Glucose uptake</i>	63
3.1.3	<i>Telomeres</i>	64
3.1.4	<i>Measurement of telomere length</i>	64
3.1.5	<i>Measurement of ROS</i>	66
3.2	AIMS.....	67
3.3	EXPERIMENTAL APPROACH.....	68
3.3.1	<i>vWF expression in HUVECs</i>	68
3.3.2	<i>Uptake of glucose in HUVECs exposed to normal or high glucose</i>	68
3.3.3	<i>Measurement of telomere length in HUVECs by Southern blotting following exposure to high and alternating glucose</i>	68
3.3.4	<i>Measurement of telomere length in HUVECs by STELA following exposure to high and alternating glucose</i>	68
3.3.5	<i>Measurement of telomere length in HUVECs by STELA following exposure to high or alternating glucose in the presence of NAC or TTFa</i>	69
3.3.6	<i>Measuring H₂O₂ in HUVECs exposed to normal, high or alternating normal and high glucose over various timepoints</i>	69
3.4	RESULTS	70
3.4.1	<i>Characterisation of HUVECs</i>	70
3.4.2	<i>Uptake of Glucose by HUVEC cultures</i>	72
3.4.3	<i>Effect of different glucose concentrations on the growth of HUVECs</i>	74
3.4.4	<i>Measuring telomere length</i>	75
3.4.4.1	Validation of Southern blotting	75
3.4.4.2	.. Effect of HG and AG on telomere length in HUVECs assessed using Southern blotting	82
3.4.4.3	Validation of STELA	87
3.4.4.4	Generation of a telomere adjacent probe for STELA	90
3.4.4.5	Effect of HG and AG on telomere length in HUVECs assessed using STELA	93
3.4.5	<i>Effect of HG and AG on ROS generation in HUVECs</i>	99
3.4.6	<i>Effect of NAC and TTFa on the rate of telomere attrition in HUVECs exposed to HG</i>	111

3.4.7	<i>Effect of NAC and TTFAs on the rate of telomere attrition in HUVECs exposed to AG</i>	119
3.5	DISCUSSION.....	124
3.5.1	<i>Preliminary experiments</i>	125
3.5.2	<i>Optimisation of telomere length measurement using Southern blotting and STELA</i>	127
3.5.3	<i>Effect of HG and AG on telomere attrition</i>	128
3.5.4	<i>Effect of HG and AG on ROS production in HUVECs</i>	131
3.5.5	<i>Role of ROS and mitochondrial function on telomere attrition</i>	134
4	INDUCTION OF A PRO-INFLAMMATORY PHENOTYPE IN ENDOTHELIAL CELLS BY HG AND MTDNA DEPLETION	135
4.1	INTRODUCTION:	135
4.1.1	<i>Mitochondrial ROS production and DNA damage</i>	135
4.1.2	<i>Markers of a pro-inflammatory phenotype in endothelial cells</i> ...	136
4.1.2.1	<i>Nitric oxide</i>	136
4.1.2.2	<i>eNOS</i>	136
4.1.2.3	<i>ICAM1</i>	137
4.1.3	<i>Models of mtDNA damage or depletion</i>	138
4.2	AIMS.....	140
4.3	EXPERIMENTAL APPROACH.....	140
4.3.1	<i>Treatment of endothelial cells in culture</i>	140
4.3.2	<i>Real time PCR</i>	140
4.3.3	<i>Western blotting</i>	141
4.3.4	<i>Amplex Red assay for measuring H₂O₂ production</i>	141
4.4	RESULTS	142
4.4.1	<i>Effect of HG and AG on mtDNA content in HUVEC cultures and the role of ROS</i>	142
4.4.1.1	<i>Effect of HG and AG on mtDNA content</i>	142
4.4.1.2	<i>Effect of NAC or TTFAs on mtDNA content changes induced by high glucose</i>	143
4.4.2	<i>Effect of high glucose and alternating glucose on the expression of eNOS and ICAM1</i>	145
4.4.2.1	<i>Optimisation of Western blotting for eNOS, ICAM1, and α-tubulin</i>	145
4.4.2.2	<i>The effect of HG or AG on eNOS expression in HUVECs</i>	149
4.4.2.3	<i>The effect of HG and AG on ICAM1 expression in HUVECs</i> ..	150
4.4.2.4	<i>The effect of NAC or TTFAs on the expression of eNOS in HUVECs treated with NG and HG</i>	153
4.4.3	<i>Effect of mtDNA depletion on pro-inflammatory phenotype in HUVECs</i>	155
4.4.3.1	<i>Formation and characterisation of Rho0 cells</i>	155
4.4.3.2	<i>Staining of Rho0 cells with vWF</i>	158
4.4.3.3	<i>Morphology of Rho0 HUVECs under TEM</i>	159
4.4.3.4	<i>The expression of eNOS and ICAM1 in Rho0 HUVECs</i>	160
4.4.4	<i>Effect of treatment of HUVECs with chloramphenicol on eNOS expression</i>	164
4.4.4.1	<i>COXI and COXIV expression</i>	164
4.4.4.2	<i>The expression of eNOS in chloramphenicol-treated HUVECs</i>	166

4.4.5	<i>Effect of ddC on eNOS and ICAM1 expression in HUVECs</i>	166
4.4.5.1	<i>Characterisation of ddC treated cells</i>	166
4.4.5.2	<i>The expression of eNOS in ddC treated HUVECs</i>	168
4.4.5.3	<i>The expression of ICAM1 in HUVECs treated with ddC</i>	170
4.4.6	<i>H₂O₂ production in Rho0 HUVECs</i>	172
4.5	DISCUSSION	173
4.5.1	<i>The effect of HG and AG on mtDNA content and the expression of eNOS and ICAM1</i>	174
4.5.2	<i>The effect of depleting mtDNA on eNOS and ICAM1 protein expression</i>	177
4.5.3	<i>Effect of depleting mtDNA on H₂O₂ production</i>	180
5	GENERAL DISCUSSION	185
5.1	HYPERGLYCAEMIA AND CARDIOVASCULAR DISEASE	185
5.2	SUMMARY OF FINDINGS	186
5.3	CLINICAL IMPLICATIONS OF THESE FINDINGS	188
5.4	FURTHER WORK	190
5.4.1	<i>Do other ROS detection systems confirm the increase in ROS and do other antioxidants and mitochondrial inhibitors show similar effects seen when using Amplex Red?</i>	190
5.4.2	<i>Is there a role for telomerase?</i>	191
5.4.3	<i>Are NADPH levels affected in Rho0 HUVECs?</i>	191
5.4.4	<i>Are other markers indicating a pro-inflammatory phenotype affected in Rho0 HUVECs?</i>	191
5.4.5	<i>Are the changes in pro-inflammatory phenotype in Rho0 HUVECs due to increased ROS?</i>	191
5.4.6	<i>Are the changes in pro-inflammatory phenotype in Rho0 HUVECs reverted by mtDNA reconstitution?</i>	192
5.4.7	<i>Is eNOS mRNA half life decreased in Rho0 HUVECs?</i>	192
5.4.8	<i>Do Rho0 HUVECs have shorter telomeres?</i>	192
5.5	PRESENTATIONS AND PUBLICATIONS ARISING FROM THIS STUDY	193
5.5.1	<i>Presentations</i>	193
5.5.2	<i>Publications</i>	193
6	APPENDICES	194
7	REFERENCES	201

LIST OF FIGURES

- Figure 1: An overview of the effect of increased glucose on cell metabolism. High glucose causes increased activity of the polyol pathway, hexosamine pathway, protein kinase C pathway and the AGE pathway. PKC = protein kinase C; NADH = reduced nicotinamide adenine dinucleotide; NADPH = reduced nicotinamide adenine dinucleotide phosphate; DAG = diacylglycerol; AGE = advanced glycation end-products; DHAP = dihydroxyacetone phosphate; UDP-Glc-Nac = uridine diphosphate N-acetylglucosamine; GFAT = glutamine:fructose-6-phosphate amidotransferase. (Adapted from Brownlee, 2001)..... **4**
- Figure 2: The reactions that occur in the formation of advanced glycation end-products. An aldehyde reacts with an amino group to form a Schiff's base, rearranges to form Amadori's product and further changes lead to the formation of AGEs. (Basta *et al.*, 2004). **6**
- Figure 3: Overview of the respiratory transport chain and oxidative phosphorylation showing complexes 1 to 5. Complex 1 is the NADH-Coenzyme Q dehydrogenase responsible for transferring a pair of electrons (e^-) from NADH to coenzyme Q and transporting protons from the matrix of the mitochondria to the cytosol. Complex II, otherwise known as succinate-coenzyme Q reductase transfers electrons from ($FADH_2$) to coenzyme Q. Complex III otherwise known as coenzyme Q-cytochrome c reductase is where reduced coenzyme Q passes its electrons to cytochrome c via the Q cycle and further protons (H^+) are transferred from the matrix to the cytosol. Complex IV is also known as cytochrome c oxidase and this is where electrons are transferred from cytochrome c to O_2 to form water (H_2O). Due to the increase in the proton concentration in the cytosol, H^+ is pumped back out of the cytosol into the matrix via complex V (ATP synthase) which converts ADP to ATP (oxidative phosphorylation). Blue arrows indicate movement of electrons. NADH = reduced nicotinamide adenine dinucleotide; ADP = adenosine diphosphate; ATP = adenosine triphosphate; $FADH_2$ = reduced flavin adenine dinucleotide. (Adapted from Garrett and Grisham, 1995, Elliot and Elliot, 2001, Matthews *et al.*, 2000). **11**
- Figure 4: The structure of a mitochondrion. Illustrates how the inner membrane projects inwards to form cristae. (Adapted from Frey and Mannella, 2000). **16**
- Figure 5: The overall primary structure of telomeric DNA. Illustrates the telomeric regions and the subtelomeric regions. (Adapted from Baird, 2005). **18**
- Figure 6: The overall structure of a telomere when expression is not occurring. Illustrating the t and d-loops as well as the position where TRF1 and TRF2 bind. TRF1: telomere repeat binding factor 1; TRF2: telomere repeat binding factor 2; POT1: protection of telomeres-1. (Adapted from Blasco, 2005)..... **19**

Figure 7: An example of the TRF1 and TRF2 complexes that are formed on telomeres. Both complexes are involved in telomere regulation but TRF2 is also involved in DNA repair. TANK: tankyrases, TRF1: telomere repeat binding factor 1, TRF2: telomere repeat binding factor 2, TIN2: TRF1 interacting nuclear factor 2, RAP1: repressor/activator protein-1, PTOP: POT1 and TIN2 organising protein, POT1: protection of telomeres-1, MRE11: meiotic recombination-11, NBS1: Nijmegen breakage syndrome, RAD50: a DNA repair protein, ERCC1: excision repair cross-complementing-1, ATM: ataxia telangiectasia mutated, PARP2: poly (ADP-ribose) polymerase family, WRN: werner syndrome, BLM: bloom syndrome, KU86: ku86 autoantigen related protein 1. (Adapted from Blasco, 2005). **20**

Figure 8: The variation in the telomere length between germ cells, somatic cells and cells involved in premature ageing. The telomere length in germ cells remains fairly constant over time as telomerase is always switched on. However, the telomere length in somatic cells and in premature ageing syndromes decreases as age increases due to telomerase being switched off (Blasco, 2005)..... **24**

Figure 9: The structure of a vein or an artery. Illustrates the vascular endothelial layer, the smooth muscle layer and the fibrous connective tissue (Cleaver and Melton, 2003). **25**

Figure 10: A flow chart showing the primary route of synthesising nitric oxide (NO) and the ways in which ageing can interact and affect this route. NO = nitric oxide; NOS = nitric oxide synthase; H₂O₂ = hydrogen peroxide; ONOO⁻ = peroxynitrite; MnSOD = manganese superoxide dismutase; O₂⁻ = superoxide. (Adapted from Brandes *et al.*, 2005, and Zou *et al.*, 2004)..... **27**

Figure 11: Illustrates how different cardiovascular diseases can affect the nitric oxide concentration and therefore lead to endothelial dysfunction. LDL = low density lipoproteins; AGE = advanced glycation endproducts; ox-LDL = oxidised low density lipoproteins; NO = nitric oxide; NOS = nitric oxide synthase. (Adapted from Hunt *et al.*, 2002). **28**

Figure 12: The overall process of atherosclerosis. This shows how increased LDL causes increased oxidised LDL and increased VSMC (vascular smooth muscle cell) proliferation. This leads to endothelial dysfunction and the formation of fibrous caps which ultimately leads to either the thrombotic phase or the fibrotic phase. VSMC = vascular smooth muscle cells. (Adapted from Naseem, 2005). **30**

Figure 13: The setup of tubing which was used to construct the plugs. **46**

Figure 14: The setup of Southern blots showing the position of the gel and the nylon membrane. **48**

Figure 15: The layout of the transfer cassette. This shows the position of the gel in relation to the membrane, filter paper and filter pads. **59**

Figure 16: Shows how STELA works. A telorette is ligated on to the end of the C-rich strand and then the DNA is amplified via PCR using a teltail primer and a chromosome-specific primer. (1) = telorette; (2) = teltail primer; (3) = chromosome specific primer. (Adapted from Baird et al., 2003). **66**

Figure 17: Characterisation of HUVECs with anti-vWF immunofluorescence. HUVECs were grown on coverslips until 80% confluent. The cells were fixed, permeabilised and blocked (as described in section 2.2.2). They were then incubated with a 1 in 200 dilution of anti-von Willebrand factor overnight and mounted using a DAPI mountant. They were sealed using clear nail varnish and viewed using FITC and DAPI filters. **71**

Figure 18: Glucose loss from medium containing NG (5.5mM) or HG (22mM). HUVECs were cultured in either NG medium or HG medium and glucose concentration in the medium was monitored over three days using the hexokinase assay. Values are expressed in pmoles/cell/day. Values are mean + SEM, n=2. **73**

Figure 19: Growth curves for HUVECs exposed to different glucose concentrations. The cumulative population doubling levels of HUVECs when exposed to NG, HG or AG. (■) = NG; (▲) = HG; (▼) = Alternating normal/high glucose (AG). Values are mean of n=3. **75**

Figure 20: Effect of cell number on Southern blot signal. Radioactively labelled blot when 0.5×10^6 cells (lanes 1 and 2), 1.0×10^6 cells (lanes 3 and 4), and 1.5×10^6 cells (lanes 5 and 6) were suspended in a 1cm plug. Lanes 1, 3 and 5 from donor number 1 and lanes 2, 4 and 6 from donor number 2. The labels are shown in kb for marker (M). **76**

Figure 21: Yield of DNA from different cell numbers. As the number of cells increased, the concentration of DNA extracted from HUVECs extraction kit increased. Values shown are single values, n=1. **77**

Figure 22: Southern blot comparing extracted DNA with suspension of cells in agarose plugs. DNA was digested using Hinf1 at 37°C for 16 hours. Lanes a to c and g to j show DNA of cells that were suspended in a tube of agarose and lanes d to f and k to n shows DNA that has been extracted using a DNA extraction kit. All cell samples are from the same donor. M = marker. The labels are shown in kb for marker. **78**

Figure 23: Comparison of different digestion protocols on TRF length by Southern analysis. HUVECs (same donor) were suspended in agarose plugs were digested under different conditions. **81**

Figure 24: Examples of Southern blots performed for the glucose experiment showing telomeric DNA from cells at passage 0 and at passage 4. Section 1 shows DNA from cells that were treated with NG medium, section 2 shows DNA from cells that were treated with HG medium and section 3 shows DNA from cells that were treated with AG medium every 48 hours. The labels are shown in kb for marker. **83**

Figure 25: Effect of HG and AG on telomere attrition in HUVECs. (A) The mean (of medians) telomere length (kb) at different cumulative population doublings for HUVECs treated with NG (■), HG (▲) or AG (▼) every 48 hours. Telomere length was assessed using Southern blotting and the blots were analysed using Telometric software. The data were analysed using linear regression. Values are \pm SEM, n=6. (B) The mean telomere decrease per population doubling (pd) level for HUVECs treated with NG, HG or AG. ***P<0.01 vs NG. Values are + SEM, n=6. **85**

Figure 26: Effect of HG and AG on telomere length heterogeneity in HUVECs. (A) The semi-interquartile range (SIR) was calculated from Southern blots (using Telometric software) and plotted against the cumulative population doublings for HUVECs treated with NG (■), HG (▲) or AG (▼) every 48 hours. The data were analysed using linear regression. Values are \pm SEM, n=6. (B) The mean SIR decrease per population doubling level for HUVECs treated with NG, HG or AG. ***P<0.001 vs NG. Values are + SEM, n=6. **86**

Figure 27: Effect of different dNTP concentrations, magnesium chloride concentrations and number of PCR cycles on STELA bands. A DNA concentration of 20pg/ μ l was used in the PCR reaction. The ligation reaction contained 0.9 μ M telorette 2. Each PCR reaction contained 0.5 μ M of the primers and 1 unit of a 10:1 mixture of taq polymerase and PWO polymerase. The blot was hybridised using the telomere probe. M=marker in kb. **88**

Figure 28: Effect of DNA concentration on STELA. A range of DNA concentrations were used ranging from 75pg/ μ l to 13pg/ μ l of DNA. The ligation reaction contained 0.9 μ M telorette 2. Each reaction contained 0.3mM of dNTP's, 0.5 μ M of the primers, 1 unit of a 10:1 mixture of taq polymerase and PWO polymerase and 2mM of magnesium chloride. The blot was hybridised using the telomere probe. M=marker in kb. **90**

Figure 29: Amplification of chromosome specific subtelomeric sequence by PCR using a chromosome specific and a subtelomeric sequence primer. Shows an example gel (1.25% agarose gel) with the amplified DNA sequence at 400bp. Lanes one to three represent repeats using 2ng/ μ l of DNA in the PCR reaction vial. **91**

Figure 30: The homology of the isolated and sequenced telomere adjacent probe with the human telomere associated repeat sequence as shown by NCBI database..... **92**

Figure 31: STELAs from DNA from HUVECs cultured in NG medium. Each lane represents a single PCR reaction using 40pg/ μ l of HUVEC DNA. The ligation reaction contained 0.9 μ M telorette 2. Each PCR reaction contained 0.3mM of dNTP's, 0.5 μ M of the primers, 1 unit of a 10:1 mixture of taq polymerase and PWO polymerase and 2mM of magnesium chloride. (See section 2.2.5 and 2.2.6 for details about gel electrophoresis and Southern blotting). The blot was hybridised using the telomere-adjacent probe. Examples are shown for passages 0, 2 and 4. M=marker in kb..... **94**

Figure 32: STELAs from DNA from HUVECs cultured in HG medium. Each lane represents a single PCR reaction using 40pg/μl of HUVEC DNA. The ligation reaction contained 0.9μM telorette 2. Each PCR reaction contained 0.3mM of dNTP's, 0.5μM of the primers, 1 unit of a 10:1 mixture of taq polymerase and PWO polymerase and 2mM of magnesium chloride. (See section 2.2.5 and 2.2.6 for details about gel electrophoresis and Southern blotting). The blot was hybridised using the telomere-adjacent probe. Examples are shown for passages 0, 2 and 4. M=marker in kb..... **95**

Figure 33: STELAs from DNA from HUVECs cultured in AG medium. Each lane represents a single PCR reaction using 40pg/μl of HUVEC DNA. The ligation reaction contained 0.9μM telorette 2. Each PCR reaction contained 0.3mM of dNTP's, 0.5μM of the primers, 1 unit of a 10:1 mixture of taq polymerase and PWO polymerase and 2mM of magnesium chloride. (See section 2.2.5 and 2.2.6 for details about gel electrophoresis and Southern blotting). The blot was hybridised using the telomere-adjacent probe. Examples are shown for passages 0, 2 and 4. M=marker in kb..... **96**

Figure 34: Effect of HG and AG on telomere attrition in HUVECs by STELA. (A) The mean (of medians) telomere length (kb) over ~6 cumulative population doublings for HUVECs treated with NG (■), HG (▲) or AG (▼) every 48 hours. Telomere length was assessed using STELA and the blots were analysed using Telometric software. The data were analysed using linear regression. Values are ± SEM, n=3. (B) The mean telomere loss per population doubling level for HUVECs treated with NG, HG or AG over whole experiment. Values are + SEM, n=3. **97**

Figure 35: Effect of HG and AG on telomere length heterogeneity in HUVECs. (A) The semi-interquartile range (SIR) was calculated from STELA blots (using Telometric software) and plotted against the cumulative population doublings for HUVECs treated with NG (■), HG (▲) or AG (▼) every 48 hours. The data were analysed using linear regression. Values are ± SEM, n=3. (B) The mean SIR decrease per population doubling level for HUVECs treated with NG, HG or AG. Values are + SEM, n=3. **98**

Figure 36: HG induces ROS production in HUVECs. HUVECs were treated with 16.5mM glucose, 50μM menadione, 3mM NAC, 25μM TTFA, 16.5mM 3-O-methylglucose, or 16.5mM mannitol for 1 hour. H₂O₂ production was assessed using the Amplex Red assay and expressed relative to the protein content (section 2.2.7). **P<0.005 vs NG. ***P<0.001 vs NG. Values represent mean +SEM, n=6..... **100**

Figure 37: Effect of NAC or TTFA on HG-induced H₂O₂ production by HUVECs. Cells were treated with HG for 1 hour in absence or presence of NAC (3mM), or TTFA (25μM). H₂O₂ production was assessed using the Amplex Red assay and expressed relative to the protein content (section 2.2.7). *P<0.05 vs NG. ***P<0.001 vs NG. Values represent mean +SEM, n=6..... **101**

Figure 38: Time course of H₂O₂ production by HUVECs exposed to medium containing NG or HG. H₂O₂ production was measured using the Amplex Red assay in the media of cells exposed to NG (■) or HG (■) over a period of 24 hours (section 2.2.7). Values are mean ± SEM, n=6 for each timepoint. **102**

Figure 39: Time course of H₂O₂ production in HUVECs exposed to NG over a period of 10 days. H₂O₂ was measured using the Amplex Red assay and expressed relative to the protein content (section 2.2.7). Values are mean +SEM, n=6..... **103**

Figure 40: H₂O₂ production in HUVECs exposed to NG or HG over a period of 10 days. H₂O₂ was measured using the Amplex Red assay and expressed relative to the protein content (section 2.2.7). (A) H₂O₂ production for HUVECs cultured in NG or HG medium for 2 days. Values are mean +SEM, n=3. (B) H₂O₂ production for HUVECs cultured in NG or HG for 6 days. Values are mean +SEM, n=3. *P<0.05. (C) H₂O₂ production for HUVECs cultured in NG or HG for 10 days. Values are mean +SEM, n=6. ***P<0.001. **104**

Figure 41: The protocol for measuring ROS for HUVECs exposed to AG medium. Cells were seeded at 50% confluence in 96 well plate 48 hours prior to measuring ROS using the Amplex Red assay. Measurements were performed at 2, 6 and 10 days. **106**

Figure 42: Time course of H₂O₂ production in HUVECs exposed to NG or AG (ending with NG) over a period of 10 days. H₂O₂ was measured using the Amplex Red assay and expressed relative to the protein content (section 2.2.7). (A) H₂O₂ production for HUVECs cultured in NG or AG medium for 2 days. Values are mean +SEM, n=3. (B) H₂O₂ production for HUVECs cultured in NG or AG for 6 days. Values are mean +SEM, n=3. **P<0.005. (C) H₂O₂ production for HUVECs cultured in NG or AG for 10 days. Values are mean +SEM, n=6. *P<0.05. **108**

Figure 43: Time course of H₂O₂ production in HUVECs exposed to NG or AG (ending with HG) over a period of 10 days. H₂O₂ was measured using the Amplex Red assay and expressed relative to the protein content (section 2.2.7). (A) H₂O₂ production for HUVECs cultured in NG or AG medium for 2 days. Values are mean +SEM, n=3. (B) H₂O₂ production for HUVECs cultured in NG or AG for 6 days. Values are mean +SEM, n=3. *P<0.05. (C) H₂O₂ production for HUVECs cultured in NG or AG for 10 days. Values are mean +SEM, n=6. ***P<0.001. **110**

Figure 44: Effect of HG and AG on telomere attrition in HUVECs measured by STELA. (A) The mean (of medians) telomere length (kb) over ~6 cumulative population doublings for HUVECs treated with NG (■), HG (▲) or AG (▼) glucose every 48 hours. Telomere length was assessed using STELA and the blots were analysed using Telometric software. The data were analysed using linear regression. Values are ± SEM, n=3. (B) The mean telomere loss per population doubling level for HUVECs treated with NG, HG or AG. *P<0.05 vs NG. Values are + SEM, n=3. **112**

Figure 45: Effect of NAC or TTFA on telomere attrition due to NG. (A) The mean telomere length (kb) versus the cumulative population doublings for HUVECs treated with NG (■), NG and NAC (▲) or NG and TTFA (▼). Telomere length was assessed using STELA and the blots were analysed using Telometric software. The data were analysed using linear regression. Values are \pm SEM, n=3. (B) The mean telomere loss per population doubling level for HUVECs treated with NG, NG + NAC or NG + TTFA. Values are + SEM, n=3. 113

Figure 46: STELAs from DNA from HUVECs cultured in NG medium. Each lane represents a single PCR reaction using 40pg/ μ l of HUVEC DNA. The ligation reaction contained 0.9 μ M telorette 2. Each PCR reaction contained 0.3mM of dNTP's, 0.5 μ M of the primers, 1 unit of a 10:1 mixture of taq polymerase and PWO polymerase and 2mM of magnesium chloride. (See section 2.2.5 and 2.2.6 for details about gel electrophoresis and Southern blotting). The blots were hybridised using the telomere-adjacent probe. Examples are shown for passages 0, 2 and 3. M=marker in kb. 114

Figure 47: STELAs from DNA from HUVECs cultured in HG medium. Each lane represents a single PCR reaction using 40pg/ μ l of HUVEC DNA. The ligation reaction contained 0.9 μ M telorette 2. Each PCR reaction contained 0.3mM of dNTP's, 0.5 μ M of the primers, 1 unit of a 10:1 mixture of taq polymerase and PWO polymerase and 2mM of magnesium chloride. (See section 2.2.5 and 2.2.6 for details about gel electrophoresis and Southern blotting). The blots were hybridised using the telomere-adjacent probe. Examples are shown for passages 0, 2 and 3. M=marker in kb. 115

Figure 48: STELAs from DNA from HUVECs cultured in HG medium with 3mM NAC. Each lane represents a single PCR reaction using 40pg/ μ l of HUVEC DNA. The ligation reaction contained 0.9 μ M telorette 2. Each PCR reaction contained 0.3mM of dNTP's, 0.5 μ M of the primers, 1 unit of a 10:1 mixture of taq polymerase and PWO polymerase and 2mM of magnesium chloride. (See section 2.2.5 and 2.2.6 for details about gel electrophoresis and Southern blotting). The blots were hybridised using the telomere-adjacent probe. Examples are shown for passages 0, 2 and 3. M=marker in kb. 116

Figure 49: Effect of NAC on telomere attrition due to HG. (A) The mean telomere length (kb) versus the cumulative population doublings for HUVECs treated with NG (■), HG (▲) or HG and 3mM NAC (▼). Telomere length was assessed using STELA and the blots were analysed using Telometric software. The data were analysed using linear regression. Values are \pm SEM, n=3. (B) The mean telomere loss per population doubling level for HUVECs treated with NG, HG or HG + NAC. *P<0.05 vs NG; #P<0.05 vs HG. Values are + SEM, n=3. 117

Figure 50: STELAs from DNA from HUVECs cultured in HG medium with 25µM TTFA. Each lane represents a single PCR reaction using 40pg/µl of HUVEC DNA. The ligation reaction contained 0.9µM telorette 2. Each PCR reaction contained 0.3mM of dNTP's, 0.5µM of the primers, 1 unit of a 10:1 mixture of taq polymerase and PWO polymerase and 2mM of magnesium chloride. (See section 2.2.5 and 2.2.6 for details about gel electrophoresis and Southern blotting). The blots were hybridised using the telomere-adjacent probe. Examples are shown for passages 0, 2 and 3. M=marker in kb..... **118**

Figure 51: Effect of TTFA on telomere attrition due to HG. (A) The mean telomere length (kb) versus the cumulative population doublings for HUVECs treated with NG (■), HG (▲) or HG and 25µM TTFA (▼). Telomere length was assessed using STELA and the blots were analysed using Telometric software. The data were analysed using linear regression. Values are ± SEM, n=3. (B) The mean telomere loss per population doubling level for HUVECs treated with NG, HG or HG + TTFA. *P<0.05 vs NG; #P<0.05 vs HG. Values are + SEM, n=3. **119**

Figure 52: STELAs from DNA from HUVECs cultured in AG medium. Each lane represents a single PCR reaction using 40pg/µl of HUVEC DNA. The ligation reaction contained 0.9µM telorette 2. Each PCR reaction contained 0.3mM of dNTP's, 0.5µM of the primers, 1 unit of a 10:1 mixture of taq polymerase and PWO polymerase and 2mM of magnesium chloride. (See section 2.2.5 and 2.2.6 for details about gel electrophoresis and Southern blotting). The blots were hybridised using the telomere-adjacent probe. Examples are shown for passages 0, 2 and 3. M=marker in kb..... **120**

Figure 53: STELAs from DNA from HUVECs cultured in AG medium with 3mM NAC. Each lane represents a single PCR reaction using 40pg/µl of HUVEC DNA. The ligation reaction contained 0.9µM telorette 2. Each PCR reaction contained 0.3mM of dNTP's, 0.5µM of the primers, 1 unit of a 10:1 mixture of taq polymerase and PWO polymerase and 2mM of magnesium chloride. (See section 2.2.5 and 2.2.6 for details about gel electrophoresis and Southern blotting). The blots were hybridised using the telomere-adjacent probe. Examples are shown for passages 0, 2 and 3. M=marker in kb..... **121**

Figure 54: Effect of NAC on telomere attrition due to AG. (A) The mean telomere length (kb) versus the cumulative population doublings for HUVECs treated with NG (■), AG (▲) or AG and NAC (▼). Telomere length was assessed using STELA and the blots were analysed using Telometric software. The data were analysed using linear regression. Values are ± SEM, n=3. (B) The mean telomere loss per population doubling level for HUVECs treated with NG, AG or AG + NAC. Values are + SEM, n=3..... **122**

Figure 55: STELAs from DNA from HUVECs cultured in AG medium with 25µM TTFA. Each lane represents a single PCR reaction using 40pg/µl of HUVEC DNA. The ligation reaction contained 0.9µM telorette 2. Each PCR reaction contained 0.3mM of dNTP's, 0.5µM of the primers, 1 unit of a 10:1 mixture of taq polymerase and PWO polymerase and 2mM of magnesium chloride. (See section 2.2.5 and 2.2.6 for details about gel electrophoresis and Southern blotting). The blots were hybridised using the telomere-adjacent probe. Examples are shown for passages 0, 2 and 3. M=marker in kb..... **123**

Figure 56: Effect of TTFA on telomere attrition due to AG. (A) The mean telomere length (kb) versus the cumulative population doublings for HUVECs treated with NG (■), AG (▲) or AG and TTFA (▼). Telomere length was assessed using STELA and the blots were analysed using Telometric software. The data were analysed using linear regression. Values are ± SEM, n=3. (B) The mean telomere loss per population doubling level for HUVECs treated with NG, AG or AG + TTFA. Values are + SEM, n=3. **124**

Figure 57: Shows the overall reaction for the hexokinase kit. The kit measures the production of NADH at 340nm which is proportional to the glucose concentration. **126**

Figure 58: mtDNA content in HUVECs following exposure to HG over a number of passages. HUVECs were cultured for up to 8 passages in the presence of HG and samples of cells were taken at 0, 6 and 8 in order to assess mtDNA content by QPCR. All values are relative to mtDNA within NG treated cells. Values are mean +SEM, n=3..... **142**

Figure 59: mtDNA content in HUVECs following exposure to AG over a number of passages. HUVECs were cultured for up to 8 passages in the presence of AG and samples of cells were taken at 0, 6 and 8 in order to assess mtDNA content by QPCR. All values are relative to mtDNA within normal glucose treated cells. Values are mean +SEM, n=3. **143**

Figure 60: mtDNA content in HUVECs following exposure to HG and NAC over 8 passages. HUVECs were cultured for up to 8 passages in the presence of HG and NAC and samples of cells were taken at 0, 6 and 8 in order to assess mtDNA content by QPCR. All values are relative to mtDNA within HG treated cells. Values are mean +SEM, n=3. **144**

Figure 61: mtDNA content in HUVECs following exposure to high glucose and TTFA over 8 passages. HUVECs were cultured for up to 8 passages in the presence of HG and TTFA and samples of cells were taken at 0, 6 and 8 in order to assess mtDNA content by QPCR. All values are relative to mtDNA within HG treated cells. Values are mean +SEM, n=3. **145**

Figure 62: Effect of different primary antibody dilutions on eNOS band intensity. 30µg of protein from HUVEC lysates were loaded in each well of an SDS-PAGE gel. The protein was separated via electrophoresis and analysed by Western blotting (section 2.2.8). The membrane was incubated with the primary antibody overnight at 4°C, followed by the rabbit anti-mouse secondary antibody (1 in 10000 dilution) for 1 hour at room temperature. ... **146**

Figure 63: Effect of different primary antibody dilutions on eNOS band intensity. 20µg of protein from HUVEC lysates were loaded in each well of an SDS-PAGE gel. The protein was separated via electrophoresis and analysed by Western blotting (section 2.2.8). The membrane was incubated with the primary antibody overnight at 4°C, followed by the rabbit anti-mouse secondary antibody (1 in 10000 dilution) for 1 hour at room temperature. ... **146**

Figure 64: Effect of different primary antibody dilutions on ICAM1 band intensity. 30µg of protein from Raji and HUVEC lysates were loaded in each well of an SDS-PAGE gel. The protein was separated via electrophoresis and analysed by the use of Western blotting (section 2.2.8). The membrane was incubated with the primary antibody overnight at 4°C, followed by the goat anti-rabbit secondary antibody (1 in 10000 dilution) for 1 hour at room temperature. **147**

Figure 65: Effect of different primary antibody dilutions on ICAM1 band intensity. 20µg of protein from HUVEC lysates were loaded in each well of an SDS-PAGE gel. The protein was separated via electrophoresis and analysed by the use of Western blotting (section 2.2.8). The membrane was incubated with the primary antibody overnight at 4°C, followed by the goat anti-rabbit secondary antibody (1 in 10000 dilution) for 1 hour at room temperature. ... **148**

Figure 66: The different intensities of protein bands when a range of concentrations were used for the anti-α-tubulin antibody (Ab). 30µg of protein from HUVEC lysates were loaded in each well of an SDS-PAGE gel. The protein was separated via electrophoresis and analysed by the use of Western blotting (section 2.2.8). A 1 in 30 000 and a 1 in 40 000 dilution of the rabbit anti-mouse secondary antibody were tested. **148**

Figure 67: The different intensities of protein bands when a range of concentrations were used for the anti-α-tubulin antibody. 20µg of protein from HUVEC lysates were loaded in each well of an SDS-PAGE gel. The protein was separated via electrophoresis and analysed by the use of Western blotting (section 2.2.8). A 1 in 20 000 dilution of the rabbit anti-mouse secondary antibody was used. **149**

Figure 68: The effect of NG, HG or AG on eNOS expression. Protein lysate from HUVECs treated with NG, HG or AG were analysed on a SDS-PAGE gel, transferred and probed using the primary antibodies anti-eNOS and anti- α -tubulin. eNOS was measured by densitometry and expressed relative to α -tubulin. (A) An example of a Western blot obtained. N=normal glucose, H=high glucose, A=alternating glucose. (B) eNOS protein content in HUVECs over a number of cumulative population doubling levels when treated with either NG, HG or AG. Values are mean \pm SEM, n=3. Squares (■) NG. Triangles (▲) HG. Circles (●) AG. **150**

Figure 69: ICAM1 protein expression for HUVECs treated with NG, HG or AG. Protein lysate from HUVECs treated with NG, HG or AG were analysed on a SDS-PAGE gel, transferred and probed using the primary antibodies anti-ICAM1 and anti- α -tubulin. ICAM1 was measured by densitometry and expressed relative to α -tubulin. Values are mean \pm SEM, n=3. (A) An example of a Western blot obtained. N=normal glucose, H=high glucose, A=alternating glucose. (B) ICAM1 protein content in HUVECs at passage 0 and passage 8 when treated with NG. *p<0.05. (C) ICAM1 protein in HUVECs at passage 0 and passage 8 when treated with HG. (D) ICAM1 protein in HUVECs at passage 0 and passage 8 when treated with AG. **152**

Figure 70: eNOS protein levels in HUVECs cultured in NG, NG and NAC or NG and TTFA. Cell lysates were separated by SDS-PAGE and Western blots performed using antibodies to eNOS and α -tubulin. eNOS protein levels were measured by densitometry and expressed relative to α -tubulin when HUVECs were treated with NG, NG and NAC or NG and TTFA at passage 0 and passage 7. The data are represented graphically. Values are mean \pm SEM, n=3. **154**

Figure 71: eNOS protein levels in HUVECs cultured in HG, HG and NAC or HG and TTFA. Cell lysates were separated by SDS-PAGE and Western blots performed using antibodies to eNOS and α -tubulin. (A) An example of a Western showing the expression of eNOS at passage 0 and passage 7 when treated with HG (X), HG and NAC (Y) or HG and TTFA (Z). (B) eNOS protein levels were measured by densitometry and expressed relative to α -tubulin when HUVECs were treated with HG, HG and NAC or HG and TTFA at passage 0 and passage 7. Values are mean \pm SEM, n=3. **154**

Figure 72: eNOS protein levels in HUVECs cultured in AG, AG and NAC or AG and TTFA. Cell lysates were separated by SDS-PAGE and Western blots performed using antibodies to eNOS and α -tubulin. (A) An example of a Western showing the expression of eNOS at passage 0 and passage 7 when treated with AG (X), AG and NAC (Y) or AG and TTFA (Z). (B) eNOS protein levels were measured by densitometry and expressed relative to α -tubulin when HUVECs were treated with AG, AG and NAC or AG and TTFA at passage 0 and passage 7. Values are mean \pm SEM, n=3. **155**

Figure 73: Effect of ethidium bromide on HUVECs growth rate, mtDNA content and the expression of mitochondrial proteins. (A) Cumulative population doubling levels of control and Rho0 HUVECs. ANCOVA shows the slopes are significantly different $p < 0.0001$. (■) = control cells. (▲) = Rho0 cells. Values are mean \pm SEM, $n=3$. (B) mtDNA was measured over a number of days in Rho0 HUVECs and compared to control HUVECs using real time PCR and expressed as a percent of the control. $n=1$. (C) Western blots using the primary antibodies anti-COXI (1 in 500 dilution), anti-COXIV (1 in 1000 dilution) and anti- α -tubulin. Protein cell lysates from HUVECs (C) and Rho0 HUVECs (R) at passages 0 and 3 were separated on a SDS-PAGE gel and analysed by Western blotting. **157**

Figure 74: vWF staining of control and Rho0 HUVECs. Control and Rho0 HUVECs were grown on coverslips until 80% confluent. The cells were fixed, permeabilised and blocked. They were then incubated overnight with a 1 in 200 dilution of antibody to von Willebrand factor and mounted using a DAPI mountant. They were sealed using clear nail varnish and viewed using FITC and DAPI filters. Magnification = x 200. **159**

Figure 75: Morphological appearance of control and Rho0 HUVECs. Samples were processed for TEM as described (section 2.2.9.1) by the Department of Biochemistry, University of Leicester. **160**

Figure 76: The effect of ethidium bromide treatment on eNOS protein levels in HUVECs and Rho0 HUVECs. Cell lysates were separated by SDS-PAGE and Western blots performed using antibodies to eNOS and α -tubulin. (A) A Western blot of eNOS at passage 0, 2, 4, and 6 for control (C) and Rho0 (R) HUVECs. (B) eNOS protein levels were measured by densitometry and expressed relative to α -tubulin for control HUVECs and HUVECs treated with ethidium bromide over 8 cumulative population doubling levels. Control HUVECs = (■). Rho0 HUVECs = (▲). Values are mean \pm SEM, $n=3$ **161**

Figure 77: The effect of ethidium bromide treatment on ICAM1 protein content in HUVECs. Cell lysates were separated by SDS-PAGE and Western blots performed using antibodies to ICAM1 and α -tubulin. (A) A Western blot of ICAM1 at passage 0, 2, 4, and 6 for control (C) and Rho0 (R) HUVECs. (B) The protein expression of ICAM1 over 6 passages measured by densitometry and expressed relative to α -tubulin in control HUVECs. The data are represented graphically. Values are mean \pm SEM, $n=3$. (C) The protein expression of ICAM1 over 6 passages measured by densitometry and expressed relative to α -tubulin in Rho0 HUVECs. Values are mean \pm SEM, $n=3$. ** $P < 0.01$ vs passage 0. **163**

Figure 78: Effect of chloramphenicol on cell growth, and mitochondrial protein expression. HUVECs were cultured in medium containing 20µg/ml of chloramphenicol for up to 27 days. Cell lysates were extracted from control and chloramphenicol-treated HUVECs at passage 0 and 4. The protein was separated by SDS-PAGE and transferred to a membrane via a Western blot. The membranes were probed with antibodies to COXI, COXIV and α-tubulin. (A) Cumulative population doubling levels of control and chloramphenicol treated HUVECs. Control HUVECs = (■). Chloramphenicol treated HUVECs = (■). Values are mean ±SEM, n=3. (B) A Western blot of COXI and α-tubulin at passage 0 and passage 4 for control and chloramphenicol treated HUVECs. Anti-COXI was used at a dilution of 1 in 500. C=control HUVECs, C*=chloramphenicol treated HUVECs. (C) A Western blot of COXIV and α-tubulin at passage 0 and passage 4 for control and chloramphenicol treated HUVECs. Anti-COXIV was used at a dilution of 1 in 1000. C=control HUVECs, C*=chloramphenicol treated HUVECs. Western blots (B) and (C) are examples of blots obtained for 3 analyses.165

Figure 79: The effect of chloramphenicol on eNOS expression in HUVECs. Cell lysates were extracted from control and chloramphenicol-treated HUVECs at passages 0, 1, 2 and 3. The protein was separated by SDS-PAGE and analysed by a Western blot. The membranes were probed with antibodies to eNOS and α-tubulin. C=control HUVECs, C*=chloramphenicol treated HUVECs.166

Figure 80: Effect of ddC treatment on cell growth and mtDNA content. (A) Cumulative population doubling levels of control and ddC treated HUVECs up to 34 days. Values are mean ±SEM, n=3. (●) = 0µM ddC. (■) = 5µM ddC. (▲) = 10µM ddC. (▼) = 15µM ddC. (B) mtDNA content in ddC treated HUVECs relative to control HUVECs was assessed using real time PCR at days 0, 10 and 15. (■) = 5µM ddC. (▲) = 10µM ddC. (▼) = 15µM ddC. ...168

Figure 81: Effect of ddC on eNOS protein expression in HUVECs. Cell lysates were extracted from control and ddC-treated HUVECs. The protein was separated by SDS-PAGE and transferred to a membrane via a Western blot. The membranes were probed with antibodies to eNOS and α-tubulin. eNOS was measured by densitometry and expressed relative to α-tubulin. (A) Example of Westerns at passage 0 (P0) and passage 6 (P6) showing eNOS expression when HUVECs were treated with 0, 5 or 10µM ddC. (B) Expression of eNOS over 8 to 10 cumulative population doubling levels in control HUVECs (●) and HUVECs treated with 5µM ddC (▼). Values are mean ±SEM, n=3. (C) Expression of eNOS over 8 to 10 cumulative population doubling levels in control HUVECs (●) and HUVECs treated with 10µM ddC (▲). Values are mean ±SEM, n=3.....169

Figure 82: Effect of ddC on ICAM1 protein expression in HUVECs. Cell lysates were extracted from control and ddC-treated HUVECs. The protein was separated by SDS-PAGE and transferred to a membrane via a Western blot. The membranes were probed with antibodies to ICAM1 and α -tubulin. ICAM1 was measured by densitometry and expressed relative to α -tubulin. Values are mean +SEM, n=3. (A) Examples of a Western at passage 0 (P0), 4 (P4) and 6 (P6) showing ICAM1 expression when HUVECs were treated with 0, 5 or 10 μ M ddC. (B) Expression of ICAM1 in control HUVECs at passage 0, 4 and 6. (C) Expression of ICAM1 in 5 μ M ddC treated HUVECs at passage 0, 4 and 6. (D) Expression of ICAM1 in 10 μ M ddC treated HUVECs at passage 0, 4 and 6. **171**

Figure 83: Effect of mtDNA depletion on H₂O₂ production in HUVECs. HUVECs and Rho0 HUVECs were cultured in 96 well plates and treated as described in section 2.2.7. H₂O₂ production was assessed using the Amplex Red assay over 1 hour and expressed relative to the protein content (section 2.2.7). (A) H₂O₂ production in control HUVECs with 16.5mM glucose, 50 μ M menadione, 3mM NAC, 25 μ M TTFA, 16.5mM 3-O-methylglucose, or 16.5mM mannitol for 1 hour. Values are mean +SEM, n=3. ***P<0.001 vs NG. (B) H₂O₂ production in Rho0 HUVECs with 16.5mM glucose, 50 μ M menadione, 3mM NAC, 25 μ M TTFA, 16.5mM 3-O-methylglucose, or 16.5mM mannitol for 1 hour. Values are mean +SEM, n=6. *P<0.05 vs NG. **173**

Figure 84: Menadione generates superoxide by redox cycling. MD = menadione; MDH/MDH₂ = reduced menadione; O₂⁻ = superoxide (Nutter *et al.*, 1992). **183**

Figure 85: Hypothesis for increased glucose mediated endothelial cell ageing and/or dysfunction. **187**

LIST OF TABLES

Table 1: A list of reactive oxygen and reactive nitrogen species (Yu and Chung, 2001).	9
Table 2: The composition of HUVEC (human umbilical vein vascular endothelial cells) media.	33
Table 3: The composition of VSMC (vascular smooth muscle cells) media... ..	33
Table 4: The composition of Raji media.	34
Table 5: The primers used for PCR in STELA and their corresponding sequences.	36
Table 6: The primers used for mtDNA and nuclear DNA PCR and their corresponding sequences.	38
Table 7: Preparation of DNA standards. Table shows the mass of DNA (ng) contained within each well of the 96 well plate, and the volume in μ l of both the TE buffer and the lambda DNA diluted stock needed to achieve this concentration.	45
Table 8: Preparation of protein standards. The volumes of lysis buffer and 1mg/ml BSA required making final BSA concentrations between 0.0 to 0.5 mg/ml.	57
Table 9: Comparison of telomere restriction fragments (TRF) values obtained from cell plugs or extracted DNA. The median telomere length and semi-interquartile range (SIR) for telomeric DNA from either plugs or extracted DNA were calculated. The samples were all from the same cell donor.	80
Table 10: Details the type and volume of digestive enzyme used and the type of buffer added to each lane letter (corresponds to Figure 23).	81
Table 11: The dNTP concentration, the magnesium chloride concentration and the number of PCR cycles for lanes a to h. Corresponds to Figure 27. .	88
Table 12: Effect of different methods on the amount of protein extracted from 2×10^5 HUVECs. HUVECs were grown until 70% confluent in a 6 well plate then protein was extracted by sonication, freeze thaw, cell lytic M buffer or NP40 buffer. Protein concentration was measured using the Bradford assay (section 2.2.8.3). n=2.	99
Table 13: Details the effect of depleting mtDNA on ROS release in different Rho0 cells. Shows a range of different methods used to measure ROS release.	139

ABBREVIATIONS

ABB = alkaline blotting buffer
ADP = adenosine diphosphate
AG = alternating glucose
AGE = advanced glycation end-products
APS = ammonium persulphate
AP1 = activator protein 1
AP2 = activator protein 2
ATM = ataxia telangiectasia mutated
ATP = adenosine triphosphate
BER = base excision repair
BLM = bloom syndrome
cGMP = cyclic guanosine monophosphate
COXI = cytochrome c oxidase subunit I
COXIV = cytochrome c oxidase subunit IV
CuZnSOD = copper/zinc superoxide dismutase
DAG = diacylglycerol
DCF = dichlorofluoroscein
ddC = dideoxycytidine
ddI = dideoxyinosine
DHAP = dihydroxyacetone phosphate
DHE = dihydroethidine
DNA = deoxyribonucleic acid
DTT = dithiothreitol
eNOS = endothelial nitric oxide synthase
ERCC1 = excision repair cross-complementing-1
FADH = reduced flavin adenine dinucleotide
FPG = fasting plasma glucose
GFAT = glutamine:fructose-6-phosphate amidotransferase
Gpx1 = glutathione peroxidase 1
HBSS = hank's buffered salt solution
HG = high glucose
HMW = high molecular weight

HNE = 4-hydroxynonenal
HRP = horse radish peroxidase
HUVEC = human umbilical vein vascular endothelial cells
H₂O₂ = hydrogen peroxide
ICAM1 = intercellular adhesion molecule 1
IFG = impaired fasting glucose
IGT = impaired glucose tolerance
iNOS = inducible nitric oxide synthase
KU86 = Ku86 autoantigen related protein 1
MDA = malondialdehyde
MnSOD = manganese superoxide dismutase
MRE11 = meiotic recombination 11
mtDNA = mitochondrial DNA
NAC = N-acetylcysteine
NADH = reduced nicotinamide dinucleotide
NADPH = reduced nicotinamide adenine dinucleotide phosphate
NBS1 = Nijmegen breakage syndrome
NEB2 = nuclear extraction buffer
NER = nucleotide excision repair
NF-κB = nuclear factor kappa B
NG = normal glucose
nNOS = neuronal nitric oxide synthase
NO = nitric oxide
PBS = phosphate buffered saline
PCR = polymerase chain reaction
PGC1-α = PPAR-γ coactivator 1α
PKC = protein kinase C
PNK = polynucleotide kinase
POT1 = protection of telomeres-1
PPAR-γ = peroxisome proliferator-activated receptor-γ
PTOP = POT1 and TIN2 organising protein
RAGE = receptor for advanced glycation endproduct
RAP1 = repressor/activator protein 1
RNA = ribonucleic acid

RNS = reactive nitrogen species
ROS = reactive oxygen species
SDS = sodium dodecyl sulphate
SDS-PAGE = sodium dodecyl sulphate polyacrylamide gel electrophoresis
SEM = standard error of the mean
SIR = semi-interquartile range
STELA = single length telomere length analysis
SSC = saline sodium citrate buffer
TANK = tankyrases
TCA = tricarboxylic acid cycle
TEMED = tetramethylethylenediamine
TIN2 = TRF1 interacting nuclear factor 2
TNF α = tumour necrosis factor α
TRF = telomere restriction fragment
TRF1 = telomere repeat binding factor 1
TRF2 = telomere repeat binding factor 2
TTFA = thenoyltrifluoroacetone
UDP-Glc-Nac = uridine diphosphate N-acetylglucosamine
VEGF = vascular endothelial growth factor
VCAM1 = vascular adhesion molecule 1
vWF = von Willebrand Factor
WRN = werner syndrome

1 Introduction

1.1 High glucose in humans

1.1.1 Hyperglycaemia and diabetes

Diabetes mellitus (diabetes) is a chronic metabolic disease of growing prevalence (Bartnik *et al.*, 2007). It is characterised by periods of hyperglycaemia which is the presence of excess glucose in the blood (Ahmed, 2005). The symptoms of diabetes include polyuria and weight loss (Bartnik *et al.*, 2007). Diabetes is diagnosed using one of two methods (McCance *et al.*, 1997). The first method is where the patient fasts for 8 hours and the fasting plasma glucose (FPG) level is measured. A FPG of ≥ 7.0 mmol/l indicates a provisional diagnosis of diabetes. Often if the fasting glucose test is high or borderline (5.6-6.9 mmol/l) then the second method is performed - an oral glucose tolerance test (American Diabetes Association, 2009). This test involves the patient taking a glucose load containing the equivalent of 75g anhydrous glucose dissolved in water. A plasma glucose ≥ 11.1 mmol/l after a 2 hour post glucose load is diagnostic for diabetes mellitus (American Diabetes Association, 2004). If glucose levels are above the normal range but do not satisfy the conditions for diabetes, patients are diagnosed with prediabetes (the presence of impaired fasting glucose/glycaemia (IFG) and/or impaired glucose tolerance (IGT)) (Twigg *et al.*, 2007). IFG and IGT are both associated with insulin resistance but the site of insulin resistance varies between the two conditions (Abdul-Ghani *et al.*, 2006). IFG is diagnosed when the FPG is ≥ 6.1 and < 7.0 mmol/l but the response to the 2 hour post glucose load is normal. IGT is diagnosed when the FPG is ≥ 5.6 and < 7.0 mmol/l and the 2 hour post glucose load is ≥ 7.8 and < 11.1 (Genuth *et al.*, 2003). Patients with prediabetes are at an increased risk of developing diabetes and cardiovascular disease (Twigg *et al.*, 2007).

An increased plasma glucose level in diabetes is due to either insulin deficiency or insulin resistance (Ahmed, 2005). Insulin aids in the uptake of

glucose by cells and the conversion of glucose to glycogen so that it can be stored in a form that has little effect on cell functions (Srivastava and Pandey, 1998). However, when insulin is not present for some reason or the body is resistant to insulin, less glucokinase is induced. Therefore less glucose is converted to glucose-6-phosphate and to glycogen (an energy store for liver and muscles) (Garrett and Grisham, 1995). This results in an increased extracellular glucose concentration which leads to hyperglycaemia and subsequently to all of the common effects seen in diabetes (Garrett and Grisham, 1995).

There are two different forms of diabetes – type 1 and type 2 (Jay *et al.*, 2006). Type 1 is where the β -cells of the pancreas are destroyed and therefore the production of insulin is impaired. Type 2 often occurs in later life and is where insulin is still being released but cells do not respond to the insulin (Elliot and Elliot, 2001).

1.1.2 High glucose and the vascular endothelium

1.1.2.1 Entry of glucose into endothelial cells

One of the most important molecules taken up by the endothelium is glucose since it is essential for the synthesis of ATP. Glucose enters the cells via glucose transporters (Mueckler, 1994). In the intestine and kidney, glucose is co-transported with sodium (Turk *et al.*, 1994; Turner and Moran, 1982). There are a number of different transporters present in other human cells but all belong to the GLUT family (Olson and Pessin, 1996). These receptors span the membrane twelve times generating internal and external cellular regions that glucose binds to, and is transported across (Brown, 2000). GLUT1 receptors are responsible for the transport of glucose across many different endothelial cells (Mueckler, 1994). In retinal vascular endothelial cells, glucose uptake was increased in cells exposed to higher concentrations of glucose. This was not due to increased expression of GLUT1 receptors but was shown to be dependent on microtubule integrity (Busik *et al.*, 2002). Another class of receptors that are present on cardiac

muscle and adipose tissue are GLUT4. These are responsible for glucose transport in an insulin dependent manner (Brown, 2000). Insulin increases the rate at which the GLUT4 receptor reaches and becomes incorporated into the membrane (Watson and Pessin, 2000). It is also known to decrease the rate at which the GLUT4 receptor is exocytosed out of the membrane (Watson and Pessin, 2001). Therefore, when cells have a resistance to insulin as in Type 2 diabetes, the receptors for glucose do not transport glucose so efficiently into the cells (Karnieli et al., 1981).

1.1.2.2 High glucose activates the polyol, protein kinase C, hexosamine and the AGE pathways

High glucose in the blood has a number of damaging effects on the endothelium (Schalkwijk and Stehouwer, 2005). This damage is believed to occur through four different pathways: the polyol pathway, the hexosamine pathway, the protein kinase C (PKC) pathway and the advanced glycation endproduct (AGE) pathway (Das Evcimen and King, 2007). The different pathways are summarised in Figure 1.

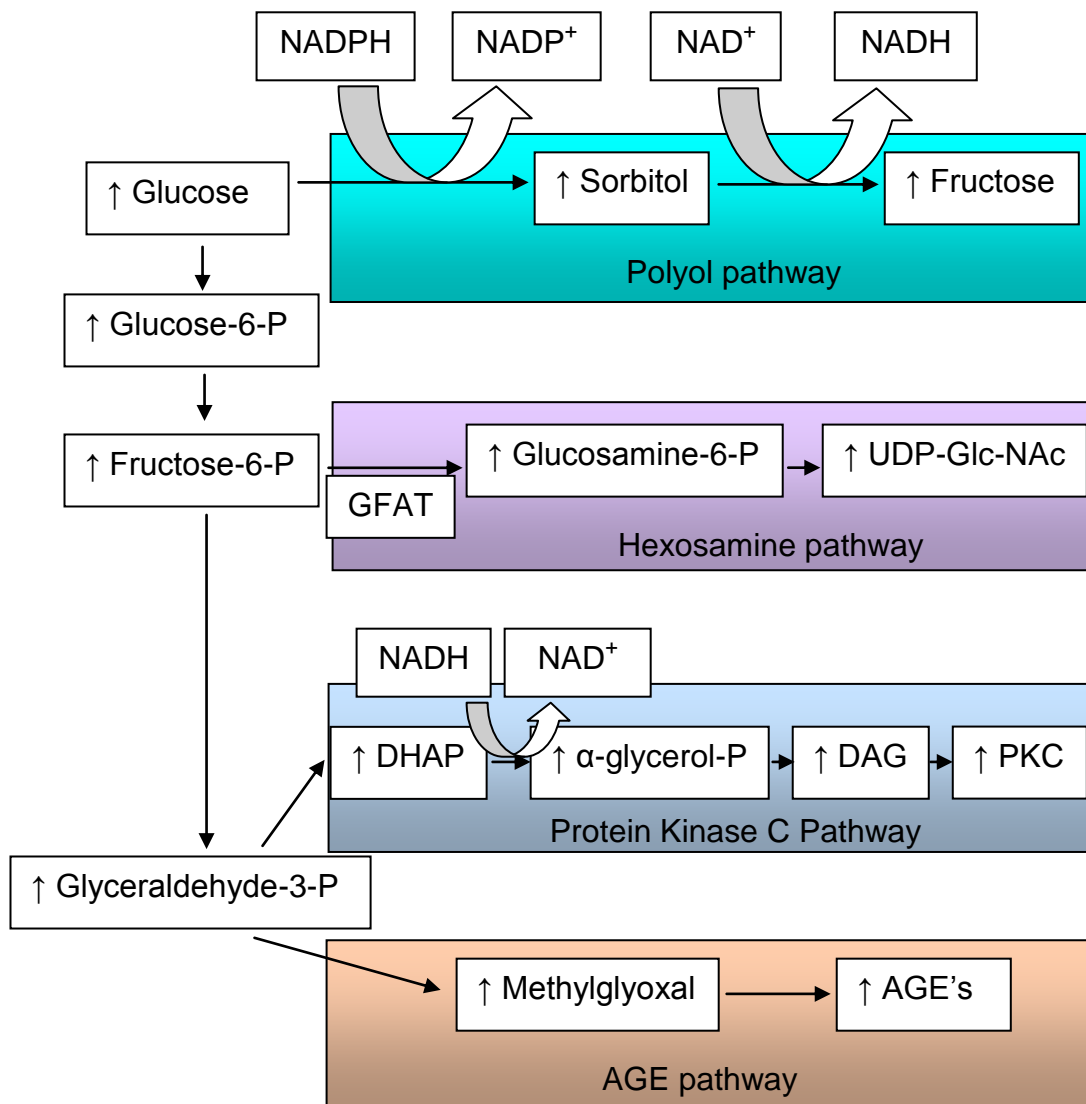


Figure 1: An overview of the effect of increased glucose on cell metabolism. High glucose causes increased activity of the polyol pathway, hexosamine pathway, protein kinase C pathway and the AGE pathway. PKC = protein kinase C; NADH = reduced nicotinamide adenine dinucleotide; NADPH = reduced nicotinamide adenine dinucleotide phosphate; DAG = diacylglycerol; AGE = advanced glycation end-products; DHAP = dihydroxyacetone phosphate; UDP-Glc-Nac = uridine diphosphate N-acetylglucosamine; GFAT = glutamine:fructose-6-phosphate amidotransferase. (Adapted from Brownlee, 2001).

The polyol pathway uses two enzymes that are both involved in the production of reactive oxygen species (ROS) (Brownlee, 2001). The first is aldose reductase that converts glucose into sorbitol and the second enzyme

is sorbitol dehydrogenase which is responsible for converting sorbitol into fructose, generating NADH (Berrone *et al.*, 2006). Only a small percentage of the available glucose is metabolised via the polyol pathway when glucose conditions are normal, however this increases dramatically during hyperglycaemia (Toth *et al.*, 2007).

During exposure to high glucose, there is known to be an increase in PKC activation (Schalkwijk and Stehouwer, 2005). The implication of increased PKC activation is decreased nitric oxide production, and increased production of endothelin-1, both of which can lead to abnormalities in the blood flow (Schalkwijk and Stehouwer, 2005). PKC activation can also increase vascular endothelial growth factor (VEGF). This leads to angiogenesis and increased ROS production, due to increased activity of NAD(P)H oxidases (Brownlee, 2001).

Furthermore, AGEs are formed in the presence of high glucose by a nonenzymic reaction (Dutta *et al.*, 2005). Aldehydes or ketone groups of a reducing sugar (in this case glucose) form a covalent link to free amino groups of proteins to form a Schiff's base. This ketoamine then undergoes rearrangement to form a more stable product known as an Amadori product. This in turn rearranges to form AGEs (Basta, 2008). Further to this, glucose, Schiff's base or Amadori's products can rearrange to form dicarbonyl intermediates which can then react again with free amino acid groups to form AGEs (Basta *et al.*, 2004) (Figure 2).

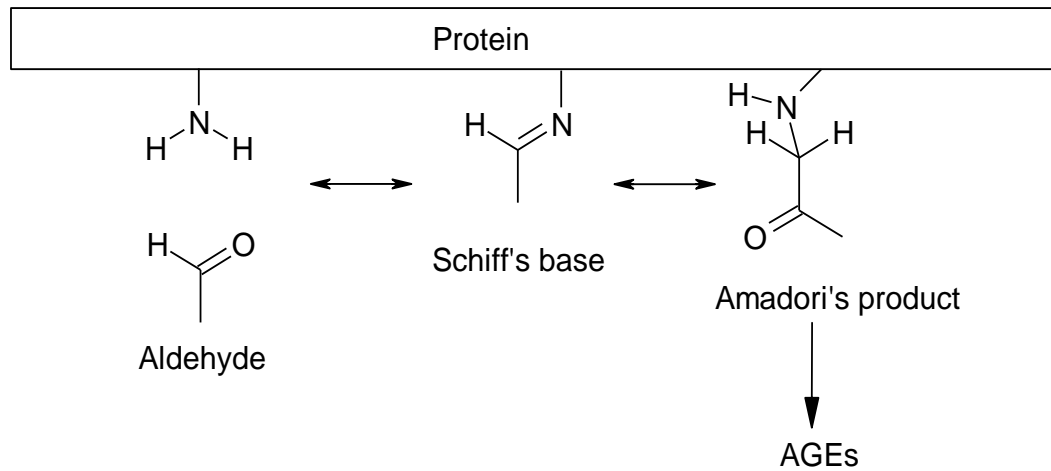


Figure 2: The reactions that occur in the formation of advanced glycation end-products. An aldehyde reacts with an amino group to form a Schiff's base, rearranges to form Amadori's product and further changes lead to the formation of AGEs. (Basta *et al.*, 2004).

AGEs can occur on both long-lived and short-lived proteins despite the length of time required in the formation of these molecules (Ahmed, 2005). They fall into one of three categories – fluorescent cross-linking AGEs such as pentosidine, non-fluorescent cross-linking AGEs such as alkyl formyl glycosyl pyrrole, or lastly non-cross-linking AGEs such as pyralline (Ahmed, 2005).

The effects of increased glucose include modifying enzyme activity and immune responses, and decreasing ligand binding (Vlassara and Palace, 2002). AGEs can form on the DNA bases adenine and guanine with major consequences for DNA function but are also known to form on phospholipids leading to lipid peroxidation (Baynes, 2002). AGEs are taken up into cells by the receptor RAGE (Basta, 2008). The expression of RAGE is enhanced during diabetes and inflammation (Ritthaler *et al.*, 1995).

AGEs are known to be involved in a number of the complications that occur in diabetes such as diabetic retinopathy, diabetic cataract, and diabetic atherosclerosis (Yamagishi *et al.*, 2008; Sun *et al.*, 1998; Bras *et al.*, 2007).

The extent to which they are involved in these complications is unknown (Vlassara and Palace, 2002).

Diabetic atherosclerosis is one of the most lethal consequences of diabetes. AGEs may contribute to atherosclerosis by firstly causing mechanical dysfunction of the blood vessel walls by forming cross-bridges trapping molecules such as low density lipoprotein (LDL) (Sell and Monnier, 1989). Secondly, AGEs can cause circulating blood cells to adhere to the vessel wall (Basta *et al.*, 2004). Thirdly, AGEs can contribute to atherosclerosis changing cellular function by binding to receptors present on endothelial cells, vascular smooth muscle cells, and macrophages. An example of altered cellular function is when binding of AGEs to endothelial cells causes increased oxidative stress (Yan *et al.*, 1994). This in turn can activate NF- κ B leading to the increased transcription of inflammatory genes which contribute to atherosclerosis (Wautier *et al.*, 2001).

There are a number of compounds used to protect against the effects of AGEs. One such compound is a drug called aminoguanidine (Stoppa *et al.*, 2006). It prevents the formation of AGEs by reacting with the carbonyl groups from reducing sugars or the dicarbonyl intermediates (Edelstein and Brownlee, 1992). Another drug that prevents the formation of AGEs is aspirin. This is thought to block the amino group of proteins therefore preventing these from reacting with sugars; however the effect that this may have on other proteins is still very much debated (Harding and Ganea, 2006). Alternatively, enzymes such as amadoriases may be used to inactivate intermediates such as 3-deoxyglucosones (a dicarbonyl intermediate) or deglycate Amadori products (Brown *et al.*, 2005).

1.1.3 Effect of high glucose and diabetes on ROS production

Cells cultured in high glucose and cells from subjects with diabetes have been shown to release higher levels of ROS (Giardino *et al.*, 1996 and Yu *et al.*, 2006). This increased ROS was shown to originate from the

mitochondrial electron transport chain and was reduced by the presence of uncoupling protein-1 and an inhibitor of complex II of the electron transport chain (Nishikawa *et al.*, 2000). This increased ROS from mitochondria during high glucose exposure is thought to be linked to mitochondrial fragmentation (Yu *et al.*, 2006).

There are a number of reasons which explain why there are dramatic increases in oxidative stress in cells from diabetic subjects. Diabetic vascular cells have increased PKC-dependent activation of NAD(P)H oxidases which leads to increased oxidative stress (Yorek, 2003). Furthermore, the four pathways that increase in diabetes (PKC, AGE, hexokinase and polyol pathways) are known to cause the overproduction of superoxide by the mitochondrial electron transport chain (Bayraktutan, 2002).

1.1.4 Effect of high glucose and diabetes on atherosclerosis

Atherosclerosis is one of the major consequences of diabetes and high glucose concentration (Libby *et al.*, 2002). It involves the build up of lipids and inflammatory cells within the walls of arteries forming a plaque. This plaque may rupture causing the release of thrombogenic factors including tissue factor, leading to the formation of a blood clot (thrombus). In the case of the coronary artery, thrombus formation can ultimately cause myocardial infarction (Libby, 2006). As mentioned, the formation of AGEs can be one of the major causes of atherosclerosis; however, there are a number of other possible causes. Firstly, increased glucose causes increased ROS production leading to increased oxidised LDL (Jay *et al.*, 2006). Secondly, an increase in endothelial cell dysfunction may arise, for example, by increased expression of endothelial cell adhesion molecules and increased permeability to circulating lipoproteins such as LDL (Ross, 1999). Thirdly, an increase in glucose leads to higher levels of ROS in monocytes and macrophages, causing activation and release of cytokines that aid in the progression of atherosclerosis (Ross, 1999, Dhindsa *et al.*, 2004).

1.2 Reactive Oxygen and Nitrogen Species

1.2.1 Definition

ROS and reactive nitrogen species (RNS) are relatively reactive reduced forms of oxygen or nitrogen respectively. As illustrated in Table 1, they can either be radicals whereby they have an unpaired electron or non-radicals whereby all electrons present are in a paired state (Yu and Chung, 2001).

Table 1: A list of reactive oxygen and reactive nitrogen species (Yu and Chung, 2001).

	Radicals	Non-radicals
Reactive Oxygen Species (ROS)	Superoxide ($O_2^{\cdot-}$) Hydroxyl (HO^{\cdot}) Hydroperoxyl (HOO^{\cdot})	Hydrogen peroxide (H_2O_2) Hydrochlorous acid ($HOCl$) Ozone (O_3)
Reactive Nitrogen Species (RNS)	Nitric oxide (NO^{\cdot}) Nitrogen dioxide (NO_2^{\cdot})	Nitrous acid (HNO_2) Dinitrogen trioxide (N_2O_3) Peroxynitrite ($ONOO^{\cdot}$)

1.2.2 Origin of ROS and RNS

Reactive species can originate from a number of different sources. One of the main cellular sources is from the mitochondrial electron transport chain during the process of respiration (Evans and Cooke, 2004). They can also arise during exposure to radiation and xenobiotics (Dias and Bailly, 2005). Other sources of reactive species include phagocytic cells which kill foreign bodies by a respiratory burst, and peroxisomes that produce hydrogen peroxide (H_2O_2) as a by-product of breaking down fatty acids and other molecules (Ames *et al.*, 1993).

The electron transport chain forms a major part of the latter stages of glucose metabolism in humans, and superoxide anions are most commonly

synthesised in the electron transport chain, predominantly at complex I and III (Raha and Robinson, 2000). An overview of the electron transport chain can be seen in Figure 3.

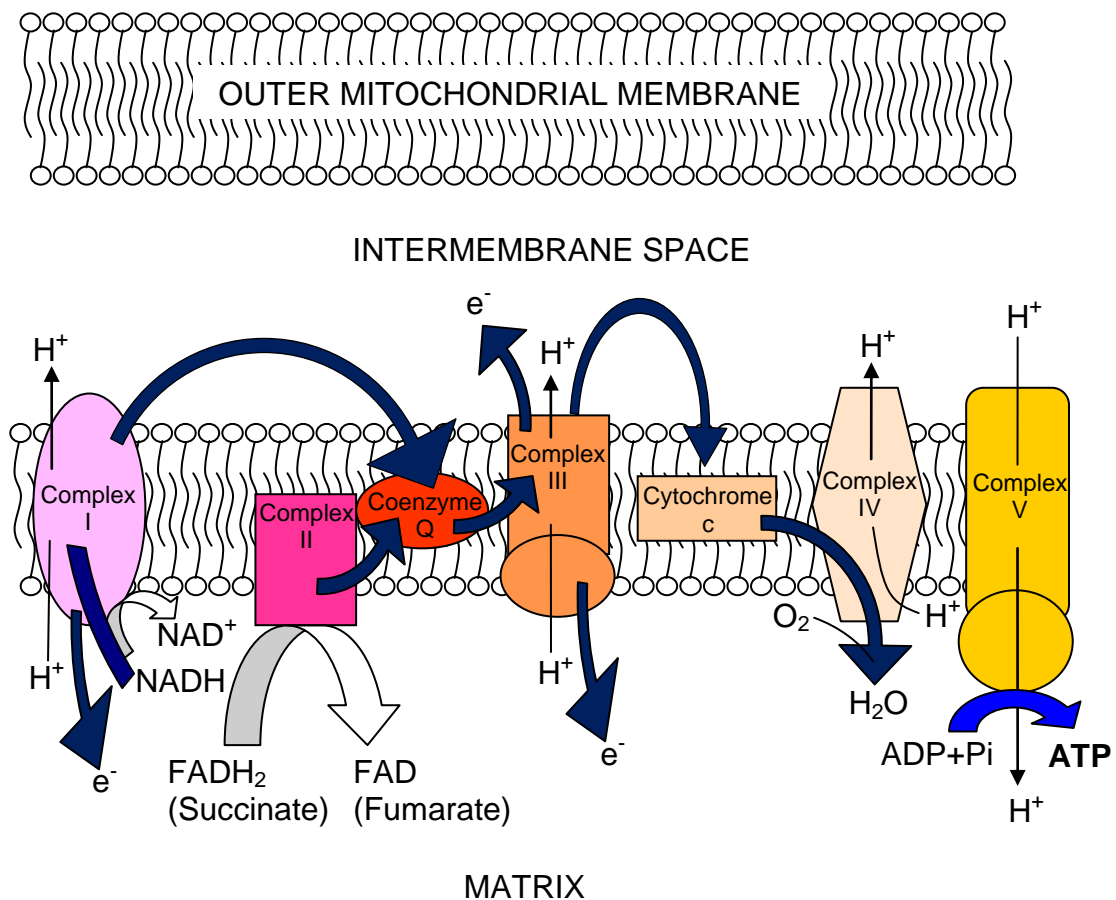


Figure 3: Overview of the respiratory transport chain and oxidative phosphorylation showing complexes 1 to 5. Complex 1 is the NADH-Coenzyme Q dehydrogenase responsible for transferring a pair of electrons (e^-) from NADH to coenzyme Q and transporting protons from the matrix of the mitochondria to the cytosol. Complex II, otherwise known as succinate-coenzyme Q reductase transfers electrons from ($FADH_2$) to coenzyme Q. Complex III otherwise known as coenzyme Q-cytochrome c reductase is where reduced coenzyme Q passes its electrons to cytochrome c via the Q cycle and further protons (H^+) are transferred from the matrix to the cytosol. Complex IV is also known as cytochrome c oxidase and this is where electrons are transferred from cytochrome c to O_2 to form water (H_2O). Due to the increase in the proton concentration in the cytosol, H^+ is pumped back out of the cytosol into the matrix via complex V (ATP synthase) which converts ADP to ATP (oxidative phosphorylation). Blue arrows indicate movement of electrons. NADH = reduced nicotinamide adenine dinucleotide; ADP = adenosine diphosphate; ATP = adenosine triphosphate; $FADH_2$ = reduced flavin adenine dinucleotide. (Adapted from Garrett and Grisham, 1995, Elliot and Elliot, 2001, Matthews *et al.*, 2000).

ROS and RNS produced in excess of the cells antioxidant capacity can have dire consequences on cell metabolism, damaging DNA and other biomolecules and activating pathways that can initiate cell death (Norbury and Zhivotovsky, 2004).

1.2.3 Protection against ROS and RNS – antioxidants

There are a wide variety of antioxidants that form a protective mechanism against free reactive oxygen and reactive nitrogen species. These include vitamins such as vitamin A, C, E and glutathione, and enzymes such as glutathione peroxidase, superoxide dismutase and catalase which act either individually or synergistically to exert their effects (Maritim *et al.*, 2003).

Vitamins are provided from the diet and directly interact with the free radicals to detoxify them. For example, vitamin E interacts with peroxy and superoxide radicals and protects membranes from lipid peroxidation (Weber *et al.*, 1997). Superoxide dismutases (SOD) are antioxidant enzymes that convert superoxide anions to H_2O_2 (Afonso *et al.*, 2007). Different isoforms of SOD are located within different parts of the cell – CuZnSOD is located in the cytoplasm and the nucleus whereas MnSOD is confined to the mitochondria (Qi *et al.*, 1997). H_2O_2 is then converted to water by glutathione peroxidase with reduced glutathione as the electron donor (Chang *et al.*, 2004). The major isoform glutathione peroxidase 1 (Gpx1) is present within the cytosol however a small fraction is located within the mitochondrial matrix (Qi *et al.*, 1997). H_2O_2 can also be converted to water by the thioredoxin dependent enzyme peroxiredoxin (Lin and Beal, 2006). Peroxiredoxin III is specifically expressed within the mitochondria (Lin and Beal, 2006). Furthermore, H_2O_2 is also converted to water by the enzyme catalase (Muzykantov, 2001).

1.2.4 Effects of increased ROS/RNS

1.2.4.1 Nuclear and mtDNA damage by ROS/RNS

Oxidative stress can have major effects on DNA by causing DNA damage. Types of DNA damage that can occur include single and double strand breaks, base oxidation (e.g. guanine to 8-oxoguanine), inter and intrastrand crosslinks and DNA-protein crosslinks (Cooke *et al.*, 2003). More specifically, oxidative damage can cause telomere shortening, microsatellite instability and damage to specific sites within the DNA sequence depending on higher order chromosomal structure, protein distribution, and the types of bases present (Evans and Cooke, 2004). In order to prevent these DNA alterations being fatal and causing altered gene expression, the cell has a number of control mechanisms in place such as BER (base excision repair) and NER (nucleotide excision repair) (Moreira *et al.*, 2008).

As expected, oxidative damage to certain specific sequences can have a greater effect than others. For example, damage to DNA that encodes for a promoter can result in a gene sequence not being transcribed. It may result in the transcription factor not binding to its corresponding sequence – e.g. Sp1 binds to a highly guanine rich sequence which is highly prone to oxidative damage (Cooke *et al.*, 2006). Methylated sequences (CpG islands), are also highly prone to oxidative damage (Ehrlich, 2003). These sequences are often involved in the silencing of gene sequences but DNA damage at these sites can result in increased expression of genes (Evans and Cooke, 2004).

The mechanism by which ROS and RNS cause DNA damage is thought to be either by a direct reaction or indirectly through the interaction with endogenous genotoxins formed from the break down of lipid hydroperoxide (Lee and Blair, 2001). Lipid hydroperoxides are formed when poly-unsaturated fatty acids undergo attack by free radicals (Spiteller, 2007). These molecules are often short-lived and are converted to less reactive fatty acid alcohols or react with metals to form highly reactive breakdown

products such as malondialdehyde (MDA) and 4-hydroxynonenal (HNE) (Marnett, 2000). Both MDA and HNE are mutagens and therefore will cause damage to DNA (Burcham, 1998).

Mitochondrial DNA (mtDNA) is thought to be more prone to oxidative damage due to it being closer to the site where ROS/RNS are produced and secondly it lacks the higher order structure that nuclear DNA possesses (Evans and Cooke, 2004). The effectiveness of mtDNA repair has been controversial but evidence suggests that it can protect mtDNA at least to some extent (Druzhyina *et al.*, 2008).

Oxidative stress is also thought to lead to telomere shortening. Studies performed by Kurz *et al.*, (2004), showed that when endothelial cells were treated with *tert*-Butylhydroperoxide (a chemical known to interfere with the antioxidant responses of the cell) telomere shortening per population doubling was greater in treated cells compared to the control cells. A reason for this shortening may be due to the highly sensitive guanines present in the telomeric repeat sequence. These three guanines are susceptible to oxidative damage leading to the formation of 8-oxodG (Oikawa and Kawanishi, 1999). Furthermore, these residues display reduced binding of telomere repeat binding factor 1 (TRF1) and telomere repeat binding factor 2 (TRF2) further disrupting the closed structure of telomeres (Opresko *et al.*, 2005). Sustained telomere shortening and uncapping often results in the initiation of the DNA damage response ultimately leading to senescence (Evans *et al.*, 2002; Li *et al.*, 2001).

1.2.4.2 Increased ROS and ageing

As cells age (either over time or through cardiovascular diseases such as diabetes), there is an increase in oxidative stress (Balaban *et al.*, 2005; Beckman and Ames, 1998; Finkel and Holbrook, 2000; Furumoto *et al.*, 1998; Yorek, 2003). Cells are exposed to a greater concentration of superoxide anions and H₂O₂ thought to be due to increased leakage of

electrons from the mitochondrial electron transport chain as discussed in section 1.2.2. Also, as cells age the concentration of antioxidants decrease, which in turn increases ROS and RNS (Sohal *et al.*, 2002). There is also known to be a decrease in nitric oxide bioavailability. This is suggested to lead to an increased activity of caspases and this can therefore result in increased apoptosis (Haendeler, 2005). As cells age, oxidative DNA damage also increases. In fact, oxidative DNA damage is used as a biomarker for age (de Magalhaes and Church, 2006). Furthermore, mtDNA damage also increases with age which leads to impaired expression of mitochondrial proteins and further ROS production (Harman, 2003; Vina *et al.*, 2003). Oxidative damage to mtDNA is also believed to lead to a reduction in the number of mitochondria (Burns *et al.*, 1979).

1.3 Mitochondria

1.3.1 Structure

Mitochondria are present in all eukaryotic cells. Each mitochondrion is surrounded by a double membrane – the outer membrane and inner membrane. The inner membrane projects inwards forming cristae; this increases the surface area for ATP synthesis (Frey and Mannella, 2000; Mannella, 2006).

Mitochondria contain their own DNA – a closed circular double stranded DNA molecule (Garesse and Vallejo, 2001). However, although the DNA codes for the basic machinery of protein synthesis and some components of the electron transport chain, it does not code for enzymes that are involved in replication, repair, transcription and translation (Schapira, 2006). Therefore, in order for the mitochondria to continue functioning, it requires the protein to be synthesised outside of the mitochondrion using nuclear DNA for transcription and then importation into the mitochondria (Schapira, 2006). The structure of mitochondria is illustrated in Figure 4.

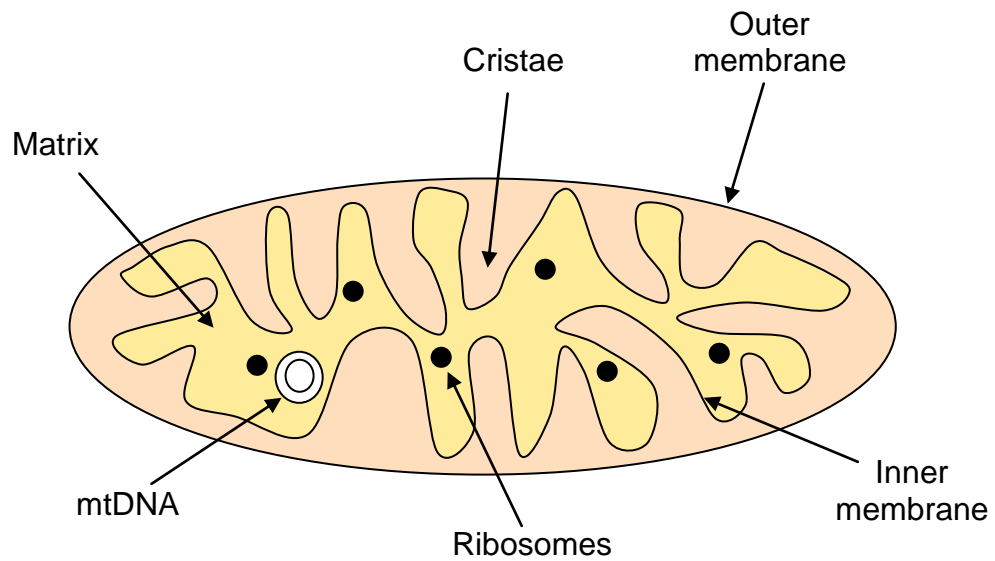


Figure 4: The structure of a mitochondrion. Illustrates how the inner membrane projects inwards to form cristae. (Adapted from Frey and Mannella, 2000).

1.3.2 Dysfunction

Mitochondrial ageing and dysfunction are known to play a prominent role in the pathogenesis of many diseases. This in many cases is thought to be due to the damage of mtDNA (Davidson and Duchon, 2007). mtDNA is more susceptible to damage as it is much more exposed than nuclear DNA and there are more inefficient repair systems present within the mitochondria (Olgun and Akman, 2007). The mitochondrial theory of ageing leading to mitochondrial dysfunction is where there is a decline in mitochondrial function and impairment of cell function due to vicious cycles of increased ROS production and mtDNA damage (Madamanchi and Runge, 2007).

1.4 Telomeres

1.4.1 Structure

For organisms to be successful and to pass on their genes to their progeny, DNA replication is essential. It is performed by synthesising new strands of DNA alongside the existing DNA (Greider, 1999). The synthesis of new DNA occurs in the 5' to 3' direction by the attachment of RNA primers to specific points along the sequence to be transcribed. The primers are recognised by DNA polymerases that bind and initiate the synthesis of Okazaki fragments which are short sequences of DNA that begin just after where the primer ends (Snustad and Simmons, 2000). These fragments are connected together by DNA ligase following the excision of the RNA primers and the replacement with new DNA by the DNA polymerase involved in the synthesis of the lagging DNA strand - thus forming a long strand of transcribed DNA (Snustad and Simmons, 2000).

Eukaryotic organisms have linear chromosomes (Takahashi *et al.*, 2000). When a RNA primer binds to the end of the chromosome for replication, the part of the DNA bound to the primer is not copied. This means the gradual loss of the end of the chromosome and therefore the eventual loss of genetic material (Snustad and Simmons, 2000; Boukamp, 2001). To prevent the loss of vital information, the ends of eukaryotic chromosomes are protected by telomeres (Greider, 1999).

Telomeres are gene-poor, short, repetitive sequences- TTAGGG in humans (Greider, 1999). The lengths of the telomeres vary between different organisms. In humans, the telomeres are approximately 20kb whereas in rats the length can vary between 20 and 100kb (Cherif *et al.*, 2003). The extreme end of the guanine-rich 3' template of a telomere overhangs its complementary strand. The length of this overhang varies but it is thought that for humans it is between 100 and 200 bases (Neidle and Parkinson, 2003). Figure 5 shows the overall structure of the end of a chromosome.

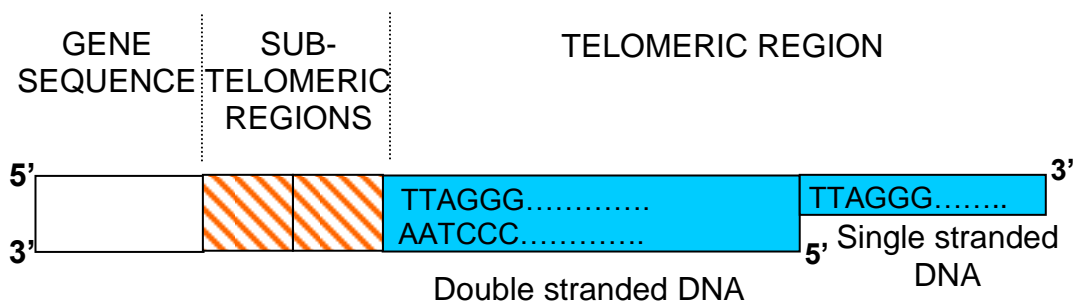


Figure 5: The overall primary structure of telomeric DNA. Illustrates the telomeric regions and the subtelomeric regions. (Adapted from Baird, 2005).

When transcription is not occurring at or near telomeres, it is thought that telomeres form a loop – called a t-loop (a so called ‘closed structure’). This means that the enzyme telomerase cannot gain access to the G-strand overhang and it also prevents any DNA degradation machinery from breaking down the ends of DNA (Goytisolo and Blasco, 2002). The formation of this loop is thought to be aided by TRF1 and TRF2 which both bind directly via a helix-turn-helix to double stranded telomeric DNA (Rhodes *et al.*, 2002). This telomeric structure can be seen in Figure 6.

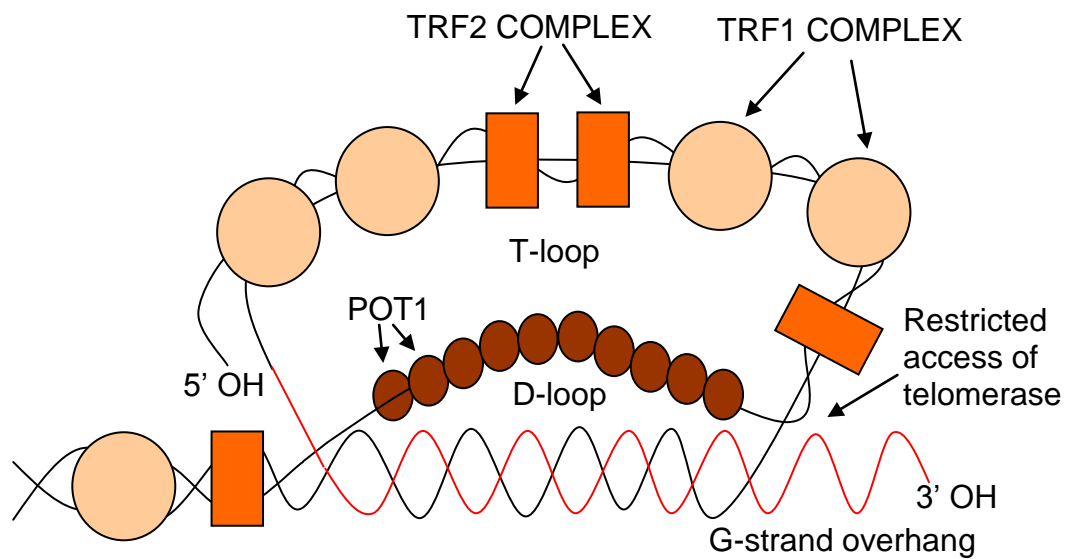


Figure 6: The overall structure of a telomere when expression is not occurring. Illustrating the t and d-loops as well as the position where TRF1 and TRF2 bind. TRF1: telomere repeat binding factor 1; TRF2: telomere repeat binding factor 2; POT1: protection of telomeres-1. (Adapted from Blasco, 2005).

The overall structure (i.e. the tertiary conformation) of telomeres is thought to be similar to constitutive heterochromatin – *in vivo* telomeres are bound to nucleosome arrays (Tommerup *et al.*, 1994). These are complex structures that contain high levels of histone 3 and 4 trimethylated at lysine 9 and lysine 20 respectively (Garcia-Cao *et al.*, 2004; Schotta *et al.*, 2004). This is further thought to have an influence on maintaining a higher overall stability of telomeres and preventing any nucleolytic cleavage (Blasco, 2005).

1.4.2 Telomeric proteins

Telomeres consist of both the DNA sequence but also telomeric proteins. These include proteins that bind directly to the telomere sequence, such as the shelterin proteins TRF1, TRF2, POT1, and others that interact with the DNA through the telomere binding proteins such as the shelterin proteins - TIN2, TPP2, Rap1 (de Lange, 2005). In addition to these six shelterin

proteins, there are also a number of non-shelterin proteins that bind non-directly to the DNA and these include Mre11, WRN and BLM (de Lange, 2005). An example of the TRF1 and TRF2 complex that is formed *in vivo* can be seen in Figure 7. The proteins that bind directly to the telomere either bind to both strands of DNA on the 3' end, such as TRF1, or bind to just the single strand of DNA found at the end of the telomere such as hPot1 (Greider, 1999). Each of these proteins has a unique function but in general their role is to protect telomere length and function (Blasco, 2005).

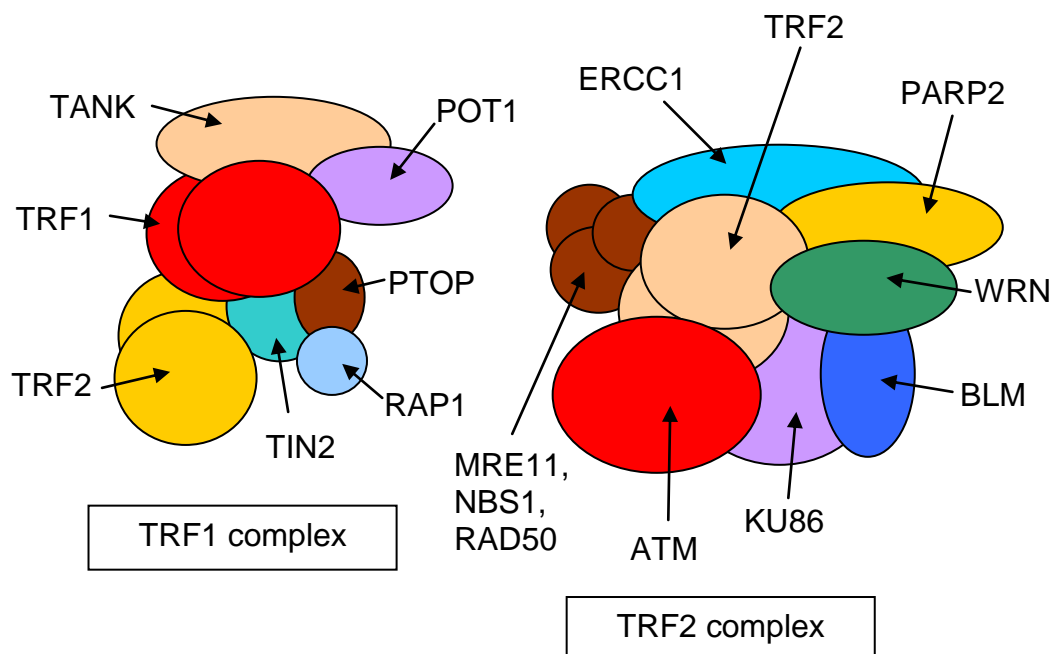


Figure 7: An example of the TRF1 and TRF2 complexes that are formed on telomeres. Both complexes are involved in telomere regulation but TRF2 is also involved in DNA repair. TANK: tankyrases, TRF1: telomere repeat binding factor 1, TRF2: telomere repeat binding factor 2, TIN2: TRF1 interacting nuclear factor 2, RAP1: repressor/activator protein-1, POT1: POT1 and TIN2 organising protein, POT1: protection of telomeres-1, MRE11: meiotic recombination-11, NBS1: Nijmegen breakage syndrome, RAD50: a DNA repair protein, ERCC1: excision repair cross-complementing-1, ATM: ataxia telangiectasia mutated, PARP2: poly (ADP-ribose) polymerase family, WRN: werner syndrome, BLM: bloom syndrome, KU86: ku86 autoantigen related protein 1. (Adapted from Blasco, 2005).

1.4.3 Function

Telomeres prevent the gradual shortening of the chromosomes (Dong *et al.*, 2005). However, they do have a number of other functions. Telomeres prevent the ends from being recognised as a double strand breaks, they prevent the chromosome from being degraded by nucleases, and they protect chromosomes from recombination and fusion with other chromosomes (Broccoli, 2004; Wang and Baumann, 2008). In addition, in certain cells, telomeres must also allow telomerase access to the chromosomes so that the length of telomeres can be maintained (Greider, 1999).

1.4.4 Telomeres in vascular disease

Shorter telomeres have been observed to occur in leukocytes from patients with vascular diseases such as in atherosclerosis (Samani *et al.*, 2001; Okuda *et al.*, 2000; Matthews *et al.*, 2006). It has also been found that in patients with premature myocardial infarction (i.e. myocardial infarction under the age of 50) there is an abundance of leukocytes with shorter telomeres compared to the controls (Brouillette *et al.*, 2003; Salpea *et al.*, 2008). Furthermore, increased telomere attrition has also been observed in monocytes from patients with diabetes (Jeanclos *et al.*, 1998; Sampson *et al.*, 2006).

1.4.5 Result of telomere loss

The loss of telomeres can either occur after each replication or can occur sporadically (Lansdorp, 2005). The polymerase 'end problem' is the main reason for telomere loss. However, other mechanisms can lead to the shortening of telomeres (Broccoli, 2004; Proctor and Kirkwood, 2002). These include damage to the telomere via oxidative stress (von Zglinicki *et al.*, 2000), incorrect nucleolytic cleavage of the telomere performed during the process of creating the G-strand overhang (Makarov *et al.*, 1997), and

deletion of the t-loops leading to telomere loss by homologous recombination (Wang *et al.*, 2004).

1.4.6 Telomere loss leads to replicative senescence

Senescence that occurs after extended cell replication, often following telomere shortening, is known as replicative senescence (Erusalimsky and Kurz, 2005). Senescent cells are still viable however they do not divide i.e. they withdraw from the cell cycle. Senescent cells appear flatter, enlarged and have increased granularity (Foreman and Tang, 2003).

When telomeres shorten or are damaged (as is the case in ageing and many cardiovascular diseases) there are mechanisms in place to recognise this loss (Hao *et al.*, 2005). However, the route by which this telomere damage is detected is unknown. It is thought that the simple loss of telomeric repeats may somehow activate the pathways that lead to senescence (de Lange, 2002). Alternatively, it is thought that as telomeres get shorter, the telomeric proteins that bind will do so less efficiently. This in itself could cause the activation of certain pathways (de Lange, 2002). Lastly, it has been proposed that chromosomes with shorter telomeres are less likely to form t-loops and this could once again signal certain pathways to be activated (d'Adda di Fagagna *et al.*, 2003). Telomere shortening has also been found to activate the DNA damage response pathway and this process could lead to senescence and ultimately apoptosis (d'Adda di Fagagna *et al.*, 2003).

As discussed in section 1.4.4, telomeres have been associated with several cardiovascular diseases and premature ageing syndromes. Therefore, understanding the mechanisms and the reasons for telomere loss may provide a greater insight for both the pathogenesis and treatment of several diseases.

1.5 Telomerase

1.5.1 Structure and Function

As discussed in section 1.4, telomeres are present at the ends of chromosomes and they prevent the genetic material from being lost. However, telomeres do shorten over time. In human fibroblasts after every cell division, 33 to 120 base pairs of telomeric DNA can be lost (Takubo *et al.*, 2002). Therefore, to prevent telomeric DNA loss, the enzyme telomerase is present in many cells (Louis and Vershinin, 2005). Telomerase consists of two different components - a catalytic 127kDa part called TERT (telomerase reverse transcriptase) and a non-catalytic 451 nucleotide part called Terc (telomerase RNA component) (Dong *et al.*, 2005). The assembly of telomerase requires the chaperones Hsp90 and p23 and takes place in the nucleus (Dong *et al.*, 2005).

Telomerase recognises the 3' hydroxyl group and binds to the overhang present on the guanine rich strand (Blackburn, 2001). It then adds multiple copies of the repetitive unit (TTAGGG in humans) to the G-rich strand (Blackburn, 2001).

1.5.2 Differences in the expression of telomerase

The gene coding for the enzyme telomerase is highly expressed in germ cells (and some cancer cells) but is switched off in adult somatic cells (Serrano and Andres, 2004). Figure 8 shows how the length of telomeres differs in different cell types. Telomere loss in somatic cells results in the gradual erosion of the guanine rich strand after every cell division (therefore the length of chromosomes tends to be age-dependent) ultimately reaching a point called replicative senescence whereby the telomere length reaches a critical size and all replication is halted (Blasco, 2005). This can and often does lead to apoptosis of the cell.

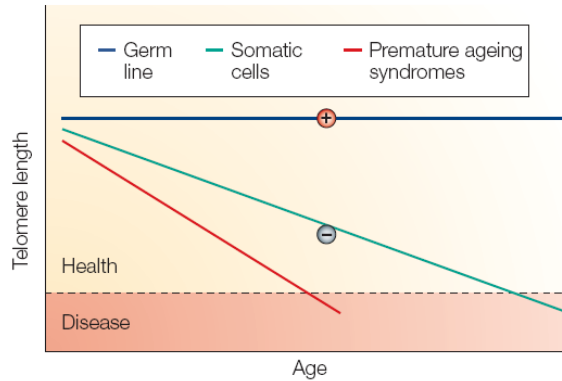


Figure 8: The variation in the telomere length between germ cells, somatic cells and cells involved in premature ageing. The telomere length in germ cells remains fairly constant over time as telomerase is always switched on. However, the telomere length in somatic cells and in premature ageing syndromes decreases as age increases due to telomerase being switched off (Blasco, 2005).

1.6 Vascular Endothelium

1.6.1 Structure and Function of blood vessels

The vascular endothelium lies between the wall of all blood vessels and the blood flow. The general structure of a blood vessel illustrating the position of the endothelium can be seen in Figure 9 (Brandes *et al.*, 2005). The primary function of the endothelium is to act as a protective barrier, but another still very important function of the endothelium is the control of tone and homeostasis of vascular muscle (Hsueh and Quinones, 2003). This is performed via the release of autacoids such as nitric oxide and prostacyclin which are relaxing and growth-inhibiting factors, and thromboxane A2 and angiotensin II which perform the opposite function - they vasoconstrict and promote the growth of vascular smooth muscle (Vanhoutte, 2002).

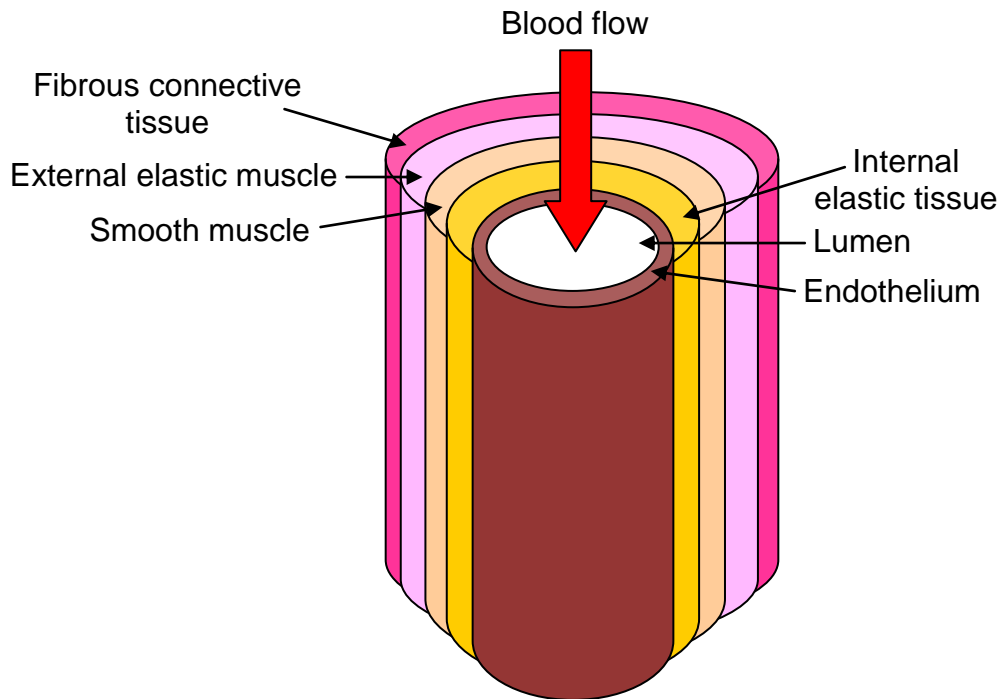


Figure 9: The structure of a vein or an artery. Illustrates the vascular endothelial layer, the smooth muscle layer and the fibrous connective tissue (Cleaver and Melton, 2003).

1.6.2 Endothelial Ageing

1.6.2.1 Changes in Structure and Function

Apart from the normal changes that are associated with ageing in the blood vessels such as increased vascular stiffness and enlargement of the lumina, it is known that ageing also affects the endothelial layer within the blood vessels (Yildiz, 2007). As endothelial cells age, there are a number of changes that occur. These include changes in the structure of the cells e.g. alterations in the cytoskeleton and an increase in the number of cells with polyploid nuclei (Najjar *et al.*, 2005). The production of certain growth factors and vasodilatory factors are also known to alter in ageing cells. These changes can either individually or collectively lead to vascular endothelial dysfunction. This in turn can play a vital role in the cause and advancement of all cardiovascular diseases (Brandes *et al.*, 2005).

1.6.2.2 Mechanisms Leading to Endothelial Dysfunction

The mechanisms that lead to vascular endothelial dysfunction as organisms age, is very difficult to assess in humans. However, by looking at organisms such as the rat, a mechanism has been proposed (Brandes *et al.*, 2005). It has been often stated that in endothelial dysfunction, there is a decrease in the production of nitric oxide (Csiszar *et al.*, 2002; Barton *et al.*, 1997). Nitric oxide is one of the main autacoids/vasodilators released by the endothelium. It plays a vital role in the control of the vascular tone and permeability but it is also important for inhibiting leukocytes from adhering to the endothelial wall, and inhibiting thrombocyte aggregation (Brandes *et al.*, 2005). The reason and mechanisms for decreased nitric oxide production as cells age is still very much debated but it is thought that ageing may bring about the following. Firstly, ageing may bring about a decrease in the expression of endothelial nitric oxide synthase (eNOS) (the enzyme responsible for the synthesis of nitric oxide from L-arginine) by a decrease in the production of estrogens and growth factors (Tanabe *et al.*, 2003; Kleinert *et al.*, 1998). Secondly, a decrease in the number of substrates and cofactors available for eNOS may occur in ageing cells, and problems with the activation of nitric oxide synthase may also occur. Lastly, with age, there may be an increased reaction of nitric oxide with superoxide leading to the formation of a peroxynitrite ion (Cai and Harrison, 2000). van der Loo *et al.* (2000) suggests that the reason for decreased nitric oxide production is purely due to an increase in ROS – in particular superoxide (their data suggests that the expression of NOS and the conversion of L-arginine to nitric oxide is unchanged as cells age). The reasons for increased superoxide production in ageing endothelial cells may be due to increased leakage of electrons from the mitochondrial electron transport chain, increased activity of NAD(P)H oxidases, increased transfer of electrons to O₂ rather than to nitric oxide by increased uncoupling of eNOS and lastly a decreased concentration of antioxidants (Brandes *et al.*, 2005).

Figure 10 shows how ageing cells can affect the concentration of nitric oxide and therefore lead to endothelial dysfunction.

1.6.3 Diseases associated with endothelial dysfunction

Vascular endothelial ageing is very relevant to many cardiovascular diseases such as diabetes, atherosclerosis and hypertension (Bayraktutan, 2002; Cai and Harrison, 2000). Age is the principal risk factor for cardiovascular diseases in general. Such diseases are associated with endothelial dysfunction often caused by decreased concentrations of nitric oxide by superoxide anions (Naseem, 2005). Figure 11 shows how a number of different cardiovascular diseases can lead to endothelial ageing and dysfunction.

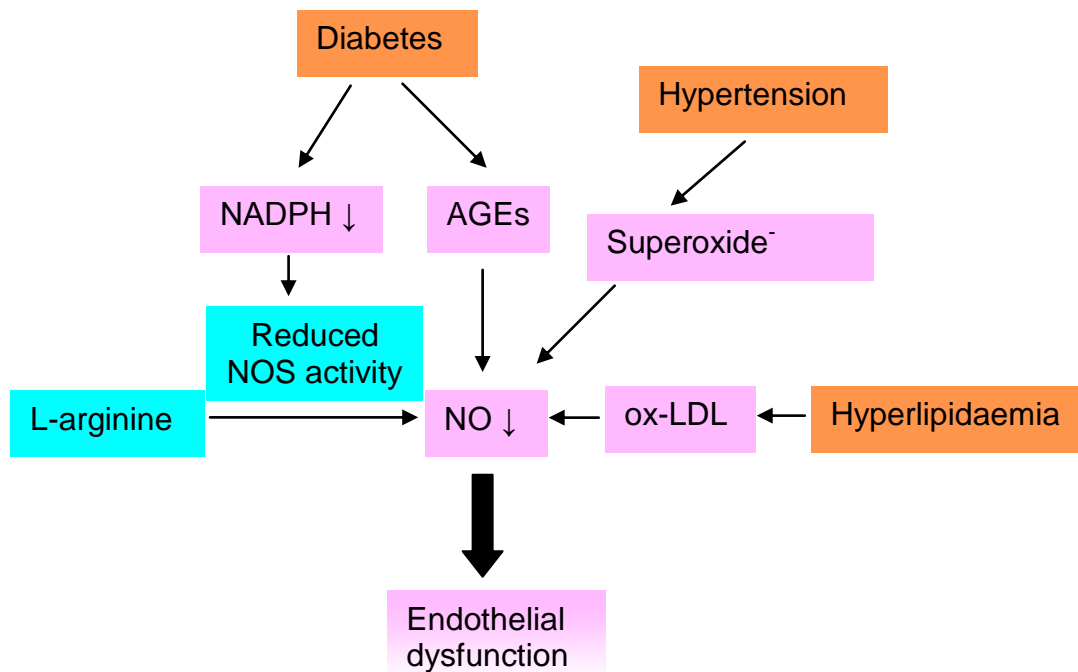


Figure 11: Illustrates how different cardiovascular diseases can affect the nitric oxide concentration and therefore lead to endothelial dysfunction. LDL = low density lipoproteins; AGE = advanced glycation endproducts; ox-LDL = oxidised low density lipoproteins; NO = nitric oxide; NOS = nitric oxide synthase. (Adapted from Hunt *et al.*, 2002).

1.6.3.1 Diabetes

Diabetes is associated with decreased NADPH (a cofactor for the NOS enzyme). The reason for this decrease is due to an increase in aldose reductase activity (Okuda *et al.*, 1997). This enzyme converts the glucose into sorbitol using NADPH as a cofactor (Jay *et al.*, 2006). Under hyperglycaemic conditions, the amount of glucose converted to sorbitol increases. This results in less NADPH for NOS (Figure 1) (Hunt *et al.*, 2002). Furthermore, diabetes is also associated with increased AGEs (Meerwaldt *et al.*, 2008). AGEs cause oxidative modification of low density lipoprotein (LDL), which directly inactivates nitric oxide. Furthermore, hyperglycaemia leads to increased superoxide production either through NADPH oxidase or mitochondria (Zou *et al.*, 2004). This can often lead to increased production of peroxynitrite (van der Loo *et al.*, 2000). Increased peroxynitrite can cause eNOS uncoupling and increased prostacyclin synthase nitration – both can accelerate the onset of endothelial dysfunction (Zou *et al.*, 2004). Other effects of diabetes include decreases in the levels of catalase and glutathione peroxidase (both convert H₂O₂ to water) and decreases in antioxidants such as glutathione and ascorbate (which mop up ROS) (Bayraktutan, 2002).

1.6.3.2 Atherosclerosis

Endothelial dysfunction also occurs in atherosclerosis. There are increases in the circulating lipid concentration, in particular LDL. The LDL interacts directly with the endothelium causing the release of chemokines that attract monocytes and the expression of adhesion molecules. These adhesion molecules help the monocytes attach to the endothelial wall, migrate into the sub-endothelium and differentiate into macrophages (Libby, 2006). The macrophages release free radicals causing the oxidation of LDL. This in turn causes a decrease in the concentration of nitric oxide via the disruption of the complexes that cause the activation of NOS (Vidal *et al.*, 1998). This therefore ultimately leads to endothelial dysfunction (Naseem, 2005). The general process leading to atherosclerosis can be seen in Figure 12.

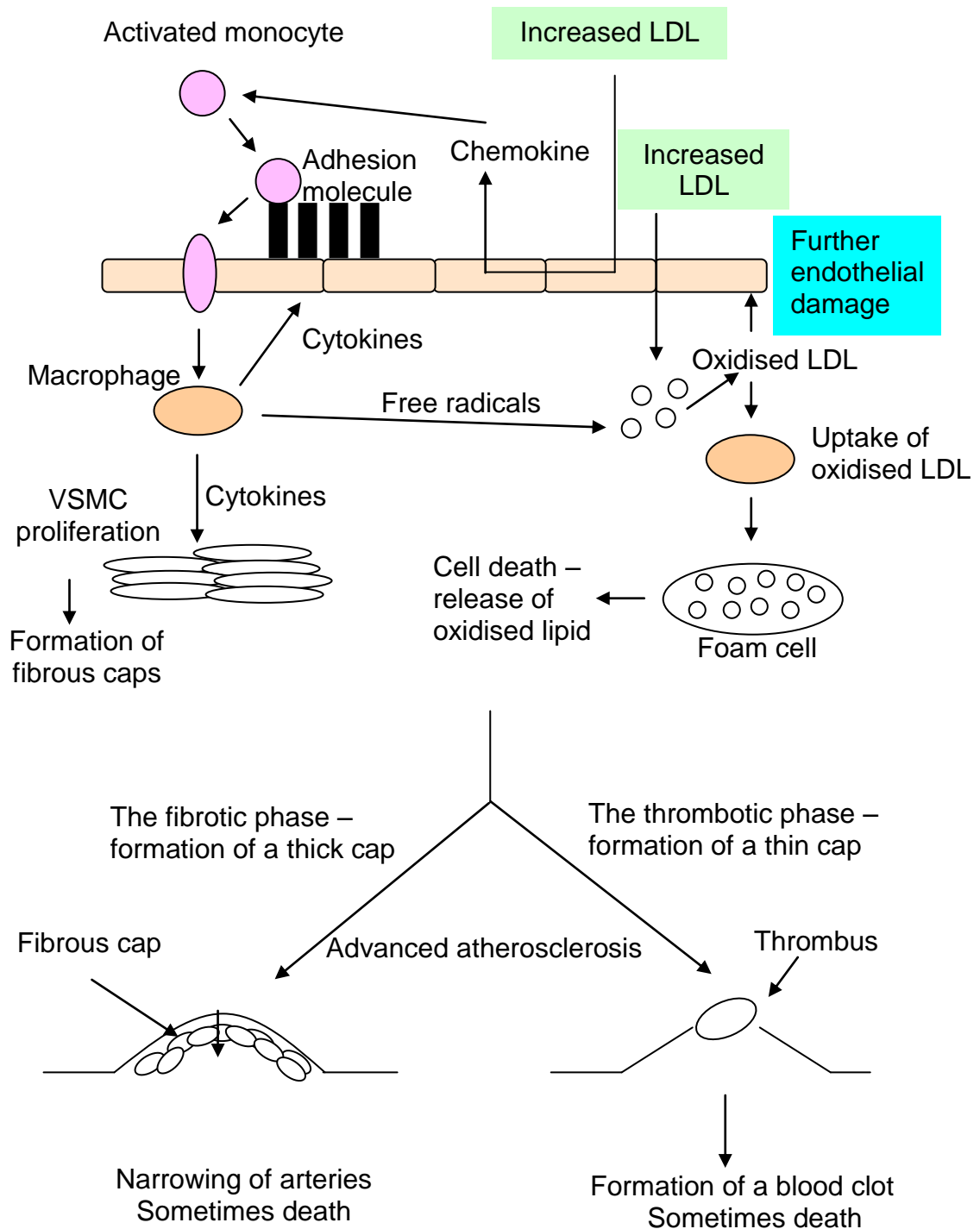


Figure 12: The overall process of atherosclerosis. This shows how increased LDL causes increased oxidised LDL and increased VSMC (vascular smooth muscle cell) proliferation. This leads to endothelial dysfunction and the formation of fibrous caps which ultimately leads to either the thrombotic phase or the fibrotic phase. VSMC = vascular smooth muscle cells. (Adapted from Naseem, 2005).

In conclusion therefore, vascular endothelial dysfunction has a large number of consequences often leading to the development and progression of many cardiovascular diseases such as diabetes and atherosclerosis. The major reason for endothelial dysfunction is believed to be due to decreases in the nitric oxide concentration. Elucidation of mechanisms leading to loss of nitric oxide or NOS will aid an understanding of cardiovascular diseases. Moreover, it is thought that identifying factors that help to preserve nitric oxide concentration will help to alleviate some of the many effects/pathological mechanisms seen in cardiovascular diseases.

1.7 Hypothesis and Aims:

Diabetes is a metabolic disorder that affects millions of people worldwide (Schalkwijk and Stehouwer, 2005). It is associated with increased ageing of the vasculature which is believed to play a major role in the progression of diabetic complications such as diabetic atherosclerosis (Ceriello, 2003; Quagliaro *et al.*, 2007; Jay *et al.*, 2006). Diabetes is linked to increased ROS/RNS leakage thought to occur from damage to the mitochondrial electron transport chain (Yorek, 2003). Increased ROS production has been linked to telomere loss (Kurz *et al.*, 2004; Furumoto *et al.*, 1998; Opresko *et al.*, 2005) and mtDNA damage (Genova *et al.*, 2004; Passos *et al.*, 2007; Li *et al.*, 2001).

The hypothesis investigated within this thesis is:

High glucose accelerates endothelial cell ageing and dysfunction by increased ROS production which leads to increased telomere attrition rates and mtDNA damage.

Therefore the aims of this thesis were:

1. To establish a model human endothelial cell system and characterise the effects of alternating normal/high and high glucose on growth and glucose uptake.
2. To investigate the effect of high glucose and alternating normal/high glucose on telomere attrition.
3. To look at whether the loss of telomeres is mediated by mitochondrial ROS production.
4. To study the effect of high glucose on ROS production.
5. To study the effect of high glucose and alternating glucose on mtDNA content.
6. To investigate the effect of high glucose and alternating glucose on the expression of pro-inflammatory markers.
7. To setup a human endothelial cell line with depleted levels of mtDNA and mitochondrial protein and to measure the effect on pro-inflammatory markers eNOS and ICAM1.

2 Materials and methods

2.1 Materials and equipment

2.1.1 Cell culture

Table 2 shows the composition of human umbilical vein vascular endothelial cells (HUVEC) media, Table 3 shows the composition of vascular smooth muscle cell (VSMC) media and Table 4 shows the composition of Raji media.

Table 2: The composition of HUVEC (human umbilical vein vascular endothelial cells) media.

	Final Concentrations
Foetal calf serum (Invitrogen)	20%
Endothelial cell growth supplement. Bovine pituitary (Sigma-Aldrich)	15µg/ml
Hepes buffer (Sigma-Aldrich)	20mM
Penicillin/ Streptomycin mixture (Invitrogen)	100 units penicillin 100µg streptomycin
Heparin sodium IV flush solution (LRI pharmacy)	0.1IU/ml
Sodium pyruvate (Sigma-Aldrich)	0.2mM
Made up to volume using Medium 199 (Lonza)	

Table 3: The composition of VSMC (vascular smooth muscle cells) media.

	Final Concentrations
Foetal calf serum	10%
Hepes buffer	20mM
SM growth supplement (20X) (Invitrogen)	1%
Glutamine	2mM
Penicillin/ Streptomycin	100 units penicillin 100µg streptomycin
Made up to volume using RPMI 1640 (Lonza)	

Table 4: The composition of Raji media.

	Final Concentration
Foetal calf serum	10%
Glutamine	2mM
Made up to volume using RPMI 1640 (Lonza)	

PBS and 10X trypsin/EDTA (5g/l trypsin and 2g/l EDTA) were obtained from Lonza. Gelatin solution type B from Bovine skin (2%) used to coat the flasks for growing HUVECs was obtained from Sigma-Aldrich.

2.1.2 Immunofluorescence

10X TBS consisted of 165mM of tris (Fisher Scientific), 913mM of sodium chloride (Fisher Scientific), and 18mM of potassium chloride (Fisher Scientific). The TBS was adjusted to pH 7.4 with hydrochloric acid and autoclaved. Triton X-100 was obtained from Sigma-Aldrich, von Willebrand factor polyclonal antibody was obtained from Dako (mouse), and the FITC labelled secondary antibody (rabbit anti-mouse) was obtained from Sigma-Aldrich. The DAPI labelled VECTASHIELD mounting medium was purchased from Vector laboratories. The DAPI was provided at a concentration of 1.5µg/ml and has an excitation of 360nm and an emission of 460nm.

2.1.3 Measurement of glucose concentration

High glucose media were made by adding D-glucose (Fisher Scientific) at a concentration of 17.0mM to HUVEC media to yield a final concentration of 22mM. The glucose hexokinase kit was obtained from Sigma-Aldrich. The UV/Visible spectrophotometer that was used to take the measurements at 340nm was from Amersham Pharmacia Biotech, model no. 80-2097-62.

2.1.4 Assessment of telomere length and heterogeneity using Southern blotting and STELA

2.1.4.1 Plugs

Buffer L consisted of 0.1M EDTA (Fisher Scientific), 10mM tris, 20mM NaCl made up in ultra pure water. The cells in the plugs were lysed using proteinase K (Sigma-Aldrich) and sarkosyl (Fisher Scientific). The digestion enzymes Rsa1 and Hinf1 were purchased from New England Biolabs with 10X NEB2 buffer.

2.1.4.2 DNA extraction, quantification and digestion

The DNA was extracted using a DNA extraction kit was from Qiagen (QIAamp DNA blood mini kit). The Picogreen kit to determine DNA concentration was purchased from Invitrogen. The digestion enzymes Hinf1 and Rsa1 were purchased from New England Biolabs with 10X NEB2 buffer and 10X React 1. 1X TE buffer consisted of 10mM tris and 1mM EDTA (Fisher Scientific) made up to a final volume of 500ml using ultra pure water. The pH was adjusted to 8.0 using hydrochloric acid.

2.1.4.3 Ligation and PCR for STELA

The ligation step and the PCR step of STELA were performed using the primers listed in Table 5. These primers were obtained from Invitrogen – synthesised on a scale of 50nmol. In addition to this, the following reagents were used. T4 DNA ligase and 10X ligation buffer from GE Healthcare , PCR grade water from Sigma-Aldrich, Taq Polymerase from ABgene, magnesium chloride from ABgene, ABgene buffer from ABgene, dNTP's from Invitrogen, PWO polymerase from Roche Applied Sciences. PCR was performed using Hybaid PCRSprint, Hybaid Limited, UK.

Table 5: The primers used for PCR in STELA and their corresponding sequences.

Primer	Sequence
XpYpE2	5' TTGTCTCAGGGTCCTAGTG 3'
Telorette 2	5' TGCTCCGTGCATCTGGCATCTAACCCCT 3'
Teltail	5' TGCTCCGTGCATCTGGCATC 3'
XpYpB2A	5' TCTGAAAGTGGACCAATCAG 3'

2.1.4.4 DNA electrophoresis

Electrophoresis buffer (50 X TAE) consisted of 2M tris, 1M glacial acetic acid (Fisher Scientific), 50mM EDTA, pH 8.0. 50 X TAE was diluted 1 in 50 to obtain a working concentration for running the electrophoresis gels. The 'bluejuice' gel loading buffer was purchased from Invitrogen. The 1kb ladder was purchased from Invitrogen and was diluted 1 in 5 prior to use. The high molecular weight (HMW) markers were obtained from Invitrogen and were diluted in the following ratio: - 4 HMW marker: 2 bluejuice gel loading buffer (diluted previously by a 1 in 5 dilution): 14 ultra pure water. The gels were viewed under a UV transilluminator (Alphalmager 1220) from Alpha Innotech Corporation (Flowgen, England), model no. 95-0291-02.

2.1.4.5 Southern blotting

Depurinating solution consisted of 0.13M hydrochloric acid made up with distilled water. Denaturing solution/alkaline blotting buffer (ABB) consisted of 1.5M sodium chloride, 0.5M sodium hydroxide (Fisher Scientific). The blotting paper was obtained from Sigma-Aldrich and the nylon membrane used for Southern blotting was purchased from GE Healthcare .

2.1.4.6 Radioactive labelling of the membrane

The telomere adjacent probe was purified using the Takara Recochip from Takara. Prehybridisation buffer contained 500mM Na₂PHO₄ anhydrous (Fisher Scientific), 1mM EDTA, 242mM SDS, 150mM BSA (Sigma-Aldrich)

and the pH was adjusted to 7.2 with phosphoric acid. Radioactive labelling of the telomere DNA probe (AATCCC)₄ obtained from Invitrogen was performed using polynucleotide kinase (PNK) and 10X PNK buffer from Sigma-Aldrich and γ ³²P-ATP from GE Healthcare. Radioactive labelling of the 1kb ladder, the HMW marker and the telomere-adjacent probe were performed using ³²P-dCTP and the Rediprime kit both from GE Healthcare. The marker probe, telomere probe and telomere-adjacent probe were purified using the QIAquick Nucleotide Removal kit from Qiagen. SSC consisted of 0.3M tri-sodium citrate (Fisher Scientific), 9M NaCl. The pH was checked to ensure it was between 7 and 8. It was then autoclaved before use. 0.1% SDS was made up in distilled water. The Kodak X-omat autoradiography film used was purchased from Sigma-Aldrich.

2.1.5 Measuring ROS using the Amplex Red assay

Amplex Red, N-acetylcysteine (NAC), Thenoyltrifluoroacetone (TTFA), HBSS, HRP stock, menadione and cell lytic M buffer were purchased from Sigma-Aldrich. The fluorescence was measured using a CytoFluor Multiwell Plate Reader Series 4000 from PerSeptive Biosystems with excitation at 530nm and emission at 580. The protein concentration in each well was determined using the Bradford Reagent purchased from Biorad, UK. The change in absorbance was measured at 595nm using an ELx808IU Ultra Microplate Reader from Bio-Tex Instruments Inc.

2.1.6 Treatment of cells to deplete mitochondria

Ethidium bromide, pyruvate, uridine, chloramphenicol and ddC were all purchased from Sigma-Aldrich.

2.1.7 Real time PCR

Real time PCR was performed using the Brilliant SYBR green QPCR core reagent kit and MX4000 tube and cap strips from Stratagene. The real time

PCR was performed using the primers listed in Table 6. These primers were obtained from Invitrogen – synthesised on a scale of 50nmol.

Table 6: The primers used for mtDNA and nuclear DNA PCR and their corresponding sequences.

Primer	Sequence
Nuclear 36B4d (sense)	5'CCCATTCTATCATCAACGGGTACAA 3'
Nuclear 36B4u	5'CAGCAAGTGGGAAGGTGTAATCC 3'
Mt14620 (sense)	5'CCCCACAAACCCCATTAATAACCCA 3'
Mt 14841	5'TTTCATCATGCGGAGATGTTGGATGG 3'

Real time PCR was performed using the MX4000 spectrofluorometric thermal cycler (Stratagene, Amsterdam, Netherlands, UK). SYBR green fluorescence was determined using the FAM filter set (excitation wavelength 492nm, emission wavelength 516nm). To compensate for non-PCR related variations in fluorescence, the sample was also analysed for ROX at excitation of 585nm and emission of 610nm.

2.1.8 Protein extraction and quantification

Protein lysis buffer consisted of 5mM magnesium acetate (Sigma-Aldrich), 50mM potassium chloride, 50mM tris, pH 7.4 with HCl, 3mM EDTA, 3mM β -mercaptoethanol (Sigma-Aldrich) and 1X protease inhibitor cocktail (Roche-Applied Sciences).

2.1.9 Western blotting

The protein MW marker was purchased from Biorad, UK. Methanol and hydrochloric acid were purchased from Fisher. Marvel dried skimmed milk powder was purchased locally. Ponceau S, glycine, and Tween-20 were purchased from Sigma-Aldrich. TBS-tween was made using 1X TBS with 0.1% Tween-20. 10% blocking solution was made using 10% Marvel

powdered milk (purchased from the local supermarket) with 1X TBS-Tween. The hybond ECI and hyperfilm ECI were purchased from GE Healthcare. The ECI reagents – P-coumaric acid and luminal were from Sigma-Aldrich. All Western blotting apparatus was purchased from Biorad, UK.

The 10% resolving gel consisted of 0.37M tris-HCl pH8.8, 10% Acrylamide/Bis solution 29:1, 0.1% (w/v) SDS, 0.05% (w/v) APS, 0.05% (v/v) TEMED. The 15% resolving gel consisted of 0.37M tris-HCl pH8.8, 15% Acrylamide/Bis solution 29:1, 0.1% (w/v) SDS, 0.05% (w/v) APS, 0.05% (v/v) TEMED. The 4% stacking gel consisted of 0.12M tris-HCl pH6.8, 4% Acrylamide/Bis solution 29:1, 0.1% (w/v) SDS, 0.05% (w/v) APS, 0.05% (v/v) TEMED. 2X loading buffer was made up with 0.02M DTT, 0.05% bromophenol blue, 0.063M tris-HCl pH6.8, 2% SDS, and 10% (v/v) glycerol. 5X SDS PAGE electrophoresis buffer consisted of 125mM tris base, 960mM glycine and 17mM SDS. The transfer buffer consisted of 25mM tris-base, 192mM glycine and 10% (v/v) methanol.

The antibody to endothelial nitric oxide synthase (mouse) was purchased from BD biosciences, anti-ICAM1 and rabbit antimouse-HRP were purchased from ABCAM. The antibody to α -tubulin and goat antirabbit-HRP were purchased from Sigma-Aldrich. Antibodies to cytochrome c oxidase 1 (COXI) and cytochrome c oxidase IV (COXIV) were purchased from Invitrogen. The lyophilised powder was reconstituted by the addition of 200 μ l 2mM sodium azide solution (a final concentration of 500 μ g/ml).

The ECI solution consisted of 100 μ M tris-HCl pH8.5, 198 μ M p-Coumaric acid, 1.25mM luminol and 0.03% (v/v) H₂O₂ (all from Sigma-Aldrich). The stripping buffer consisted of 62.7mM tris base, 69.4mM SDS and 0.7% (v/v) β mercaptoethanol. The pH was adjusted to 6.8 with HCl.

2.2 Methods:

2.2.1 Cell Culture

2.2.1.1 Reviving frozen cells

A cryotube containing frozen cells was removed from the nitrogen store and placed into a small plastic box. The cells were warmed up slowly by firstly placing the cryotube in the palm of hands followed by a 37°C water bath. Once the cells were defrosted, they were immediately pipetted into a 15ml centrifuge tube containing 2ml of either HUVEC or VSMC media, already warmed to room temperature.

To remove any cells that were remaining in the cryotube, medium (1ml) was then added to the cryotube and this too was pipetted into the centrifuge tube. The cells were then centrifuged at 200g for 5 min. The supernatant was then discarded and the pellet was resuspended into 1ml of medium. This cell suspension was pipetted into a T75 flask containing 13ml of medium for VSMC and Raji. However, for HUVECs, the T75 flask was coated prior to the addition of any media with 1% gelatin (Sigma-Aldrich) for 10 minutes. The flask was then placed into a humidified 37°C incubator with 5% CO₂.

2.2.1.2 Sub-culture/passaging of cells

The T75 flask was removed from the 37°C, 5% CO₂ incubator and placed into a biosafety level 2 cabinet. The medium was aspirated off the flask and was placed into a waste bucket. The adhered cells were washed by aspirating a few ml's of PBS onto the side of the flask. The cell layer was washed by gently rotating the flask and then the PBS was removed. Warmed trypsin/EDTA (2ml) was pipetted onto the cell layer, at which point the flask was put back into the incubator for 5 minutes. Then, the flask was removed from the incubator, given a gentle but firm tap and placed under a 10X objective to visualise how many cells had detached from the base of the flask. If successful, 2ml of medium was added to the flask and the

resultant cell suspension transferred to a tube and centrifuged at 200g for 5 minutes. The supernatant was discarded and the pellet was resuspended into 3ml of medium. 1ml (1 in 3 split), 1.5ml (1 in 2 split) or 2ml (1 in 1.5 split) of this suspension was pipetted into a gelatin-coated T75 flask containing 13ml of medium (the split performed depended on how confluent the cells were before being trypsinised). The flask was then placed into a 37°C incubator with 5% CO₂.

2.2.1.3 Media changing of cells

Media was aspirated from the flasks and the adhered cells were washed by aspirating a few ml of PBS onto the side of the flask and then the cell layer was washed by gently rotating the flask and then this was removed. Freshly warmed medium (13ml) was added into the flask and the flask was then placed back into the incubator.

2.2.2 Phenotypic characterisation of HUVECs

Coverslips of about 25mm in diameter were immersed in 70% ethanol for a few minutes and were then removed and were left to dry in a Class II biosafety cabinet. Once they were dry, a single coverslip was placed into a well of a six-well plate. This was repeated for the other wells. For culture of HUVECs, the wells were coated with 1% gelatin - this was not performed for VSMC. At this stage, 2ml of medium (either HUVEC or VSMC medium) was added to each well followed by the addition of 7.5×10^4 cells. The plate was then incubated until the cells were approximately 80% confluent on all of the coverslips.

The medium was aspirated off and then each cell layer was washed twice with 1ml PBS. Methanol was added to each coverslip. The plate was incubated at -20°C for 10 minutes and the coverslips washed twice in TBS for 2 minutes. TBS/0.5% triton X-100 was added to each of the coverslips for 10 minutes at room temperature followed by rinsing twice in TBS/0.1%

triton (TBS/triton) for 5 minutes. Blocking was performed with 3% BSA in TBS/triton (BSA/TBS/triton) for 45 minutes at room temperature. The von Willebrand factor antibody was then added at a dilution of 1:33.3 in BSA/TBS/triton to the wells and incubated at 4°C overnight. The coverslips were washed three times in PBS/0.1% triton for 2 minutes. FITC conjugated antibody was added to each at a dilution of 1:200. The coverslips were incubated for 1 hour at 37°C in the dark in a humidified chamber followed by three washes in TBS/triton for 5 minutes and then twice in distilled water. Each coverslip was mounted on a slide using a fluorescent mountant containing DAPI and was sealed using clear nail varnish. Once dry, each slide was viewed under a fluorescent microscope using FITC and DAPI filters.

2.2.3 Measurement of glucose concentration in media

2.2.3.1 Cell and media preparation

HUVECs were seeded into 2 wells of eight, six-well plates at approximately 50% confluency. The plates were placed in the incubator overnight. The next day (day 0), two of the plates were removed from the incubator, the cells were trypsinised from the wells and a cell count was performed. Once the cell count was performed, three of the other plates were removed and the medium was aspirated off the two wells and replaced with normal glucose medium. At this point, normal glucose medium was pipetted into two wells without cells – this was performed for all three plates. The remaining three plates were removed from the incubator and the medium on the cells was aspirated off the two wells and replaced with high glucose medium. At this point, high glucose medium was pipetted into two wells without cells – this was performed for all three plates. A 1ml sample of both the normal glucose and high glucose medium was put onto ice and the glucose concentration was tested using the hexokinase kit. All six plates were placed back into the incubator and at day 1, one of the plates with normal glucose and one of the plates with high glucose was removed. The

medium from the wells was put onto ice in preparation for the assay and a cell count was performed. This was repeated for days 2 and 3.

2.2.3.2 Hexokinase assay

Glucose concentrations were measured using the hexokinase method according to the kit instructions.

For the standard curve, four standard concentrations of glucose were made up from a stock solution of 1mg/ml: 100µg/ml, 200µg/ml, 300µg/ml and 400µg/ml (each was in a volume of 250µl).

For the medium aspirated off the cells at each timepoint the following procedure was performed. The medium that contained the low concentrations of glucose (5.5mM or less) was diluted 1 in 3 to obtain a concentration of glucose between 50µg and 5000µg/ml. The medium that contained the high concentrations of glucose (22mM or less) was diluted 1 in 15 to obtain a concentration of glucose between 50µg to 5000µg. For the assay, 1ml of the glucose assay reagent was pipetted into 12 eppendorfs, 1ml of deionised water was pipetted into another 12 eppendorfs, and 100µl of deionised water was added to another eppendorf. The assay was started by the addition of 1ml reagent blank to 100µl deionised water and the absorbance was measured at 340nm 15 minutes later. Each of the four standards and diluted samples (100µl) were then added to eppendorf tubes containing the deionised water and also to eppendorf tubes containing the glucose assay reagent – the absorbance was measured at 340nm 15 minutes after the addition.

2.2.4 Measuring telomere length and heterogeneity using Southern blotting

2.2.4.1 DNA extraction from cells

Cells were trypsinised off the surface of T75 flasks by the addition of trypsin/EDTA and were centrifuged in a 15ml centrifuge tube at 200g for 5 minutes. The supernatant was discarded and the pellet was resuspended in 2ml of medium for a T75 flask or 5ml of medium for a T175 flask. A cell count was performed by the use of a haemocytometer, and the required numbers of cells were pipetted into a 1.5ml eppendorf tube. Following centrifugation at 275g for 5 minutes, the supernatant was aspirated off and the pellet was resuspended in 200µl of PBS. At this point, 20µl of proteinase k was added followed by the addition of 200µl of buffer AL. The tube was then vortex mixed for 15 seconds and incubated at 56°C for 10 min. It was centrifuged and 200µl of ethanol was added. The sample was transferred to a QIAamp spin column placed in a 2ml collection tube. This was centrifuged at 11600g for 1 minute and the tube containing the filtrate was discarded. The spin column was placed into a clean collection tube and 500µl of buffer AW1 was added. It was centrifuged at 4400g for 1 minute, the filtrate was discarded and the column was placed into a clean collection tube. 500µl of buffer AW2 was added to the column, which was centrifuged at 11600g for 3 minutes and the column placed into a clean 1.5ml eppendorf tube. A volume of buffer AE was added (varied between 20 to 40µl depending on the initial cell count) and the column was incubated at room temperature for 5 minutes. Following centrifugation for 1 minute at 11600g the filtrate which contained the DNA was frozen at -80°C until it was required for analysis.

2.2.4.2 DNA quantification

Quantification was performed using the Picogreen kit. The lambda DNA stock solution of 2µg/µl was prepared by diluting 4µl of this solution in 196µl of TE buffer. The stock solutions (containing 0, 4, 10, 20, 50 and 100ng

DNA per well) were then prepared from the diluted stock. Table 7 shows the dilutions performed on the lambda DNA provided within the kit.

Table 7: Preparation of DNA standards. Table shows the mass of DNA (ng) contained within each well of the 96 well plate, and the volume in μl of both the TE buffer and the lambda DNA diluted stock needed to achieve this concentration.

Mass of DNA in each well (ng)	Volume of lambda DNA from the diluted stock (μl)	Volume of TE buffer (μl)
0	0.0	150.0
4	3.0	147.0
10	7.5	142.5
20	15.0	135.0
50	37.5	112.5
100	75.0	75.0

In a 96 well, flat bottomed plate, 100 μl of each of the six standards were added to six wells. All of the samples were then diluted by performing a 1 in 50 dilution in TE buffer – this was performed in eppendorf tubes. A volume of 90 μl of TE buffer was added to a 96-well plate followed by the addition of 10 μl of each diluted sample. A stock solution of Picogreen reagent was made up by performing a 1 in 200 dilution (in TE) and then 100 μl of this was added to each of the individual wells (total volume in each well was 200 μl). The plate was covered in foil to minimise exposure to light and the fluorescence was measured immediately at 485nm excitation and 530nm emission using a Cytofluor plate reader.

2.2.4.3 Plug formation

Cells were trypsinised from the surface of T75 flasks by the addition of trypsin/EDTA to the flask and then centrifuged in a 15ml centrifuge tube at 200g for 5 minutes. The required numbers of cells were pipetted into clean eppendorfs and then centrifuged at 275g for 5 minutes. The supernatant was removed, the eppendorf was placed in a 56°C water bath and then an

equal volume of buffer L and 1.2% low melting agarose solution was pipetted into the eppendorf (the total volume determined the length of the agarose plug). The volume within this tube was aspirated up using the setup shown in Figure 13. The P1000 pipette was then removed from the tubing, which was left on ice for 30 minutes for the agarose to set.

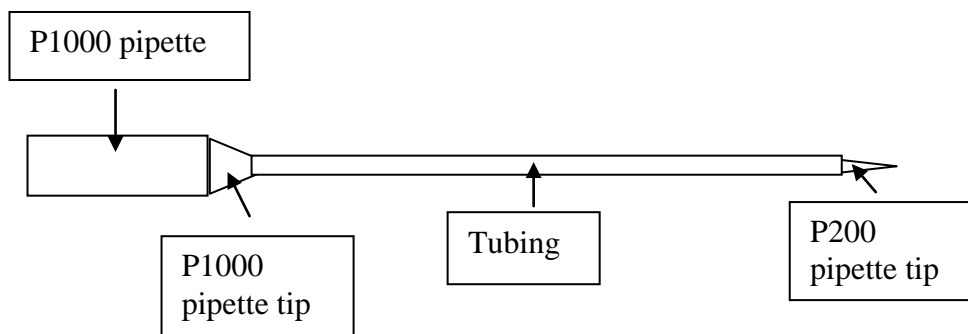


Figure 13: The setup of tubing which was used to construct the plugs.

Once the agarose had set, the plug was squeezed out of the tubing using a P1000 pipette into an eppendorf containing a solution of TE buffer with 1% sarkosyl and 1mg/ml of proteinase K. The plugs were incubated for a minimum of 16 hours (maximum 70 hours) at 50°C. The plugs were then placed on ice for 5 minutes and then washed for 30 minutes with gentle agitation in each of the following buffers: TE for 30 minutes, TE with 1mM phenylmethanesulphonylfluoride (PMSF) for 30 minutes, followed by two 30 minute washes in TE. Plugs were stored in TE buffer at 4°C until further use.

2.2.4.4 Digestion of plugs or extracted DNA

Plugs

The plugs were cut into 1cm lengths and each was incubated with TE buffer containing 1X nuclear extraction buffer 2 (NEB2) containing 4-8µl of digestive enzymes for 20 hours at 37°C.

DNA extract

The DNA extracted using the QIAGEN DNA extraction kit was digested by the addition of 1X NEB2 or 1X React 1 and 4-8µl of digestive enzyme. This was incubated for 20 hours at 37°C.

2.2.4.5 Gel Electrophoresis

A 0.5% agarose solution was made up by the addition of 1.5g of agarose to 300ml of TAE buffer which was heated until boiling. The molten agarose was then cooled to ~60°C, and then 5µl of 10mg/ml ethidium bromide was added. The agarose was poured onto a plate with the comb already in position and left to set for approximately 15 minutes.

If plugs were being run on the gel, they were taken out of the 37°C water bath and placed on ice for 10 minutes. The solution was aspirated off and 500µl TAE was pipetted into the tubes – these were left for 30 minutes at room temperature. The plugs were then put into the wells of the gel before the plate was placed in the electrophoresis tank.

If DNA extract was being run on the gel, the gel was placed in the electrophoresis tank containing 2.5 litres of 1X TAE with 50µl of 10mg/ml ethidium bromide solution. 4µl of bluejuice gel loading buffer was added to each of the samples and then the solutions were pipetted into the wells of the gel.

For the markers, 22.5µl of marker was then loaded into one well of the gel. This was performed when the plate was in the electrophoresis tank and the wells were submerged in TAE buffer. Electrophoresis was carried out at 40V for approximately 16 hours. The gels were viewed under a UV transilluminator.

2.2.4.6 Southern blotting

The gel was placed in depurinating solution for exactly 10 minutes, and then in alkaline blotting buffer (ABB) for 15 minutes. This was replaced with fresh ABB and the gel was incubated for a further 20 minutes. During this time, the nylon membrane and the filter paper were cut to the appropriate size. These were then placed into distilled water for 5 minutes followed by ABB for 5 minutes. The Southern blot was then set up as shown in Figure 14.

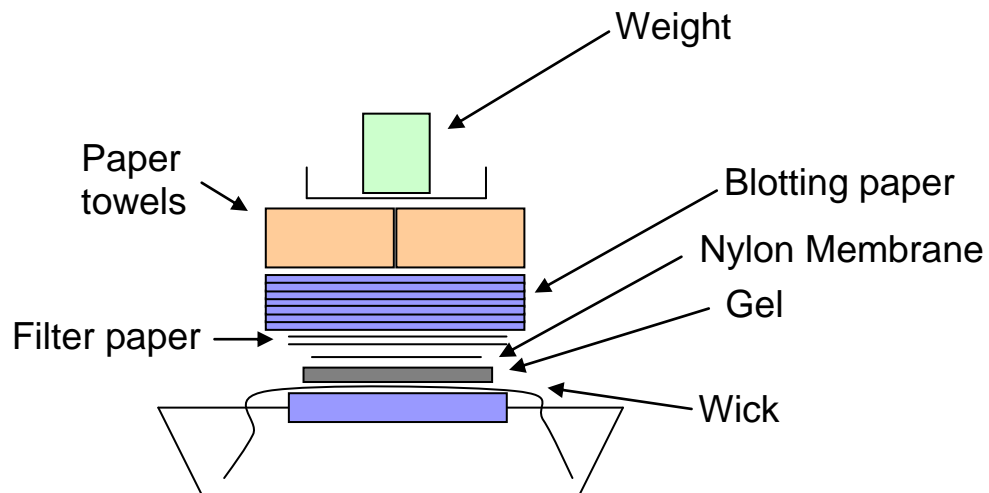


Figure 14: The setup of Southern blots showing the position of the gel and the nylon membrane.

This blot was left between 16 to 50 hours until the all the DNA from the gel had been transferred and ensuring during this time the liquid in the tray did not completely evaporate. The Southern blot was disassembled and the gel was put into 1 litre of distilled water with 30 μ l of ethidium bromide, left for 30 minutes then viewed under a UV transilluminator to ensure that the entire DNA had been transferred. The nylon membrane was baked at 80°C for 4

hours. It was then wrapped in clingfilm and placed at 4°C until development.

2.2.5 Measuring telomere length and telomere length heterogeneity using STELA

2.2.5.1 DNA preparation

DNA was extracted from HUVECs, and then quantified as described in 2.2.4.1 and 2.2.4.2. If the concentration was above 20ng/μl it was suitable for use in STELA. The DNA (volume between 15μl and 40μl) was digested in 1X NEB2 and 8μl of Hinf1 at 37°C for 16 hours.

2.2.5.2 Reconstitution of the primers for PCR

Primers were synthesised on a scale of 50nmoles. Each primer was reconstituted with 70μl of TE buffer under a class II biosafety cabinet. For quantitation, 5μl of reconstituted primer was diluted in 995μl of 10mM tris, pH 7.5. This 1ml was pipetted into a cuvette and the absorbance was measured at 260nm (the spectrophotometer was zeroed with 1ml 10mM tris, pH 7.5).

2.2.5.3 Ligation of teltail onto the end of DNA

After digestion, the DNA was diluted to 10ng/μl with PCR grade water. The ligation mixture was made up using 1μl of 10ng/μl of digested DNA, 0.9μl of 10μM telorette 2, 1μl of 10X ligation buffer, 0.5μl of T4 DNA ligase and 6.6μl of PCR water (final volume 10μl). The eppendorfs were then incubated at 35°C for 12 hours.

2.2.5.4 PCR

After 12 hours, the eppendorfs were placed on ice and the DNA was diluted to concentrations between 1ng/μl and 50pg/μl. The PCR reaction mixtures

were made up in a final volume of 10 μ l: 5.7 μ l of PCR water, 1 μ l of 10X ABgene buffer, 0.3 μ l of 0.3mM dNTP's, 0.8 μ l of 25mM magnesium chloride, 0.5 μ l of 10mM XpYpE2, 0.5 μ l of 10mM Teltail, 0.2 μ l of a 10:1 mix of taq polymerase and PWO polymerase and 1 μ l of DNA. PCR was performed in a thermal cycler for 25 to 29 cycles of: 94.0 $^{\circ}$ C for 20 seconds, 65 $^{\circ}$ C for 30 seconds, and 68 $^{\circ}$ C for 10 minutes. Once the PCR had finished, 4 μ l of bluejuice gel loading buffer was added to each of the 10 μ l samples. They were then loaded onto a gel. The gel was electrophoresed and Southern blotted as described in 2.2.4.5 and 2.2.4.6.

2.2.6 Radioactively labelling the membrane

2.2.6.1 Preparing the membrane

The membrane was wrapped in mesh and then placed in a hybridisation bottle containing 10ml prehybridisation buffer. It was then placed onto a rotator in the hybridisation oven at 50 $^{\circ}$ C for approximately 3 hours ensuring that as the bottle rotated, the nylon membrane unwound in the bottle.

2.2.6.2 Labelling the telomere probe

To radioactively label the telomere DNA probe (AATCCC)₄ 35.2 μ l of ultrapure water, 5 μ l of 10X PNK buffer, 2 μ l of 5 μ M (TTAGGG)₄, 2 μ l PNK and 5 μ l of γ ³²P-ATP were added into a screw cap eppendorf. This was incubated at 37 $^{\circ}$ C for 30 min, then at 80 $^{\circ}$ C for 10 minutes followed by pulse centrifugation.

2.2.6.3 Labelling the marker probe

In a 1.5ml eppendorf, 2 μ l of 1kb ladder stock was added to 998 μ l of ultra pure TE. This was mixed well and 2.5 μ l of this solution was added to 32.5 μ l TE in a screw cap eppendorf tube. In another eppendorf, 2 μ l of HMW stock was added to 38 μ l of TE. This was mixed thoroughly and 10 μ l of this was added to the 1kb markers (final volume of 45 μ l for labelling). The tube was

then heated at 100°C for 5 minutes, and then placed on ice for 5 minutes. The tube was spin-pulsed. The denatured probe was transferred to a Rediprime tube without mixing. Five µl of labelled ³²P-dCTP were added to the tube and the contents mixed well by pipetting up and down at least 20 times. It was incubated for 10 min at 37°C, spin-pulsed and then 2µl of 0.5M EDTA was added to stop the reaction.

2.2.6.4 Labelling the telomere adjacent probe

Synthesis of the telomere adjacent probe

DNA from HUVECs was extracted and then quantified as described in sections 2.2.4.1 and 2.2.4.2. If the concentration of the DNA was above 30ng/µl, then it was used for the synthesis of the probe. To 20µl of DNA solution, 3µl of NEB2 was added followed by 7µl of Hinf1. This was incubated at 37°C for 16 hours. Once the DNA was digested, 2x10µl were put into two clean 1.5ml eppendorf tubes. The DNA was then diluted to 20ng/µl. The following solution was then made up – 3µl of ABgene buffer, 2.4µl of MgCl₂ (when using 2.0mM) or 3.6µl of MgCl₂ (when using 3.0mM), 0.9µl of dNTP's, 1.5µl of XpYpE2, 1.5µl of XpYpB2A, and 1.2µl of a 10:1 mixture of Taq polymerase and PWO polymerase (for details see Materials Section). To this solution, the diluted DNA was added to give a final concentration between 1.0ng/µl to 4.0ng/µl. To each reaction mixture, PCR water was added to give a final volume of 30µl. The eppendorf tube was then placed in the thermal cycler and the PCR setup for 94°C for 20 seconds, 65°C for 30 seconds and 68°C for 10 minutes for 25 to 33 cycles.

Purification of the amplified telomere adjacent probe

The amplified PCR reaction product was electrophoresed on a 1.25% agarose gel. To the PCR sample (30µl), 4µl of bluejuice gel loading buffer was added and then 34µl was loaded into a single well of the gel. 10µl of 1kb ladder were added to each of the required wells. Electrophoresis was carried out at 100V for 2 hours and the gel was viewed under a UV

transilluminator. The 400bp band was removed from the gel by the use of a Takara Recochip. The Takara Recochip was firstly dipped into electrophoresis buffer to fill up the recovery space (space between the black surface and the cellulose membrane). It was placed into the gel just below the DNA band (on the positive side) ensuring that the black surface faced toward the DNA band and the white surface faced towards the anode side. The gel was then placed back into the electrophoresis chamber and electrophoresis was performed again for 8 minutes. After 8 minutes, electrophoresis was stopped and the Recochip was taken out of the gel and placed into a 2.0ml tube and centrifuged at 5000rpm for 5 seconds. The DNA in the tube was quantified by running the sample on a 1.25% mini agarose gel. The gel was prepared and the DNA was loaded into the lanes. In addition, 10 μ l of hyperladder I was loaded in an adjacent well. The gel was run for 2 hours at 100V and the 400bp band was quantified using the Alphasizer software.

Sequencing of the telomere adjacent probe

The DNA was diluted to a concentration between 25 to 40ng. 8 μ l and 9 μ l was then pipetted into a separate eppendorf. The XpYpE2 primer was diluted to a concentration between 0.8-1.0 μ M and 10 μ l was pipetted into a separate eppendorf. Sequencing was performed by the Protein and Nucleic acid Laboratory, Department of Biochemistry using the chain termination technique. The sequencing data were analysed using FinchTV.

Radioactive labelling of the telomere adjacent probe

DNA (20ng) was suspended in 45 μ l of TE buffer. The tube was then heated at 100 $^{\circ}$ C for 5 min and then placed on ice for 5 minutes. The tube was spin-pulsed. The denatured probe was transferred to a Rediprime tube without mixing. Five μ l of labelled 32 P-dCTP were added to the tube and this was mixed well by pipetting up and down at least 20 times. It was incubated for 10 minutes at 37 $^{\circ}$ C, spin-pulsed and then 2 μ l of 0.5M EDTA was added to

stop the reaction. The labelled DNA was then denatured by heating to 95-100°C for 5 minutes and then snap cooling on ice for 5 minutes.

Purification of the probe

The telomere probe, telomere-adjacent probe and the marker probe were all purified using the Qiagen Qiaquick Nucleotide Removal kit (Qiagen). To each tube, 10 volumes of buffer PN (promotes the adsorption of oligonucleotides to the membrane) were added followed by transfer to individual spin columns. The columns (in their collection tubes) were centrifuged for 1 minute at 2500g and the wash through was discarded. The column was transferred to a new collection tube and 500µl of buffer PE was added. It was centrifuged at 2500g for 1 minute and the flow-through was discarded. The tube was then centrifuged again for 1 minute at 11600g. Elution buffer (200µl) was then added to the tubes, followed by centrifugation at 11600g for 1 minute.

2.2.6.5 Hybridisation of the membrane

When the telomere probe was used, 8µl of the marker probe was added to 42µl of TE buffer. This was then added to the total 200µl volume of the telomere probe. When the telomere adjacent probe was used, 50µl of the diluted marker probe was added to 128µl of telomere-adjacent probe. This volume (either 250µl if using the telomere probe or 178µl if using the telomere adjacent probe) was added to the hybridisation solution and then added to the hybridisation bottle. This was put in the hybridisation oven at 50°C for approximately 14 hours.

The blot was then washed in 1X SSC, 0.1% SDS for about 5 minutes and then placed in a clean tray containing 1X SSC, 0.1% SDS and was washed for approximately 10 minutes with gentle agitation at room temperature (the amount of radioactivity on the blot, assessed by hand-held radiation monitor, determined the length and the number of washes). The blot was

wrapped in clingfilm and placed in a cassette. A film was placed on top of the blot in a darkroom and this was placed at -80°C and left for 6 to 20 hours depending on the strength of the radioactivity. The film was then developed in an automatic developer.

2.2.6.6 Analysis of the blots using Telometric software

The bands/smears on the film were analysed on the blot using Telometric software. A photo of the gel was taken using the Alphamager software and the image was opened in Telometric software. The image was then calibrated - the markers were clicked and the molecular weights were entered. The molecular weights were entered in descending order. When the lowest molecular weight was entered, the 'calibrate' button was pressed a second time. A box was then placed around one of the smears. The 'mark a lane' button was then pressed and the remaining boxes were placed around each of the smears. The 'remove background' button was then clicked and an area which had sufficient background was selected. The 'generate stats' button was then pressed to display the median telomere restriction fragment (TRF), and semi-interquartile range (SIR).

2.2.7 Measuring extracellular H_2O_2 concentration using Amplex Red

2.2.7.1 Performing the Amplex Red assay

Extracellular H_2O_2 production was measured over a number of timepoints and in the presence of various inhibitors, ROS producers and antioxidants. HUVECs were grown into wells of a 96 well plate always leaving 12-15 wells free for the standard curve. When the cells were approximately 80% confluent in the wells, the medium was removed and the wells were washed with PBS. At this point, treatment of the cells was performed. Treatment with D-glucose, L-glucose, 3-O-methylglucose or mannitol, required the addition of each to a final concentration of 16.5mM (this was in addition to 5mM glucose within the normal HUVEC medium) and 200 μl of this medium

was pipetted into the wells and the plate was incubated at 37°C 5% CO₂. When HUVECs were treated with menadione, NAC, or TFA these reagents were added to the wells at a concentration of 50µM, 3mM, and 25µM respectively. Each treatment was performed in triplicate. Approximately 15 minutes before treatment ended, the reaction mixture containing 50µM of Amplex Red and 0.1U/ml of horse radish peroxidase (HRP) was made up in the dark and heated to 37°C. When the treatments were completed, the medium was aspirated off the wells and 10µl of HBSS was added to each of the wells containing cells. For the standard curve the following H₂O₂ solutions were made up: 0µM, 4.5µM, 9.0µM and 13.5µM H₂O₂. 10µl of these solutions were added in triplicate to each of the wells (in total 12 wells). At this point, 50µl of the reaction mixture was added to each of the wells. The fluorescence in the plate was measured at a number of timepoints over 150 minutes at 530 excitation and 580 emission. Between measurements, the plate was placed back into the 37°C incubator in the dark. Following measurement of fluorescence, the amount of protein in each well was quantified.

2.2.7.2 Optimisation of the lysis of HUVECs in wells

Sonication

HUVECs were grown until 80% confluent into the wells of a 6 well plate, washed with PBS, trypsinised, centrifuged in Eppendorf tubes at 1000rpm for 5 minutes, and then the cells were resuspended into 40µl of lysis buffer. The cells were sonicated for 10 seconds, put on ice for 10 seconds and then sonicated for a further 10 seconds. Protein content was then measured using the Bradford assay (section 2.2.8.3).

Freeze-thaw

HUVECs were grown until 80% confluent into the wells of a six well plate. The cells were washed with PBS and then 150µl, 300µl or 450µl of lysis buffer were added to the wells. The plate was then frozen at -20°C for 12

hours then defrosted and the liquid was pipetted into 1.5ml eppendorfs. The protein content was then measured using the Bradford assay.

NP-40 buffer

HUVECs were grown until 80% confluent into the wells of a six well plate. The cells were washed with PBS and then 150µl or 300µl of NP-40 buffer was added to the wells. The plate was incubated for 30 minutes on ice and then the plate was gently tapped and the liquid was pipetted into 1.5ml eppendorfs. The protein content was then measured using the Bradford assay.

Cell lytic M buffer

HUVECs were grown until 80% confluent into the wells of a six well plate. The cells were washed with PBS and then 150µl or 300µl of Cell lytic M buffer was added to the wells. The plate was incubated for 30 minutes on ice and then the plate was gently tapped and the liquid was pipetted into 1.5ml eppendorfs. The protein content was then measured using the Bradford assay.

2.2.7.3 Bradford Assay

Bovine serum albumin (BSA, 0.01g) was dissolved in 10ml of UP H₂O. This solution was further diluted in 1.5ml eppendorfs. The dilutions used for the Bradford assay were between 0.0 to 0.5mg/ml (Table 8).

Table 8: Preparation of protein standards. The volumes of lysis buffer and 1mg/ml BSA required making final BSA concentrations between 0.0 to 0.5 mg/ml.

BSA concentration (mg/ml)	Volume of 1mg/ml BSA stock required (μl)	Volume of lysis buffer required (μl)
0.0	0	100
0.1	10	90
0.2	20	80
0.3	30	70
0.4	40	60
0.5	50	50

The eppendorfs tubes were vortex mixed for a few seconds and left on ice. Each sample was then diluted using a 1 in 25 dilution (2 μ l of sample and 48 μ l of lysis buffer). These were vortexed to mix. Following this, 10 μ l of each of the standards and the samples were pipetted into a well of a 96 well plate in duplicate. The protein assay dye reagent was made up by diluting the concentrate by the addition of 2ml protein assay dye reagent to 8ml of UP H₂O. An aliquot of this (200 μ l) was then pipetted into each of the standard and sample wells and this was incubated at room temperature for 10 minutes. The absorbance was measured at 595nm using a plate reader. A standard curve of the BSA concentration (mg/ml) versus the absorbance was constructed in Excel and the protein concentration of samples was determined via this standard curve.

2.2.8 Measurement of the expression of pro-inflammatory markers in HUVECs

2.2.8.1 Cell lysis and Western blotting

The cells were washed with PBS and resuspended into protein lysis extraction buffer (20 μ l for 10⁶ cells). The samples were sonicated for 10 seconds followed by 10 seconds on ice followed by a further 10 seconds of sonication. The lysed cells were then placed on ice for 60 minutes after which they were centrifuged for 10 minutes at 4°C at 13000rpm. The

supernatants were transferred to clean eppendorfs and the protein content was measured using the Bradford assay.

The mini-gel spacer and the short plates were assembled together in the casting frame and secured into the casting stand. For eNOS and ICAM1, a 10% resolving gel was set up. 7ml of this solution was pipetted between the short and the spacer plates and the gel was left to set at room temperature for 40 minutes. The stacking gel was then prepared, and once the resolving gel had set, the stacking gel was pipetted on the top. A toothed comb was slotted into the stacking gel and the gel was left to set for 40 minutes. Once the gel had set, the comb was removed, the cast was removed from the casting stand and the wells were washed with SDS-PAGE running buffer. The casts were placed in the electrophoresis tank and the tank was filled with electrophoresis buffer.

To denature the samples, loading buffer was added to the samples and the samples were heated at 95°C for 5 minutes. The samples were then placed immediately on ice for 10 minutes. A pre-stained marker was loaded into one of the wells followed by the samples. Electrophoresis was then carried out at 120V for 70 minutes during which time the transfer buffer was prepared.

At the end of the electrophoresis, the nitrocellulose membrane was placed into ultrapure water for 2 minutes, and then into transfer buffer for 5 minutes. The filter paper and the transfer sponges were also soaked in transfer buffer. The plates containing the gels were separated and stacking gel was removed from the resolving gel. The transfer cassette was then opened up and the filter paper, filter pad, the resolving gel, and the membrane were placed onto the black surface (shown in Figure 15).

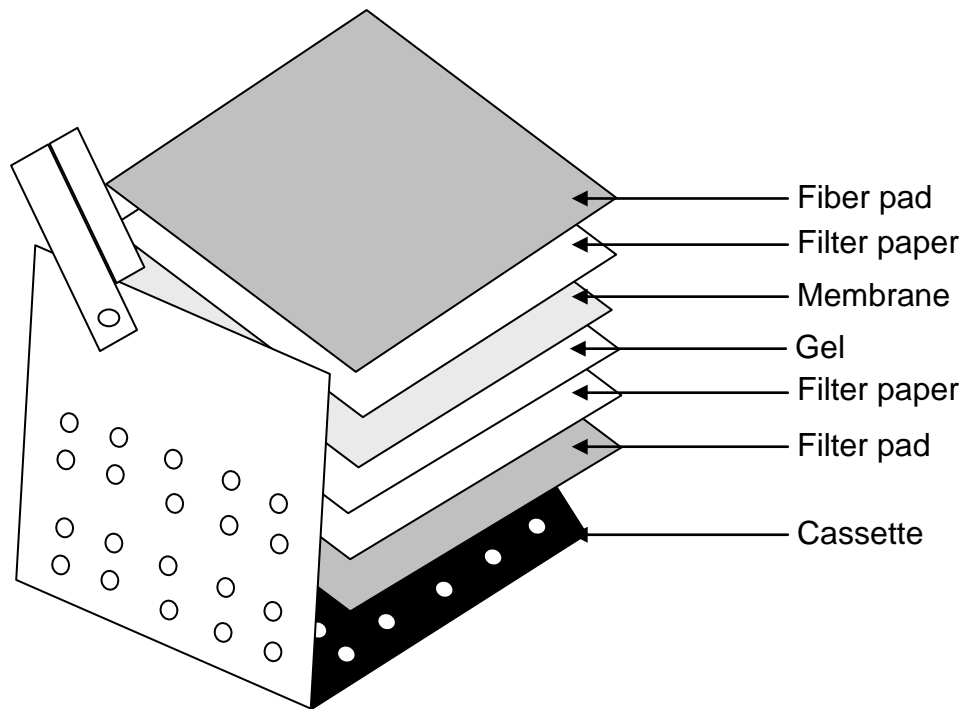


Figure 15: The layout of the transfer cassette. This shows the position of the gel in relation to the membrane, filter paper and filter pads.

The bubbles were rolled out using a 1ml stripette and then the cassette was gently closed. The cassette was placed into the clamp with the black surface facing the black side – this was repeated with the other cassette (the current runs from black to red therefore from gel to nitrocellulose membrane). Electrophoresis was then carried out at 64V for 1 hour.

After 1 hour the transfer tank was disassembled and the membranes were placed in ultrapure water on a rocking platform for 2 to 3 minutes. The water was discarded and Ponceau S Stain was poured onto the membranes for 5 minutes at room temperature. The membranes were washed twice with water to remove any excess stain and the bands of protein were visualised to ensure that correct transfer had occurred. 0.1M sodium hydroxide was then poured onto the blot for 30 seconds to remove the stain and was washed three times in water. The 10% blocking solution was then poured onto the membrane and left for 1 hour at room temperature. The membranes were washed in two fifteen minute washes with TBS tween.

Once washing had occurred, the membranes were probed with a primary and secondary HRP labelled antibody.

2.2.8.2 Stripping protocol

After the film had been developed, the membrane was washed four times for 5 minutes in TBS tween. The membranes were then incubated in 15ml stripping buffer for 30 minutes at 50°C on a rocking platform. The membrane was then washed six times for 5 minutes in TBS tween, blocked in 5% milk for 1 hour and then probed with the primary and secondary labelled antibody.

2.2.9 Depletion of mitochondrial DNA

2.2.9.1 Treatment with ethidium bromide (Rho0 HUVECs)

Creation and confirmation of Rho0 HUVECs

Rho0 HUVECs were generated by the addition of ethidium bromide to the stock media. A 10g/ml stock of ethidium bromide was filter sterilised and then diluted to 10µg/ml. A stock concentration of 5mg/ml of uridine and 5mg/ml of sodium pyruvate was also filter sterilised. These were added to HUVEC medium at a final concentration of 50ng/ml of ethidium bromide, 100µg/ml of sodium pyruvate and 50µg/ml of uridine. HUVECs were cultured in this medium for at least 7 days before experimental use.

mtDNA was determined via real time PCR. DNA was extracted using the Qiagen DNA blood mini kit from HUVECs prior to treatment and following treatment with ethidium bromide. It was quantified using the Picogreen kit (section 2.2.4.2). The DNA was stored at -80°C until real time PCR was performed.

Real time PCR was performed using the Stratagene Brilliant SYBR green QPCR reagent kit. All reactions were run in triplicate and no-template controls were always included.

A linear SYBR green standard curve was generated by performing a dilution series of 1, 1 in 5, 1 in 25, and a 1 in 125. The starting concentration of the reference DNA used to set up this standard curve was 10ng/μl for genomic and mtDNA real time PCR. The samples were diluted down to 1ng/μl in TE buffer when genomic DNA real time PCR was performed. When mtDNA real time PCR was performed the samples were diluted to 0.1ng/μl in TE buffer.

Mitochondrial and nuclear protein expression was determined by Western blotting. Protein from control HUVECs and Rho0 HUVECs was extracted and a Western blot was run (section 2.2.8). For the COXI western, a 10% resolving gel was prepared and for the COXIV western, a 15% resolving gel was prepared.

TEM of rho0 HUVECs

Control and Rho0 HUVECs were viewed under Transmission Electron Microscopy (TEM). They were trypsinised off 6 T175 flasks (3T175 control HUVECs and 3T175 Rho0 HUVECs), washed in PBS and then resuspended in PBS. TEM was then performed by the Department of Biochemistry.

2.2.9.2 Treatment of HUVECs with chloramphenicol

A stock solution of chloramphenicol (10mg/ml) was made up and filter sterilised. This was then added to cell culture medium at a concentration of 20μg/ml.

2.2.9.3 Treatment of HUVECs with ddC

A stock solution of 1mM ddC was made up and filter sterilised. This was then added to cell culture medium at final concentrations of 2, 5, 10 and 15 μ M.

2.2.9.4 Analysis of eNOS and ICAM1 protein expression in Rho0 HUVECs, chloramphenicol treated HUVECs and ddC treated HUVECs

Protein was extracted from control HUVECs and treated HUVECs and eNOS and ICAM1 protein was measured by Western blotting (section 2.2.8).

2.2.9.5 Statistical Analysis of the data

All statistical analysis was performed using GraphPad Prism 4. Points were fitted using either linear or non linear regression. Slopes were compared using an analysis of covariance (ANCOVA). When two groups of data were compared, a two-tailed unpaired t test was performed. When three or more groups of data were compared, a one-way ANOVA was performed.

3 The effect of high glucose on telomere length and ROS production in HUVECs

3.1 Introduction

3.1.1 Glucose in diabetes

Hyperglycaemia characterised by uncontrolled glucose regulation, is the main factor in the development of diabetes and the complications that occur as a result of the disease. Hyperglycaemia is thought to cause increased AGE production, activation of PKC, increased hexosamine pathway activity and increased polyol pathway flux. These pathways have a wide range of effects including increased ROS production, and modifications of proteins by AGE precursors leading to altered gene expression (Brownlee, 2001). Furthermore, hyperglycaemia leads to increased mitochondrial ROS production by increased glucose metabolism (Yu *et al.*, 2006). This is due to increased leakage of electrons from the ETC and increased production of NADH which leads to increased proton gradients and increased production of superoxide (Jay *et al.*, 2006).

3.1.2 Glucose uptake

There are four different transporter isoforms of GLUT which take up glucose – GLUT1 to GLUT4 (Olson and Pessin, 1996). GLUT1 is insulin independent and is present at high levels in human erythrocytes and in endothelial cells that line the brain and the vascular system (Brown, 2000). GLUT4 is the major insulin responsive transporter present in striated muscle and adipose tissue (Brown, 2000). GLUT1 to GLUT3 are localised on the cell membrane but GLUT4 is not localised on the cell membrane, instead it is present in small vesicles which are only translocated to the membrane when there is an increase in circulating insulin due to increases in circulating glucose (Watson and Pessin, 2000).

3.1.3 Telomeres

Telomeres are located at the ends of chromosomes and are composed of non coding units of DNA. They consist of a six base repeat – TTAGGG in humans. The main function of telomeres is to protect against the loss of vital genetic information (Saretzki and von Zglinicki, 2002). Shortening of telomeres in peripheral leukocytes occurs in a number of different cardiovascular diseases and is thought to occur due to increased oxidative stress (Fuster and Andres, 2006). A correlation has recently been noted between circulating leukocyte and vascular wall telomere length supporting the contention that leukocyte telomeres are a good surrogate marker for vascular wall telomere length (Wilson *et al.*, 2008). Furthermore, a paper published by Kurz *et al.*, (2004) showed a greater increase in heterogeneity in telomere length for endothelial cells that were treated with *tert*-butylhydroperoxide compared to the control cells.

3.1.4 Measurement of telomere length

Telomere length can be measured using a number of different techniques. Southern blotting and QPCR are often used to measure telomere length (Lin and Yan, 2005). A much newer method to measure telomere length is STELA (single telomere length analysis) which involves amplifying individual telomeres via the polymerase chain reaction (PCR) and then analysing the amplified telomeres by electrophoresis, and Southern blotting (Baird, 2005).

Southern blotting otherwise known as telomere restriction fragment (TRF) analysis is still the most common method to determine telomere length because it involves using standard molecular biology techniques. It does however have a number of drawbacks. The first disadvantage is that it requires microgram amounts of DNA. Secondly, the telomere restriction fragments in human DNA contain a number of other sequences such as the subtelomeric sequence and telomere repeat variants. These vary significantly in length between each TRF resulting in a distorted length and

false measurements of TRF. Furthermore, because the probe used to label the blot is a telomere repeat, it means that less of the probe will bind to shorter sequences and therefore there is a threshold below which the probe will not detect (Baird, 2005).

STELA (single telomere length analysis) is another technique for measuring telomere length and heterogeneity but on a single chromosome. It involves amplifying single telomeric sequences using a PCR based technique and then analysing them using Southern blotting and radioactive labelling. The PCR technique uses a telorette that is ligated onto the end of the telomeric sequence. The telorette (1 in Figure 16) consists of two major sequences – one of which is complementary to the end of the telomere and to the opposite G-rich sequence and the other which is non complementary to the G-strand overhang but is complementary to a primer called the teltail primer (2 in Figure 16). There are six different telorettes corresponding to the six different bases of the telomere repeat TTAGGG that can be used - for example one telorette may begin with TTAGGG and another telorette may begin with TAGGGT and so forth. One of the telorettes is ligated onto the sequence, and then PCR is performed using a chromosome specific primer (3 in Figure 16) and a teltail primer (Baird *et al.*, 2003; Baird and Kipling, 2004; Cheung *et al.*, 2004). The amplified DNA is then analysed by gel electrophoresis, Southern blotting followed by radioactive labelling of the blot (as explained in the methods section 2.2.5 and 2.2.6).

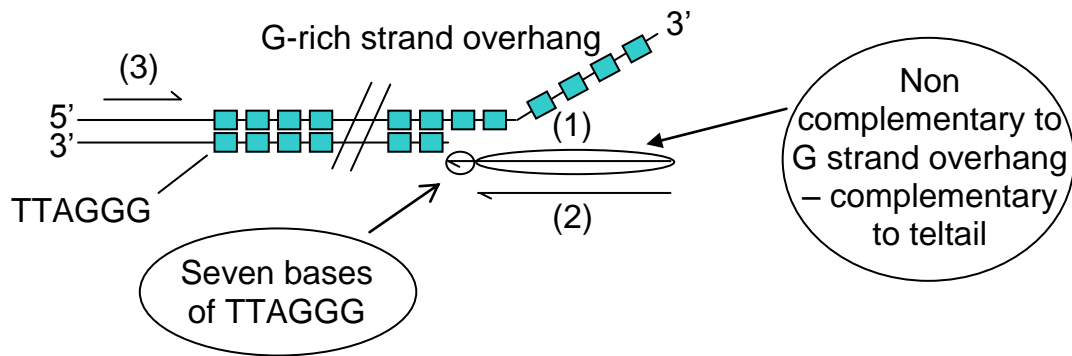


Figure 16: Shows how STELA works. A telorette is ligated on to the end of the C-rich strand and then the DNA is amplified via PCR using a telotail primer and a chromosome-specific primer. (1) = telorette; (2) = telotail primer; (3) = chromosome specific primer. (Adapted from Baird et al., 2003).

The finished blot has approximately 8 to 10 bands - each band represents a single telomere length however the intensity of the band reflects the number of telomeres at this length – i.e. if the intensity of a band is twice as strong then in theory this means that there are double the number of telomeres with that telomere length (Baird et al., 2003; Baird and Kipling., 2004; Cheung *et al.*, 2004).

3.1.5 Measurement of ROS

The increased production of ROS can have dire consequences on cells and their DNA. Increased ROS is associated with a number of cardiovascular diseases (Molavi and Mehta, 2004; Griending and FitzGerald, 2003). Therefore, monitoring ROS production is essential to be able to find circumstances where ROS is increased. The main methods to monitor ROS are through chemiluminescence assays, fluorescence-based assays, enzymatic assays and electron-spin resonance (Munzel *et al.*, 2007).

Chemiluminescence is often used to detect superoxide in vascular tissue (Skatchkov *et al.*, 1999). One of the most widely used compounds is lucigenin (Gyllenhammar, 1987; Ohara *et al.*, 1993; Rajagopalan *et al.*, 1996). This compound is extremely sensitive and detects superoxide when

other methods fail to do so (Skatchkov *et al.*, 1999). However recently, there have been a number of reports on how this method may over-estimate superoxide production due to a phenomenon known as redox cycling (Liochev and Fridovich, 1997).

Other methods to detect ROS include fluorescence-based assays (Maeda, 2008). A major fluorescence compound often used is dihydroethidine (DHE). This measures superoxide by reacting with superoxide to form ethidium which then intercalates with DNA (Benov *et al.*, 1998; Miller *et al.*, 1998). This fluorescence is observed using an emission wavelength of 520nm and an excitation wavelength of 610nm (Munzel *et al.*, 2007). A second fluorescence based compound that is often used is dichlorofluoroscein (DCF). DCFH is oxidised to DCF which is fluorescent (Soh, 2006). However, DCF is not specific and measures a wide range of reactive oxygen species such as H₂O₂ and peroxynitrite (Wardman, 2007).

Additionally, a number of different enzymatic assays such as aconitase have been used to measure ROS (Anderson *et al.*, 2008; Vincent *et al.*, 2005). Aconitase catalyses the conversion of citrate to isocitrate and is inactivated by superoxide (Han *et al.*, 2005). Therefore, the activity of aconitase reflects the amount of superoxide present in cells (Munzel *et al.*, 2007).

3.2 Aims

The first aim of this chapter was to establish whether high and alternating glucose caused telomere shortening and increased telomere length heterogeneity in endothelial cell cultures over short term treatment. Furthermore, if glucose did shorten telomeres, the next aim was to analyse if glucose caused increased ROS and whether this was causing the decrease in telomere length.

3.3 Experimental Approach

3.3.1 vWF expression in HUVECs

HUVECs were grown on coverslips in three wells of a six well plate. VSMC were grown on coverslips in three wells of another six well plate. vWF expression was then assessed in both cell types by immunofluorescence which is detailed in section 2.2.2.

3.3.2 Uptake of glucose in HUVECs exposed to normal or high glucose

The uptake of glucose in HUVECs was measured over a period of 3 days when exposed to either normal or high glucose containing medium. The method is detailed in section 2.2.3.

3.3.3 Measurement of telomere length in HUVECs by Southern blotting following exposure to high and alternating glucose

HUVECs were cultured in normal, high or alternating high/normal glucose medium for a number of passages. Cells were trypsinised from the flasks at each passage, and suspended in agarose in the form of plugs. The plugs were then digested, and each plug was placed into a single well of an agarose gel. The gel was run overnight, and a Southern blot was set up. More detailed methodology is shown in section 2.2.4. Once the DNA was transferred to the membrane, the blot was radioactively labelled using the telomere probe (section 2.2.6).

3.3.4 Measurement of telomere length in HUVECs by STELA following exposure to high and alternating glucose

HUVECs were cultured in normal, high or alternating normal/high glucose medium for a number of passages. Cells were trypsinised from the flasks at each passage and the DNA was extracted. The DNA was stored at -80°C until the cell work was completed. The DNA in each sample was quantified

and STELA was performed on these samples. For each sample, five separate PCR reactions were setup using 400pg of DNA. STELA was performed as detailed in 2.2.5 and 2.2.6.

3.3.5 Measurement of telomere length in HUVECs by STELA following exposure to high or alternating glucose in the presence of NAC or TTFA

HUVECs were cultured in normal, high or alternating normal/high glucose with or without NAC and TTFA over 5 passages. Cells were removed at each passage and the DNA was extracted. The DNA was stored at -80°C until the cell work was completed. The DNA in each sample was quantified and STELA was performed on these samples. For each sample, five separate PCR reactions were set up using 400pg of DNA. STELA was performed as detailed in 2.2.5 and 2.2.6.

3.3.6 Measuring H₂O₂ in HUVECs exposed to normal, high or alternating normal and high glucose over various timepoints

HUVECs were cultured in 96 well plates and exposed to normal glucose medium, high glucose medium, normal glucose medium with 50µM menadione, normal or high glucose medium with 3mM NAC, normal or high glucose medium with 25µM TTFA and normal glucose medium with either 16.5mM 3-O-methylglucose or 16.5mM mannitol for 1 hour. The Amplex Red assay was then performed which is detailed in section 2.2.7.

Furthermore, HUVECs were cultured in either normal or high glucose medium over a period of 24 hours or with normal, high or alternating glucose medium for 10 days. The Amplex Red assay was then performed which is detailed in section 2.2.7.

3.4 Results

3.4.1 Characterisation of HUVECs

In order to be more certain that the cells used in the following experiments were indeed of an endothelial nature, HUVECs were stained by immunofluorescence using an antibody to von Willebrand Factor (vWF) and a FITC labelled secondary antibody. When HUVECs were stained with anti-vWF and viewed under a FITC filter, the cells displayed characteristic cytoplasmic granular staining (Figure 17). In order to visualise the percentage of cells stained within the population of endothelial cells, the nuclei were stained with DAPI. Enumeration of cells showed that over 90% stained positive for the vWF marker.

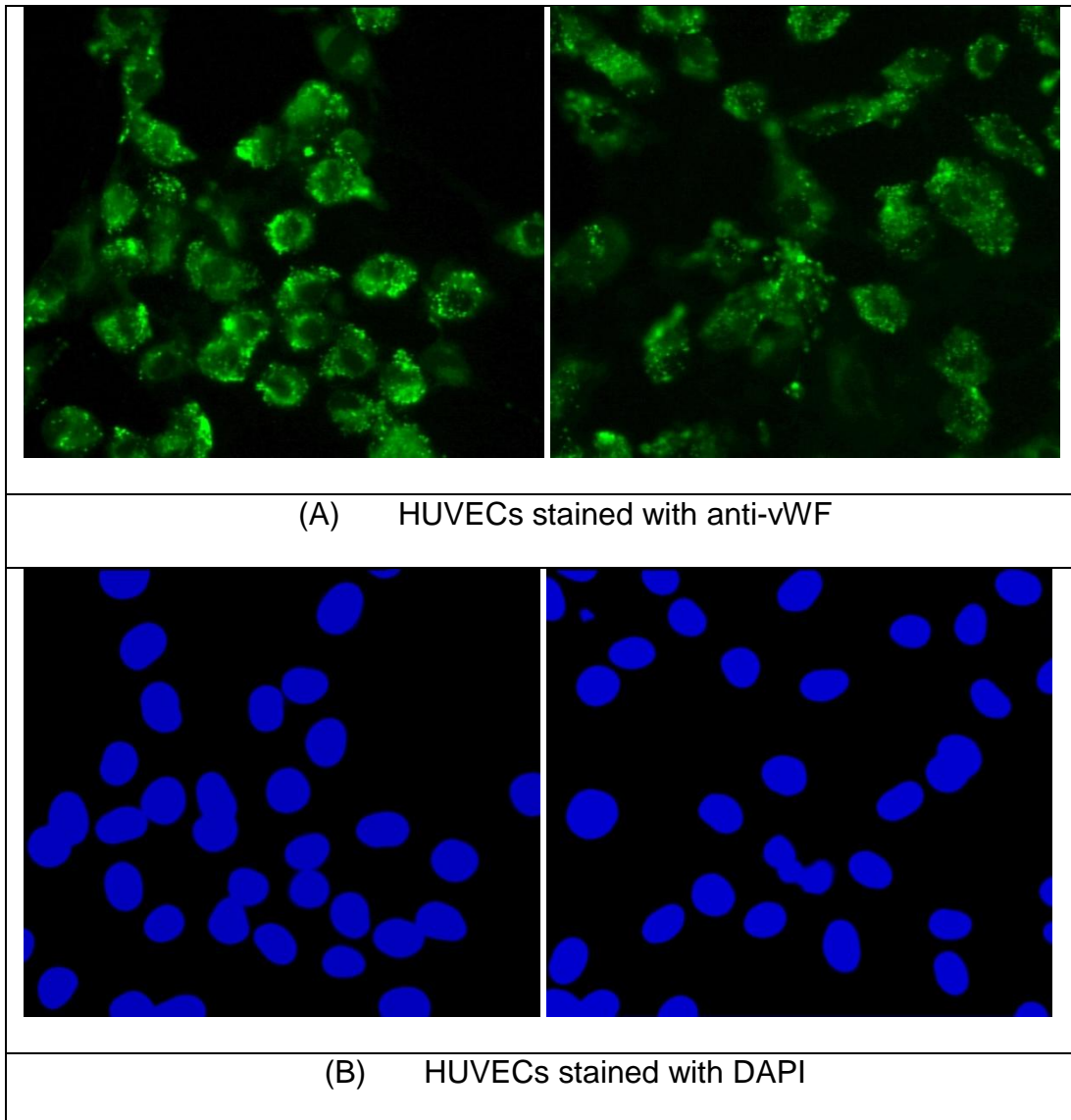


Figure 17: Characterisation of HUVECs with anti-vWF immunofluorescence. HUVECs were grown on coverslips until 80% confluent. The cells were fixed, permeabilised and blocked (as described in section 2.2.2). They were then incubated with a 1 in 200 dilution of anti-von Willebrand factor overnight and mounted using a DAPI mountant. They were sealed using clear nail varnish and viewed using FITC and DAPI filters.

As a control, VSMC were also stained with vWF. When these cells were stained with vWF no staining occurred.

3.4.2 Uptake of Glucose by HUVEC cultures

Determination of glucose uptake by HUVEC cultures was performed for two reasons. Firstly, glucose uptake was determined for experimental reasons. When longer term experiments were performed using alternating glucose it was essential to know by how much the glucose concentration in the media decreased and therefore whether it needed to be changed on a daily basis. Secondly, to determine whether glucose uptake was increased in cells exposed to higher concentrations of glucose. Uptake was determined by measuring the concentration of glucose in media following culture of HUVECs for one, two or three days. The concentration of glucose was determined using kits from Sigma. The GO assay kit from Sigma was first used but it was found that the results were not consistent. Therefore, an alternative, the hexokinase kit, was used.

As described in the method (section 2.2.3), HUVECs were cultured in wells of a flat bottom plate for 24, 48 or 72 hours in medium containing either normal glucose (NG) (5.5mM) or high glucose (HG) (22mM). As a control, NG and HG medium was placed into wells containing no cells for 24, 48 and 72 hours. Any glucose loss from the medium in the wells with cells was corrected with glucose loss from the medium in the wells without cells. This control confirmed glucose loss in the medium with HUVECs was due to glucose uptake and not general glucose loss from medium. The media was aspirated off the wells and was placed at 4°C until the amount of glucose was determined (maximum of one hour). The cells were trypsinised from the base of the wells and a cell count was performed using a haemocytometer.

Over a period of three days, the glucose concentration in NG medium without cells decreased by about 1.0mM, whereas when cells were present, the glucose concentration fell by approximately 2.5mM over three days. As with the NG medium, the concentration drop for medium containing HG without cells was approximately 0.5mM and the concentration drop for HG medium with cells over a three day period was approximately 3.5mM.

The overall decrease in glucose in the medium when cells were present was corrected by the drop in glucose when no cells were present. The difference in the glucose concentration each day was worked out and the amount of glucose in nmoles utilised per cell was calculated. This value was averaged and then worked out in pmoles/cell/day then in pmol/10⁶ cells/min.

It was calculated that the average drop in glucose concentration for NG medium was 13.9 pmoles/cell/day (96 pmol/10⁶cells/min) and the average drop in glucose concentration for high glucose medium was 27.7 pmoles/cell/day (192 pmol/10⁶cells/min) (Figure 18).

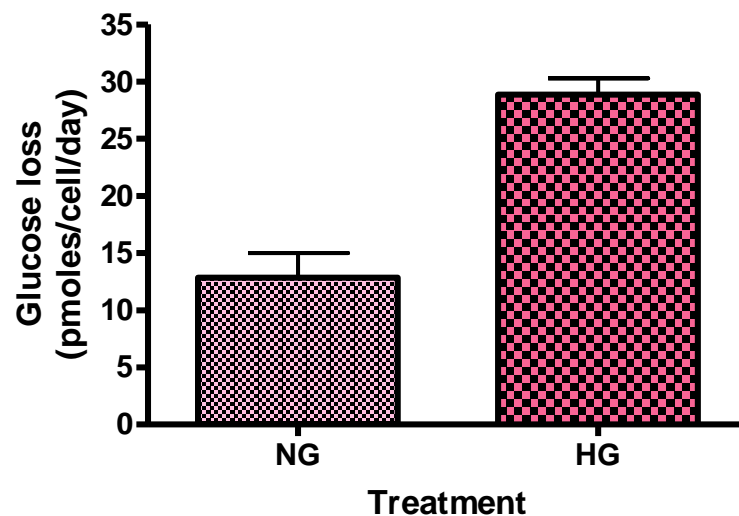


Figure 18: Glucose loss from medium containing NG (5.5mM) or HG (22mM). HUVECs were cultured in either NG medium or HG medium and glucose concentration in the medium was monitored over three days using the hexokinase assay. Values are expressed in pmoles/cell/day. Values are mean + SEM, n=2.

This value was calculated in terms of concentration decrease in a T75 flask over two days for a cell count that increased by ~1.5 X 10⁶ cells. The

reason this value was determined over a two day period was to ensure that the medium could be changed every two days (or 48 hours). When calculated for cells exposed to NG medium, glucose loss/utilisation worked out to be about 3.5mM and when calculated for cells exposed to HG medium, glucose loss/utilisation worked out to be about 7.2mM.

3.4.3 Effect of different glucose concentrations on the growth of HUVECs

The growth of HUVECs was also monitored following exposure to NG, HG or alternating normal/high glucose (AG). Cumulative population doublings of HUVECs, when exposed to the different treatments were determined via cell counts at each passage. As can be seen (Figure 19), the cumulative population doublings were very similar. The general trend however was for the growth rate to be highest in HUVECs exposed to NG medium and lowest in HUVECs exposed to AG medium. This change in growth rate was more apparent in cells at later passages.

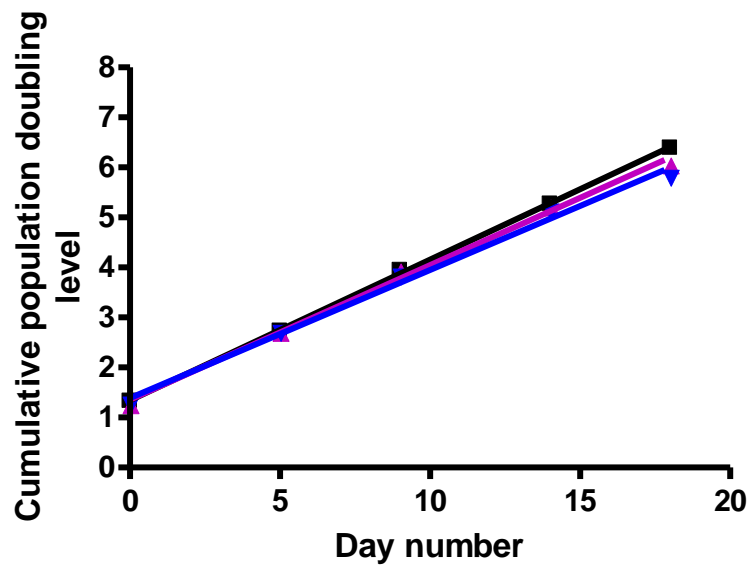


Figure 19: Growth curves for HUVECs exposed to different glucose concentrations. The cumulative population doubling levels of HUVECs when exposed to NG, HG or AG. (■) = NG; (▲) = HG; (▼) = Alternating normal/high glucose (AG). Values are mean of n=3.

3.4.4 Measuring telomere length

To analyse the effect of shorter term treatment (over 5 passages) on telomere length, telomere length was investigated over a few passages using two different techniques – STELA and Southern blotting.

3.4.4.1 Validation of Southern blotting

Before telomere length shortening was investigated using Southern blotting, the technique was optimised. An experiment was initially performed to analyse the number of cells to use in each 1cm long agarose plug. Three different amounts of cells were used – 0.5×10^6 , 1.0×10^6 , and 1.5×10^6 . It was found that the signal was proportional to the number of cells used. When 0.5×10^6 cells were used, the signal was very low, 1.0×10^6 cells provided a higher signal and 1.5×10^6 cells provided a very high signal (Figure 20).

Therefore, in future experiments, 1.0×10^6 cells were resuspended in each agarose plug.

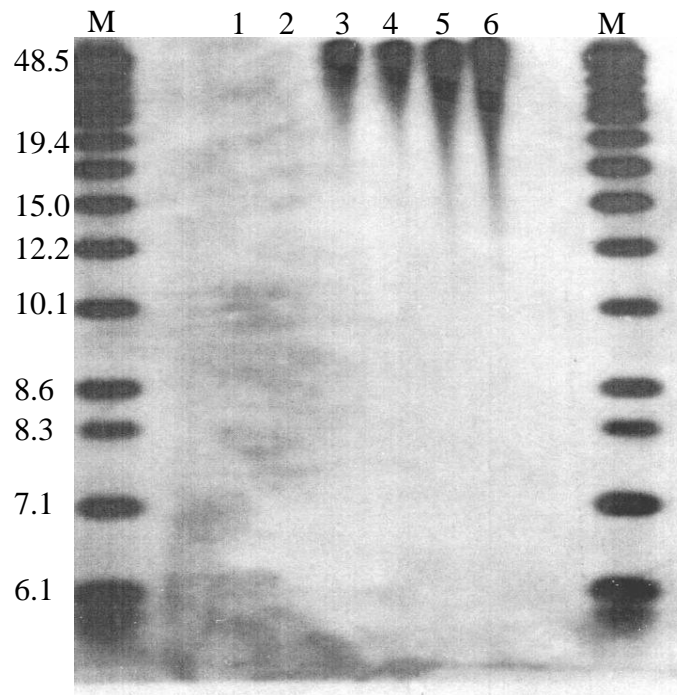


Figure 20: Effect of cell number on Southern blot signal. Radioactively labelled blot when 0.5×10^6 cells (lanes 1 and 2), 1.0×10^6 cells (lanes 3 and 4), and 1.5×10^6 cells (lanes 5 and 6) were suspended in a 1cm plug. Lanes 1, 3 and 5 from donor number 1 and lanes 2, 4 and 6 from donor number 2. The labels are shown in kb for marker (M).

Subsequently, the amount of DNA extracted from increasing numbers of cells was analysed. Four different numbers of cells were used – 0.25×10^6 , 0.5×10^6 , 0.75×10^6 and 1.0×10^6 cells. When using 0.5×10^6 cells, the amount of DNA extracted was $1.0 \mu\text{g}$, for 0.75×10^6 cells the amount of DNA was $1.4 \mu\text{g}$, and for 1.0×10^6 , the amount of DNA extracted was $1.8 \mu\text{g}$ (Figure 21). Therefore, it was decided that for future experiments, 1.0×10^6 cells would be used.

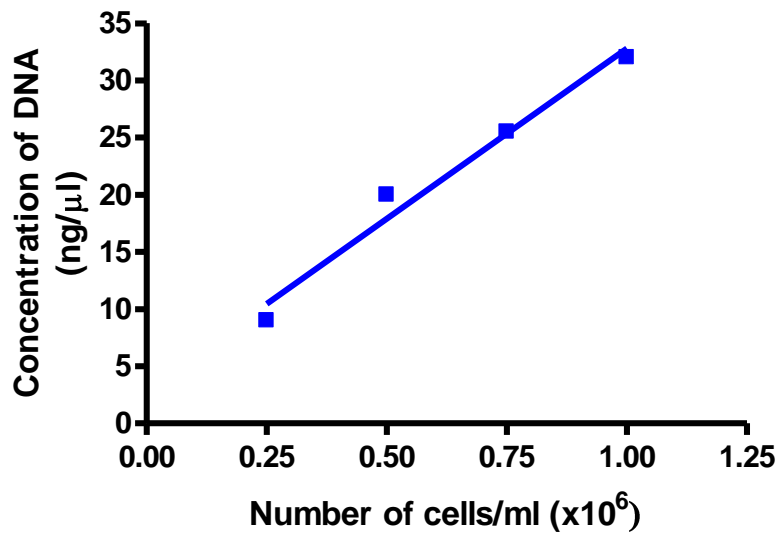


Figure 21: Yield of DNA from different cell numbers. As the number of cells increased, the concentration of DNA extracted from HUVECs extraction kit increased. Values shown are single values, n=1.

To compare two different methods of extracting DNA from HUVECs, a Southern blot was performed with 7 lanes of extracted DNA and 7 lanes of cells suspended into agarose plugs (Figure 22). Telomere lengths were longer when cells were encased into plugs (Figure 22).

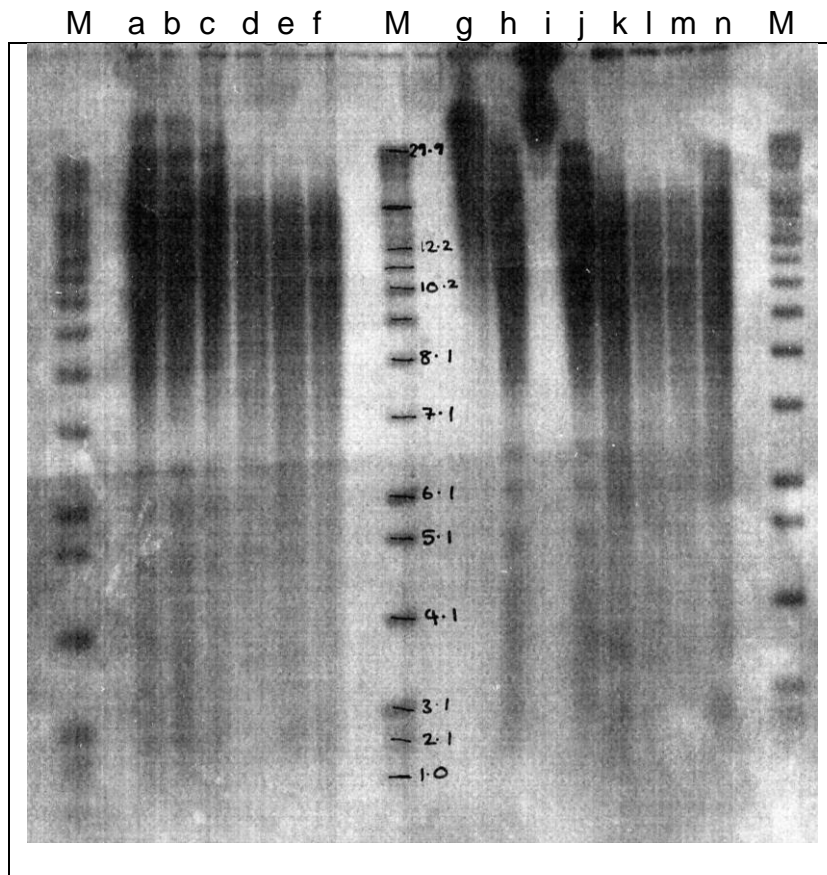


Figure 22: Southern blot comparing extracted DNA with suspension of cells in agarose plugs. DNA was digested using Hinf1 at 37°C for 16 hours. Lanes a to c and g to j show DNA of cells that were suspended in a tube of agarose and lanes d to f and k to n shows DNA that has been extracted using a DNA extraction kit. All cell samples are from the same donor. M = marker. The labels are shown in kb for marker.

The blot (Figure 22) was analysed using the Telometric software which provided data on median TRF and the semi-interquartile range (SIR) (section 2.2.6.6). The TRF is the telomeric fragment that results from the cleavage of DNA following digestion with the restriction enzyme (endonuclease) Hinf1. The median TRF is the middle TRF and SIR measures the spread of telomere fragments and is defined by one half of the difference between the 75th and the 25th percentile. As the DNA within the plugs was not completely digested in lanes g and i (Figure 22), these

two lanes were not included in the calculation of the mean of the median TRF lengths, and the mean SIR of the TRF lengths (Table 9).

The median and SIR values were all higher when using plugs. The range of the medians for the plugs was 16.06 to 17.10 whereas for the DNA extract the range of the medians was 12.94 to 14.09 (Table 9). The average SIR value for the plugs was 6.14, whereas the average SIR value for the DNA extract was 5.69. The SIR indicates the heterogeneity of TRF length and the larger the value is, the higher the heterogeneity. The coefficient of variation was determined for the median and SIR for both the plugs and the DNA extract and it was calculated that this value was always below 3% indicating a high degree of precision between the replicates. However, because longer TRF lengths were observed in HUVECs suspended into plugs, all future Southern blotting experiments used plugs.

Table 9: Comparison of telomere restriction fragments (TRF) values obtained from cell plugs or extracted DNA. The median telomere length and semi-interquartile range (SIR) for telomeric DNA from either plugs or extracted DNA were calculated. The samples were all from the same cell donor.

Lane	Plug or DNA extraction	Median	SIR
a	Plug	16.21	5.96
b	Plug	16.06	5.98
c	Plug	16.12	6.07
d	DNA extract	13.26	5.44
e	DNA extract	12.94	5.27
f	DNA extract	13.19	5.43
h	Plug	17.10	6.40
j	Plug	16.90	6.27
k	DNA extract	13.99	5.69
l	DNA extract	13.37	5.67
m	DNA extract	13.60	5.87
n	DNA extract	14.09	5.79

Different digestion enzymes were also compared. DNA was digested with Rsa1 or Hinf1 alone or both Rsa1 and Hinf1 for 16 hours at 37°C. DNA digested with Rsa1 alone showed lower mobility (higher molecular weight) than DNA digested with Hinf1 alone (Figure 23 and Table 10). Also, lanes o and p compared to lanes f and g showed very little difference in digestion when just one enzyme or a combination of enzymes were used. Therefore, Hinf1 alone was used to digest DNA in future experiments.

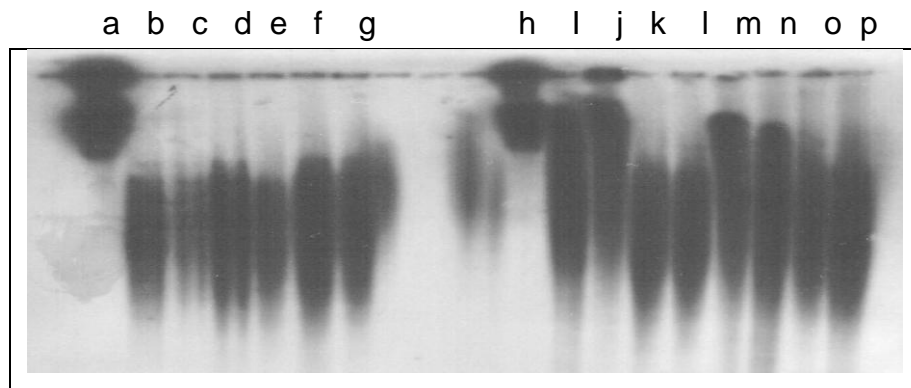


Figure 23: Comparison of different digestion protocols on TRF length by Southern analysis. HUVECs (same donor) were suspended in agarose plugs were digested under different conditions.

Table 10: Details the type and volume of digestive enzyme used and the type of buffer added to each lane letter (corresponds to Figure 23).

Lane number	Rsa1 added?	Hinf1 added?	React 1 or NEB2?
a	No	No	Neither
b	2µl initially	2µl initially	React 1
c	2µl initially	2µl initially	React 1
d	2µl initially 2µl 3 hours later	2µl initially 2µl 3 hours later	React 1
e	2µl initially 2µl 3 hours later	2µl initially 2µl 3 hours later	React 1
f	2µl initially 2µl 3 hours later	2µl initially 2µl 3 hours later	NEB2
g	2µl initially 2µl 3 hours later	2µl initially 2µl 3 hours later	NEB2
h	No	No	Neither
i	2µl initially 2µl 3 hours later	No	React 1
j	2µl initially 2µl 3 hours later	No	React 1
k	No	2µl initially 2µl 3 hours later	NEB2
l	No	2µl initially 2µl 3 hours later	NEB2
m	4µl initially 4µl 3 hours later	No	React 1
n	4µl initially 4µl 3 hours later	No	React 1
o	No	4µl initially 4µl 3 hours later	NEB2
p	No	4µl initially 4µl 3 hours later	NEB2

3.4.4.2 Effect of HG and AG on telomere length in HUVECs assessed using Southern blotting

Once Southern blotting was optimised, the effect of HG and AG on telomere length was investigated. Early passage HUVECs were treated either with NG medium (5.5mM), HG medium (22mM) or AG (5.5mM/22mM) medium. The medium was changed every 48 hours and nine individual T75 flasks containing HUVEC's were used for each treatment – six flasks for Southern blotting and three flasks for STELA (see section 3.4.4.5). Cells were trypsinsed at passage 0 (cells before treatment), passage 1 (cells after 4 days treatment), passage 2 (cells after 8 days of treatment), passage 3 (cells after 12 days of treatment), and passage 4 (cells after 16 days of treatment). A cell count was performed (this was later used to determine the population doublings) and the DNA from the cells was used for Southern blotting or stored for STELA once the DNA was extracted.

Figure 24 shows examples of two blots that were performed for the glucose experiment at passage 0 and at passage 4. The blot containing DNA from cells at passage 4 did not run straight during electrophoresis. This however, did not pose a major problem during analysis as the markers either side of the sections were used during analysis.

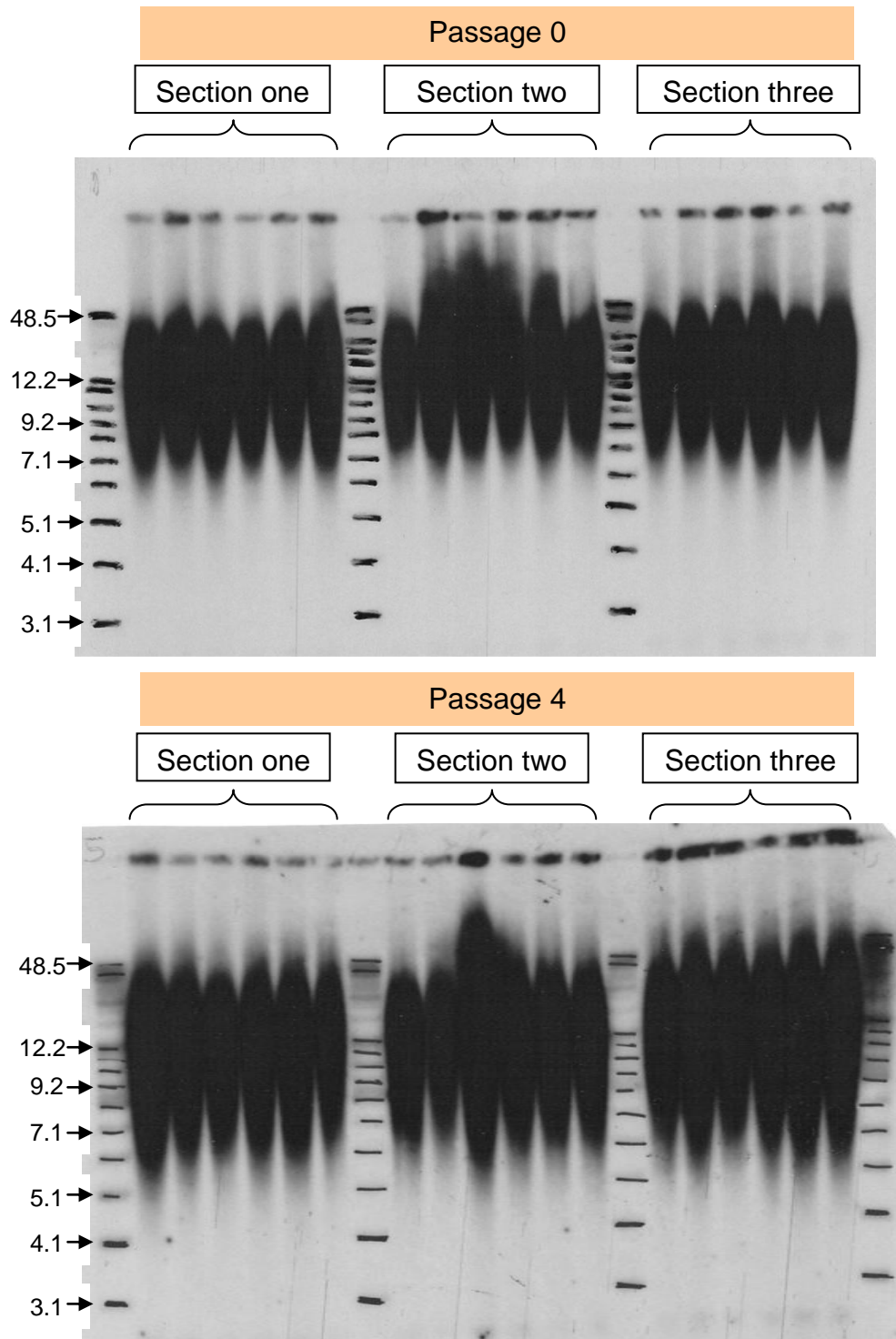


Figure 24: Examples of Southern blots performed for the glucose experiment showing telomeric DNA from cells at passage 0 and at passage 4. Section 1 shows DNA from cells that were treated with NG medium, section 2 shows DNA from cells that were treated with HG medium and section 3 shows DNA from cells that were treated with AG medium every 48 hours. The labels are shown in kb for marker.

Figure 25(A) and (B) show the mean (of the individual median TRFs) telomere lengths of DNA when HUVECs were exposed to the different treatments. When HUVECs were treated with medium containing NG, the mean telomere loss was 170 ± 47 bp/pd. Treatment with HG significantly increased the mean telomere loss to 1106 ± 75 bp/pd ($p<0.001$) (Figure 25). These values demonstrated that HG greatly accelerated telomere loss. AG also significantly increased ($p<0.001$) the mean telomere loss in HUVECs (859 ± 26 bp/pd) (Figure 25) compared with NG alone.

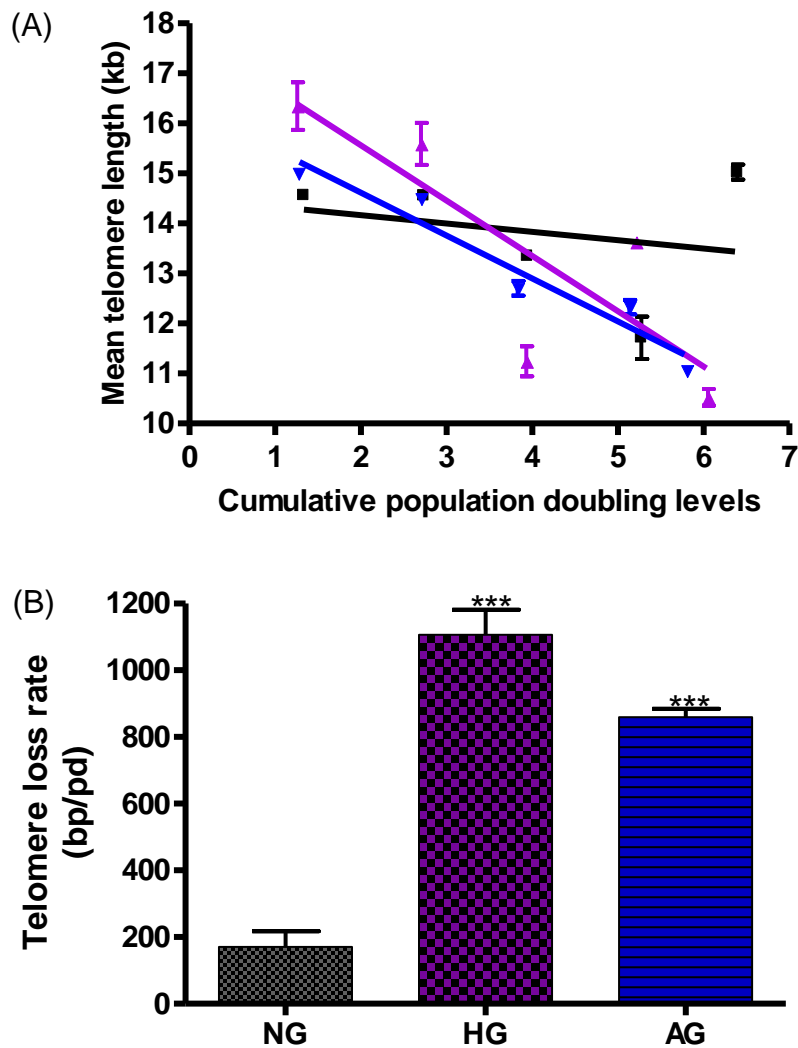


Figure 25: Effect of HG and AG on telomere attrition in HUVECs. (A) The mean (of medians) telomere length (kb) at different cumulative population doublings for HUVECs treated with NG (■), HG (▲) or AG (▼) every 48 hours. Telomere length was assessed using Southern blotting and the blots were analysed using Telometric software. The data were analysed using linear regression. Values are \pm SEM, n=6. (B) The mean telomere decrease per population doubling (pd) level for HUVECs treated with NG, HG or AG. ***P<0.01 vs NG. Values are \pm SEM, n=6.

The SIR decreased for HUVECs exposed to NG, HG and AG (Figure 26). HG significantly accelerated mean SIR decrease per population doubling (425 ± 32 bp/pd) compared with NG (132 ± 20 bp/pd; $p < 0.001$). AG significantly accelerated mean SIR decrease (438 ± 16 bp/pd) compared with NG ($p < 0.001$). The difference between the SIR decrease for HUVECs

cultured in HG medium or HUVECs cultured in AG medium was not statistically significant (Figure 26).

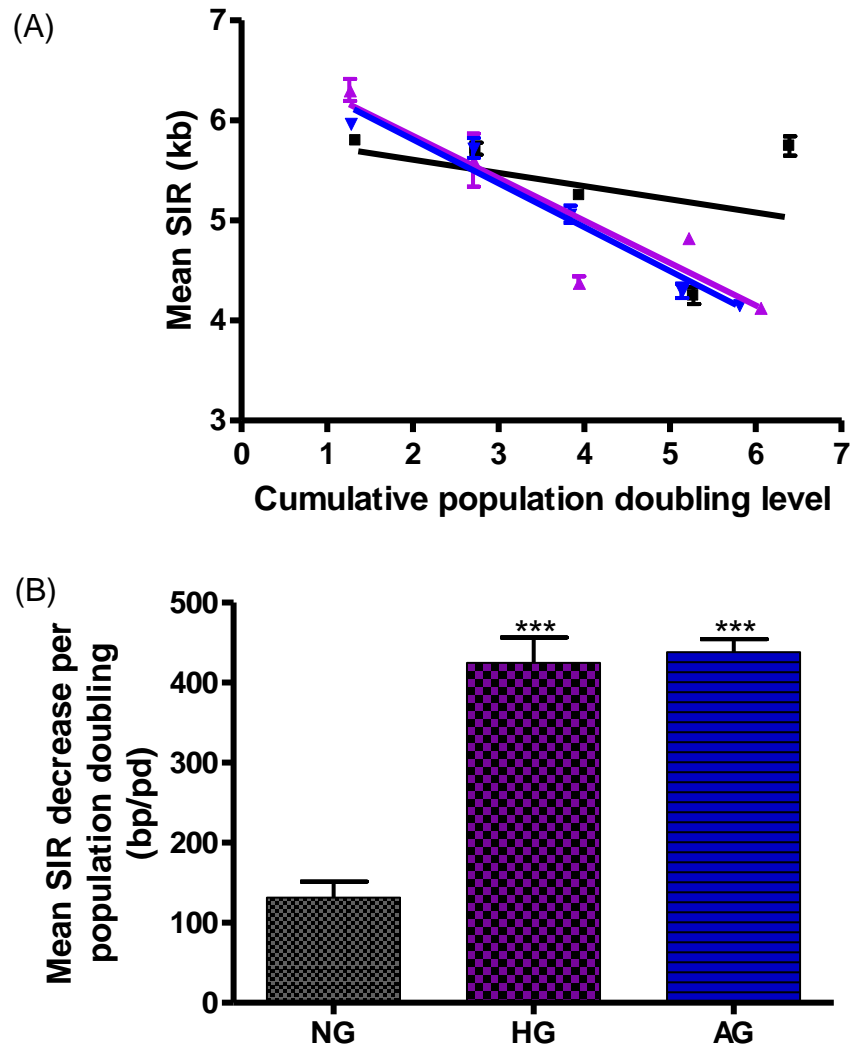


Figure 26: Effect of HG and AG on telomere length heterogeneity in HUVECs. (A) The semi-interquartile range (SIR) was calculated from Southern blots (using Telometric software) and plotted against the cumulative population doublings for HUVECs treated with NG (■), HG (▲) or AG (▼) every 48 hours. The data were analysed using linear regression. Values are \pm SEM, n=6. (B) The mean SIR decrease per population doubling level for HUVECs treated with NG, HG or AG. ***P<0.001 vs NG. Values are + SEM, n=6.

3.4.4.3 Validation of STELA

As telomere length decrease in HUVECs exposed to NG, HG or AG was successfully determined using Southern blotting, telomere length decrease was also determined by STELA which measures telomere length at a specific chromosome – in this case the XpYp chromosome.

When STELA was initially attempted as published (Baird *et al.*, 2003), it was unsuccessful. When the blots were radioactively labelled, there was very little DNA on the blots. It was believed that these problems arose from problems with the PCR reaction. In order to overcome these problems, the PCR part of the STELA was optimised in terms magnesium chloride concentration, the concentration of DNA and in the number of PCR cycles. When a number of factors were changed, the number of bands on the STELA blot increased.

Subsequently, the six different telorettes were compared - it was found that the use of telorette 2 provided the most bands indicating that human telomeres preferentially ended in the sequence AATCCCAA (complementary strand TTAGGGTT). It was also found that using 0.3mM of dNTP's and 2mM of magnesium chloride for PCR was optimal (Figure 27; Table 11). Furthermore, a blot looking at the number of PCR cycles showed that 27 cycles appeared to give the best results in terms of the band intensity (Figure 27; Table 11).

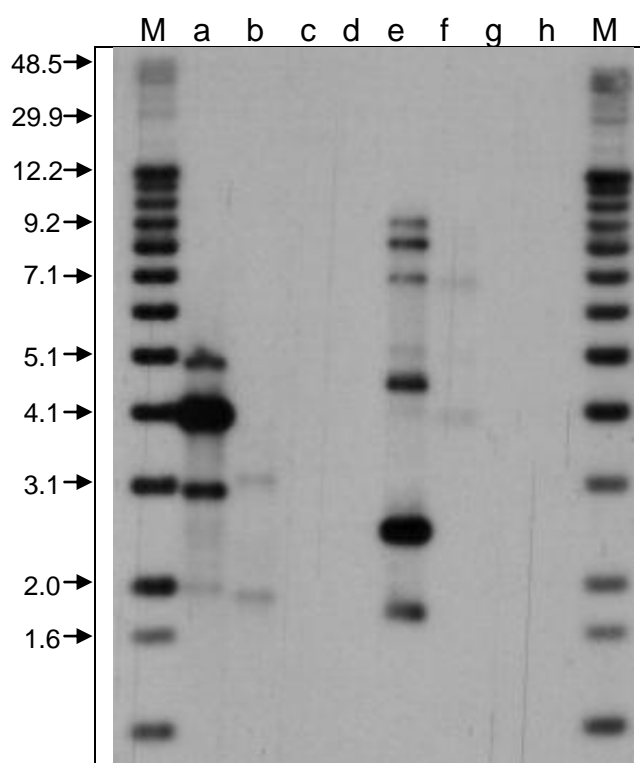


Figure 27: Effect of different dNTP concentrations, magnesium chloride concentrations and number of PCR cycles on STELA bands. A DNA concentration of 20pg/ μ l was used in the PCR reaction. The ligation reaction contained 0.9 μ M telorette 2. Each PCR reaction contained 0.5 μ M of the primers and 1 unit of a 10:1 mixture of taq polymerase and PWO polymerase. The blot was hybridised using the telomere probe. M=marker in kb.

Table 11: The dNTP concentration, the magnesium chloride concentration and the number of PCR cycles for lanes a to h. Corresponds to Figure 27.

Lane number	dNTP concentration (mM)	Magnesium chloride concentration (mM)	Number of PCR cycles
a, b	0.3	2.0	25
c, d	0.9	2.5	25
e, f	0.3	2.0	27
g, h	0.9	2.5	27

To optimise STELA further, a range of different DNA concentrations was investigated when performing the PCR reaction (Figure 28). Each lane represents DNA from a single lane PCR reaction (therefore 5 different

reactions vials per concentration of DNA). Ideally, STELA should show 8 to 10 bands within a single lane. Concentrations of DNA above 50pg/ μ l provided more prominent smears towards the top end of the blot. However, this blot also showed that 12.5pg/ μ l of DNA was too low as in two of the lanes three or fewer bands were observed. Therefore future STELA experiments used DNA concentrations of 25pg/ μ l in the initial PCR reaction.

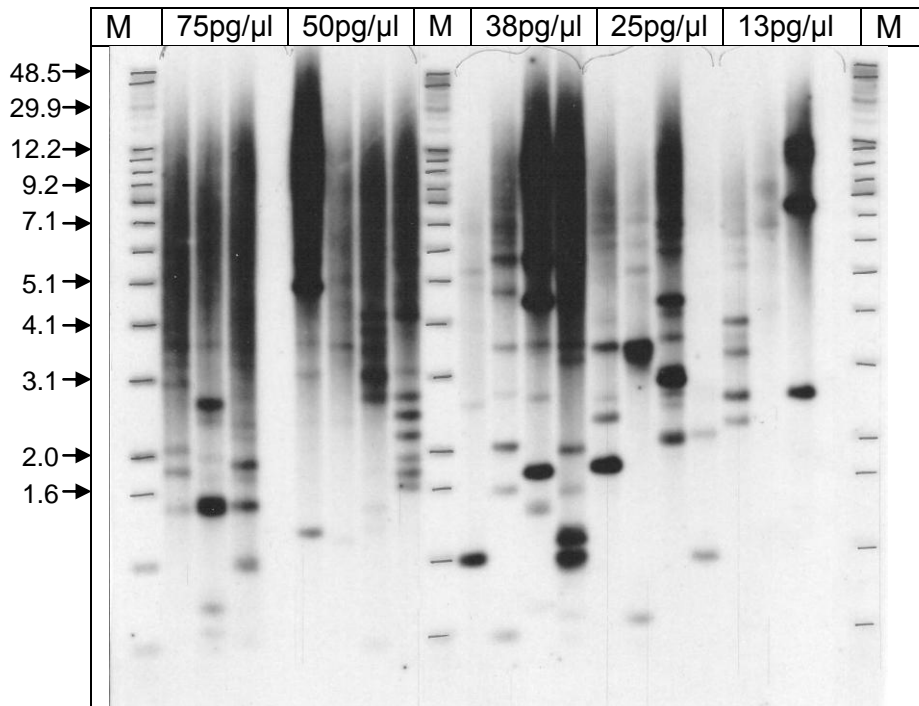


Figure 28: Effect of DNA concentration on STELA. A range of DNA concentrations were used ranging from 75pg/ μ l to 13pg/ μ l of DNA. The ligation reaction contained 0.9 μ M telorette 2. Each reaction contained 0.3mM of dNTP's, 0.5 μ M of the primers, 1 unit of a 10:1 mixture of taq polymerase and PWO polymerase and 2mM of magnesium chloride. The blot was hybridised using the telomere probe. M=marker in kb.

3.4.4.4 Generation of a telomere adjacent probe for STELA

Blots obtained by Southern blotting were probed using a telomere repeat probe. This probe was 4 repeats of TTAGGG. However, one of the drawbacks with this probe was its size. As the probe was very short (only 24 base pairs) it meant that the probe could bind more than once to telomeres longer than 48 base pairs and most telomeres are composed of many thousands of bases/repeats. Therefore following hybridisation of a blot, longer telomeric sequences showed increased signal not necessarily due to increased numbers of telomeres at that length. This increased signal due to the probe was accounted for when the data analysis was performed. However, this was a disadvantage that could be eliminated in STELA with the use of a probe that bound to a telomere adjacent sequence specific to the chromosome that was amplified in STELA (Cheung *et al.*, 2004). In this

case, the telomere adjacent sequence was specific to the short arm of the X and Y chromosome.

Unlike the telomere repeat probe (only 24bp long), the telomere adjacent probe required synthesis because the probe was 400bp long. Therefore, the probe was amplified from HUVEC DNA using two primers – a chromosome specific primer (XpYpE2) and a primer with a sequence found within the subtelomeric sequence via PCR- termed the XpYpB2A/T (Baird *et al.*, 2003; Cheung *et al.*, 2004). The PCR reaction product was then purified using gel electrophoresis.

When the amplified DNA was electrophoresed on an agarose gel, a band was observed at 400bp (Figure 29). The 400bp band was excised from the gel using a Qiagen gel extraction kit. However, the yield when using this kit was very low. To overcome this problem, the band was extracted from the gel using a Takara Recochip.

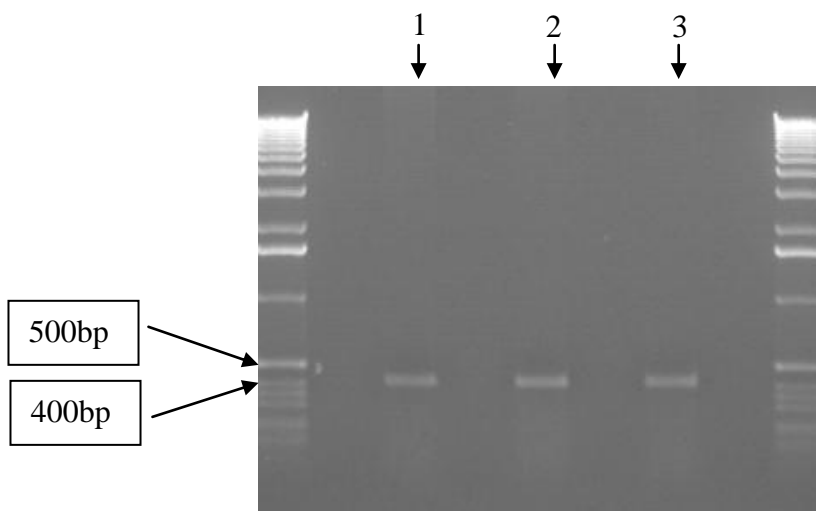


Figure 29: Amplification of chromosome specific subtelomeric sequence by PCR using a chromosome specific and a subtelomeric sequence primer. Shows an example gel (1.25% agarose gel) with the amplified DNA sequence at 400bp. Lanes one to three represent repeats using 2ng/ μ l of DNA in the PCR reaction vial.

To confirm the generation of the correct target sequence, the excised DNA was sequenced. When the sequence was analysed in BLAST, it was found to be 98% homologous to the human telomere associated repeat sequence on chromosome XpYp (Figure 30).

```

>gb|M57751.1|HUMTARS7AL Human telomere associated repeat sequence, complete sequence
Length=2036

Score = 644 bits (325), Expect = 0.0
Identities = 343/349 (98%), Gaps = 0/349 (0%)
Strand=Plus/Plus

Query 30      AATGAAGACGCGGAACCTCGCGGTGAGTGTTACAGTTCTTAAAGGTGGCATGTCCGGAGT 89
            |
Sbjct 1661     AATGAAGACGCGGAACCTCGCGGTGAGTGTTACAGTTCTTAAAGGTGGCGCGTCCGGAGT 1720

Query 90      TTGTTTCTTCTGATGTTTCAGATGTGTTCTGAGTTTCTTCTTTCTGGTGGGGTTGTGGTCT 149
            |
Sbjct 1721     TTGTTTCTTCTGATGTTTCAGATGTGTTCTGAGTTTCTTCTTTCTGGTGGGGTTGTGGTCT 1780

Query 150     CACTGGCTCAGGAGTGAAGCTGCAGACCTTTGCGGTGAGTGTCACAGCTCAGAAAGGCAG 209
            |
Sbjct 1781     CACTGGCTCAGGAGTGAAGCTGCAGACCTTTGCGGTGAGTGTCACAGCTCATAAAGGCAG 1840

Query 210     TGTGGACCCAAAAGAGTGAGCAGTAGCAAGATTTATTGCAAAGAGTGAAAGAACGAAAGCTT 269
            |
Sbjct 1841     TGTGGACCCAAAAGAGTGAGCAATAGCAAGATTTATTGCAAAGAGTGAAAGAACGAAAGCTT 1900

Query 270     CCACAGTATGGAAGGGACCCCATTTGGGTTGCCACTGCTGGCTCAGGCAGTCTGCTTTTA 329
            |
Sbjct 1901     CCACAGTATGGAAGGGACCCCATTTGGGTTGCCACTGCTGGCTCAGGCAGTCTGCTTTTA 1960

Query 330     TTCTCTAATCTGCTCCCTCCCACATCCTGCTGATAGGTCCACTTTCAGA 378
            |
Sbjct 1961     TTCTCTAATCTGCTCCCAACCACATCCTGCTGATAGGTCCACTTTCAGA 2009

```

Figure 30: The homology of the isolated and sequenced telomere adjacent probe with the human telomere associated repeat sequence as shown by NCBI database.

Following successful isolation of the telomere adjacent probe, the probe was radioactively labelled using random prime labelling and STELA blots were labelled using this probe. Labelling using this probe provided a weaker signal than when the telomere probe was used and therefore resulted in fewer bands on the STELA blot. This meant that the initial

concentration of DNA was increased from 25pg/μl to 40pg/μl in subsequent analyses.

3.4.4.5 Effect of HG and AG on telomere length in HUVECs assessed using STELA

As described in section 3.4.4.2, twenty-seven flasks were treated with NG, HG or AG medium over a number of passages (nine flasks for each treatment). DNA from three of the nine flasks (for each treatment – in total nine flasks) were extracted and frozen at -80°C. Once optimised, STELA was performed using these DNA samples. For each flask, five separate PCR reactions were set up. This meant that for each flask, five individual lanes were electrophoresed on an agarose gel. As each treatment was performed in triplicate, at every passage for each treatment, there were a total of 15 lanes.

Figure 31, 32 and 33 show examples of lanes from the STELA blots using DNA from HUVECs treated with NG, HG or AG medium.

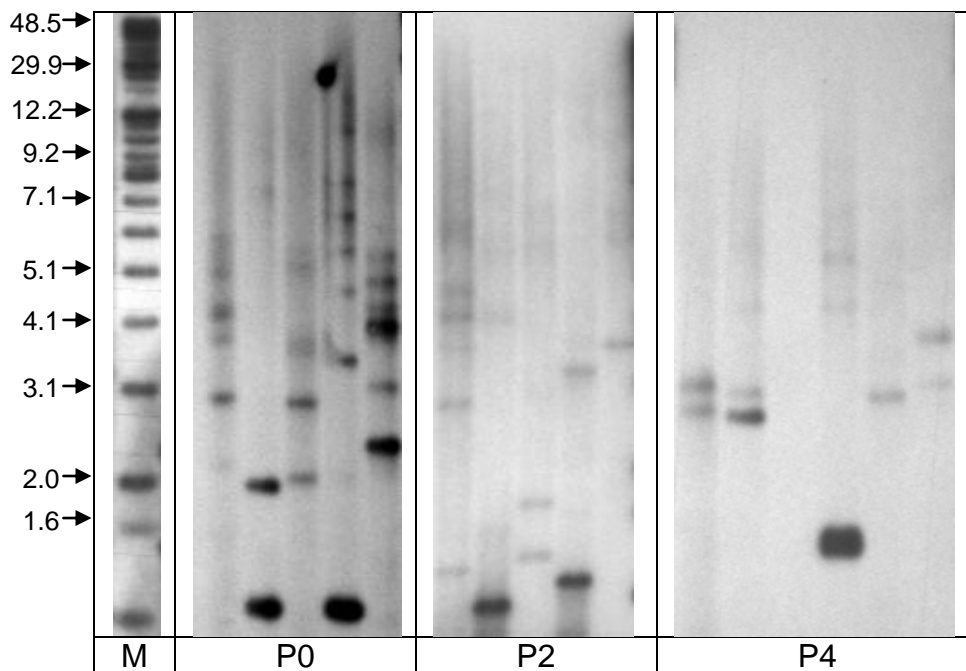


Figure 31: STELAs from DNA from HUVECs cultured in NG medium. Each lane represents a single PCR reaction using 40pg/ μ l of HUVEC DNA. The ligation reaction contained 0.9 μ M telorette 2. Each PCR reaction contained 0.3mM of dNTP's, 0.5 μ M of the primers, 1 unit of a 10:1 mixture of taq polymerase and PWO polymerase and 2mM of magnesium chloride. (See section 2.2.5 and 2.2.6 for details about gel electrophoresis and Southern blotting). The blot was hybridised using the telomere-adjacent probe. Examples are shown for passages 0, 2 and 4. M=marker in kb.

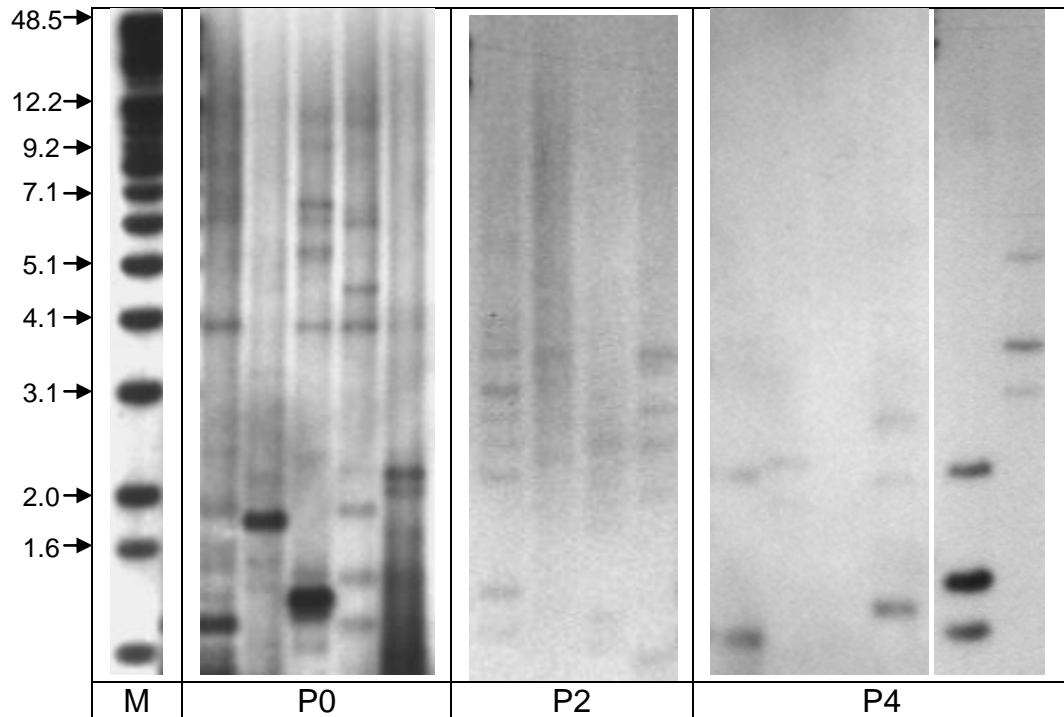


Figure 32: STELAs from DNA from HUVECs cultured in HG medium. Each lane represents a single PCR reaction using 40pg/ μ l of HUVEC DNA. The ligation reaction contained 0.9 μ M telorette 2. Each PCR reaction contained 0.3mM of dNTP's, 0.5 μ M of the primers, 1 unit of a 10:1 mixture of taq polymerase and PWO polymerase and 2mM of magnesium chloride. (See section 2.2.5 and 2.2.6 for details about gel electrophoresis and Southern blotting). The blot was hybridised using the telomere-adjacent probe. Examples are shown for passages 0, 2 and 4. M=marker in kb.

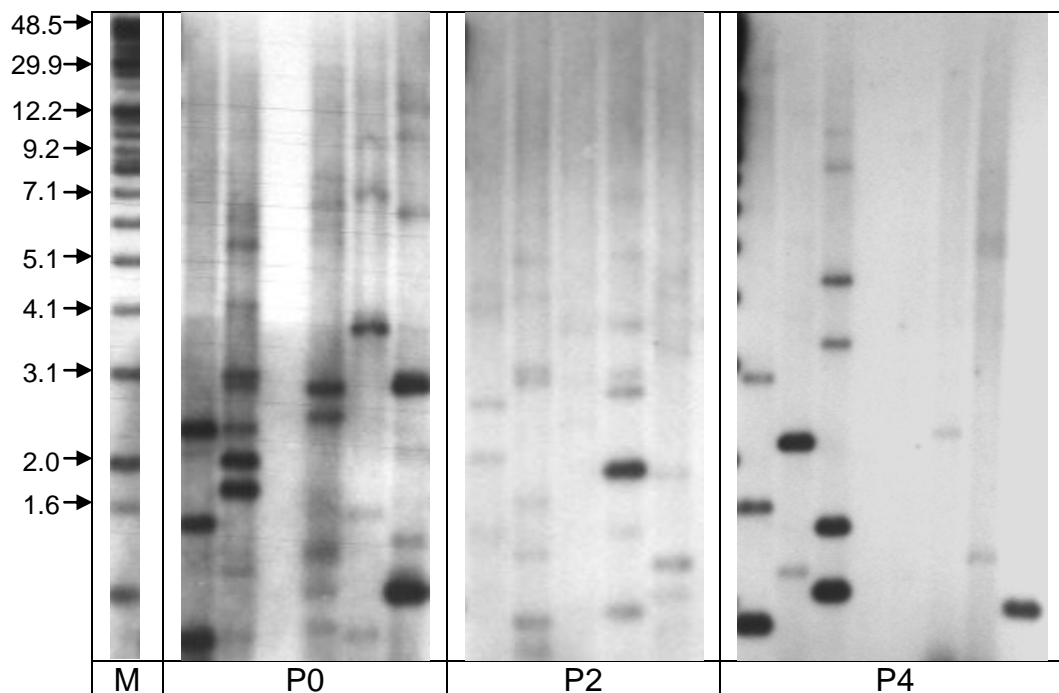


Figure 33: STELAs from DNA from HUVECs cultured in AG medium. Each lane represents a single PCR reaction using 40pg/ μ l of HUVEC DNA. The ligation reaction contained 0.9 μ M telorette 2. Each PCR reaction contained 0.3mM of dNTP's, 0.5 μ M of the primers, 1 unit of a 10:1 mixture of taq polymerase and PWO polymerase and 2mM of magnesium chloride. (See section 2.2.5 and 2.2.6 for details about gel electrophoresis and Southern blotting). The blot was hybridised using the telomere-adjacent probe. Examples are shown for passages 0, 2 and 4. M=marker in kb.

The mean of the median TRF was then calculated from these blots using Telometric software (section 2.2.6.6). When HUVECs were treated with NG medium, the mean telomere loss determined by STELA was 80 ± 46 bp/pd (Figure 34). When the cells were treated with HG, the mean telomere loss increased to 222 ± 111 bp/pd; however the difference was not statistically significant. Similarly, when HUVECs were exposed to AG the mean telomere loss increased to 348 ± 154 bp/pd. However the difference in telomere loss rate was not statistically significant (Figure 34).

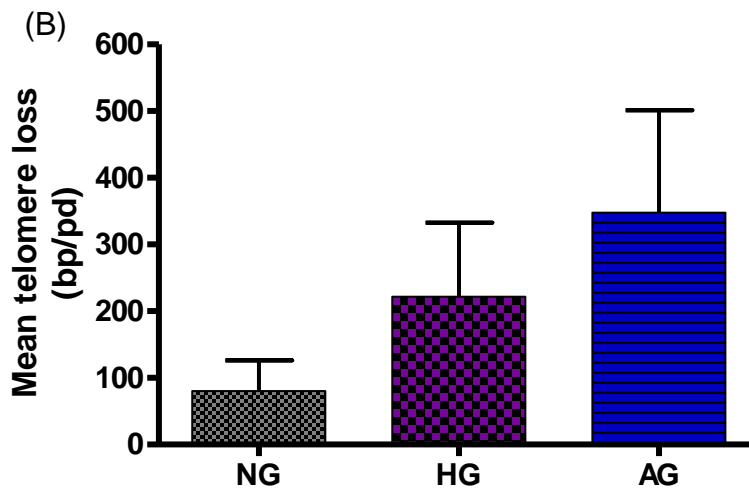
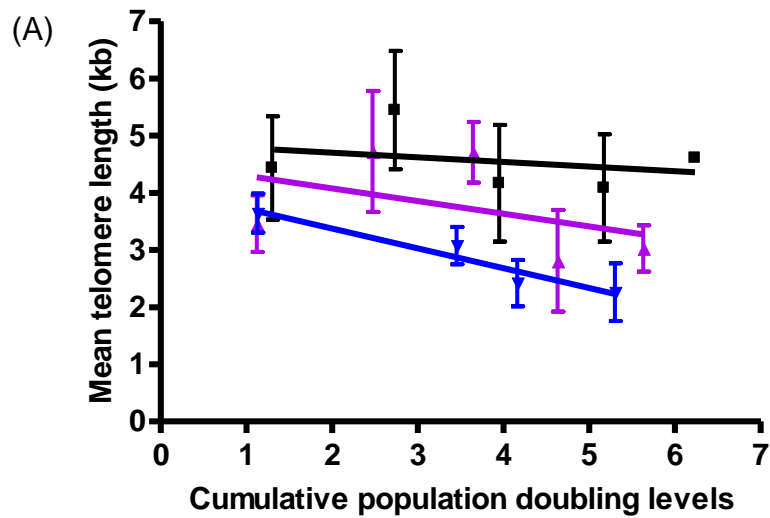


Figure 34: Effect of HG and AG on telomere attrition in HUVECs by STELA. (A) The mean (of medians) telomere length (kb) over ~6 cumulative population doublings for HUVECs treated with NG (■), HG (▲) or AG (▼) every 48 hours. Telomere length was assessed using STELA and the blots were analysed using Telometric software. The data were analysed using linear regression. Values are \pm SEM, $n=3$. (B) The mean telomere loss per population doubling level for HUVECs treated with NG, HG or AG over whole experiment. Values are \pm SEM, $n=3$.

The SIR was also measured using STELA (Figure 35). HUVECs cultured in NG, HG or AG medium showed a decrease in SIR. Unlike Southern blotting (Figure 26), the SIR decrease was similar for all three treatments. The SIR

decrease for HUVECs cultured in NG was 144.2 ± 62.32 bp/pd, for HG was 150.9 ± 26.29 bp/pd and for AG was 177.6 ± 29.25 bp/pd (Figure 35).

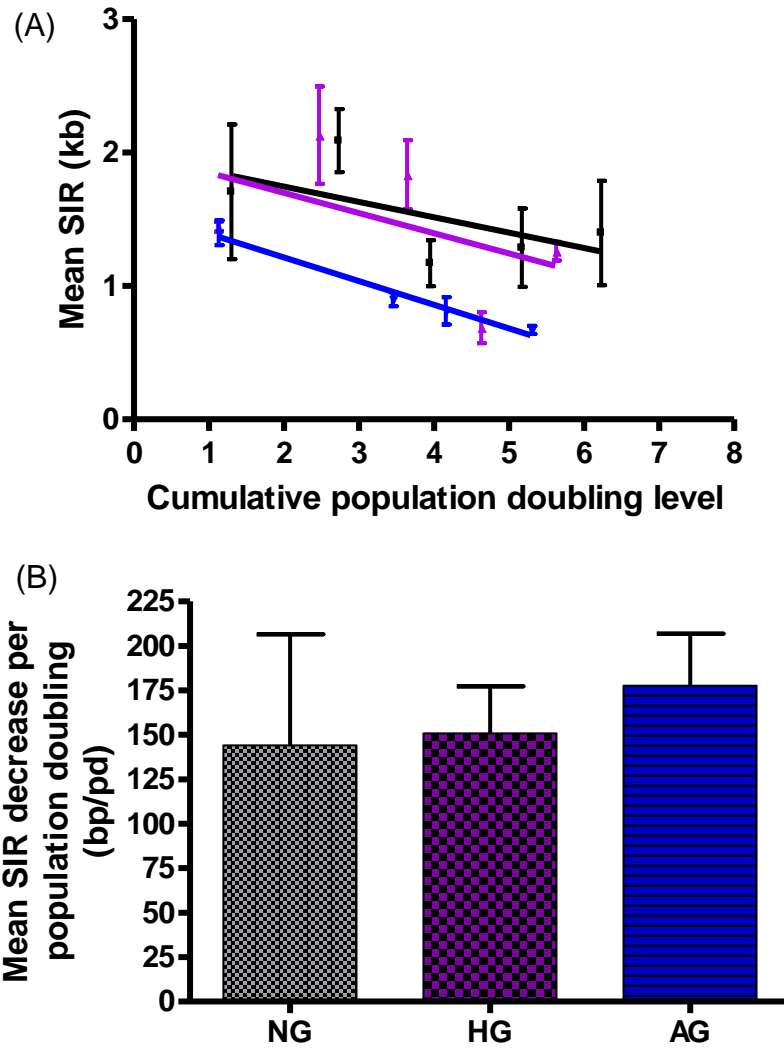


Figure 35: Effect of HG and AG on telomere length heterogeneity in HUVECs. (A) The semi-interquartile range (SIR) was calculated from STELA blots (using Telometric software) and plotted against the cumulative population doublings for HUVECs treated with NG (■), HG (▲) or AG (▼) every 48 hours. The data were analysed using linear regression. Values are \pm SEM, $n=3$. (B) The mean SIR decrease per population doubling level for HUVECs treated with NG, HG or AG. Values are \pm SEM, $n=3$.

3.4.5 Effect of HG and AG on ROS generation in HUVECs

Telomeres are believed to shorten due to increased production of ROS (von Zglinicki *et al.*, 2000). Therefore, one mechanism for the accelerated telomere shortening by HG might be increased ROS production. This was determined by measuring extracellular H₂O₂ production using the Amplex Red assay. This assay has been used for extracellular ROS production by phagocytic cells (Rinaldi *et al.*, 2007) but also has proven useful for measuring H₂O₂ that has diffused from its site of formation within cells (McNally *et al.*, 2003).

Prior to performing the Amplex Red assay on the samples, a number of factors of the assay were optimised. The number of cells needed for the assay and the volume of the reaction mixture added to each well had to be optimised as well as the H₂O₂ standard curve. Furthermore, in order to be able to compare variations in the H₂O₂ concentration, each sample was measured relative to protein concentration. Four different methods of extracting protein from the cells were tested – sonication, freeze thaw, NP-40 buffer or cell lytic M buffer. It was found that the use of cell lytic M buffer yielded the most protein (615pg of protein per cell) whereas NP40 buffer yielded the least amount of protein (15pg of protein per cell) (Table 12).

Table 12: Effect of different methods on the amount of protein extracted from 2x10⁵ HUVECs. HUVECs were grown until 70% confluent in a 6 well plate then protein was extracted by sonication, freeze thaw, cell lytic M buffer or NP40 buffer. Protein concentration was measured using the Bradford assay (section 2.2.8.3). n=2.

Method of protein extraction	Average amount of protein (mg)	Average amount of protein (pg) per cell
Sonication	0.075	375
Freeze thaw	0.063	315
Cell lytic M buffer	0.123	615
NP40 buffer	0.003	15

H₂O₂ production in HUVECs cultured in NG was just over 15 pmoles/min/mg protein (Figure 36). However, cells cultured in HG medium showed a two-fold increase (to ~35 pmoles/min/mg protein) in H₂O₂ production (p<0.005 versus NG treated HUVECs). When NG treated cells were also cultured with menadione, H₂O₂ increased greatly to 60 pmoles/min/mg protein (p<0.001; Figure 36). Furthermore, NG treated HUVECs treated with NAC and TTFA produced less H₂O₂ than HUVECs treated with NG although this did not reach statistical significance. NG treated HUVECs were also treated with agents that were not metabolised by the cells as a control for HG. 3-O-methylglucose and mannitol did not show a significant increase in H₂O₂ production compared to HUVECs treated with NG alone.

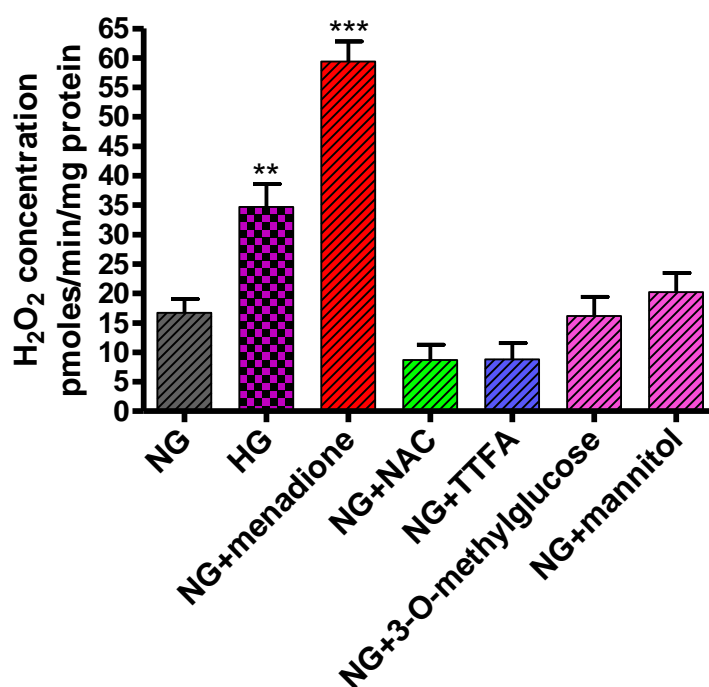


Figure 36: HG induces ROS production in HUVECs. HUVECs were treated with 16.5mM glucose, 50µM menadione, 3mM NAC, 25µM TTFA, 16.5mM 3-O-methylglucose, or 16.5mM mannitol for 1 hour. H₂O₂ production was assessed using the Amplex Red assay and expressed relative to the protein content (section 2.2.7). **P<0.005 vs NG. ***P<0.001 vs NG. Values represent mean +SEM, n=6.

HG treated HUVECs were also treated with the antioxidant NAC and the electron transport chain inhibitor TTFA (Figure 37). Both NAC and TTFA significantly decreased H₂O₂ production from 35 to 23 pmoles/min/mg protein ($p < 0.05$ versus HG control) and from 35 to 13 pmoles/min/mg protein ($p < 0.001$ versus HG control) respectively (Figure 37).

The decrease in H₂O₂ production observed in HUVECs treated with both HG and the mitochondrial ETC complex II inhibitor TTFA compared to when HUVECs were treated with HG alone, suggests a role for mitochondrial derived ROS in the production of H₂O₂.

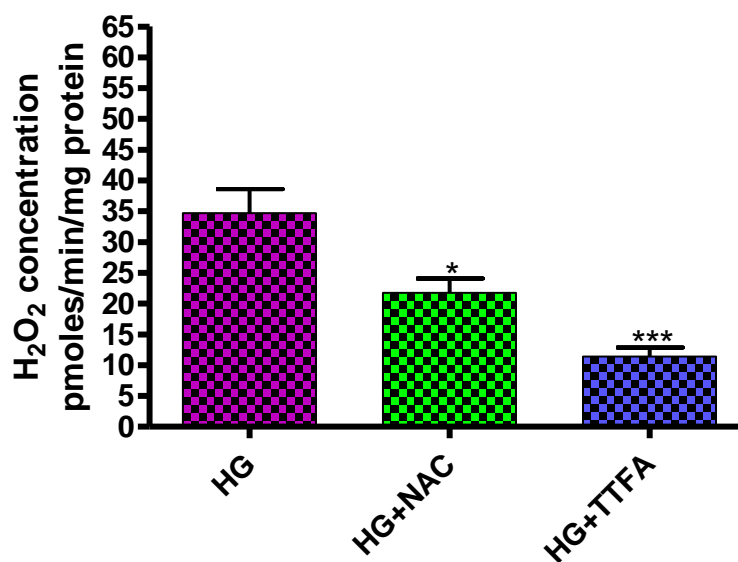


Figure 37: Effect of NAC or TTFA on HG-induced H₂O₂ production by HUVECs. Cells were treated with HG for 1 hour in absence or presence of NAC (3mM), or TTFA (25 μ M). H₂O₂ production was assessed using the Amplex Red assay and expressed relative to the protein content (section 2.2.7). * $P < 0.05$ vs NG. *** $P < 0.001$ vs NG. Values represent mean +sem, $n = 6$.

H₂O₂ production was also monitored over a 24 hour period for HUVECs cultured in medium containing NG and medium containing HG (Figure 38). H₂O₂ production in NG treated HUVECs remained relatively constant at around 25 to 30 pmoles/min/mg protein during the first 12 to 15 hours. However, after 15 hours ROS production increased steadily from

approximately 30 to 40 pmoles/min/mg protein. For HUVECs cultured in HG, H₂O₂ production increased after three hours treatment compared with the control (p=0.0889). After 6 hours, H₂O₂ production decreased to the same level as HUVECs exposed to NG. From around 6 hours, H₂O₂ production increased in parallel with the control but always remained higher than the control by approximately 5 to 10 pmoles/min/mg protein.

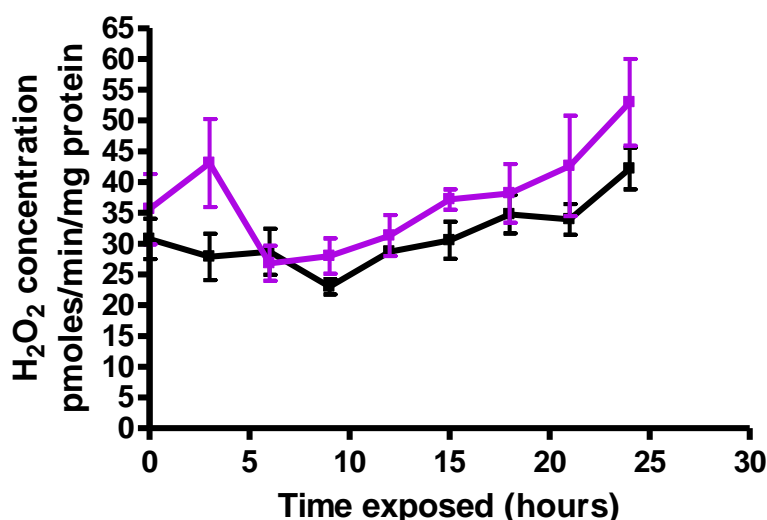


Figure 38: Time course of H₂O₂ production by HUVECs exposed to medium containing NG or HG. H₂O₂ production was measured using the Amplex Red assay in the media of cells exposed to NG (■) or HG (■) over a period of 24 hours (section 2.2.7). Values are mean ± SEM, n=6 for each timepoint.

Subsequently, ROS were also measured over a number of days of culture. This allowed the measurement of ROS in cells exposed to AG. Initially, H₂O₂ production was measured in HUVECs exposed to NG medium at 2, 6 and 10 days (Figure 39). Over 10 days, H₂O₂ production remained constant at approximately 25 to 30 pmoles/min/mg protein. No statistical differences were observed between any of the timepoints.

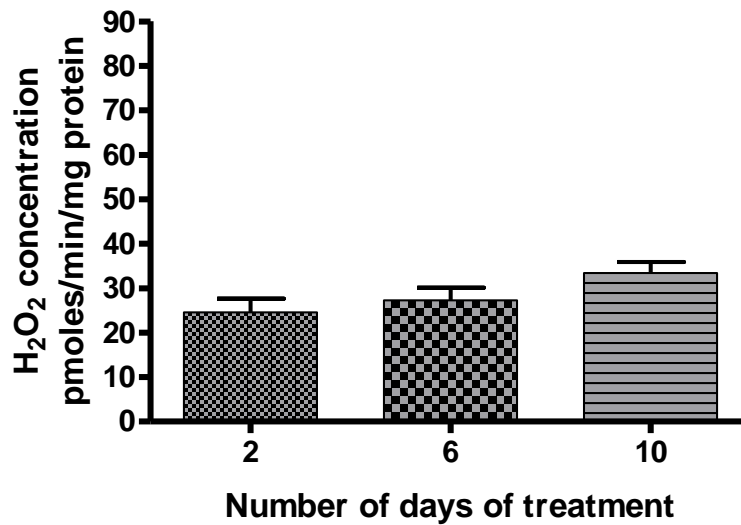


Figure 39: Time course of H₂O₂ production in HUVECs exposed to NG over a period of 10 days. H₂O₂ was measured using the Amplex Red assay and expressed relative to the protein content (section 2.2.7). Values are mean +SEM, n=6.

HUVECs were exposed to HG medium over a period of 10 days (Figure 40). There was no statistical difference between H₂O₂ production after 2 days for HUVECs treated with NG and HG (Figure 40(A)). However, at day 6, H₂O₂ production for cells cultured in HG was 45 pmoles/min/mg protein compared to ~30 pmoles/min/mg protein for cells cultured in NG medium ($p < 0.05$ versus NG day 6) (Figure 40(B)). At day 10, H₂O₂ production for cells cultured in HG was significantly higher (~60 pmoles/min/mg protein) than H₂O₂ production for cells cultured in NG medium for 10 days ($p < 0.001$ versus NG day 10) (Figure 40(C)).

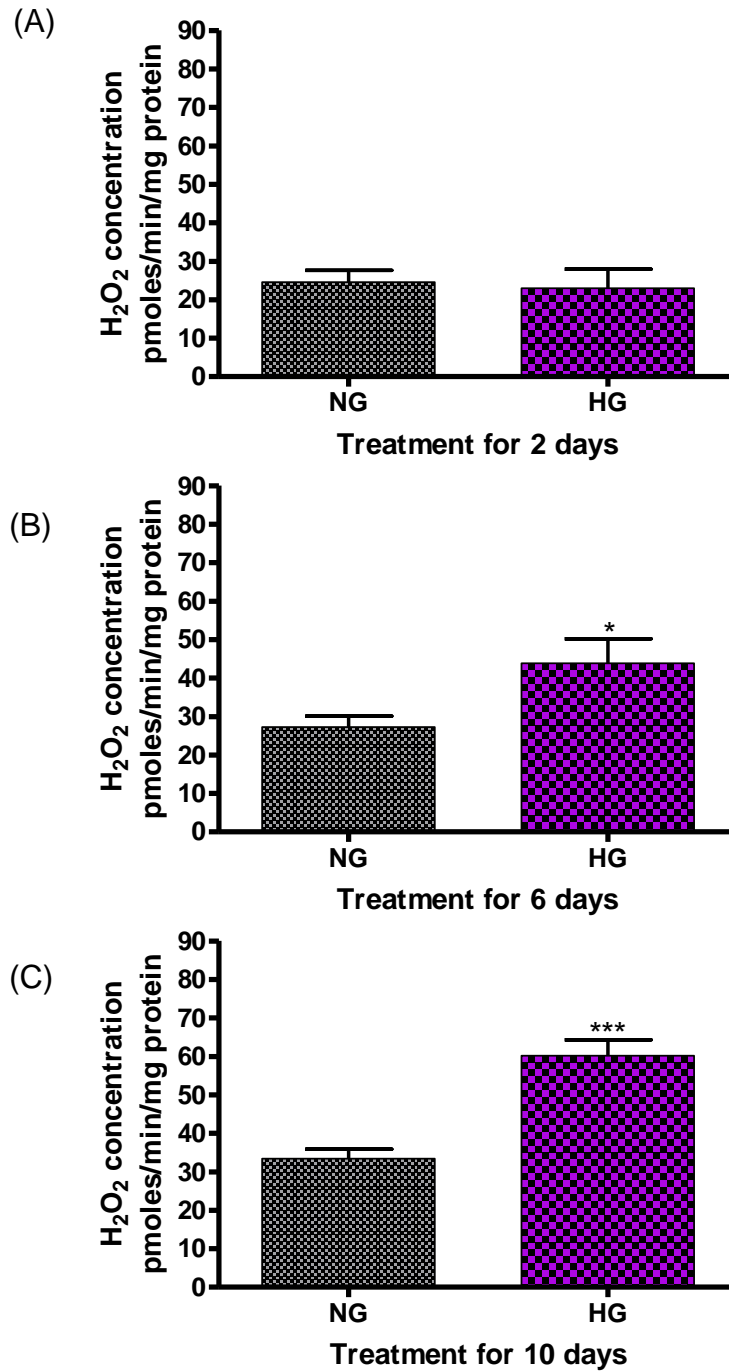


Figure 40: H₂O₂ production in HUVECs exposed to NG or HG over a period of 10 days. H₂O₂ was measured using the Amplex Red assay and expressed relative to the protein content (section 2.2.7). (A) H₂O₂ production for HUVECs cultured in NG or HG medium for 2 days. Values are mean +SEM, n=3. (B) H₂O₂ production for HUVECs cultured in NG or HG for 6 days. Values are mean +SEM, n=3. *P<0.05. (C) H₂O₂ production for HUVECs cultured in NG or HG for 10 days. Values are mean +SEM, n=6. ***P<0.001.

HUVECs were then exposed to AG for a period of 10 days. The medium was changed every 48 hours from NG to HG medium or *vice versa* and ROS were measured at day 2, 6 and 10 (Figure 41).

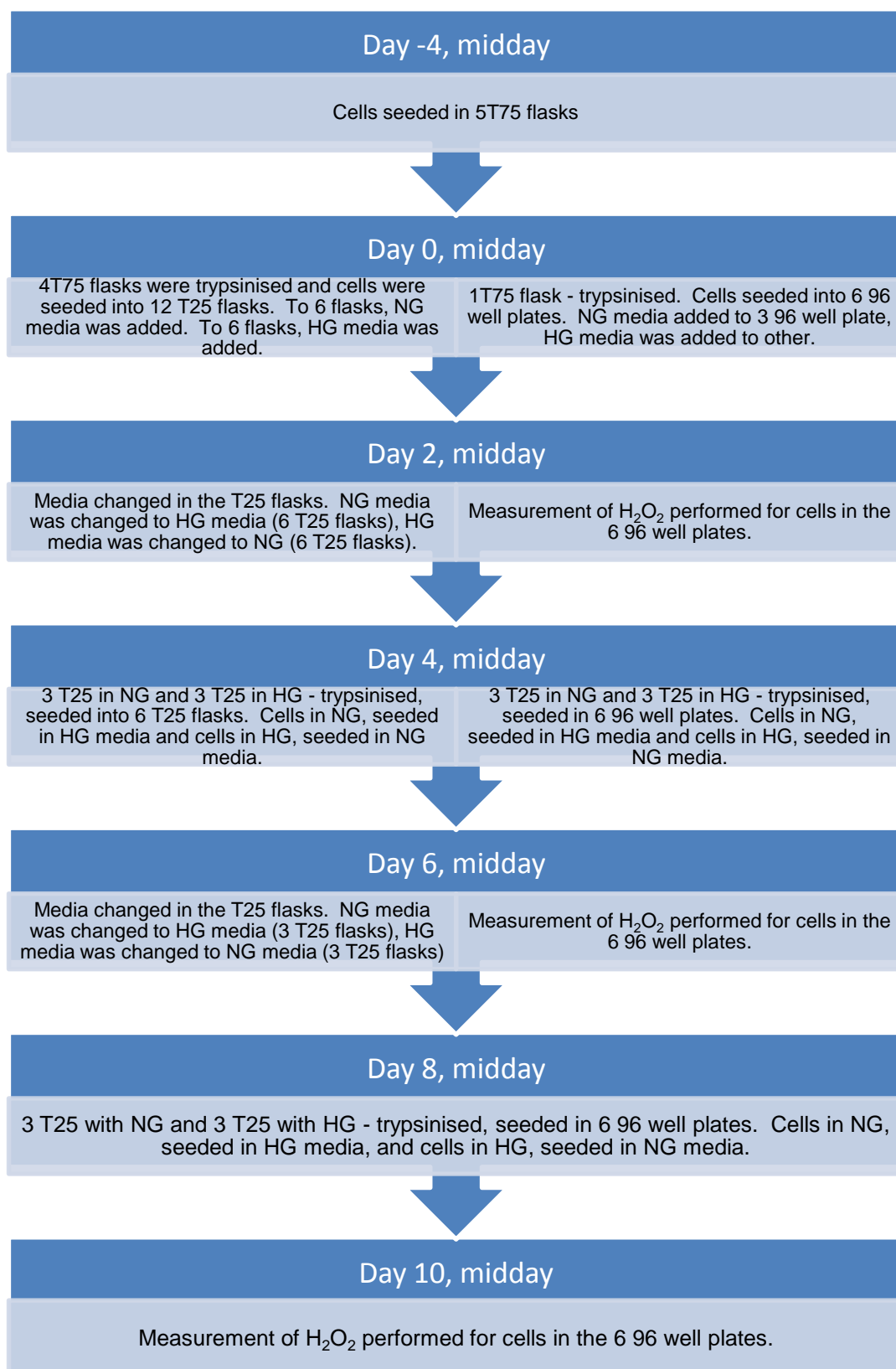


Figure 41: The protocol for measuring ROS for HUVECs exposed to AG medium. Cells were seeded at 50% confluence in 96 well plate 48 hours prior to measuring ROS using the Amplex Red assay. Measurements were performed at 2, 6 and 10 days.

Figure 42 shows H₂O₂ production in cells exposed to NG and AG medium after 2, 6 and 10 days. H₂O₂ production was measured after HUVECs were cultured in NG medium for 24 hours. Figure 43 shows H₂O₂ production in cells exposed to NG and AG after 2, 6 and 10 days. H₂O₂ production was measured after HUVECs were cultured in HG medium for 24 hours.

When HUVECs were exposed to NG or AG medium (ending with NG medium) for 2 days, H₂O₂ production was very similar (Figure 42(A)). At day 6, H₂O₂ production for cells cultured in AG was ~40 pmoles/min/mg protein compared to ~30 pmoles/min/mg protein for cells cultured in NG medium for 6 days ($p < 0.005$ versus NG day 6) (Figure 42(B)). At day 10, H₂O₂ production for cells cultured in AG was significantly higher (~50 pmoles/min/mg protein) than H₂O₂ production for cells cultured in NG medium for 10 days (~35 pmoles/min/mg protein) ($p < 0.05$ versus NG day 10) (Figure 42(C)).

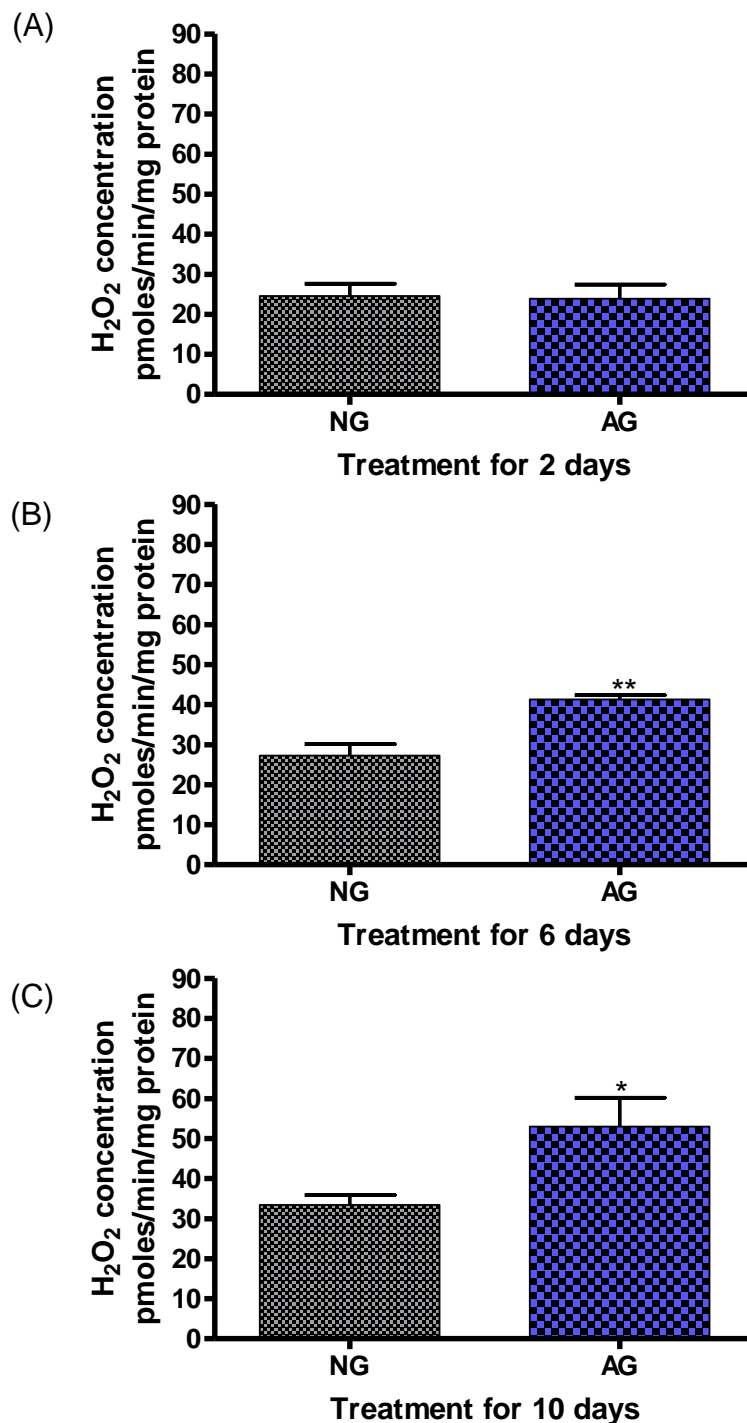


Figure 42: Time course of H₂O₂ production in HUVECs exposed to NG or AG (ending with NG) over a period of 10 days. H₂O₂ was measured using the Amplex Red assay and expressed relative to the protein content (section 2.2.7). (A) H₂O₂ production for HUVECs cultured in NG or AG medium for 2 days. Values are mean +SEM, n=3. (B) H₂O₂ production for HUVECs cultured in NG or AG for 6 days. Values are mean +SEM, n=3. **P<0.005. (C) H₂O₂ production for HUVECs cultured in NG or AG for 10 days. Values are mean +SEM, n=6. *P<0.05.

When HUVECs were exposed to AG medium over a period of 10 days ending with HG medium (Figure 43), H₂O₂ production increased. There was no statistical difference between H₂O₂ production after 2 days for HUVECs treated with NG and AG (Figure 43(A)). However, at day 6, H₂O₂ production for cells cultured in AG (ending with HG) was 40 pmoles/min/mg protein compared to ~30 pmoles/min/mg protein for cells cultured in NG medium for 6 days (p<0.05 versus NG day 6) (Figure 43(B)). At day 10, H₂O₂ production for cells cultured in AG (ending with HG) was significantly higher (~80 pmoles/min/mg protein) than H₂O₂ production for cells cultured in NG medium for 10 days (p<0.001 versus NG day 10) (Figure 43(C)). Therefore, the increase in H₂O₂ for cells exposed to AG was much greater when measured in medium containing HG.

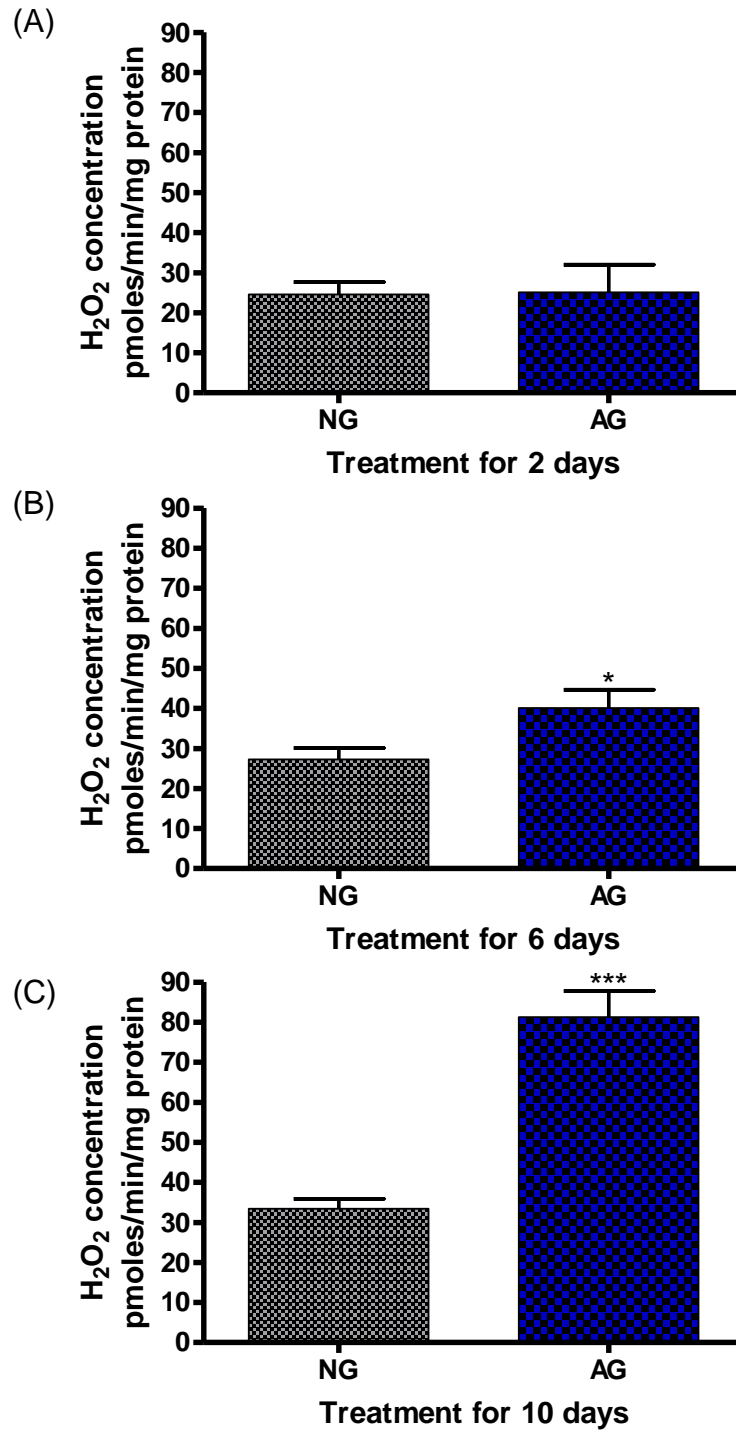


Figure 43: Time course of H₂O₂ production in HUVECs exposed to NG or AG (ending with HG) over a period of 10 days. H₂O₂ was measured using the Amplex Red assay and expressed relative to the protein content (section 2.2.7). (A) H₂O₂ production for HUVECs cultured in NG or AG medium for 2 days. Values are mean +SEM, n=3. (B) H₂O₂ production for HUVECs cultured in NG or AG for 6 days. Values are mean +SEM, n=3. *P<0.05. (C) H₂O₂ production for HUVECs cultured in NG or AG for 10 days. Values are mean +SEM, n=6. ***P<0.001.

3.4.6 Effect of NAC and TTFA on the rate of telomere attrition in HUVECs exposed to HG

Section 3.4.4.2 and 3.4.4.5 showed that telomere length decreased more rapidly in HUVECs exposed to HG or AG. Section 3.4.5 suggested that HUVECs exposed to HG or AG produced increased levels of ROS and this ROS was reduced when the HUVECs were cultured in NAC and TTFA. Therefore, in order to determine whether increased ROS was causing the telomere shortening, HUVECs were treated with HG or AG in the presence of TTFA or NAC.

Cells from a different donor were used to confirm the effect of HG and AG on telomere attrition (see section 3.4.4). This experiment (Figure 44) reconfirmed that HG and AG caused telomere shortening at an increased rate compared to HUVECs cultured in NG medium. Telomere attrition occurred at a rate of 222 ± 16 bp/pd for NG treated HUVECs, 605 ± 131 bp/pd for HG treated HUVECs and 460 ± 38 bp/pd for AG treated HUVECs (Figure 44).

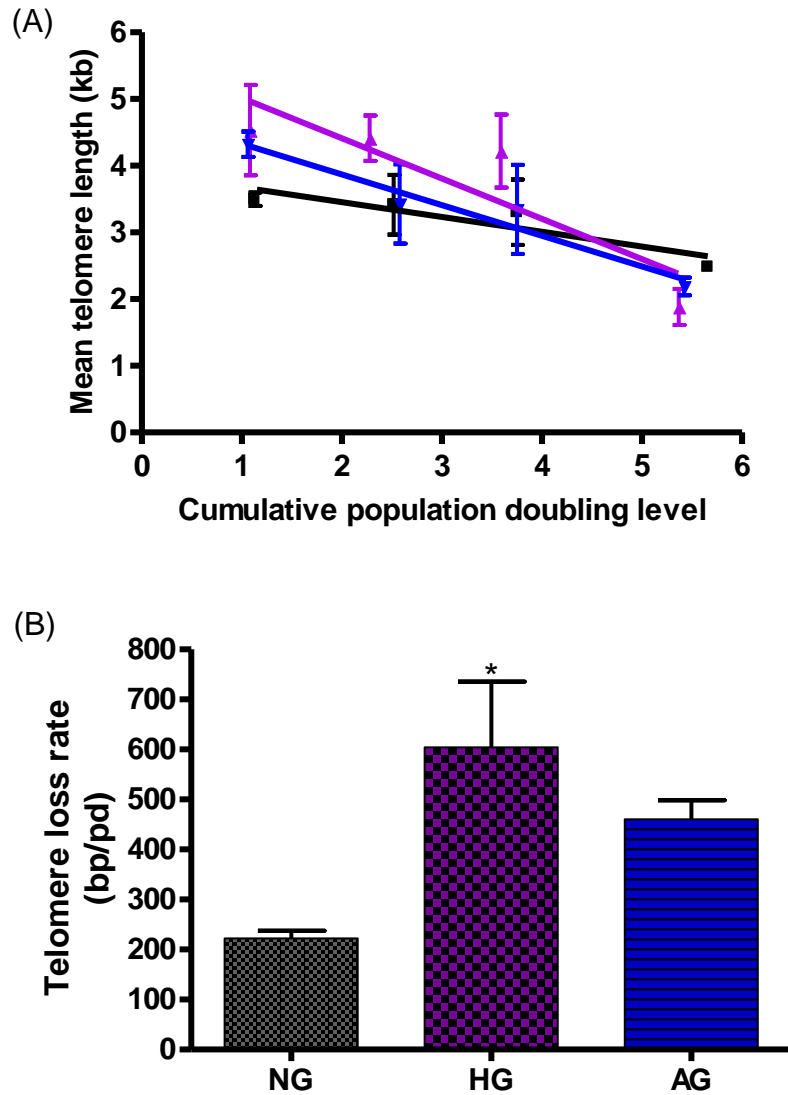


Figure 44: Effect of HG and AG on telomere attrition in HUVECs measured by STELA. (A) The mean (of medians) telomere length (kb) over ~6 cumulative population doublings for HUVECs treated with NG (■), HG (▲) or AG (▼) glucose every 48 hours. Telomere length was assessed using STELA and the blots were analysed using Telometric software. The data were analysed using linear regression. Values are \pm SEM, $n=3$. (B) The mean telomere loss per population doubling level for HUVECs treated with NG, HG or AG. * $P<0.05$ vs NG. Values are \pm SEM, $n=3$.

As a control, HUVECs treated with NG were co-treated with either NAC or TTFA (Figure 45). The rate of telomere loss was approximately equal whether HUVECs were cultured in NG or NG with TTFA. HUVECs treated with NG had a telomere loss rate of 222 ± 16 bp/pd and HUVECs treated with

NG and TTFA had a telomere attrition rate of 155 ± 50 bp/pd. This difference was not statistically significant. Similarly, culturing HUVECs in the presence of NAC did not affect telomere loss statistically, although there was a trend for higher telomere loss rate values for the cell cultured with NAC (392 ± 175 bp/pd for HUVECs treated NAC compared with 220bp/pd for HUVECs in NG alone; Figure 45).

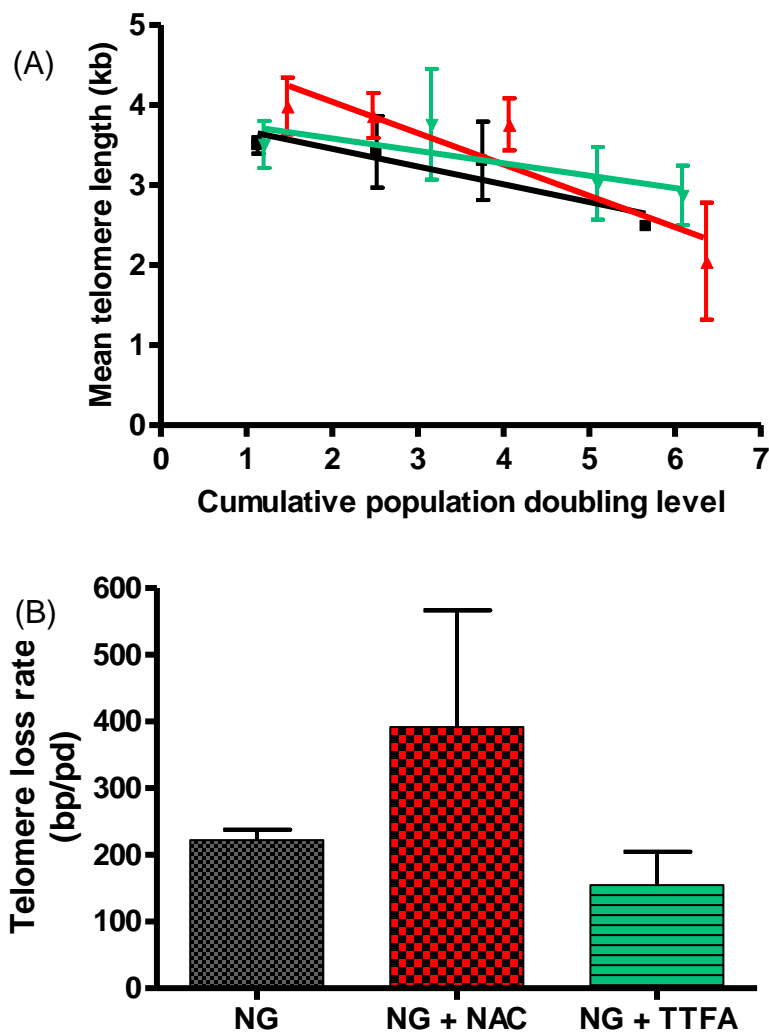


Figure 45: Effect of NAC or TTFA on telomere attrition due to NG. (A) The mean telomere length (kb) versus the cumulative population doublings for HUVECs treated with NG (■), NG and NAC (▲) or NG and TTFA (▼). Telomere length was assessed using STELA and the blots were analysed using Telometric software. The data were analysed using linear regression. Values are \pm SEM, $n=3$. (B) The mean telomere loss per population doubling level for HUVECs treated with NG, NG + NAC or NG + TTFA. Values are \pm SEM, $n=3$.

Next, the effect of NAC on telomere attrition in HUVECs exposed to HG was investigated. The telomere loss rate per population doubling level for HUVECs exposed to HG in the presence of NAC (133 ± 39 bp/pd) was reduced compared to HUVECs exposed to HG alone (605 ± 131 bp/pd; $P < 0.05$) and was restored to levels similar to when HUVECs were cultured in NG (222 ± 16 bp/pd) (Figure 46, 47, 48 and 49).

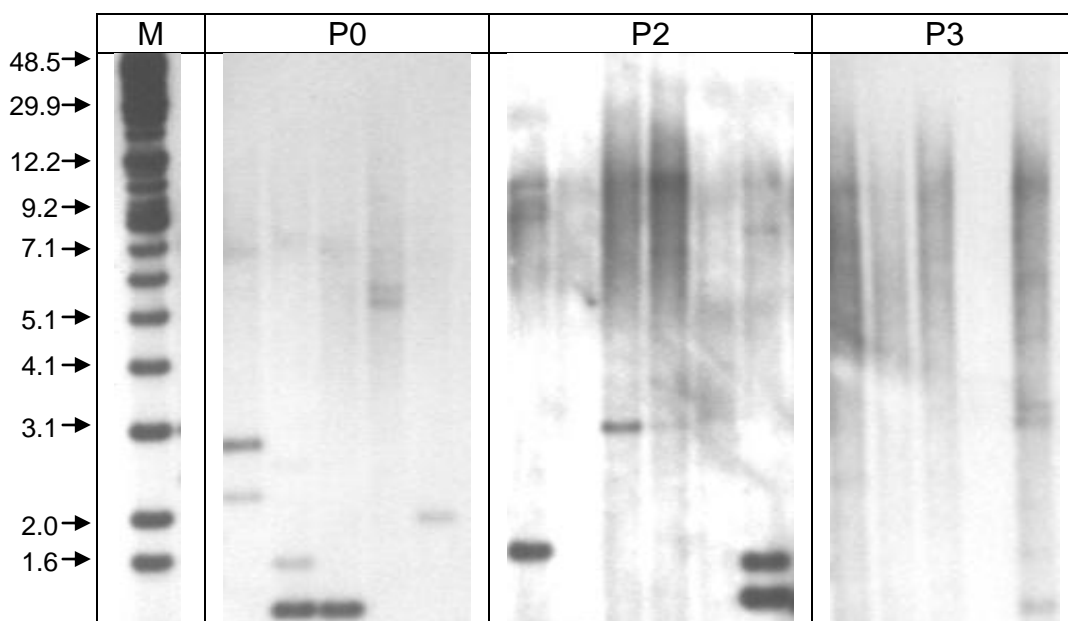


Figure 46: STELAs from DNA from HUVECs cultured in NG medium. Each lane represents a single PCR reaction using 40pg/ μ l of HUVEC DNA. The ligation reaction contained 0.9 μ M telorette 2. Each PCR reaction contained 0.3mM of dNTP's, 0.5 μ M of the primers, 1 unit of a 10:1 mixture of taq polymerase and PWO polymerase and 2mM of magnesium chloride. (See section 2.2.5 and 2.2.6 for details about gel electrophoresis and Southern blotting). The blots were hybridised using the telomere-adjacent probe. Examples are shown for passages 0, 2 and 3. M=marker in kb.

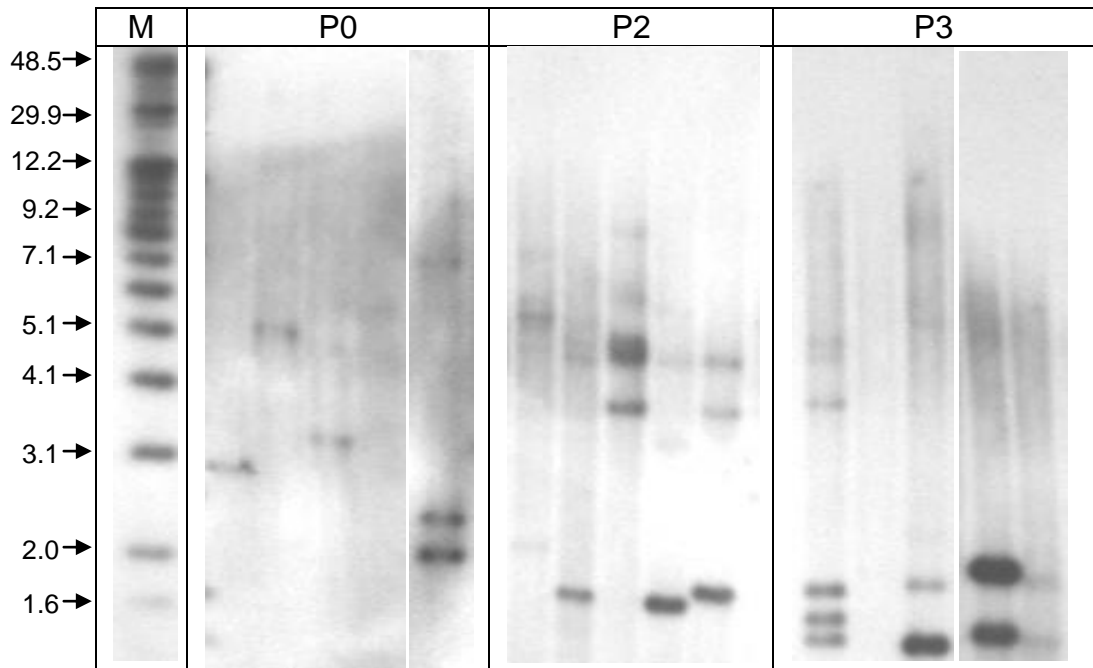


Figure 47: STELAs from DNA from HUVECs cultured in HG medium. Each lane represents a single PCR reaction using 40pg/ μ l of HUVEC DNA. The ligation reaction contained 0.9 μ M telorette 2. Each PCR reaction contained 0.3mM of dNTP's, 0.5 μ M of the primers, 1 unit of a 10:1 mixture of taq polymerase and PWO polymerase and 2mM of magnesium chloride. (See section 2.2.5 and 2.2.6 for details about gel electrophoresis and Southern blotting). The blots were hybridised using the telomere-adjacent probe. Examples are shown for passages 0, 2 and 3. M=marker in kb.

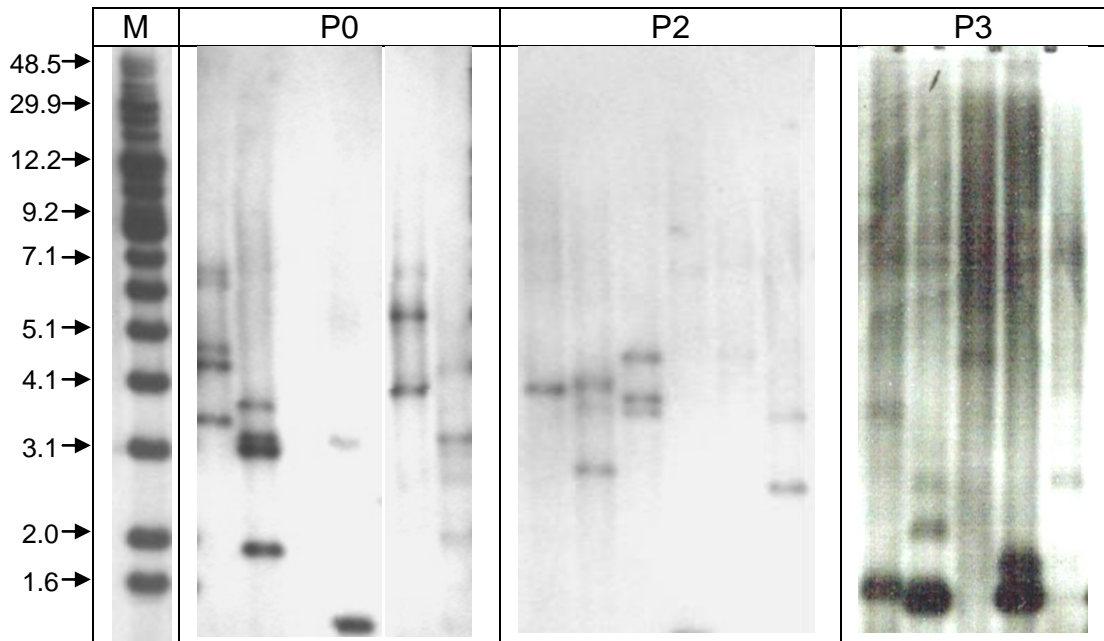


Figure 48: STELAs from DNA from HUVECs cultured in HG medium with 3mM NAC. Each lane represents a single PCR reaction using 40pg/ μ l of HUVEC DNA. The ligation reaction contained 0.9 μ M telorette 2. Each PCR reaction contained 0.3mM of dNTP's, 0.5 μ M of the primers, 1 unit of a 10:1 mixture of taq polymerase and PWO polymerase and 2mM of magnesium chloride. (See section 2.2.5 and 2.2.6 for details about gel electrophoresis and Southern blotting). The blots were hybridised using the telomere-adjacent probe. Examples are shown for passages 0, 2 and 3. M=marker in kb.

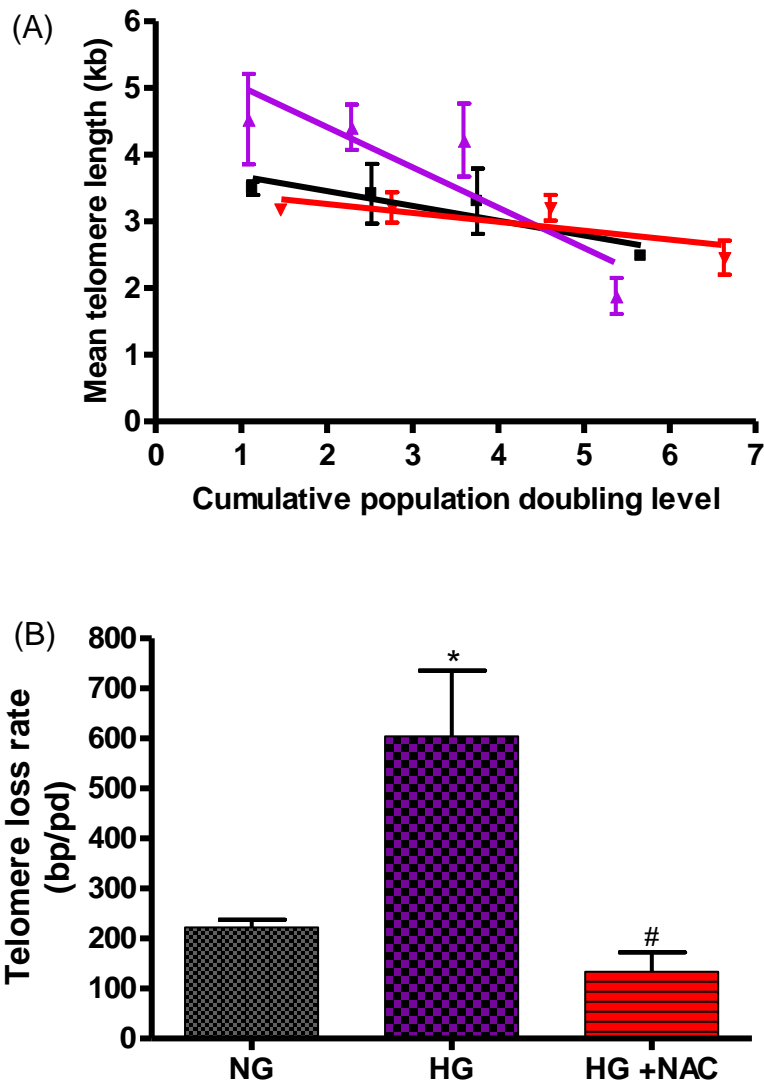


Figure 49: Effect of NAC on telomere attrition due to HG. (A) The mean telomere length (kb) versus the cumulative population doublings for HUVECs treated with NG (■), HG (▲) or HG and 3mM NAC (▼). Telomere length was assessed using STELA and the blots were analysed using Telometric software. The data were analysed using linear regression. Values are \pm SEM, $n=3$. (B) The mean telomere loss per population doubling level for HUVECs treated with NG, HG or HG + NAC. * $P<0.05$ vs NG; # $P<0.05$ vs HG. Values are \pm SEM, $n=3$.

When HUVECs were cultured in HG containing TTF α , the rate of telomere loss was once again reduced compared to HG and was restored to levels similar to when HUVECs were cultured in NG medium (Figure 46, 47, 50 and 51). The telomere attrition rate decreased from 605 ± 131 bp/pd to

202±58 bp/pd for HG and TTFA ($P < 0.05$). This value is very similar to the value obtained for HUVECs cultured in NG (220±16 bp/pd).

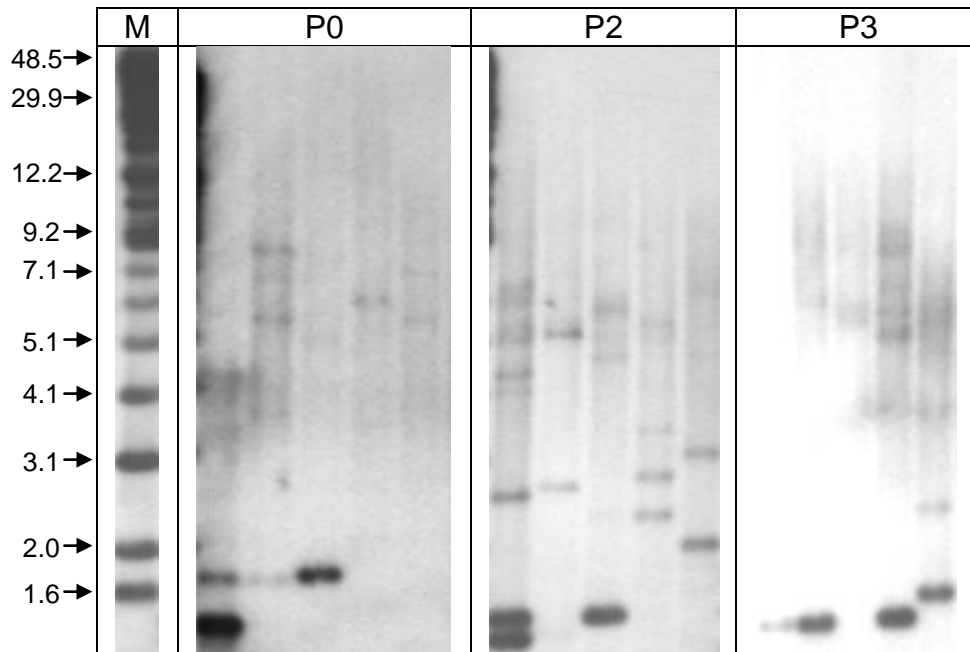


Figure 50: STELAs from DNA from HUVECs cultured in HG medium with 25µM TTFA. Each lane represents a single PCR reaction using 40pg/µl of HUVEC DNA. The ligation reaction contained 0.9µM telorette 2. Each PCR reaction contained 0.3mM of dNTP's, 0.5µM of the primers, 1 unit of a 10:1 mixture of taq polymerase and PWO polymerase and 2mM of magnesium chloride. (See section 2.2.5 and 2.2.6 for details about gel electrophoresis and Southern blotting). The blots were hybridised using the telomere-adjacent probe. Examples are shown for passages 0, 2 and 3. M=marker in kb.

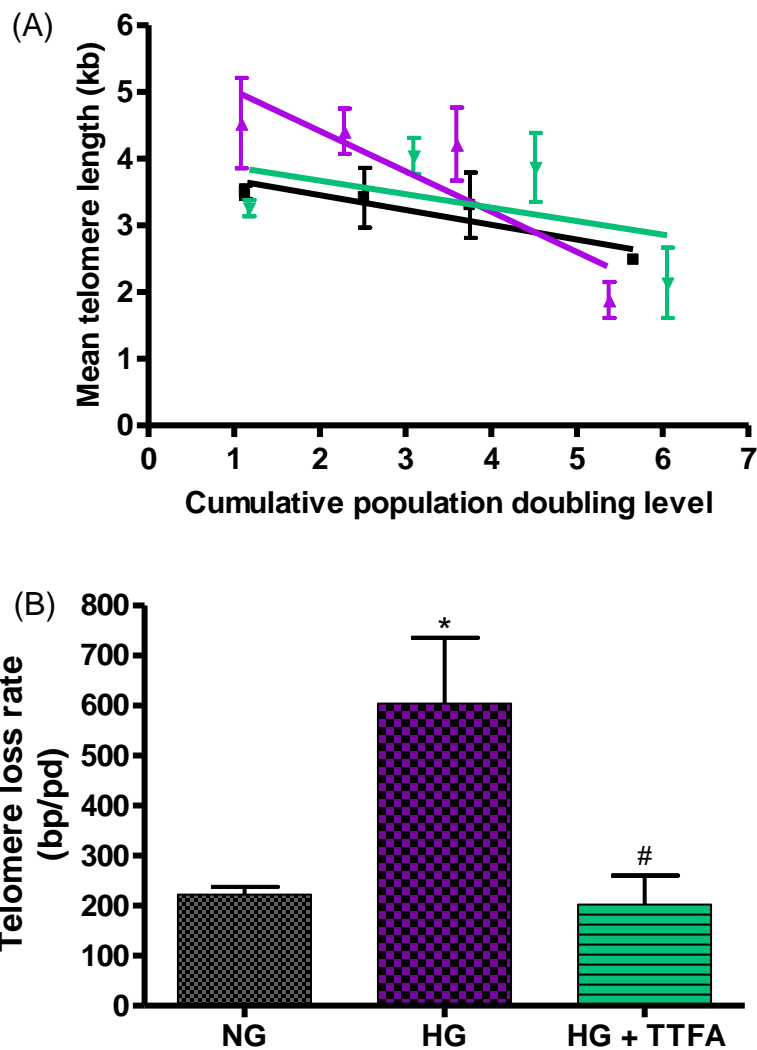


Figure 51: Effect of TTFA on telomere attrition due to HG. (A) The mean telomere length (kb) versus the cumulative population doublings for HUVECs treated with NG (■), HG (▲) or HG and 25 μ M TTFA (▼). Telomere length was assessed using STELA and the blots were analysed using Telometric software. The data were analysed using linear regression. Values are \pm SEM, n=3. (B) The mean telomere loss per population doubling level for HUVECs treated with NG, HG or HG + TTFA. *P<0.05 vs NG; #P<0.05 vs HG. Values are \pm SEM, n=3.

3.4.7 Effect of NAC and TTFA on the rate of telomere attrition in HUVECs exposed to AG

Similar experiments were performed for cells exposed to AG. Although the result was not as striking as with HUVECs cultured in HG and NAC or HG

and TTFa, it was still apparent that the addition of NAC or TTFa to either NG or HG medium (AG medium) restored the telomere loss rate to similar levels seen in HUVECs cultured in NG medium. The telomere loss rate for HUVECs cultured in AG while in the presence of NAC reduced from 460 ± 38 bp/pd (AG) to 283 ± 101 bp/pd (AG +NAC) (Figure 46, 52, 53 and 54). The telomere loss rate for HUVECs cultured in AG while in the presence of TTFa reduced from 460 ± 38 bp/pd (AG) to 261 ± 80 bp/pd (AG +NAC) (Figure 46, 52, 55 and 56). However, neither of these differences reached statistical significance but nonetheless the trend was similar to that observed for HG.

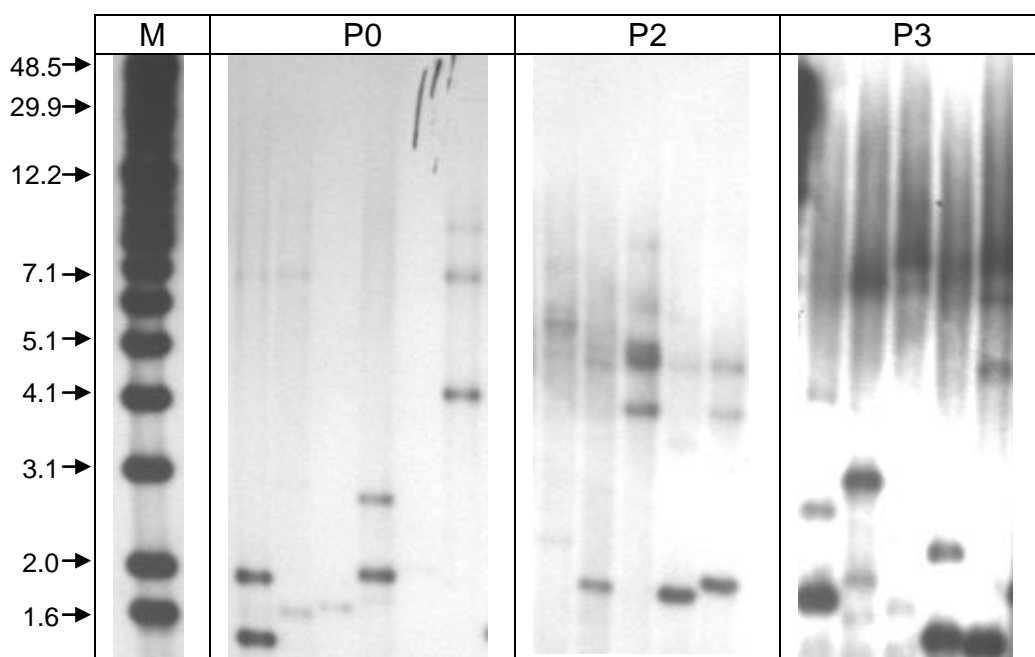


Figure 52: STELAs from DNA from HUVECs cultured in AG medium. Each lane represents a single PCR reaction using 40pg/ μ l of HUVEC DNA. The ligation reaction contained 0.9 μ M telorette 2. Each PCR reaction contained 0.3mM of dNTP's, 0.5 μ M of the primers, 1 unit of a 10:1 mixture of taq polymerase and PWO polymerase and 2mM of magnesium chloride. (See section 2.2.5 and 2.2.6 for details about gel electrophoresis and Southern blotting). The blots were hybridised using the telomere-adjacent probe. Examples are shown for passages 0, 2 and 3. M=marker in kb.

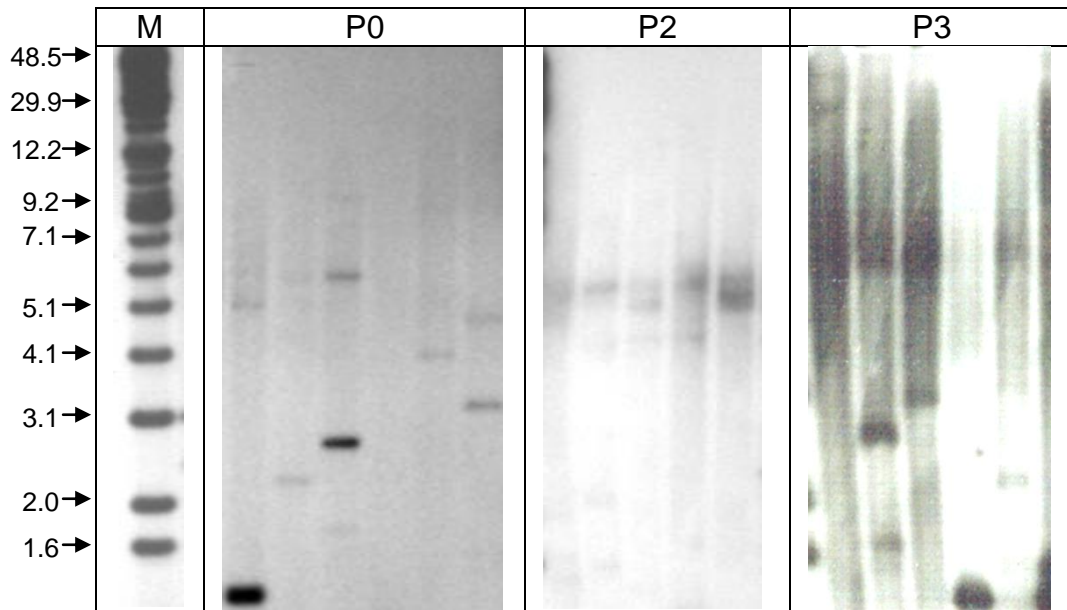


Figure 53: STELAs from DNA from HUVECs cultured in AG medium with 3mM NAC. Each lane represents a single PCR reaction using 40pg/ μ l of HUVEC DNA. The ligation reaction contained 0.9 μ M telorette 2. Each PCR reaction contained 0.3mM of dNTP's, 0.5 μ M of the primers, 1 unit of a 10:1 mixture of taq polymerase and PWO polymerase and 2mM of magnesium chloride. (See section 2.2.5 and 2.2.6 for details about gel electrophoresis and Southern blotting). The blots were hybridised using the telomere-adjacent probe. Examples are shown for passages 0, 2 and 3. M=marker in kb.

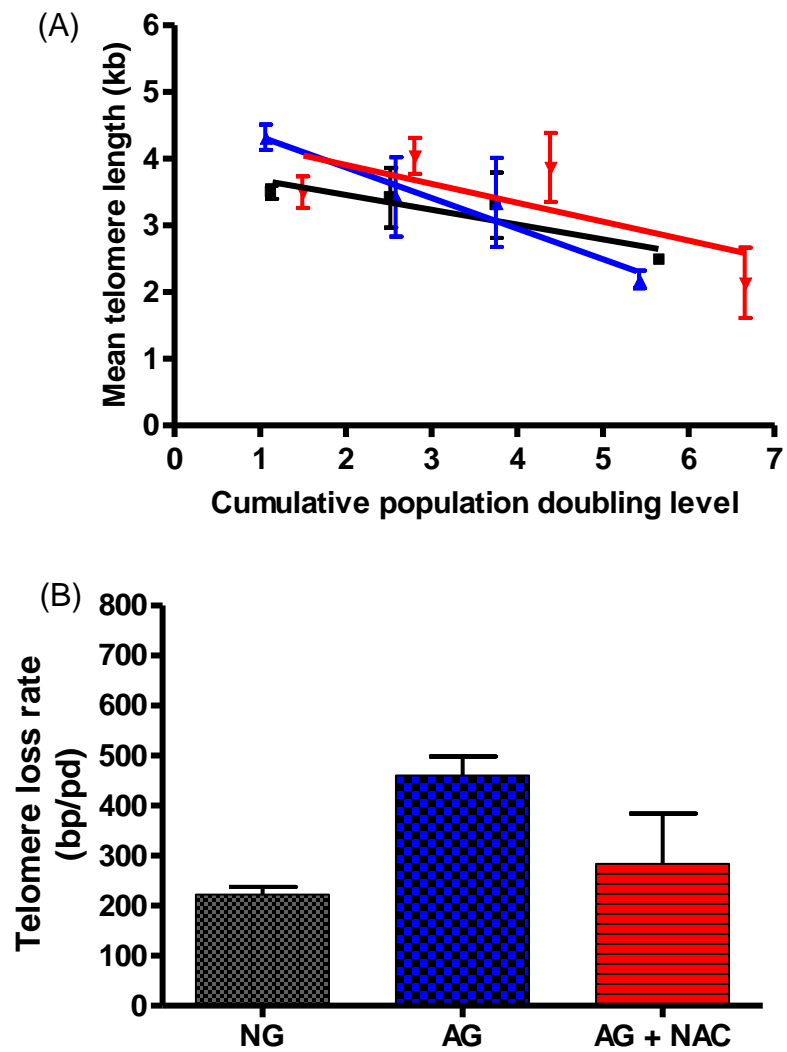


Figure 54: Effect of NAC on telomere attrition due to AG. (A) The mean telomere length (kb) versus the cumulative population doublings for HUVECs treated with NG (■), AG (▲) or AG and NAC (▼). Telomere length was assessed using STELA and the blots were analysed using Telometric software. The data were analysed using linear regression. Values are \pm SEM, $n=3$. (B) The mean telomere loss per population doubling level for HUVECs treated with NG, AG or AG + NAC. Values are \pm SEM, $n=3$.

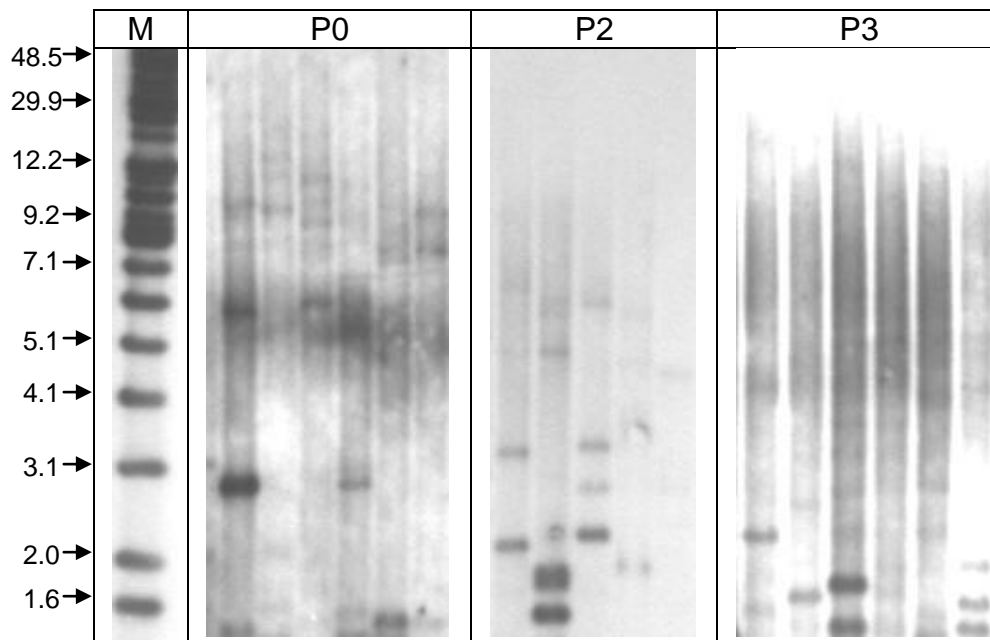


Figure 55: STELAs from DNA from HUVECs cultured in AG medium with 25 μ M TTFA. Each lane represents a single PCR reaction using 40pg/ μ l of HUVEC DNA. The ligation reaction contained 0.9 μ M telorette 2. Each PCR reaction contained 0.3mM of dNTP's, 0.5 μ M of the primers, 1 unit of a 10:1 mixture of taq polymerase and PWO polymerase and 2mM of magnesium chloride. (See section 2.2.5 and 2.2.6 for details about gel electrophoresis and Southern blotting). The blots were hybridised using the telomere-adjacent probe. Examples are shown for passages 0, 2 and 3. M=marker in kb.

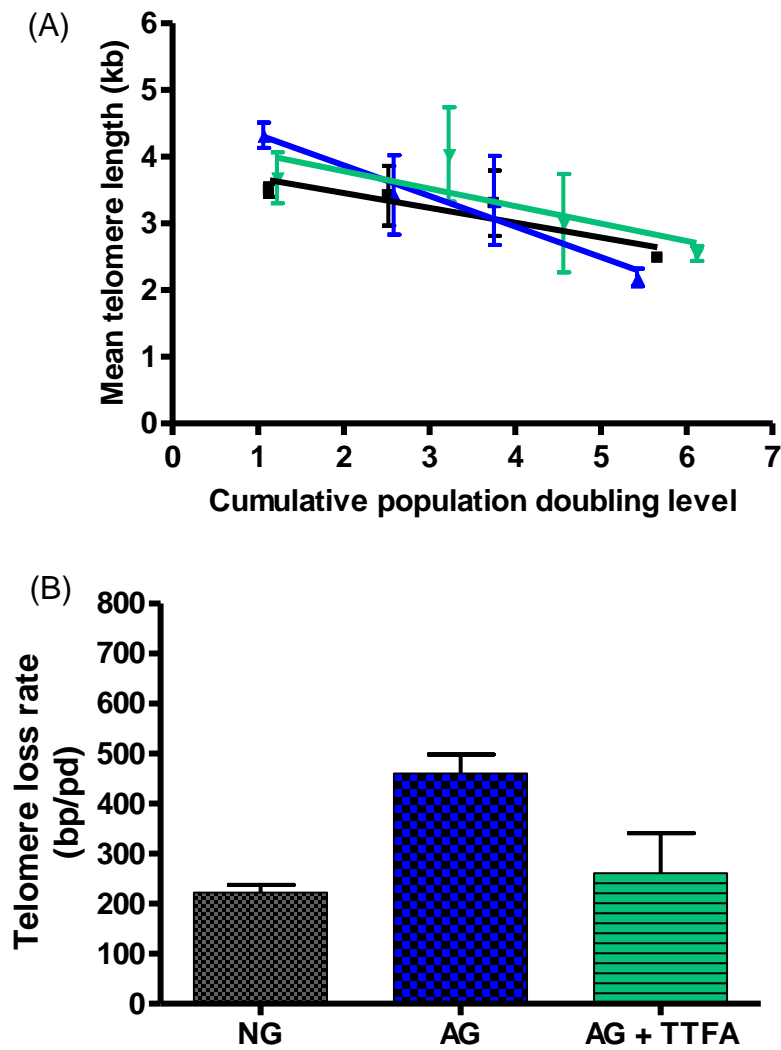


Figure 56: Effect of TTFA on telomere attrition due to AG. (A) The mean telomere length (kb) versus the cumulative population doublings for HUVECs treated with NG (■), AG (▲) or AG and TTFA (▼). Telomere length was assessed using STELA and the blots were analysed using Telometric software. The data were analysed using linear regression. Values are \pm SEM, n=3. (B) The mean telomere loss per population doubling level for HUVECs treated with NG, AG or AG + TTFA. Values are \pm SEM, n=3.

3.5 Discussion

Cardiovascular diseases are associated with shorter telomeres. Since oxidative stress accelerates telomere attrition and is implicated in cardiovascular diseases such as diabetes, this chapter analysed if cells

exposed to high concentrations of glucose had shorter telomeres by increased oxidative stress.

3.5.1 Preliminary experiments

Prior to analysing telomere length and oxidative stress in HUVECs, a number of preliminary experiments were first performed. The identity of HUVECs was confirmed by staining the cells with von Willebrand Factor (vWF), glucose uptake was measured in HUVECs following exposure to HG medium compared to NG medium, and the rate of cell growth was investigated when cells were cultured in NG, HG or AG medium.

The initial experiment performed looked at the identity of the HUVECs. As the cells had not been previously characterised, HUVECs were stained by immunofluorescence using a marker characteristic to endothelial cells - vWF. vWF is present in Weibel Palade bodies within endothelial cells and is involved in the injury response (Constans and Conri, 2006). When HUVECs were stained with anti-vWF, and viewed under a FITC filter they had granular staining. This type of staining in endothelial cells was also demonstrated by others (Sommer *et al.*, 2005 and Shi *et al.*, 2004). When the same population was also viewed under a DAPI filter to visualise nuclei, the percentage of cells staining positive for DAPI and anti-vWF was calculated to be approximately 90 to 95%. VSMC did not stain for anti-vWF. This indicated the specificity of anti-vWF to endothelial cells and that the HUVECs were indeed of an endothelial nature.

Glucose uptake was investigated for two reasons. Firstly, glucose uptake was determined for experimental reasons to determine if the medium needed to be changed on a daily basis. Secondly, to determine whether glucose uptake was increased in cells exposed to higher concentrations of glucose.

The kit used to determine glucose concentrations in the media were the hexokinase kit. This kit was based on the reaction shown in Figure 57.

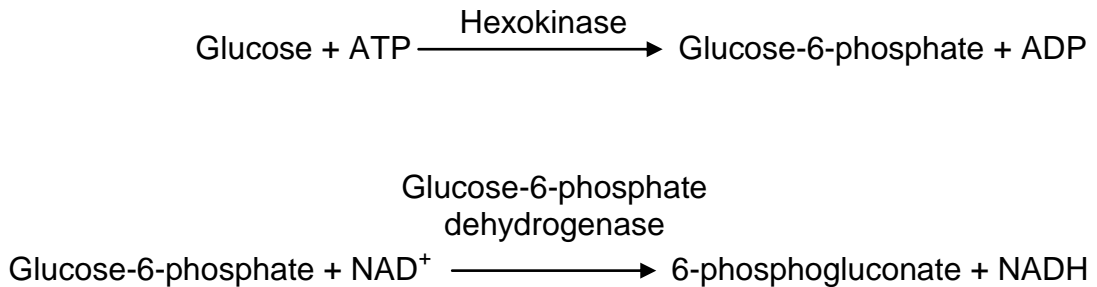


Figure 57: Shows the overall reaction for the hexokinase kit. The kit measures the production of NADH at 340nm which is proportional to the glucose concentration.

The reaction measured glucose concentration at 340nm based on the conversion of NAD to NADH which is directly proportional to the glucose concentration.

Glucose uptake for cells exposed to NG medium was measured at 96 pmoles/10⁶cells/min. This value was in close agreement with values in the literature. Glucose uptake assessed using the hexose uptake assay for bovine aortic endothelial cells ranged from 20 to 60 pmoles/10⁶cells/min (Alpert *et al.*, 2002, Alpert *et al.*, 2005). When glucose uptake for cells exposed to HG medium was measured using the hexokinase kit, glucose uptake was found to be 192 pmoles/10⁶cells/min. Again this compared to values in the literature, which ranged from 60 to 125 pmoles/10⁶cells/min for bovine aortic endothelial cells (Alpert *et al.*, 2002). The small differences may be due to different cell types and also due to different kits used to measure glucose uptake. Despite the differences in the values, the data agrees with the literature and confirms that cells cultured in higher concentrations of glucose utilise more glucose. Overall, it is concluded that the utilisation of glucose is two fold higher in cells exposed to 22mM compared with 5.5mM glucose.

The effect of HG on proliferation was also compared by measuring population doubling levels for cells exposed to NG, HG and AG. It was found that the growth rate for cells exposed to HG and AG was slightly lower than cells exposed to NG. There are a number of possible reasons for this decrease. A number of studies showed that following exposure to HG, there are increases in senescence and apoptosis (McGinn *et al.*, 2003, Hayashi *et al.*, 2006). Furthermore, studies by Abraham *et al.*, (2003) showed that heme oxygenase-1, which enhances cell growth, was decreased in cells exposed to HG. Moreover, McGinn *et al.*, (2003) and Chen *et al.*, (2007) showed that HG exposure led to altered cell cycle progression. In addition, Chen *et al.*, (2007) showed that human umbilical vein endothelial cells exposed to HG arrested in the G₀G₁ phase of the cell cycle. This was shown to be due to increased expression of p15^{INK4b}. The activity of this cyclin-dependent kinase inhibitor was itself dependent on oxidative stress as it was alleviated by the addition of the antioxidant N-acetylcysteine.

3.5.2 Optimisation of telomere length measurement using Southern blotting and STELA

Prior to performing the experiments aimed at investigating the effect of HG on telomere attrition, the Southern blotting method was optimised. This involved investigating the optimal concentration of cells to use for each experiment when using extracted DNA or using DNA that was released from cell, within agarose plugs. It was found that when DNA was extracted using the QIAGEN DNA extraction kit the optimal number of cells to use was 1x10⁶. This number of cells provided 1.8µg of DNA. For Southern blotting, it is recommended to use between 1-2µg of DNA per well. When analysing the optimal numbers of cells to use in each plug, three different concentrations of cells were used and it was concluded that 1x10⁶ cells in each lane was a sufficient number to use.

The next step compared the two different techniques of running DNA on a gel. It was decided that despite two plugs not digesting, plugs would be used to assess telomere length and heterogeneity simply due to higher median and SIR values. The reason for longer telomeres was thought to be due to the technique of plugs being gentler on the cells resulting in fewer DNA breaks being introduced. In addition, as the coefficient of variation was always below 3% when using 5 or 6 repeats, it was decided that this was a feasible number of repeats to use. Due to incomplete digestion of the DNA within plugs, different digestive enzymes and different volumes of these enzymes were investigated. It was found that there was little difference in the digestion of the DNA when using either just one enzyme, or when using a combination of enzymes. It was therefore decided that 60 to 80 units of Hinf1 alone would be used for each digestion.

Once the Southern blotting method was better optimised, the next stage was to optimise the STELA method. This was a new technique to the Department so a number of preliminary experiments were performed mainly centred on the initial PCR step. The optimum concentrations of dNTPs and magnesium chloride were evaluated, as well as the optimum concentration of DNA to use. Furthermore, a different probe was developed – ‘the telomere adjacent probe’ (see section 3.4.4.4 for further explanation). The development of this probe was not straightforward and a number of problems arose during the amplification and the purification of this probe. However, when these issues were overcome and the probe was successfully developed, it was found to be a lot more efficient and yielded much better results than the telomere probe.

3.5.3 Effect of HG and AG on telomere attrition

Once Southern blotting and STELA were optimised, telomere attrition was compared in HUVECs cultured in NG, HG and AG medium. Southern blotting showed that when HUVECs were exposed to NG, HG or AG over a number of passages, the mean rate of telomere loss decreased. However,

the rate of telomere loss decreased more rapidly in HUVECs cultured in medium containing HG or AG.

When telomere length was analysed by STELA, these once again showed a decrease in telomere length over passage number as expected. STELA showed that telomere length decreased more rapidly in cells exposed to HG or AG. However, the decrease in telomere length was more apparent in the HUVECs exposed to AG than in cells exposed to HG.

Telomere shortening occurs in the NG control due to the 'end replication problem' and therefore telomere loss occurs after each cell division (Lansdorp, 2005). However, the rate of shortening is increased in HUVECs cultured in HG medium. One reason for this decrease in telomere length in HUVECs cultured in HG medium may be due to increased oxidative stress. This predominately affects the guanine molecules within DNA (Kawanishi and Oikawa, 2004). Furthermore, oxidative stress is believed to increase the number of S1 nuclease sensitive sites in telomeres (von Zglinicki *et al.*, 2000). S1 nuclease is a single-stranded specific nuclease and causes double strand breaks (von Zglinicki *et al.*, 2000). Increased S1 nuclease sites in telomeres result in increased breakdown of the telomeres (von Zglinicki *et al.*, 2000). AG has been shown to lead to increased apoptosis, and increased oxidative stress compared to cells exposed to NG and HG (Risso *et al.*, 2001). It was therefore thought that AG may lead to increased telomere shortening. When analysing the mean telomere length, the results showed this trend. In the literature, the average decrease in telomere loss for human cells is generally between 50 to 200 base pairs per population doubling (Lansdorp, 2000). Therefore, the median telomere loss for HUVECs exposed to NG obtained from this experiment was generally within this range for both methods (Southern blotting and STELA). These novel data proposes that in conditions where cells are exposed to either constant or intermittent high glucose such as in diabetes, telomere shortening will occur more rapidly and therefore the cells will age quicker and enter senescence earlier.

In addition, when the SIR was analysed using Southern blotting and STELA it decreased with each passage/cell division in culture. SIR measures the spread of data and gives an indication of telomere length heterogeneity. It was previously shown that the SIR increased over passage number and was more rapid when human endothelial cells were exposed to increased oxidative stress caused by exposure to *tert*-butyl hydroperoxide (Kurz *et al.*, 2004). The reason for the increase in SIR following increased ROS exposure was believed to be due to alternative lengthening of telomeres (ALT) however, this mechanism was not confirmed or refuted in this paper (Kurz *et al.*, 2004). The results in this thesis do not support the data shown by Kurz *et al.*, (2004) and show that the overall trend of the SIR was to decrease. In addition, Southern blotting showed that the SIR decreased even more rapidly for HUVECs cultured in HG or AG medium (shown to lead to increased oxidative stress) compared to HUVECs cultured in NG medium. This decrease may be due to selection of a certain cell type(s) which is somehow more rapid in the presence of increased glucose. It is also important to remember that the SIR was looked at only over ~6 cumulative population doubling levels whereas Kurz *et al.*, (2004) investigated the SIR over 20 to 25 cumulative population doublings.

The telomere attrition rates in HUVECs were reasonably dissimilar when they were analysed using Southern blotting and STELA. For example, HUVECs exposed to NG medium, showed a telomere loss rate of 170 bp/pd when the samples were analysed using Southern blotting. When the same samples were analysed using STELA, telomere loss rates were much lower (80 bp/pd). Telomere loss rates in HUVECs exposed to HG and AG medium were also lower when analysis was performed using STELA compared to Southern blotting. Another difference between the two methods was Southern blotting showed HG medium had the greatest effect on the telomere loss rate, whereas STELA showed that AG had the greatest effect on the telomere loss rate. A possible explanation for the difference in telomere attrition rates is Southern blotting measures telomere length from total DNA (all chromosomes) whereas STELA only measures telomere

lengths from the XpYp chromosome. It is possible that certain telomeres are more susceptible to oxidative damage therefore telomere attrition rates may vary between chromosomes. When the two techniques are compared in terms of ease, cost and time of analysis, STELA is significantly more difficult and complicated to perform. As STELA requires at least 5 individual PCR reactions for every sample, this means that at least 5 times as many STELAs are performed for each sample. For example, 20 samples would require 1 Southern blot or 5 STELAs. In addition, Southern blotting only takes 3 days to perform whereas the STELA process takes 5 days to perform as a ligation and PCR step are required with STELA. This too increases the complexity of the method and increases the cost of performing STELA. However, despite the numerous disadvantages of STELA, it does appear however to yield realistic values and also provides data which is much easier to analyse. Moreover, it does produce data applicable to telomere lengths of specific chromosomes.

3.5.4 Effect of HG and AG on ROS production in HUVECs

To try to understand if telomere shortening was due to oxidative stress, H₂O₂ production was monitored in HUVECs exposed to HG or AG at various timepoints and with the use of different inhibitors. This analysis was performed using the Amplex Red assay. This assay is highly specific and sensitive for the detection of H₂O₂ (Rinaldi *et al.*, 2007). However, because Amplex Red can not diffuse through cell membranes, it can only measure extracellular hydrogen peroxide (Muller *et al.*, 2004). This does not pose a great problem as hydrogen peroxide is much more stable than superoxide and readily diffuses through lipid membranes (Messner and Imlay, 2002). This assay is commonly used to measure H₂O₂ production in phagocytic cells as these cells generate large amounts of hydrogen peroxide (Mohanty *et al.*, 1997). However, this assay has been used to measure hydrogen peroxide in cells that generate smaller amounts of hydrogen peroxide such as endothelial cells (Parinandi *et al.*, 2003; Brevig *et al.*, 2006).

Firstly, when H_2O_2 was measured in HUVECs, it was found to be two fold higher in cells treated with HG for 1 hour than in NG treated cells. The reason for this increase may be due to increased metabolism of glucose and increased electron leakage from complex I and complex III of the electron transport chain. As a positive control, HUVECs were exposed to NG and menadione and H_2O_2 production increased greatly in these conditions. Menadione is a quinone and when it enters cells it is reduced to a semiquinone. Semiquinones have a high affinity for the oxygen molecule and reduce oxygen to superoxide anion which in turn causes the regeneration of the quinone molecule (Hollensworth *et al.*, 2000). This leads to a cycle which generates large amounts of superoxide and is termed 'redox cycling' (Zielonka *et al.*, 2006). The superoxide molecules are then converted to H_2O_2 by spontaneous dismutation or enzymatically by superoxide dismutase (Thor *et al.*, 1982, Hollensworth *et al.*, 2000). HUVECs treated with NG and NAC or HG and NAC showed a decrease in H_2O_2 production compared to their controls. NAC is an antioxidant which reduces ROS in cells. NAC can directly scavenge free radicals however due to a lower rate constant than antioxidant enzymes such as catalase and superoxide dismutase this is unlikely to be the primary route for reducing ROS (Jones *et al.*, 2003). It has been proposed that the main way in which NAC reduces ROS is by acting as a precursor for glutathione (Atkuri *et al.*, 2007). NAC is converted to L-cysteine which is then incorporated into glutathione. Glutathione acts as a coenzyme for glutathione peroxidase and reduces the amount of H_2O_2 in the cell (Zafarullah *et al.*, 2003; Satpute *et al.*, 2008).

H_2O_2 production was lower in cells treated with NG and TTFA or HG and TTFA compared to their corresponding controls. TTFA is an inhibitor of complex II of the electron transport chain suggesting that the origin of increased ROS when cells are in hyperglycaemic conditions is from the mitochondrial electron transport chain (Yamagishi *et al.*, 2001). However, the exact source of superoxide production within the electron transport chain can not be determined from this data.

Lastly, when HUVECs cultured in NG were treated with 3-O-methylglucose (which is not metabolised by cells) or mannitol (an osmotic control) there was no significant increase in H₂O₂ concentration. These two compounds confirmed that the increase in ROS observed when cells were being cultured in HG was due to the additional glucose being metabolised and not an osmotic or chemical phenomenon.

ROS production was also determined for HUVECs cultured in either NG or HG for 24 hours. In both conditions, ROS production generally increased over 24 hours. The reason for this general increase is unknown and it would be interesting to investigate whether H₂O₂ continued to rise after 24 hours. Yu *et al.*, (2006) showed that ROS production in clone 9 cells exposed to high glucose fluctuated over a period of 24 hours. There was an initial peak of ROS production followed by a steady increase of ROS. This then decreased at 18 hours and at 24 hours ROS was observed at levels similar to those seen at 0 hours (Yu *et al.*, 2006). Similar observations were made in this thesis where H₂O₂ increased at 3 hours but at 6 hours returned to similar levels seen in cells exposed to NG. The reason why this occurs is unclear but it may be that some antioxidant enzymes are up regulated and this reduces the amount of H₂O₂ produced or present within the cells.

H₂O₂ production was then observed over an extended period of a number of days. HUVECs exposed to NG showed a slight increase in H₂O₂ supporting the effect seen over a 24 hour period. As there was a slight increase in H₂O₂ over 10 days, it suggests that oxidative stress increases with time in culture. HUVECs exposed to HG and AG showed a significant increase in H₂O₂ over 10 days indicating the possible long term effects that increased glucose levels have on ROS production. HUVECs exposed to AG medium showed higher levels of H₂O₂ production when measurements were made after HUVECs were exposed to medium containing HG for 24 hours. This suggests that HG still has the greater effect on ROS production. This also suggests that exposure to NG and then HG medium could lead to

fluctuating production of ROS which may have more damaging effects on cells than constant levels of increased ROS production.

3.5.5 Role of ROS and mitochondrial function on telomere attrition

To determine if increased telomere loss was due to increased ROS production, HUVECs were treated with either NAC or TTFAs when cultured in NG, HG or AG medium. Telomere length was then assessed using STELA. It was found that when HUVECs were cultured in HG or AG with either NAC or TTFAs (both shown to reduce ROS in HUVECs treated with high glucose), telomere loss was reduced to levels similar to those seen in NG treated HUVECs. These results suggested reducing ROS levels reduced telomere shortening rates. Furthermore, the TTFAs data suggested that telomere shortening occurred through increased production of ROS specifically from the mitochondrial electron transport chain. Oxidative stress is believed to cause this shortening through damage to the guanines within the TTAGGG repeat (Oikawa and Kawanishi, 1999) and by increasing the number of single strand breaks within telomeric DNA (Li *et al.*, 2005). Furthermore, increased oxidative stress is thought to lead to increased telomere uncapping. Voghel *et al.*, (2008) showed similar results when they analysed the effect of NAC on telomere length and cellular senescence. NAC slightly shortened telomere attrition rates in human endothelial cells. However, telomere length was not analysed in cells cultured in HG medium (the cells used were 'diseased') and telomere length was analysed using Southern blotting and not STELA.

In conclusion, this chapter shows that in HUVECs exposed to HG caused telomere shortening through increased ROS predominantly arising from the mitochondrial electron transport chain. Furthermore, by using STELA, AG appeared to have even more damaging effects on telomere attrition rates than HG alone.

4 Induction of a pro-inflammatory phenotype in endothelial cells by HG and mtDNA depletion

4.1 Introduction:

4.1.1 Mitochondrial ROS production and DNA damage

Mitochondria are present within eukaryotic cells and their primary function is to synthesise energy through the electron transport chain and oxidative phosphorylation (Falkenberg *et al.*, 2007). Each mitochondrion contains 2 to 10 copies of circular double stranded DNA (Falkenberg *et al.*, 2007). The DNA encodes for 13 of the approximate 90 polypeptides that make up the electron transport chain, 2 rRNA molecules and 22 tRNA molecules (Asin-Cayuela and Gustafsson, 2007). An overview of the electron transport chain is detailed in section 1.2.2.

Some cells, including endothelial cells, make a large proportion of their energy through glycolysis (Davidson and Duchon, 2007). Despite this, mitochondria are still thought to play a major role in ROS production (Davidson and Duchon, 2007).

Mitochondria have been increasingly shown to play a major role in the progression of many cardiovascular diseases (Ramachandran *et al.*, 2002; Watson *et al.*, 2001; Glass and Witzturn, 2001). Over the last few years, a number of the complications that occur as a result of diabetes such as lactic acidosis and myoclonic epilepsy have been linked to mutations within the mitochondrial genome (Kennedy *et al.*, 1998). Mutations in the mitochondrial genome caused by increased ROS leakage lead to reduced mitochondrial function including insufficient ATP production. This in itself may be a major factor in the progression of many cardiovascular diseases (Piechota *et al.*, 2006). Therefore, a number of studies are now focussing on looking at how mitochondrial mutations can lead to these complications.

4.1.2 Markers of a pro-inflammatory phenotype in endothelial cells

4.1.2.1 Nitric oxide

Nitric oxide is a gaseous cellular messenger (Yetik-Anacak and Catravas, 2006). One main recognised function of nitric oxide is to control vascular homeostasis. It mediates the balance between vasoconstriction and vasodilation and ultimately controls blood pressure through its effect on vascular smooth muscle cyclic guanosine monophosphate (cGMP) (Vanhoutte, 2002).

Nitric oxide is synthesised from the amino acid L-arginine (Drew and Leeuwenburgh, 2002). The reaction is catalysed by one of the three nitric oxide synthases (NOS) (Yorek, 2003). nNOS also known as NOS1 is predominantly found in neuronal tissue, iNOS also known as NOS2 is inducible in a wide range of cells and tissues, and eNOS also known as NOS3 is the constitutive isoform found in vascular endothelial cells (Alderton *et al.*, 2001). Cardiovascular diseases and vascular ageing are both associated with reduced nitric oxide production by the endothelium with important consequences for vascular function (Yetik-Anacak and Catravas, 2006; Yu and Chung, 2001; Brandes *et al.*, 2005).

4.1.2.2 eNOS

eNOS is regulated at both the transcriptional and posttranscriptional level (Dudzinski and Michel, 2007). eNOS mRNA is controlled at a basal level by numerous factors such as shear stress within the blood vessels. A number of shear stress elements in the promoter region have been identified such as the shear-responsive element (GAGACC) ~990 bp upstream of the eNOS transcription start site (Searles, 2006). In addition, the promoter region also contains a number of other cis-elements such as activator protein 1 (AP-1) and activator protein 2 (AP-2) binding sites, Sp1 motifs, and a cAMP-responsive element (Govers and Rabelink, 2001). The activation of these elements can lead to up regulation of eNOS e.g. immunosuppressive

drugs such as cyclosporine A have been shown to up regulate eNOS by the activation of AP-1 (Navarro-Antolin *et al.*, 2000).

eNOS protein activity is controlled by a series of post-translational modifications (Dudzinski and Michel, 2007). The first modification that occurs is acylation. eNOS is initially targeted to caveolae which are cholesterol-enriched microdomains (Shaul, 2003). This prevents the activation of the eNOS enzyme (Garcia-Cardena *et al.*, 1997). Dual acylation (N-myristoylation and S-palmitoylation) inactivates eNOS by anchoring the enzyme firmly to the caveolar lipid bilayer (Fernandez-Hernando *et al.*, 2006). Secondly, binding of calmodulin to eNOS disrupts the caveolin-eNOS interaction and ultimately leads to the activation of eNOS (Takahashi and Mendelsohn, 2003). Furthermore, eNOS activity is also affected by phosphorylation and de-phosphorylation. Phosphorylation at Ser 1177 and Ser 633 stimulates the activity of eNOS whereas phosphorylation at Thr 495 inhibits eNOS (Mount *et al.*, 2007).

Many diseases have been linked to changes in eNOS mRNA and protein levels. Atherosclerosis is associated with a decrease in the expression of eNOS (Albrecht *et al.*, 2003). Furthermore, eNOS gene expression and protein levels are increased in adipocytes of obese subjects (Elizalde *et al.*, 2000). Interestingly, hyperglycaemia has been linked to a decrease in eNOS expression (Srinivasan *et al.*, 2004).

4.1.2.3 ICAM1

Intercellular adhesion molecule 1 (ICAM1), is a transmembrane glycoprotein with a molecular mass ranging from 80 to 114kDa depending on the amount of glycosylation which is dependent on the cell type (Roebuck and Finnegan, 1999). Normally, ICAM1 is expressed constitutively at low levels on endothelial cells, monocytes and lymphocytes but the expression is increased following exposure to inflammatory cytokines such as tumour necrosis factor (TNF) α (Zhou *et al.*, 2006). It is involved in the trafficking of

inflammatory cells, microbial pathogenesis, and the adhesion of antigen-presenting cells to T lymphocytes (Hubbard and Rothlein, 2000).

4.1.3 Models of mtDNA damage or depletion

One of the most common methods of depleting mtDNA is treating cells with ethidium bromide, pyruvate and uridine creating a 'Rho0' cell line (Zmijewski *et al.*, 2005; Davis and Zou, 2005; Chandel *et al.*, 1998). Ethidium bromide inhibits mitochondrial transcription and mitochondrial replication (Piechota *et al.*, 2006). It inhibits both the γ and the mitochondrial polymerases in mitochondria and therefore reduces the amount of mtDNA within cells (Tarrago-Litvak *et al.*, 1978). For Rho0 cells to grow successfully, the media is supplemented with pyruvate and uridine. Uridine is synthesised by an enzyme present in the inner membrane of the mitochondria that requires mitochondrial electron transport for it to function efficiently. The mitochondrial electron transport chain is more inefficient in Rho0 cells and therefore for the cells to grow at a similar rate to control cells, the media is supplemented with uridine (King and Attardi, 1996). Pyruvate synthesis occurs by glycolysis and is a precursor of TCA cycle intermediates. It enters the TCA cycle ultimately resulting in the synthesis of ATP. However, in Rho0 cells, there is a dysfunctional respiratory chain and the normal processes that lead to NADH oxidation are reduced. Therefore, excess NADH is oxidised by the conversion of pyruvate to lactate which reduces the amount of pyruvate available to enter the TCA cycle. This ultimately leads to a reduction in ATP levels. Therefore, pyruvate is supplemented in the media to restore TCA cycling (King and Attardi, 1996).

Rho0 cells are commonly used to study the role of mitochondria in ROS production, ATP production and apoptosis in a given cell model. For example, Kennedy *et al.*, (1998) showed that ATP production was lower in INS-1 Rho0 cells and Walford *et al.*, (2004) looked at how apoptosis in bovine endothelial cells was affected when mtDNA levels were depleted. A number of studies have looked at ROS in Rho0 cells with conflicting results.

Vergani *et al.*, (2004) showed that ROS production fell in muscle and lung Rho0 cells but was not affected in bone Rho0 cells. Therefore, ROS in Rho0 appears to be dependent on not only the cell type but also on the method used to measure it (Table 13).

Table 13: Details the effect of depleting mtDNA on ROS release in different Rho0 cells. Shows a range of different methods used to measure ROS release.

Cell Type	ROS in Rho0 cells compared to the controls	Method	Reference
HUVEC	Greatly decreased	Dichlorofluoroscein (DCF)	Ali <i>et al.</i> , 2004
HUVEC	No change	DCF	Yao <i>et al.</i> , 2005
HeLa	Increased	DCF	Miranda, 1999
HeLa	Decreased	Hydroethidine	Schauen, 2006
HeLa	No change	Aconitase activity	Schauen, 2006
143B human osteosarcoma	Decreased	Amplex Red	Vaux, 2001

Depleting cells of mtDNA using ethidium bromide is not always optimal as it can also affect the expression of a number of nuclear genes (Singh *et al.*, 2005). Therefore, a number of other different agents have been used to deplete mtDNA or protein. Chloramphenicol was used to study the effects on apoptosis when mitochondrial protein expression was inhibited (Ramachandran *et al.*, 2002, Li *et al.*, 2005). In addition, a number of nucleoside reverse transcriptase inhibitors (NRTIs) have been found to affect mtDNA concentrations. NRTIs are used to treat HIV but after long term treatment cause a number of adverse effects including lactic acidosis, pancreatitis and are linked to mitochondrial toxicity (Birkus *et al.*, 2002). Two of the NRTIs have been shown to have a greater effect on mtDNA. These are dideoxycytidine (ddC) and dideoxyinosine (ddI) (Lund *et al.*, 2007).

4.2 Aims

The first aim of this chapter was to analyse if HG and AG had an effect on endothelial cell mtDNA content and to investigate whether effects were mediated by increased ROS production. Furthermore, to analyse if HG and AG alter eNOS and ICAM1 protein expression in HUVECs. Subsequently, to investigate whether changes in these endothelial cell pro-inflammatory markers occurred following a reduction in the mtDNA content.

4.3 Experimental Approach

4.3.1 Treatment of endothelial cells in culture

Early passage HUVECs were cultured as detailed in section 2.2.1. Ethidium bromide was added to the cell medium at a concentration of 10ng/ml. Chloramphenicol was added to the cell culture medium at a concentration of 20µg/ml. ddC was used at concentrations of 2, 5, 10 and 15µM. NAC and TTFA were added to the cell culture medium at concentrations of 3mM and 25µM respectively. 3-O-methylglucose was added to NG medium at a concentration of 16.5mM.

4.3.2 Real time PCR

HUVECs were cultured in NG, HG, AG, HG with NAC or HG with TTFA for 8 passages. The cells were trypsinised at each passage, and 50% of the cells were taken for analysis. The DNA was extracted using a Qiagen DNA extraction kit detailed in section 2.2.4.1 and then quantified as detailed in section 2.2.4.2. mtDNA was measured using real time PCR as detailed in section 2.2.9.1.

HUVECs were also cultured in either ethidium bromide or ddC for up to 20 days. The cells were trypsinised, and the DNA was extracted using the Qiagen DNA extraction kit detailed in section 2.2.4.1 and then quantified as

detailed in section 2.2.4.2. Real time PCR for mtDNA was then performed which is detailed in section 2.2.9.1.

4.3.3 Western blotting

HUVECs were cultured in the presence of NG medium, HG medium or AG medium. The cells were taken at between passages 0 and 7 and the protein was extracted via sonication (as detailed in section 2.2.8.1). The protein was quantified using the Bradford assay detailed in section 2.2.7.3. Once quantified, 20 or 30µg of protein was loaded into each well and SDS-PAGE and Western blotting were performed (section 2.2.8.1). The membranes were probed with anti-eNOS (dilutions between a 1 in 250 and a 1 in 4167) or anti-ICAM1 (dilutions between a 1 in 200 and a 1 in 1333). Each membrane was stripped (section 2.2.8.2) and re-probed with anti- α -tubulin (dilutions between a 1 in 10000 and a 1 in 30000) to assess equal protein loading per well and to facilitate semi-quantitation of Westerns.

Similar Westerns for eNOS (a 1 in 1000 dilution for 20µg of protein or a 1 in 3000 dilution for 30µg of protein), ICAM1 (a 1 in 400 dilution for 20µg of protein or a 1 in 1000 dilution for 30µg of protein), COX1 (a 1 in 500 dilution) or COXIV (a 1 in 1000 dilution) were performed following culture of HUVECs with ethidium bromide, chloramphenicol or ddC.

4.3.4 Amplex Red assay for measuring H₂O₂ production

Control and Rho0 HUVECs were exposed to NG medium, HG medium, menadione in NG medium, HG medium with NAC, HG medium with TTFA or NG medium with 3-O-methylglucose for 1 hour. The Amplex Red assay was then used to measure H₂O₂ production as detailed in section 2.2.7.

4.4 Results

4.4.1 Effect of HG and AG on mtDNA content in HUVEC cultures and the role of ROS

4.4.1.1 Effect of HG and AG on mtDNA content

The effect of HG and AG on mtDNA content was analysed using real time PCR. mtDNA content generally decreased over 8 passages when HUVECs were exposed to high glucose (Figure 58). After 8 passages of treatment with HG the mtDNA content decreased by ~35% however this was not statistically significant. There was also a trend for mtDNA content to decrease slightly over 8 passages when HUVECs were exposed to AG (Figure 59) although this did not reach statistical significance. However, the decrease in mtDNA content was less pronounced than for the cells exposed to near-constant HG.

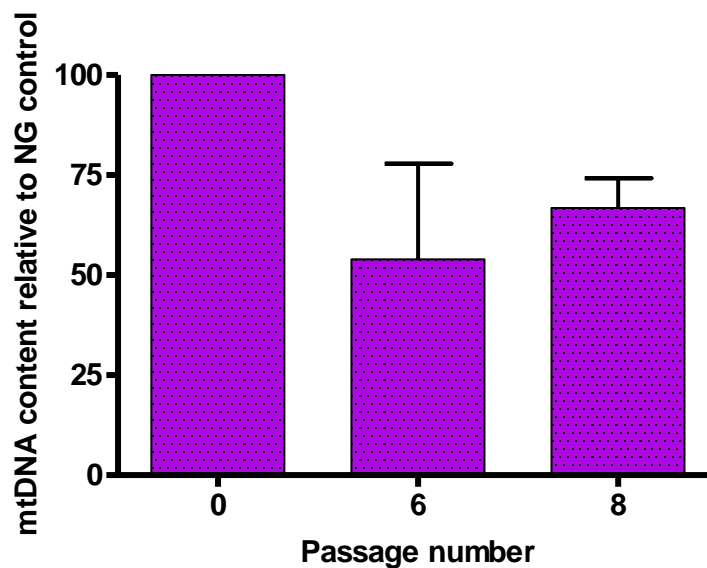


Figure 58: mtDNA content in HUVECs following exposure to HG over a number of passages. HUVECs were cultured for up to 8 passages in the presence of HG and samples of cells were taken at 0, 6 and 8 in order to assess mtDNA content by QPCR. All values are relative to mtDNA within NG treated cells. Values are mean +SEM, n=3.

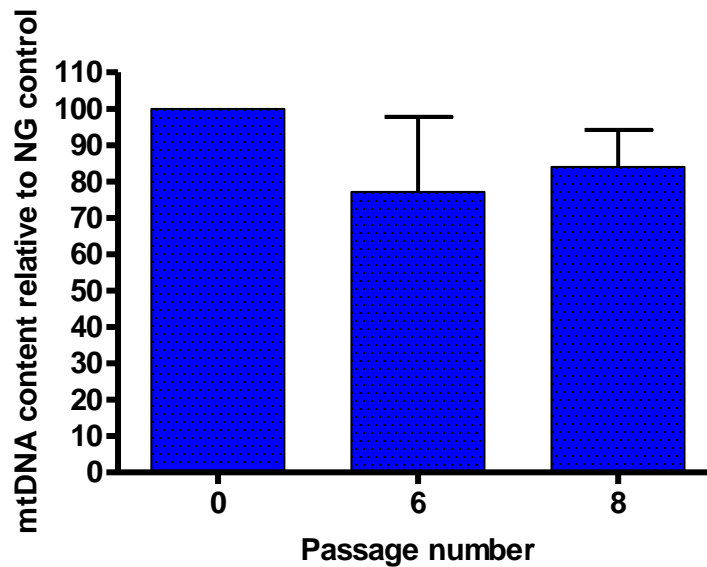


Figure 59: mtDNA content in HUVECs following exposure to AG over a number of passages. HUVECs were cultured for up to 8 passages in the presence of AG and samples of cells were taken at 0, 6 and 8 in order to assess mtDNA content by QPCR. All values are relative to mtDNA within normal glucose treated cells. Values are mean +SEM, n=3.

4.4.1.2 Effect of NAC or TTFA on mtDNA content changes induced by high glucose

In order to provide evidence that the decrease in mtDNA content was due to the production of ROS, HUVECs were exposed to HG in the presence of the antioxidant NAC or the electron transport chain inhibitor TTFA. Figure 60 and 61 show that when HUVECs were exposed to HG and NAC or HG and TTFA, mtDNA content increased over 8 passages when compared relative to mtDNA content within HG treated cells at the same passage. Within 8 passages, the mtDNA content in HUVECs exposed to HG with NAC increased by 30 to 40%. When HUVECs were exposed to HG and TTFA in 8 passages the increase in mtDNA content was about 50%, although changes were not statistically significant. Nevertheless, these data suggest that both NAC and TTFA were able to reverse the loss of mtDNA induced by the growth of HUVECs in HG.

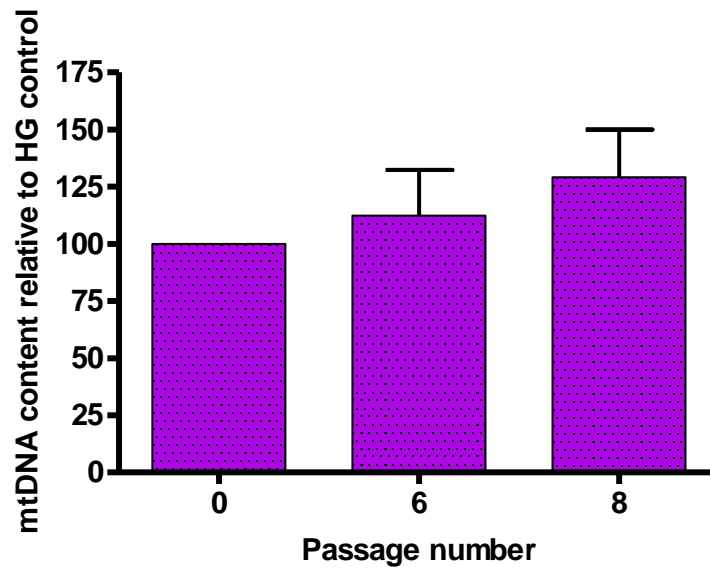


Figure 60: mtDNA content in HUVECs following exposure to HG and NAC over 8 passages. HUVECs were cultured for up to 8 passages in the presence of HG and NAC and samples of cells were taken at 0, 6 and 8 in order to assess mtDNA content by QPCR. All values are relative to mtDNA within HG treated cells. Values are mean +SEM, n=3.

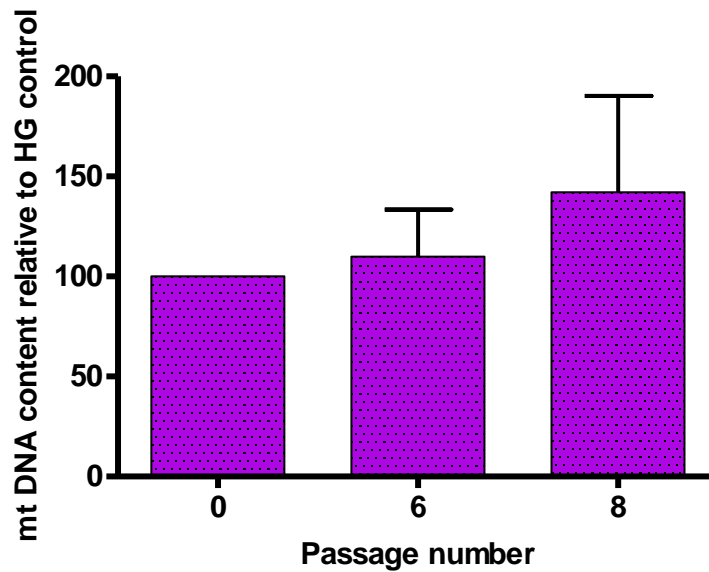


Figure 61: mtDNA content in HUVECs following exposure to high glucose and TTFA over 8 passages. HUVECs were cultured for up to 8 passages in the presence of HG and TTFA and samples of cells were taken at 0, 6 and 8 in order to assess mtDNA content by QPCR. All values are relative to mtDNA within HG treated cells. Values are mean +SEM, n=3.

4.4.2 Effect of high glucose and alternating glucose on the expression of eNOS and ICAM1

4.4.2.1 Optimisation of Western blotting for eNOS, ICAM1, and α -tubulin

One of the main aims was to analyse if HG and AG had an effect on the protein expression of two markers of endothelial dysfunction – eNOS and ICAM1. This was determined using Western blotting. However, before these Westerns were undertaken, the dilutions of the primary antibodies to eNOS and ICAM1 required optimisation. In addition, the loading control (anti- α -tubulin) was also optimised. These antibodies were optimised for both 20 μ g and 30 μ g of cell lysate protein per well. Examples of the Western blots over a range of dilutions are shown in Figure 62 to Figure 67.

The first primary antibody that was optimised was eNOS. A protein band for eNOS was observed at ~135kDa. When 30 μ g of protein was loaded into

each well, the optimum conditions were a 1 in 3000 dilution (0.08 μ g/ml) of eNOS primary antibody overnight at 4°C, and a 1 in 10000 dilution of the secondary rabbit anti-mouse antibody (0.2 μ g/ml) for 1 hour at room temperature (Figure 62). When 20 μ g of protein was loaded into each well, the optimum conditions were a 1 in 1000 dilution (0.25 μ g/ml) of the eNOS primary antibody overnight at 4°C and a 1 in 10000 dilution of the secondary rabbit anti-mouse antibody for 1 hour at room temperature (0.2 μ g/ml) (Figure 63).

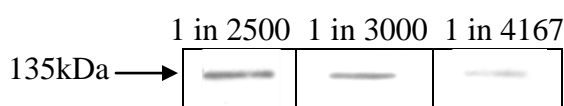


Figure 62: Effect of different primary antibody dilutions on eNOS band intensity. 30 μ g of protein from HUVEC lysates were loaded in each well of an SDS-PAGE gel. The protein was separated via electrophoresis and analysed by Western blotting (section 2.2.8). The membrane was incubated with the primary antibody overnight at 4°C, followed by the rabbit anti-mouse secondary antibody (1 in 10000 dilution) for 1 hour at room temperature.



Figure 63: Effect of different primary antibody dilutions on eNOS band intensity. 20 μ g of protein from HUVEC lysates were loaded in each well of an SDS-PAGE gel. The protein was separated via electrophoresis and analysed by Western blotting (section 2.2.8). The membrane was incubated with the primary antibody overnight at 4°C, followed by the rabbit anti-mouse secondary antibody (1 in 10000 dilution) for 1 hour at room temperature.

As ICAM1 is expressed at low levels in endothelial cells, lysates of Raji cells (a cell type that expresses this marker constitutively) were used to optimise

the Western blot. When 30µg of protein was loaded into each well, the optimum conditions were a 1 in 1000 dilution (0.2µg/ml) of the ICAM1 primary antibody overnight at 4°C and a 1 in 10000 dilution of the secondary goat anti-rabbit antibody (0.2µg/ml) for 1 hour at room temperature (Figure 64). However, HUVECs also showed a weak band at 110kDa using the same antibody dilutions. Therefore, ICAM1 primary antibody was optimised for 20µg of protein using HUVEC lysate. When 20µg of protein was loaded into each well, the optimum conditions were a 1 in 400 (0.5µg/ml) of the ICAM1 primary antibody overnight at 4°C and a 1 in 10000 dilution of the secondary goat anti-rabbit antibody (0.2µg/ml) for 1 hour at room temperature (Figure 65).

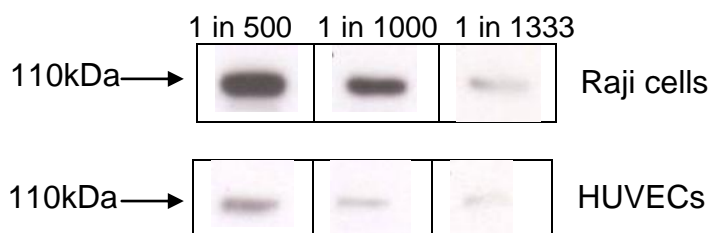


Figure 64: Effect of different primary antibody dilutions on ICAM1 band intensity. 30µg of protein from Raji and HUVEC lysates were loaded in each well of an SDS-PAGE gel. The protein was separated via electrophoresis and analysed by the use of Western blotting (section 2.2.8). The membrane was incubated with the primary antibody overnight at 4°C, followed by the goat anti-rabbit secondary antibody (1 in 10000 dilution) for 1 hour at room temperature.

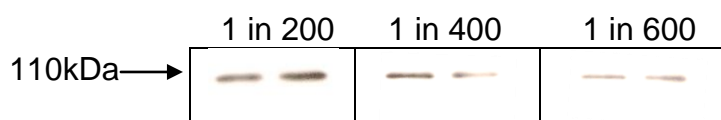


Figure 65: Effect of different primary antibody dilutions on ICAM1 band intensity. 20µg of protein from HUVEC lysates were loaded in each well of an SDS-PAGE gel. The protein was separated via electrophoresis and analysed by the use of Western blotting (section 2.2.8). The membrane was incubated with the primary antibody overnight at 4°C, followed by the goat anti-rabbit secondary antibody (1 in 10000 dilution) for 1 hour at room temperature.

The third primary antibody that was optimised was α-tubulin. This was used as a loading control for the eNOS and ICAM1 antibodies. When 30µg of protein was loaded into each well, the optimum conditions were a 1 in 30 000 dilution of α-tubulin primary antibody overnight at 4°C with a 1 in 40 000 dilution of the secondary rabbit anti-mouse antibody (0.05µg/ml) for 1 hour at room temperature (Figure 66). When 20µg of protein was loaded into each well, the optimum conditions were a 1 in 10 000 dilution α-tubulin primary antibody overnight at 4°C and a 1 in 20 000 dilution of the secondary rabbit anti-mouse antibody (0.1µg/ml) for 1 hour at room temperature (Figure 67).

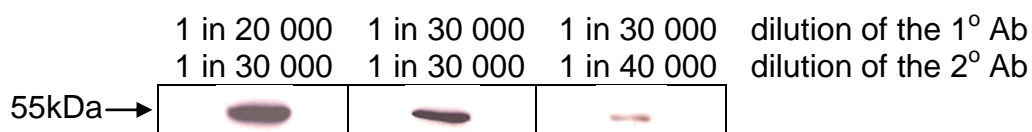


Figure 66: The different intensities of protein bands when a range of concentrations were used for the anti-α-tubulin antibody (Ab). 30µg of protein from HUVEC lysates were loaded in each well of an SDS-PAGE gel. The protein was separated via electrophoresis and analysed by the use of Western blotting (section 2.2.8). A 1 in 30 000 and a 1 in 40 000 dilution of the rabbit anti-mouse secondary antibody were tested.

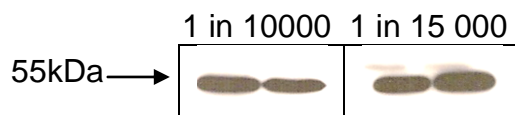


Figure 67: The different intensities of protein bands when a range of concentrations were used for the anti- α -tubulin antibody. 20 μ g of protein from HUVEC lysates were loaded in each well of an SDS-PAGE gel. The protein was separated via electrophoresis and analysed by the use of Western blotting (section 2.2.8). A 1 in 20 000 dilution of the rabbit anti-mouse secondary antibody was used.

Once the primary and secondary antibodies were optimised, eNOS and ICAM1 protein expression were analysed in HUVECs exposed to NG, HG and AG.

4.4.2.2 The effect of HG or AG on eNOS expression in HUVECs

eNOS protein expression was determined over 8 passages of HUVECs treated with HG (Figure 68). eNOS protein in NG treated HUVECs was maintained, whereas it decreased in cells exposed in HG or AG. eNOS expression for HUVECs exposed to NG was maintained at approximately 1.1 over 13 cumulative population doubling levels, whereas in HUVECs exposed to HG, eNOS expression at passage 0 was 1.0 and this decreased to ~0.7 at passage 8. An example Western is shown in Figure 68(A) and demonstrated graphically in Figure 68(B).

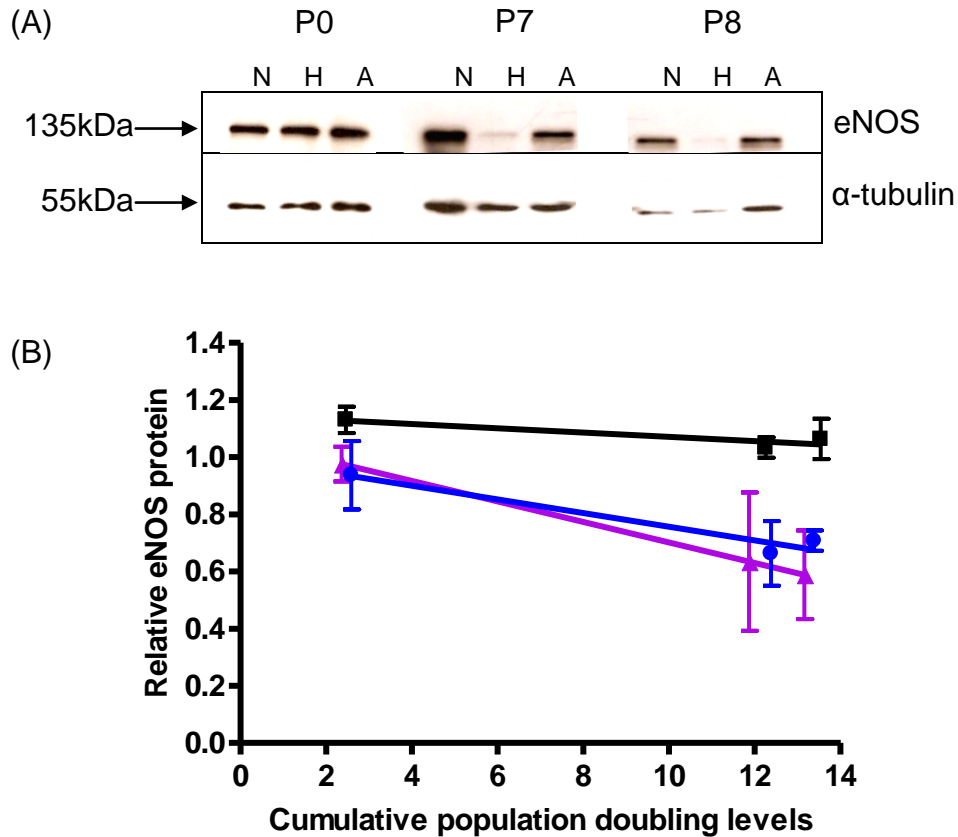


Figure 68: The effect of NG, HG or AG on eNOS expression. Protein lysate from HUVECs treated with NG, HG or AG were analysed on a SDS-PAGE gel, transferred and probed using the primary antibodies anti-eNOS and anti- α -tubulin. eNOS was measured by densitometry and expressed relative to α -tubulin. (A) An example of a Western blot obtained. N=normal glucose, H=high glucose, A=alternating glucose. (B) eNOS protein content in HUVECs over a number of cumulative population doubling levels when treated with either NG, HG or AG. Values are mean \pm SEM, n=3. Squares (■) NG. Triangles (▲) HG. Circles (●) AG.

4.4.2.3 The effect of HG and AG on ICAM1 expression in HUVECs

When HUVECs were analysed for ICAM1 protein expression, ICAM1 in cells exposed to NG was significantly lower at passage 8 (Figure 69). The ratio of ICAM1 to α -tubulin decreased from \sim 1.5 (SEM=0.17) to \sim 0.9 (SEM=0.09, $p < 0.05$) over the culture period (Figure 69(B)). In contrast, in HUVECs exposed to HG or AG, ICAM1 was maintained throughout the culture period. Although not statistically significant, there was a trend with

both HG and AG for the expression of ICAM1 to increase rather than decrease with exposure in culture (Figure 69(C) and (D)). An example of one of the Westerns is shown in Figure 69 (A) and is shown graphically in Figure 69 (B), (C) and (D).

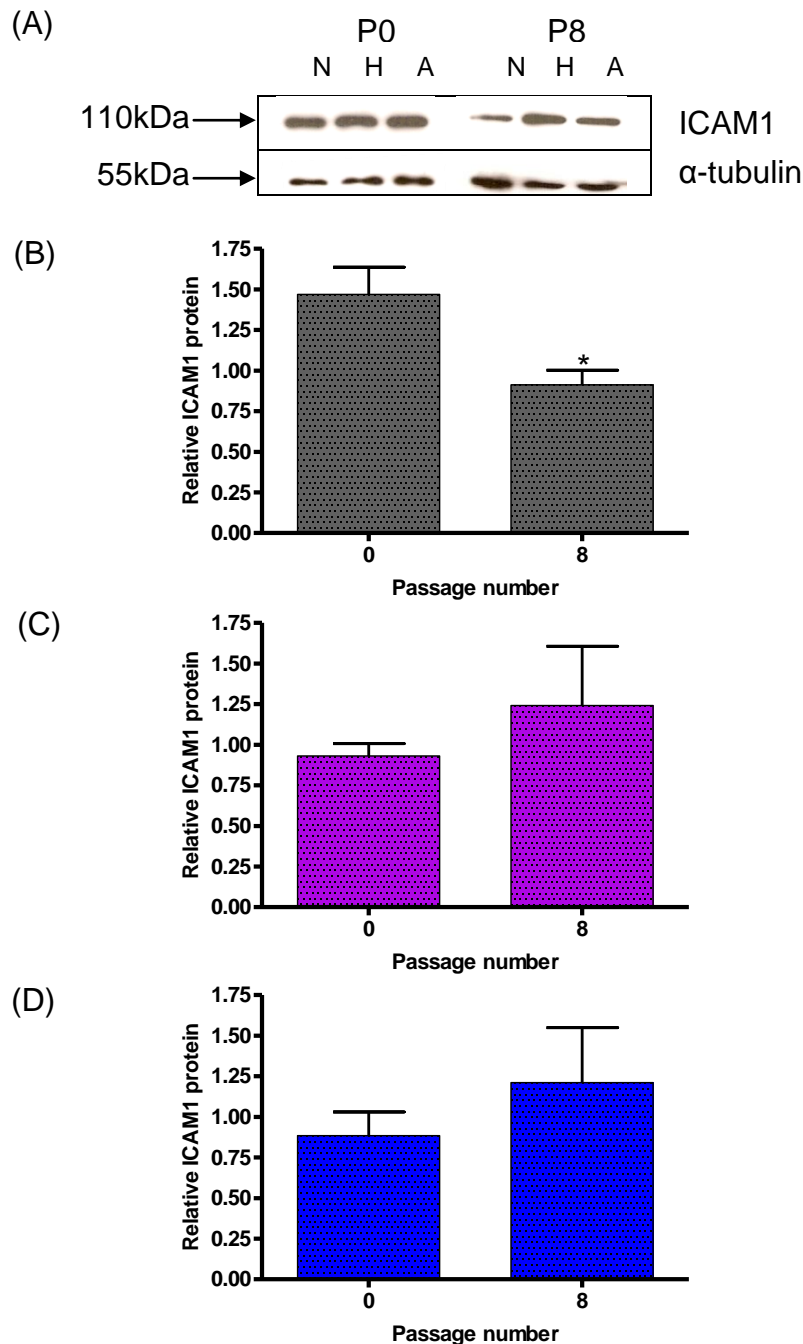


Figure 69: ICAM1 protein expression for HUVECs treated with NG, HG or AG. Protein lysate from HUVECs treated with NG, HG or AG were analysed on a SDS-PAGE gel, transferred and probed using the primary antibodies anti-ICAM1 and anti- α -tubulin. ICAM1 was measured by densitometry and expressed relative to α -tubulin. Values are mean +SEM, n=3. (A) An example of a Western blot obtained. N=normal glucose, H=high glucose, A=alternating glucose. (B) ICAM1 protein content in HUVECs at passage 0 and passage 8 when treated with NG. * $p < 0.05$. (C) ICAM1 protein in HUVECs at passage 0 and passage 8 when treated with HG. (D) ICAM1 protein in HUVECs at passage 0 and passage 8 when treated with AG.

4.4.2.4 The effect of NAC or TTFA on the expression of eNOS in HUVECs treated with NG and HG

The previous experiments had shown that eNOS protein levels tended to decrease and ICAM1 protein levels tended to increase in HUVECs exposed to HG or AG. To provide evidence for a role of ROS in such effects, HUVECs were cultured in medium containing HG or AG in the presence of NAC or TTFA. When HUVECs were cultured in NG, NG and NAC or NG and TTFA, eNOS protein levels were maintained over 7 passages (Figure 70). When HUVECs were exposed to HG, eNOS protein levels at passage 7 were similar to eNOS protein levels at passage 0 (Figure 71). However, when HUVECs were exposed to HG with NAC or TTFA, eNOS protein levels increased at passage 7 when compared to passage 0 i.e. before treatment. The mean expression of eNOS protein increased from 0.5 to 0.85 when cells were exposed to HG and NAC and from 0.5 to 0.9 when HUVECs were exposed to HG and TTFA (Figure 71). When HUVECs were exposed to AG (shown by Figure 72), relative eNOS protein decreased by about 0.1 unit. The increase in eNOS protein when HUVECs were exposed to AG and NAC was lower compared to cells exposed to HG and NAC (Figure 71 and Figure 72). Furthermore, when HUVECs were exposed to AG and TTFA, there was no increase in eNOS at passage 7.

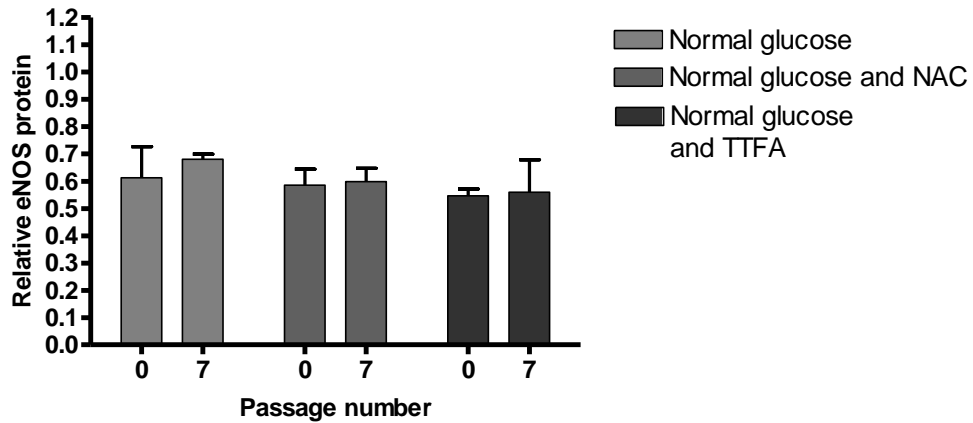


Figure 70: eNOS protein levels in HUVECs cultured in NG, NG and NAC or NG and TTFA. Cell lysates were separated by SDS-PAGE and Western blots performed using antibodies to eNOS and α -tubulin. eNOS protein levels were measured by densitometry and expressed relative to α -tubulin when HUVECs were treated with NG, NG and NAC or NG and TTFA at passage 0 and passage 7. The data are represented graphically. Values are mean +SEM, n=3.

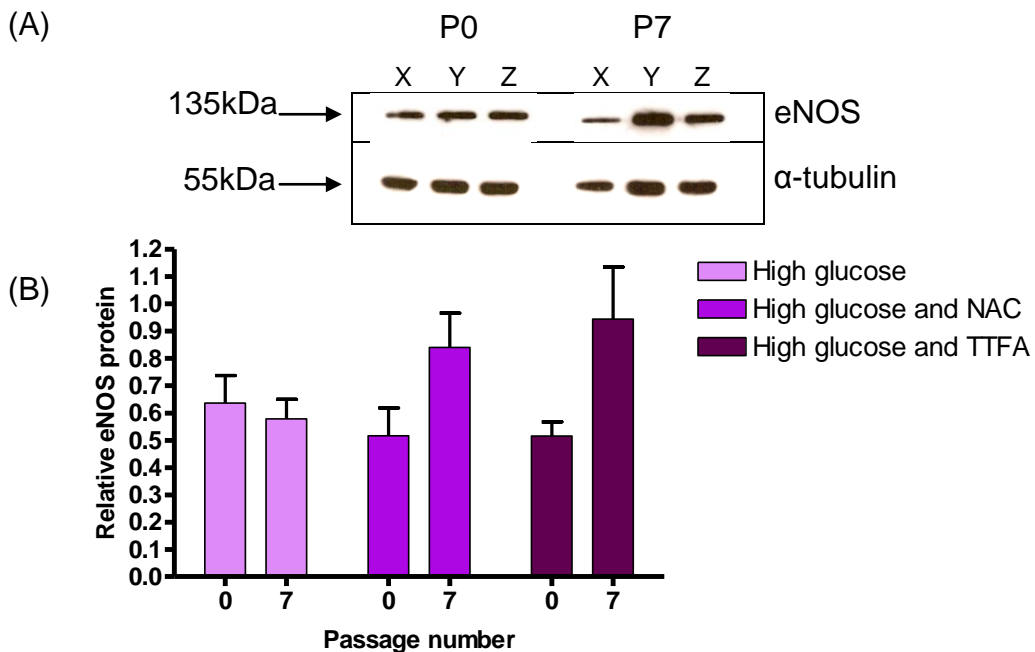


Figure 71: eNOS protein levels in HUVECs cultured in HG, HG and NAC or HG and TTFA. Cell lysates were separated by SDS-PAGE and Western blots performed using antibodies to eNOS and α -tubulin. (A) An example of a Western showing the expression of eNOS at passage 0 and passage 7 when treated with HG (X), HG and NAC (Y) or HG and TTFA (Z). (B) eNOS protein levels were measured by densitometry and expressed relative to α -tubulin when HUVECs were treated with HG, HG and NAC or HG and TTFA at passage 0 and passage 7. Values are mean +SEM, n=3.

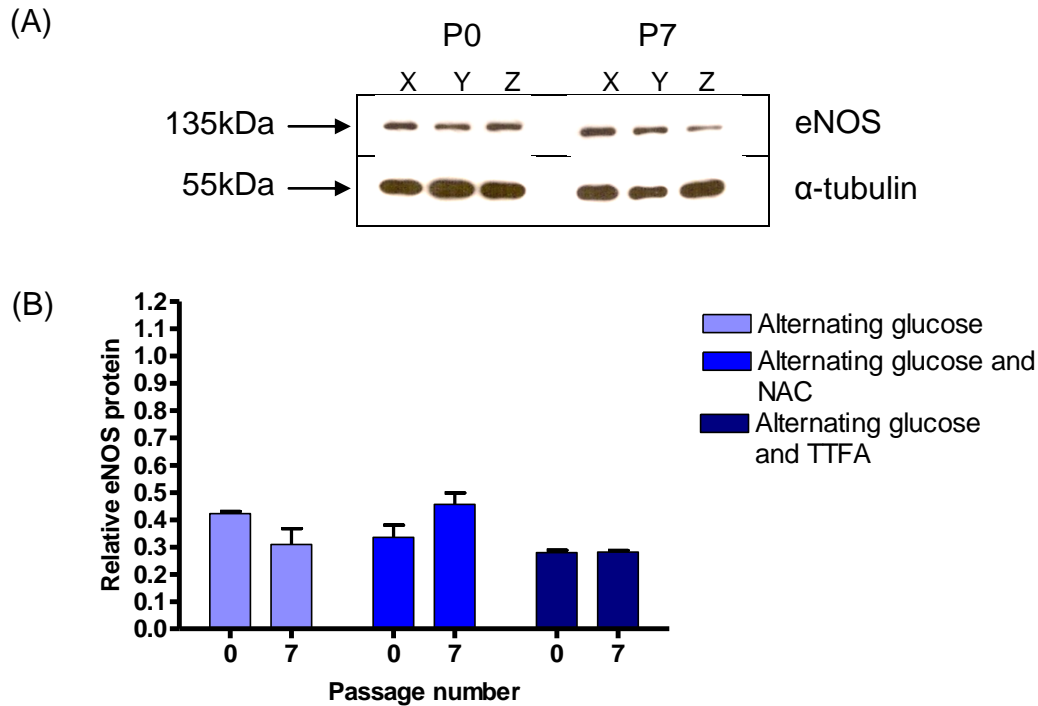


Figure 72: eNOS protein levels in HUVECs cultured in AG, AG and NAC or AG and TTFA. Cell lysates were separated by SDS-PAGE and Western blots performed using antibodies to eNOS and α -tubulin. (A) An example of a Western showing the expression of eNOS at passage 0 and passage 7 when treated with AG (X), AG and NAC (Y) or AG and TTFA (Z). (B) eNOS protein levels were measured by densitometry and expressed relative to α -tubulin when HUVECs were treated with AG, AG and NAC or AG and TTFA at passage 0 and passage 7. Values are mean +SEM, n=3.

4.4.3 Effect of mtDNA depletion on pro-inflammatory phenotype in HUVECs

4.4.3.1 Formation and characterisation of Rho0 cells

A decrease in eNOS and increase in ICAM1 in HUVECs exposed to HG and AG was observed in section 4.4.2.2 and 4.4.2.3. In order to investigate whether this might be due to a reduction in mtDNA content (as observed in Figure 58 and Figure 59), mtDNA was depleted in HUVECs. This was undertaken by the treatment of HUVECs with ethidium bromide as described in section 2.2.9.1. In order to confirm Rho0 cells were generated, mtDNA and mitochondrial encoded proteins were analysed (Figure 73).

Growth of control and Rho0 HUVECs was analysed by performing cell counts (Figure 73(A)). Rho0 HUVECs showed a lower growth rate compared to control HUVECs over time despite being supplemented with pyruvate and uridine in the media (ANCOVA showed that the difference in the slopes was statistically significant $p < 0.001$). Real time PCR confirmed that mtDNA was reduced dramatically in Rho0 cells compared to control HUVECs over 6 days. Within 2 days of culture with ethidium bromide, mtDNA in Rho0 cells was reduced to 12% of the control mtDNA and within 4 days it was reduced to $< 1\%$ (Figure 73(B)). Western blotting showed that by passage 3 (approximately 20 days), the protein expression of the nuclear encoded COXIV was unaffected. However, COXI (mitochondrial encoded protein) was below the limit of detection at passage 3 (Figure 73(C)). Taken together these data confirm that mtDNA is rapidly depleted in HUVECs cultured in ethidium bromide and that after just a few passages, this resulted in complete loss of mitochondrial encoded proteins. This suggested that a Rho0 culture was established.

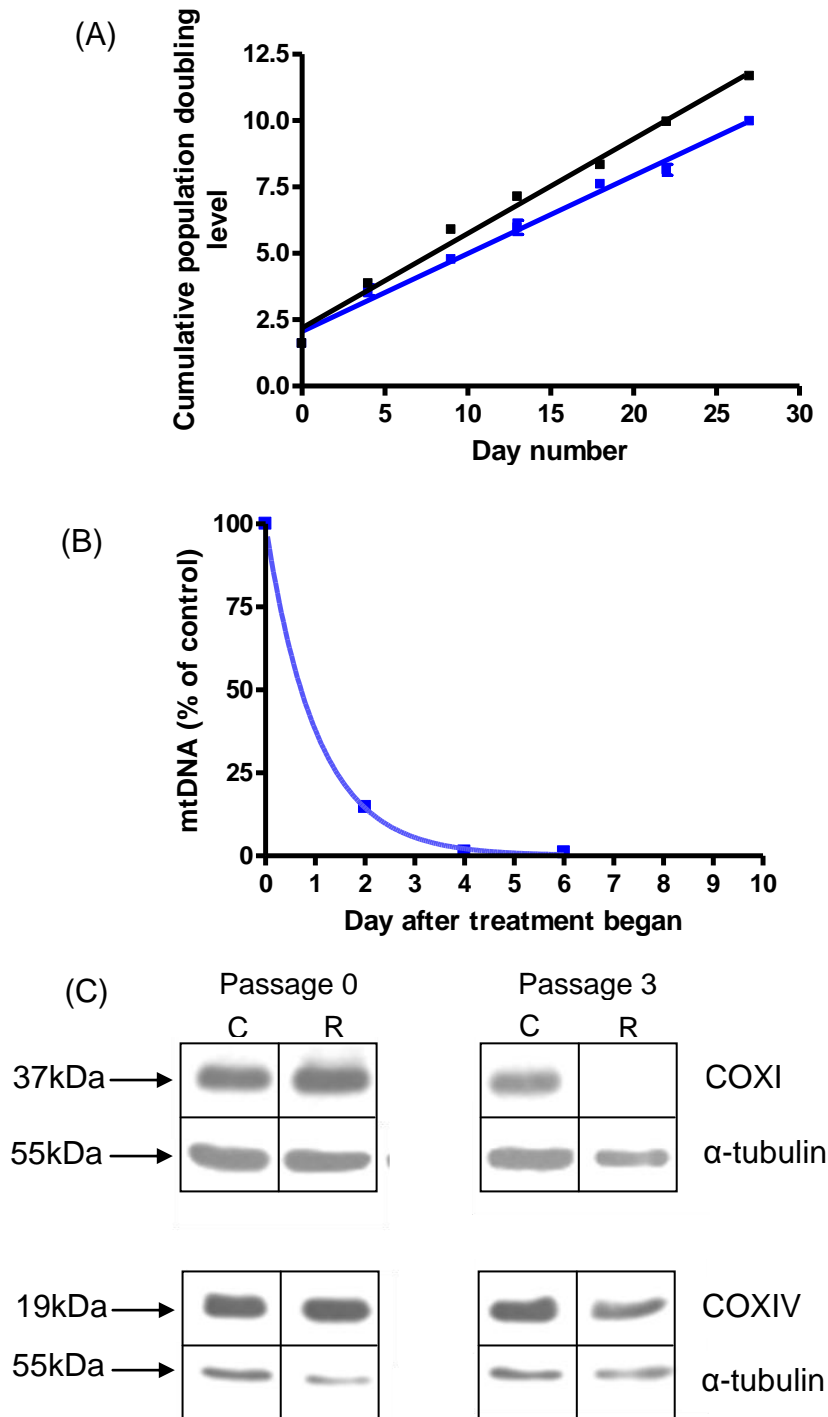


Figure 73: Effect of ethidium bromide on HUVECs growth rate, mtDNA content and the expression of mitochondrial proteins. (A) Cumulative population doubling levels of control and Rho0 HUVECs. ANCOVA shows the slopes are significantly different $p < 0.0001$. (■) = control cells. (■) = Rho0 cells. Values are mean \pm SEM, $n=3$. (B) mtDNA was measured over a number of days in Rho0 HUVECs and compared to control HUVECs using real time PCR and expressed as a percent of the control. $n=1$. (C) Western blots using the primary antibodies anti-COXI (1 in 500 dilution), anti-COXIV (1 in 1000 dilution) and anti- α -tubulin. Protein cell lysates from HUVECs (C) and Rho0 HUVECs (R) at passages 0 and 3 were separated on a SDS-PAGE gel and analysed by Western blotting.

4.4.3.2 Staining of Rho0 cells with vWF

The expression of vWF was measured in control and Rho0 HUVECs. As can be seen from Figure 74, the intensity of staining for vWF did not change in Rho0 HUVECs. However, the change in the shape of Rho0 HUVECs was dramatic. Control HUVECs when growing adherently were generally rounded. However, when Rho0 HUVECs were grown adherently, a higher proportion of the cells were more spindle-shaped and elongated than their corresponding control HUVECs (Figure 74).

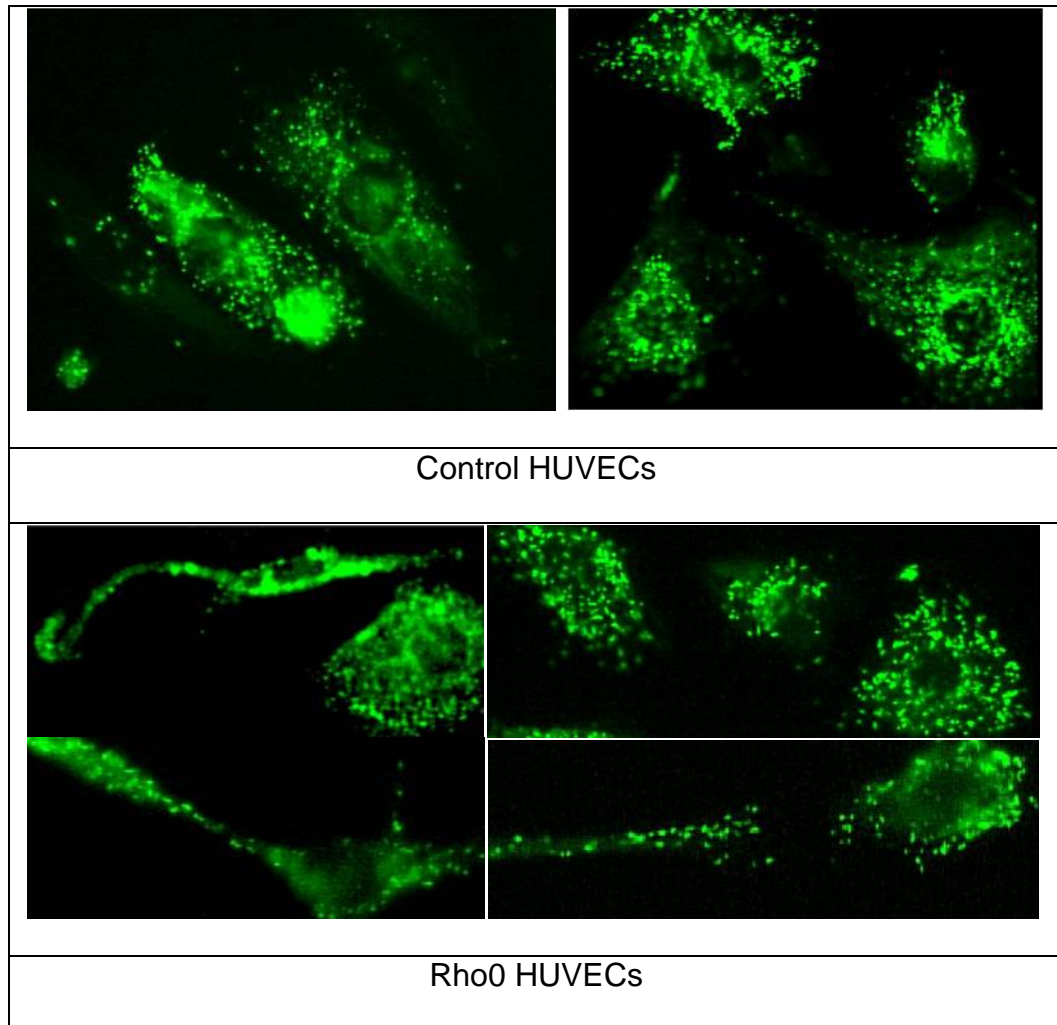


Figure 74: vWF staining of control and Rho0 HUVECs. Control and Rho0 HUVECs were grown on coverslips until 80% confluent. The cells were fixed, permeabilised and blocked. They were then incubated overnight with a 1 in 200 dilution of antibody to von Willebrand factor and mounted using a DAPI mountant. They were sealed using clear nail varnish and viewed using FITC and DAPI filters. Magnification = x 200.

4.4.3.3 Morphology of Rho0 HUVECs under TEM

The overall shape of control and Rho0 HUVECs and their mitochondria were viewed under transmission electron microscopy. The overall shape of both control and Rho0 cells was very similar although some of Rho0 cells were slightly larger than their corresponding controls (Figure 75). When the mitochondria in the HUVECs and Rho0 HUVECs were viewed, there were clear differences. Control HUVECs possessed mitochondria that were

elongated and tubular with a clear double membrane with cristae. However, in Rho0 HUVECs, the mitochondria are much more enlarged and lacked a clear double membrane and most notably cristae were far fewer in number (Figure 75).

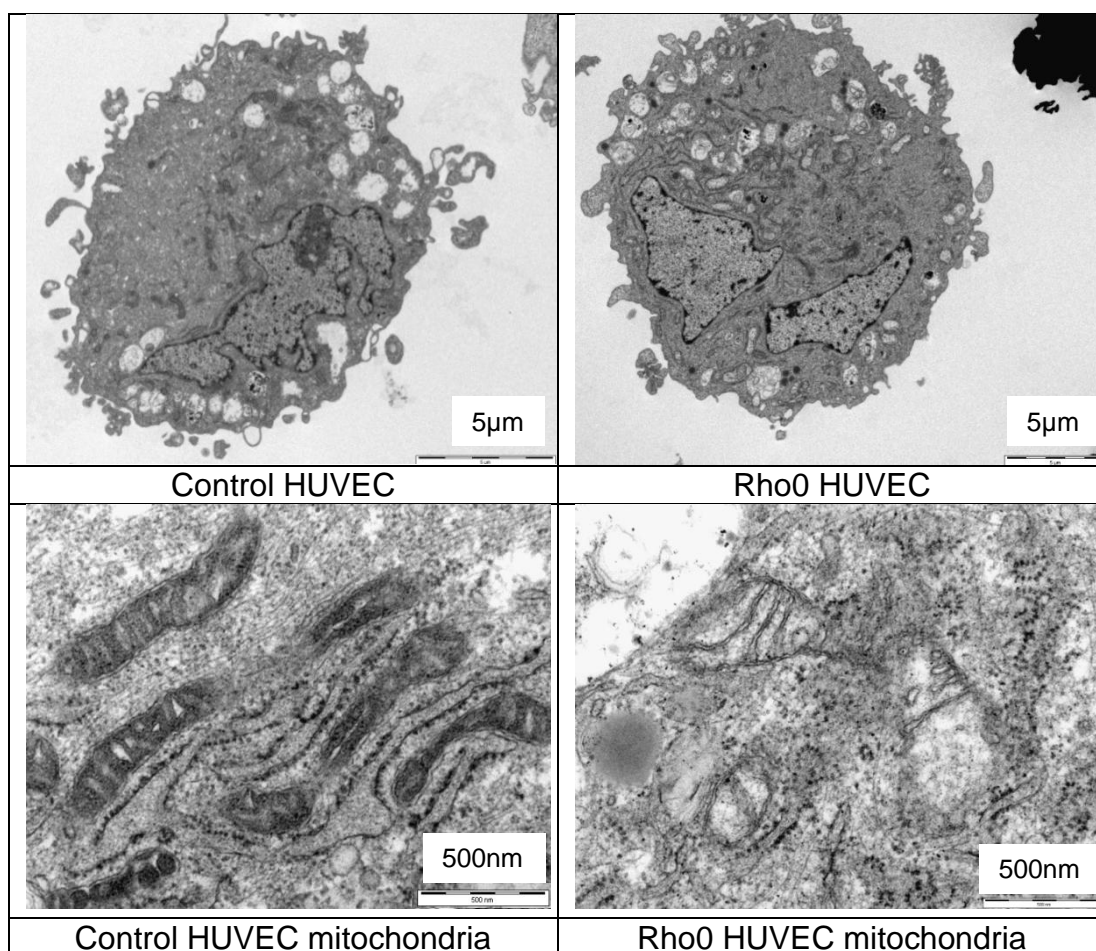


Figure 75: Morphological appearance of control and Rho0 HUVECs. Samples were processed for TEM as described (section 2.2.9.1) by the Department of Biochemistry, University of Leicester.

4.4.3.4 The expression of eNOS and ICAM1 in Rho0 HUVECs

In order to analyse if Rho0 HUVECs displayed an altered phenotype, the expression of eNOS and ICAM1 was determined. eNOS was measured over 6 passages or approximately 8 cumulative population doubling levels in

control and Rho0 HUVECs. Although eNOS protein expression was found to decrease over time in control HUVECs, in Rho0 HUVECs the decrease was more rapid (Figure 76(A) and (B)). In control HUVECs, eNOS protein tended to begin to decrease at 6 cumulative population doubling levels whereas in Rho0 HUVECs, eNOS decreased at 2.5 cumulative population doubling levels. Moreover, within 5 cumulative population doubling levels, eNOS protein expression in Rho0 HUVECs was below the limit of detection of the Western analysis.

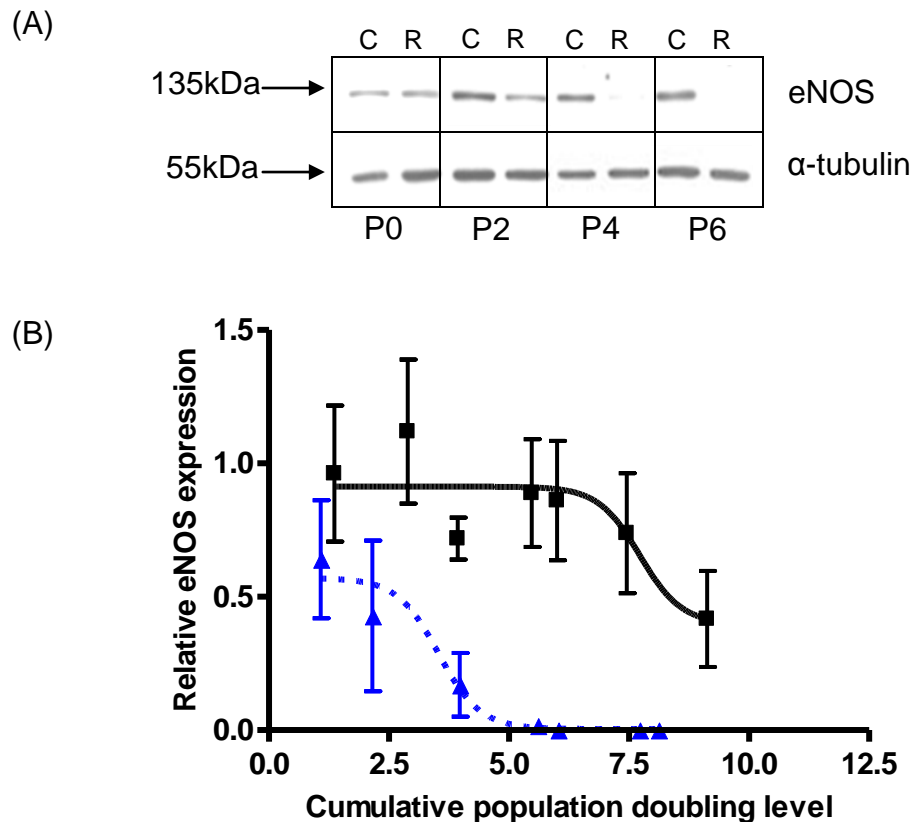


Figure 76: The effect of ethidium bromide treatment on eNOS protein levels in HUVECs and Rho0 HUVECs. Cell lysates were separated by SDS-PAGE and Western blots performed using antibodies to eNOS and α -tubulin. (A) A Western blot of eNOS at passage 0, 2, 4, and 6 for control (C) and Rho0 (R) HUVECs. (B) eNOS protein levels were measured by densitometry and expressed relative to α -tubulin for control HUVECs and HUVECs treated with ethidium bromide over 8 cumulative population doubling levels. Control HUVECs = (■). Rho0 HUVECs = (▲). Values are mean \pm SEM, n=3.

ICAM1 was then measured in control and Rho0 HUVECs over 6 cell passages (Figure 77). In control HUVECs, ICAM1 was at least maintained over 6 passages although there was a clear trend for decreasing ICAM1 with time in culture (Figure 77(B)). However, in Rho0 HUVECs, ICAM1 increased and at passage 4 and passage 6 the protein content was significantly more than at passage 0 ($p < 0.01$). ICAM1 increased from ~ 0.3 to ~ 0.75 (Figure 77(C)), a 2.5 fold increase over 6 passages.

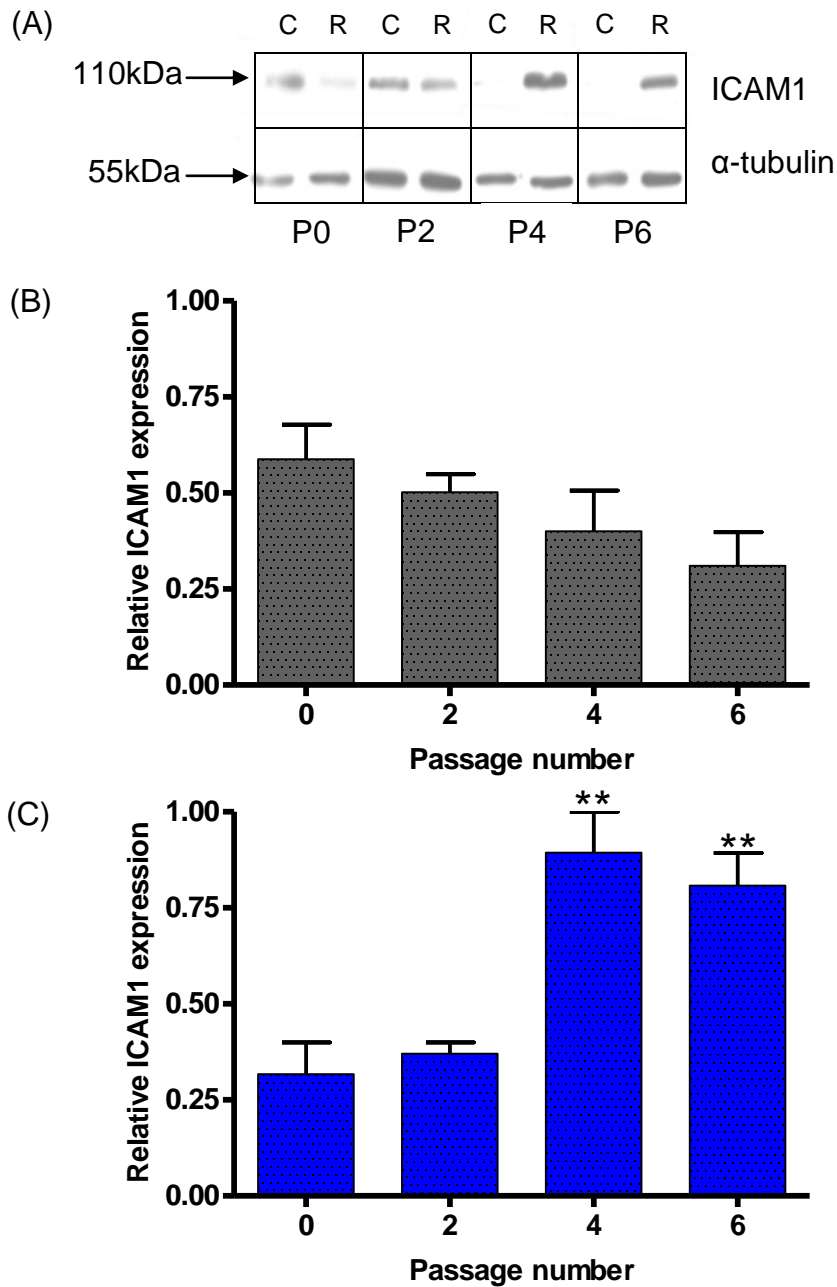


Figure 77: The effect of ethidium bromide treatment on ICAM1 protein content in HUVECs. Cell lysates were separated by SDS-PAGE and Western blots performed using antibodies to ICAM1 and α -tubulin. (A) A Western blot of ICAM1 at passage 0, 2, 4, and 6 for control (C) and Rho0 (R) HUVECs. (B) The protein expression of ICAM1 over 6 passages measured by densitometry and expressed relative to α -tubulin in control HUVECs. The data are represented graphically. Values are mean +SEM, n=3. (C) The protein expression of ICAM1 over 6 passages measured by densitometry and expressed relative to α -tubulin in Rho0 HUVECs. Values are mean +SEM, n=3. **P<0.01 vs passage 0.

4.4.4 Effect of treatment of HUVECs with chloramphenicol on eNOS expression

4.4.4.1 COXI and COXIV expression

In order to analyse whether the effect on eNOS and ICAM1 seen in Rho0 HUVECs occurred when only mitochondrial protein expression was prevented, HUVECs were treated with chloramphenicol. Firstly, the cumulative population doubling levels were compared. HUVECs treated with chloramphenicol showed a decrease in growth rate over time compared to the controls (Figure 78(A)). Following treatment with chloramphenicol, COXI and COXIV were measured by Western blotting. COXIV, which is nuclear-encoded, was not affected by the addition of chloramphenicol to cell culture media whereas COXI which is mitochondrial-encoded was below the limit of detection after 4 passages in the presence of chloramphenicol (Figure 78(B) and (C)).

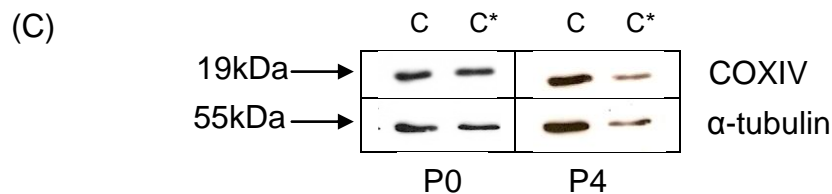
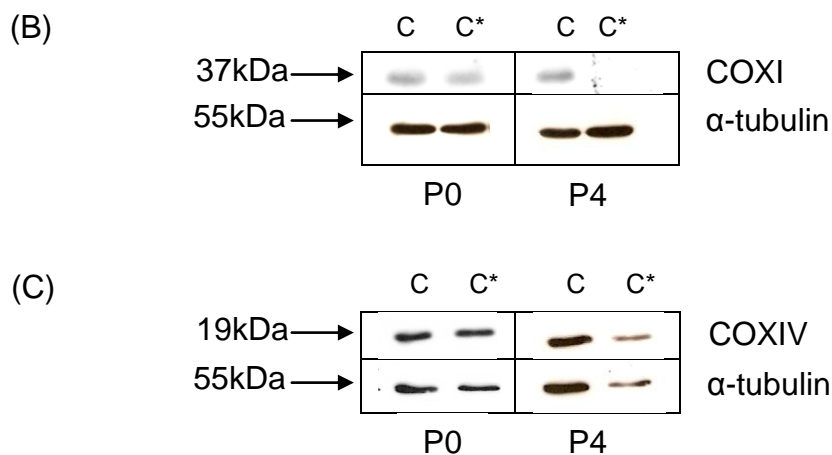
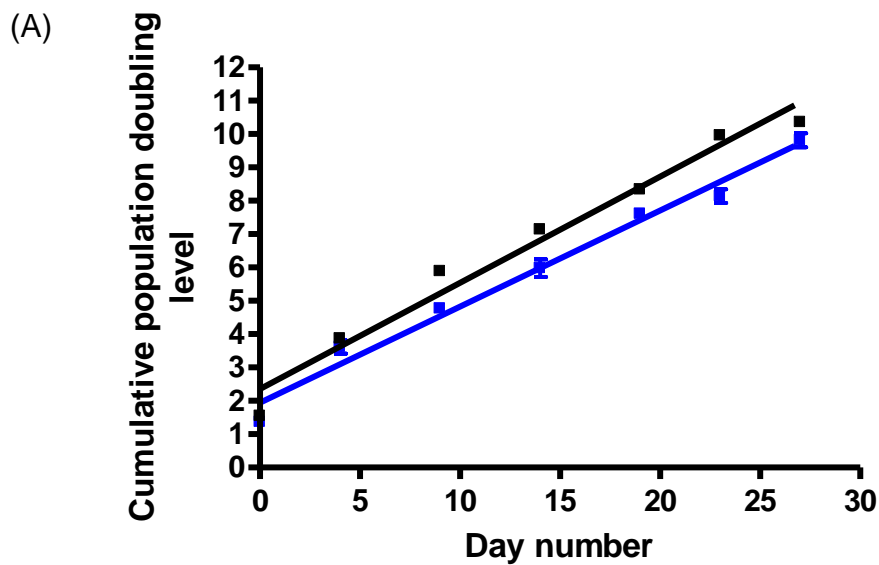


Figure 78: Effect of chloramphenicol on cell growth, and mitochondrial protein expression. HUVECs were cultured in medium containing 20µg/ml of chloramphenicol for up to 27 days. Cell lysates were extracted from control and chloramphenicol-treated HUVECs at passage 0 and 4. The protein was separated by SDS-PAGE and transferred to a membrane via a Western blot. The membranes were probed with antibodies to COXI, COXIV and α -tubulin. (A) Cumulative population doubling levels of control and chloramphenicol treated HUVECs. Control HUVECs = (■). Chloramphenicol treated HUVECs = (■). Values are mean \pm SEM, n=3. (B) A Western blot of COXI and α -tubulin at passage 0 and passage 4 for control and chloramphenicol treated HUVECs. Anti-COXI was used at a dilution of 1 in 500. C=control HUVECs, C*=chloramphenicol treated HUVECs. (C) A Western blot of COXIV and α -tubulin at passage 0 and passage 4 for control and chloramphenicol treated HUVECs. Anti-COXIV was used at a dilution of 1 in 1000. C=control HUVECs, C*=chloramphenicol treated HUVECs. Western blots (B) and (C) are examples of blots obtained for 3 analyses.

4.4.4.2 The expression of eNOS in chloramphenicol-treated HUVECs

Since chloramphenicol treatment successfully depleted COXI, but did not affect COXIV, the expression of eNOS was analysed in the cells. However, despite the decrease in mitochondrial protein expression, eNOS expression in these cells was not affected. This was investigated over a number of passages and Figure 79 shows an example of one of the Western blots illustrating eNOS protein expression at passages 0, 1, 2 and 3.

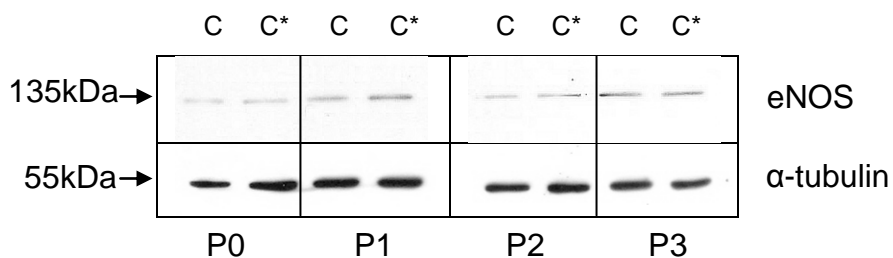


Figure 79: The effect of chloramphenicol on eNOS expression in HUVECs. Cell lysates were extracted from control and chloramphenicol-treated HUVECs at passages 0, 1, 2 and 3. The protein was separated by SDS-PAGE and analysed by a Western blot. The membranes were probed with antibodies to eNOS and α -tubulin. C=control HUVECs, C*=chloramphenicol treated HUVECs.

4.4.5 Effect of ddC on eNOS and ICAM1 expression in HUVECs

4.4.5.1 Characterisation of ddC treated cells

As preventing mitochondrial protein expression did not have any effect on eNOS, but depleting mtDNA did have an effect, another cell model was generated where mtDNA was depleted. This was performed by treating HUVECs with ddC. ddC is believed to act by inhibiting mtDNA replication (Piechota *et al.*, 2006).

4.4.5.1.1 mtDNA content

HUVECs were treated with 5 μ M, 10 μ M and 15 μ M ddC. The growth rate in these cells was decreased following ddC treatment (Figure 80(A)). However, there did not appear to be any great differences in the growth rate of cells treated with the different concentrations of ddC. Figure 80(B) shows that HUVECs treated with ddC had reduced mtDNA levels. The higher concentrations of ddC had a more rapid effect on mtDNA levels - 15 μ M ddC reduced levels to 10% of the control within 15 days. However, what was apparent with ddC, was that even when higher concentrations were used, mtDNA was not totally depleted. Also, ddC appeared to reduce mtDNA in a dose dependent manner. Due to the decreased viability of cells when cultured with 15 μ M ddC, only 5 μ M and 10 μ M ddC were used in the following experiments.

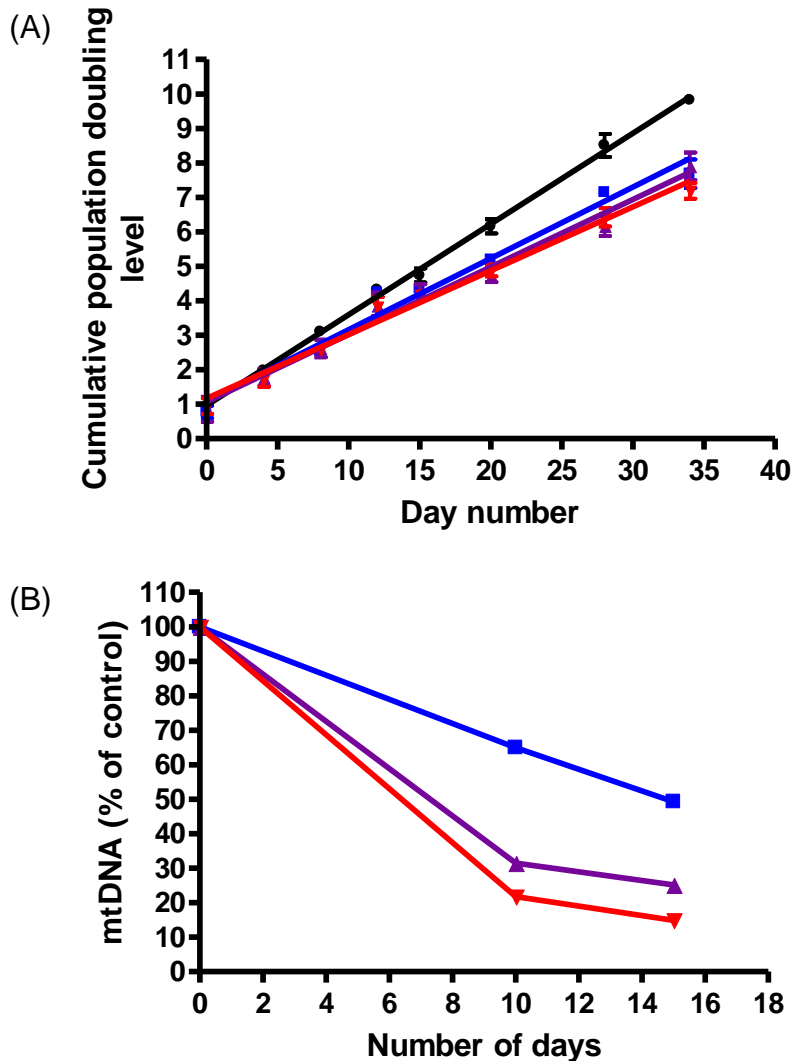


Figure 80: Effect of ddC treatment on cell growth and mtDNA content. (A) Cumulative population doubling levels of control and ddC treated HUVECs up to 34 days. Values are mean \pm SEM, n=3. (●) = 0 μ M ddC. (■) = 5 μ M ddC. (▲) = 10 μ M ddC. (▼) = 15 μ M ddC. (B) mtDNA content in ddC treated HUVECs relative to control HUVECs was assessed using real time PCR at days 0, 10 and 15. (■) = 5 μ M ddC. (▲) = 10 μ M ddC. (▼) = 15 μ M ddC.

4.4.5.2 The expression of eNOS in ddC treated HUVECs

The effect of 5 μ M and 10 μ M ddC on eNOS protein expression was analysed by Western blotting. eNOS protein expression was reduced in cells treated with ddC but the reduction was more apparent in HUVECs treated with 10 μ M ddC than in HUVECs treated with 5 μ M ddC (Figure 81).

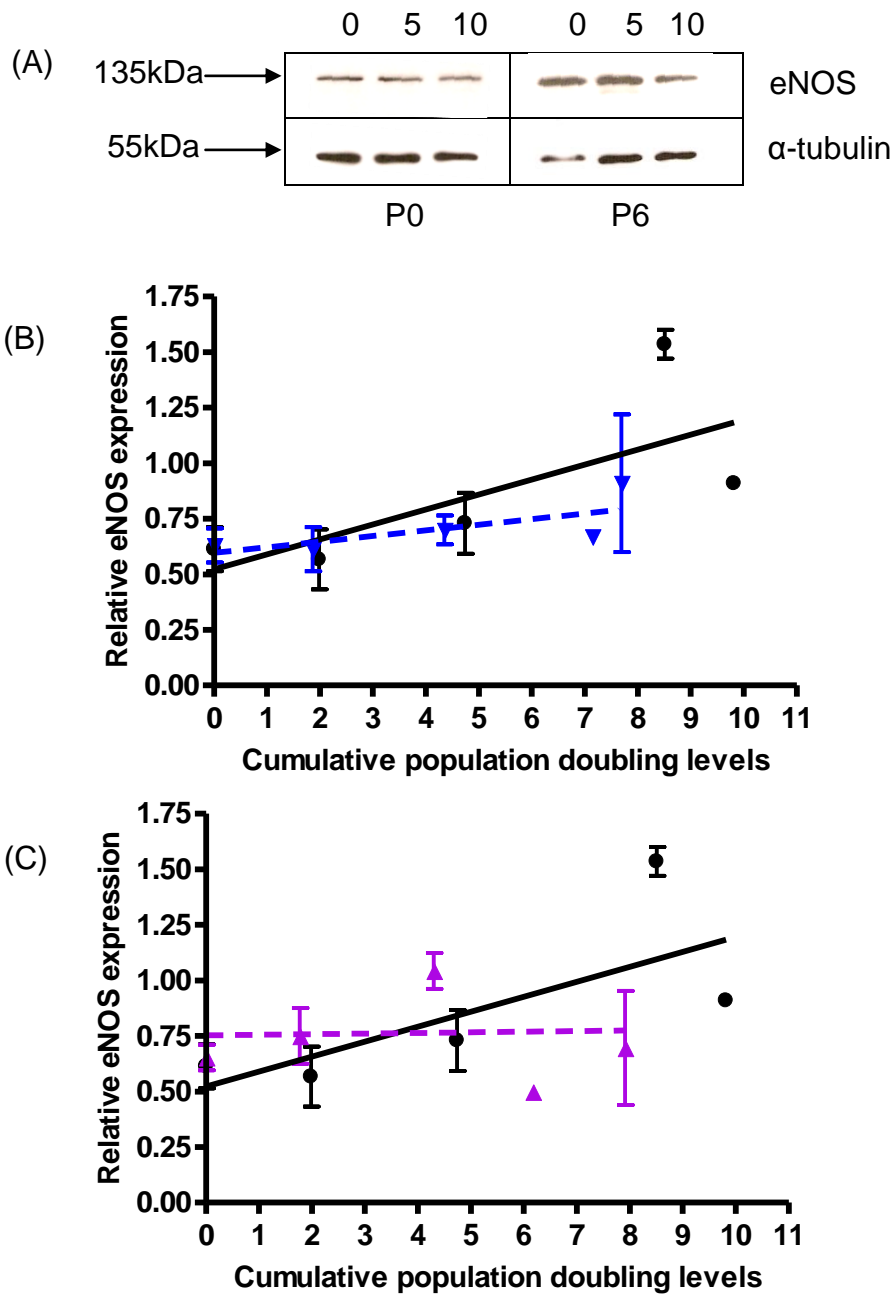


Figure 81: Effect of ddC on eNOS protein expression in HUVECs. Cell lysates were extracted from control and ddC-treated HUVECs. The protein was separated by SDS-PAGE and transferred to a membrane via a Western blot. The membranes were probed with antibodies to eNOS and α -tubulin. eNOS was measured by densitometry and expressed relative to α -tubulin. (A) Example of Westerns at passage 0 (P0) and passage 6 (P6) showing eNOS expression when HUVECs were treated with 0, 5 or 10 μ M ddC. (B) Expression of eNOS over 8 to 10 cumulative population doubling levels in control HUVECs (●) and HUVECs treated with 5 μ M ddC (▼). Values are mean \pm SEM, n=3. (C) Expression of eNOS over 8 to 10 cumulative population doubling levels in control HUVECs (●) and HUVECs treated with 10 μ M ddC (▲). Values are mean \pm SEM, n=3.

4.4.5.3 The expression of ICAM1 in HUVECs treated with ddC

As HUVECs cultured with 5 μ M and 10 μ M ddC had altered eNOS expression, the effect of ddC on ICAM1 expression was investigated (Figure 82). Over 6 passages, the expression of ICAM1 in control HUVECs was at least maintained, if not decreased slightly over 6 passages (Figure 82(B)). In HUVECs exposed to 5 μ M ddC, the relative expression of ICAM1 increased from 0.8 at passage 0 to 1.0 at passage 6 (Figure 82(C)). In HUVECs treated with 10 μ M ddC, ICAM1 also increased from 0.8 at passage 0 to 1.5 at passage 6 (~2 fold increase). However, the increase in ICAM for HUVECs treated with either 5 μ M or 10 μ M did not reach statistical significance after 6 passages (Figure 82(D)).

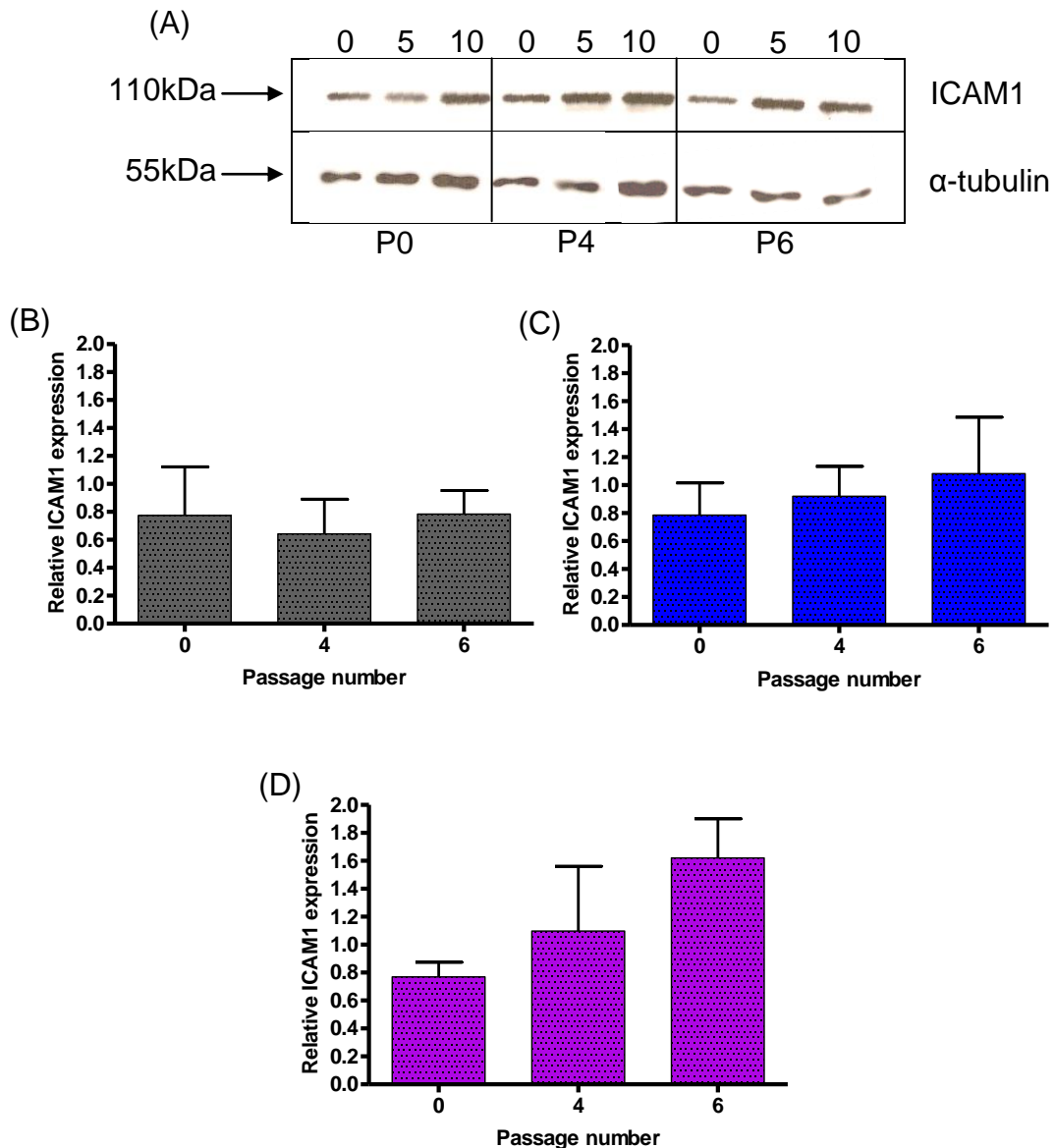


Figure 82: Effect of ddC on ICAM1 protein expression in HUVECs. Cell lysates were extracted from control and ddC-treated HUVECs. The protein was separated by SDS-PAGE and transferred to a membrane via a Western blot. The membranes were probed with antibodies to ICAM1 and α -tubulin. ICAM1 was measured by densitometry and expressed relative to α -tubulin. Values are mean +SEM, n=3. (A) Examples of a Western at passage 0 (P0), 4 (P4) and 6 (P6) showing ICAM1 expression when HUVECs were treated with 0, 5 or 10 μ M ddC. (B) Expression of ICAM1 in control HUVECs at passage 0, 4 and 6. (C) Expression of ICAM1 in 5 μ M ddC treated HUVECs at passage 0, 4 and 6. (D) Expression of ICAM1 in 10 μ M ddC treated HUVECs at passage 0, 4 and 6.

4.4.6 H₂O₂ production in Rho0 HUVECs

In order to determine whether the decrease in eNOS and increase in ICAM1 expression in Rho0 HUVECs was associated with increased ROS release, H₂O₂ was measured in Rho0 cells compared to control HUVECs. Furthermore, the effect on H₂O₂ production when culturing Rho0 HUVECs in medium containing HG was investigated.

H₂O₂ production in control HUVECs exposed to NG was approximately 28 pmoles/min/mg protein whereas H₂O₂ production in Rho0 HUVECs exposed to normal glucose was almost two fold higher (Figure 83). Exposure of HUVECs to HG increased H₂O₂ production to ~65 pmoles/min/mg protein. However, HG caused only a slight increase in H₂O₂ production in Rho0 HUVECs relative to medium containing NG. This was also the case when looking at the effect of menadione on H₂O₂ production. In control HUVECs there was a large increase in H₂O₂ production (28 to 125 pmoles/min/mg protein) but the increase was much smaller in Rho0 HUVECs (50 to 85 pmoles/min/mg protein). When both control and Rho0 HUVECs were exposed to high glucose and the antioxidant NAC, or high glucose and the electron transport chain inhibitor TTFA, H₂O₂ production decreased back to similar levels observed in cells exposed to medium containing NG. Lastly, when control and Rho0 HUVECs were exposed to 3-O-methylglucose (NG plus 16.5mM 3-O-methylglucose) there was very little difference in H₂O₂ production compared to when these cells were only exposed to NG.

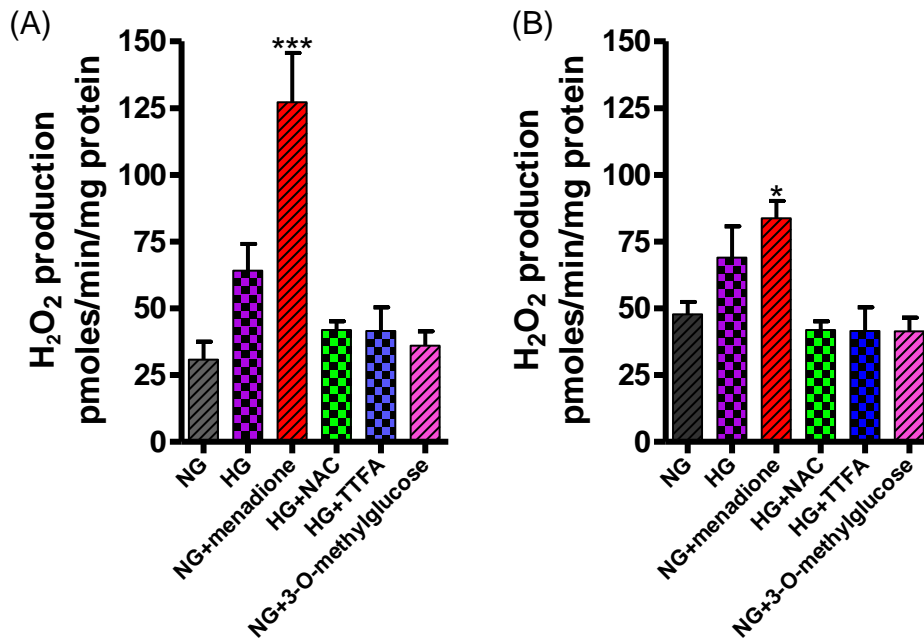


Figure 83: Effect of mtDNA depletion on H₂O₂ production in HUVECs.

HUVECs and Rho0 HUVECs were cultured in 96 well plates and treated as described in section 2.2.7. H₂O₂ production was assessed using the Amplex Red assay over 1 hour and expressed relative to the protein content (section 2.2.7). (A) H₂O₂ production in control HUVECs with 16.5mM glucose, 50μM menadione, 3mM NAC, 25μM TTFA, 16.5mM 3-O-methylglucose, or 16.5mM mannitol for 1 hour. Values are mean +SEM, n=3. ***P<0.001 vs NG. (B) H₂O₂ production in Rho0 HUVECs with 16.5mM glucose, 50μM menadione, 3mM NAC, 25μM TTFA, 16.5mM 3-O-methylglucose, or 16.5mM mannitol for 1 hour. Values are mean +SEM, n=6. *P<0.05 vs NG.

4.5 Discussion

Many cardiovascular diseases have been shown to be associated with damage to and/or depletion of mtDNA levels (Ballinger *et al.*, 2002; Simon and Johns., 1999; Reardon *et al.*, 1992). In addition, studies showed that these diseases are associated with early endothelial dysfunction characterised by decreasing nitric oxide (Albrecht *et al.*, 2003; Srinivasan *et al.*, 2004). Therefore, one of the aims of this chapter was to look at whether HG led to phenotypic changes in endothelial cells, and whether there was any evidence that this change occurred through the depletion of mtDNA.

This was investigated by treating HUVECs with HG to analyse if these cells had depleted levels of mtDNA, and displayed markers indicative of a pro-inflammatory phenotype, and by creating extreme models of mitochondrial DNA dysfunction by depleting mtDNA in endothelial cells and investigating the effect on the pro-inflammatory phenotype.

4.5.1 The effect of HG and AG on mtDNA content and the expression of eNOS and ICAM1

The effect of HG and AG on mtDNA content was investigated over a number of passages. It was found that when HUVECs were exposed to HG, the mtDNA content decreased compared to HUVECs exposed to NG. In addition, the effect of AG on mtDNA content was analysed. As mentioned in section 3.5.3, it was reported by Risso *et al.*, (2001) that AG had a more drastic effect than HG exposure on apoptosis and DNA fragmentation in endothelial cells. However, in this current study, AG caused a similar decrease in mtDNA content as cells exposed to HG. In fact, the decrease in mtDNA content was not as severe as in cells exposed to HG. This suggests that prolonged periods of exposure to HG are important in determining changes in mtDNA. However, the conditions of NG/HG alternation may be critical for the outcome on cellular mtDNA.

A number of diseases such as Parkinson's disease have been associated with a decrease in mtDNA content (Simon and Johns, 1999). However, there are also a number of occasions in cells in culture when mtDNA has been shown to increase. For example, when cells were treated with a redox active agent such as peroxide, there was an increase in mtDNA content (Lee *et al.*, 2000; Lee *et al.*, 2005). A possible reason why these data show a decrease in mtDNA content in HG treated cells, may be due to reduced nitric oxide production and decreased expression of peroxisome proliferator-activated receptor- γ (PPAR- γ) coactivator 1 α (PGC1- α) which in turn leads to decreased mitochondrial biogenesis. A study by Palmeira *et al.*, (2007) showed a reduction in mitochondrial biogenesis in hyperglycaemic

conditions. Furthermore, in diabetic and pre-diabetic subjects, the expression of PGC1- α is reduced (Patti *et al.*, 2003) and nitric oxide production is also reduced due to the increased formation of peroxynitrite (Zou *et al.*, 2004). PGC1- α is activated by nitric oxide through a guanylate-cyclase-dependent signalling pathway (Leary and Shoubridge, 2003) and PGC1- α activates many of the genes involved in mitochondrial biogenesis (Nisoli *et al.*, 2007). A reduction in nitric oxide may lead to decreased activation of PGC1- α which in turn may down regulate mitochondrial biogenesis and lead to decreased mtDNA content (Nisoli *et al.*, 2004).

In section 3.4.5, it was shown that HUVECs exposed to HG and AG released more ROS than cells cultured in NG. In order to investigate whether the observed decrease in mtDNA was due to an increase in ROS production, HUVECs were co-treated with either NAC or TTFA. As HG treatment had a greater effect on mtDNA content, only HG treated cells were treated with NAC or TTFA. NAC is an antioxidant and when HUVECs were cultured with HG and NAC, mtDNA content was maintained at higher levels than in cells treated with HG alone. TTFA is an inhibitor of complex II of the electron transport chain and once again, HUVECs treated with HG and TTFA had higher levels of mtDNA than in HUVECs treated with just HG. The treatment of cells with NAC and TTFA has been shown to decrease superoxide (Nishikawa *et al.*, 2000; Quagliario *et al.*, 2007) and decrease H₂O₂ (Section 4.4.6). Taken together, these results suggest that the decreases in mtDNA were due to increases in ROS production. However, to ensure that the increase in mtDNA following incubation with NAC and TTFA was because these agents reduced/prevented ROS production, mtDNA needs to be quantified in cells exposed to NG and NAC or NG and TTFA. This will eliminate the possibility that NAC and TTFA were directly affecting mtDNA.

A decrease in mtDNA content by HG exposure may have a number of consequences on cells. A reduction in mtDNA content has been linked to reduced ATP production, reduced glucose uptake and reduced activities of

glucose-metabolism enzymes (Park *et al.*, 2001). Additionally, the changes in mitochondrial morphology that occur in cells with depleted levels of mtDNA are very similar to the morphological changes observed in mitochondria from apoptotic cells (Gilkerson *et al.*, 2000; Burnett and Scheffler, 1981; Karbowski *et al.*, 1999) and this suggests a possible link between mtDNA depletion and mitochondrial function (Gilkerson *et al.*, 2000).

In order to investigate whether HG and AG induced a pro-inflammatory phenotype, the expression of eNOS and ICAM1 were analysed. eNOS is responsible for the synthesis of nitric oxide from L-arginine. Often nitric oxide is lower in endothelial dysfunction due to reduced levels of eNOS activity (Hoffmann *et al.*, 2001; Haendeler, 2005; Cai and Harrison, 2000). In the current study, when eNOS was measured in HUVECs exposed to HG and AG, eNOS protein expression at later passages was found to be lower than in HUVECs exposed to NG. These data support the results from Srinivasan *et al.*, (2004) who investigated the effect of HG over number of hours and days. They too found that over a period of seven days, with exposure of human aortic endothelial cells to HG, eNOS expression was reduced significantly.

In addition, the effects of culturing cells with agents that reduce ROS were used to see if eNOS expression was restored. Although the increases in eNOS were not statistically significant, it was found that NAC and TTFA generally led to an increase in eNOS expression to levels found in HUVECs treated with NG.

When ICAM1 protein content was measured in cells cultured in medium containing NG, ICAM1 expression was significantly lower after 7 passages. However, in HUVECs cultured in medium containing HG or AG, ICAM1 protein expression was raised after 7 passages.

A decrease in eNOS and an increase in ICAM1 protein expression have been detailed by a number of groups following exposure to HG (Rajesh *et al.*, 2007; Piconi *et al.*, 2004). However, a number of these only looked at protein expression over a short term – a few hours or a matter of days. We have demonstrated that exposure to HG or AG over a period of 35 days leads to expression of markers that are indicative of a pro-inflammatory phenotype. In addition, the use of agents which reduce ROS can return the cells to their more ‘normal’ physiological state.

A decrease in eNOS and an increase in ICAM1 could have detrimental effects on the cells/blood vessels *in vivo* and *in vitro*. Increased senescence (Gorgoulis *et al.*, 2003; Foreman and Tang, 2003; Matsushita *et al.*, 2001), increased vascular disease and increased formation of atherosclerotic lesions (Minamino *et al.*, 2004; Zhou *et al.*, 2006) have all been associated with decreased eNOS and increased ICAM1 expression. Factors which affect eNOS and ICAM1 expression, such as HG, may be responsible for accelerating the progression of diseases associated with endothelial dysfunction (Vanhoutte, 2002; Schalkwijk and Stehouwer, 2005).

4.5.2 The effect of depleting mtDNA on eNOS and ICAM1 protein expression

The data generated so far demonstrated that HG affected mtDNA and markers that indicate endothelial cell dysfunction. Therefore, to be able to confirm that mtDNA depletion was a possible mechanism for the change in the expression of these markers, HUVECs were depleted of mtDNA and/or mitochondrial encoded proteins. This represented an extreme model of mtDNA dysfunction. Nevertheless, it is an important means of investigating whether mtDNA plays any role in the maintenance of endothelial cell phenotype.

mtDNA or mitochondrial encoded proteins were depleted using three different agents. Firstly, HUVECs were treated with 10ng/ml ethidium

bromide. Ethidium bromide has been shown to deplete mtDNA in yeast cells (King and Attardi, 1996). It inhibits mitochondrial transcription and mitochondrial replication (Piechota *et al.*, 2006). It inhibits both the γ and the mitochondrial polymerases in mitochondria and therefore reduces the amount of mtDNA within cells (Tarrago-Litvak *et al.*, 1978). Furthermore, treatment of mammalian cells with low levels of ethidium bromide was shown to have very little effect on nuclear DNA (Nass, 1972). In light of this, HUVECs were treated over a number of passages and the mtDNA content was measured as well as the expression of mitochondrial encoded COXI and nuclear encoded COXIV. The mtDNA content fell very rapidly reflecting that it was progressively diluted as the cells divided. Every time the cells divided, the mitochondrial DNA was reduced by a half (King and Attardi, 1996). Moreover, when the Rho0 HUVECs were stained for an endothelial cell specific marker (vWF) there was no difference to the expression of this marker in control HUVECs. However, under TEM, the mitochondria in Rho0 cells were swollen and lacked cristae compared to mitochondria within control HUVECs.

Since ethidium bromide treatment successfully depleted mitochondrial DNA, the expression of two markers which are associated with endothelial dysfunction were analysed. eNOS protein expression in Rho0 cells was found to rapidly decrease and within 5 population doubling levels the protein was below the limit of detection of the Western analysis. When the protein expression of ICAM1 was analysed, it was found that it increased significantly in Rho0 cells. This was an extreme model where the entire amount of mitochondrial DNA was depleted and in cardiovascular diseases such as diabetes it is very unlikely that the entire mtDNA is depleted. However, because an effect on the markers was observed in these extreme conditions, it was feasible to look at whether there was a shift in the phenotype when affecting mitochondrial protein expression or through the reduction but not total depletion of mitochondrial DNA. Therefore, in order to investigate this, HUVECs were treated with chloramphenicol.

Chloramphenicol does not affect nuclear or mitochondrial DNA or nuclear gene expression. However, it prevents mitochondrial protein expression or translation (Li *et al.*, 2005). When the expression of COXI and COXIV were analysed, COXI protein expression was reduced significantly whereas COXIV protein expression was unaffected. However, when eNOS was analysed in these cells, there was no difference in the expression of eNOS compared to the control cells. (These data therefore differ from the observations on eNOS depletion in Rho0 HUVECs). Therefore, this raised a number of questions about the Rho0 data. Was the decrease in eNOS protein expression due to the ethidium bromide preventing the expression of this gene? Is the difference because the two agents target mitochondrial gene expression by different mechanisms? It was possible that ethidium bromide affected eNOS transcription however this was not a generalised suppression of nuclear gene expression as an increase in ICAM1 protein expression in Rho0 HUVECs was observed. Nevertheless, the effect of ethidium bromide on eNOS transcription should be investigated. In response to the second question, ethidium bromide depletes mtDNA by preventing replication and also inhibits mtDNA transcription whereas chloramphenicol only affects mitochondrial protein expression by targeting mitochondrial protein translation (Piechota *et al.*, 2006). Therefore, it may have been possible that a decrease in eNOS and an increase in ICAM1 in Rho0 cells were observed because somehow the markers are affected by mtDNA content or mtDNA transcription.

In an attempt to verify either the Rho0 data or the chloramphenicol data, mtDNA was depleted in HUVECs using ddC (Piechota *et al.*, 2006). Although, a number of studies on mtDNA had used ddC to deplete mtDNA (Pan-Zhou *et al.*, 2000; Ashley *et al.*, 2005; Glynn and Yazdanian, 1998), there were very few reports using human endothelial cells. So prior to measuring eNOS and ICAM1, mitochondrial DNA content was measured in HUVECs exposed to a range of ddC concentrations. By taking into account the percentage viability and the amount of mtDNA depleted, 5 μ M and 10 μ M ddC were used. After 15 days treatment with 5 μ M ddC, the percentage of

DNA compared to the control was 55%, but after 15 days of treatment with 10 μ M ddC, approximately 25% of DNA remained compared to the control. eNOS protein expression decreased in ddC treated HUVECs with the decrease more apparent in 10 μ M ddC than in 5 μ M ddC HUVECs. When the effect of ddC on ICAM1 protein expression was analysed, ICAM1 protein was higher than in control HUVECs and once again in 10 μ M ddC treated HUVECs expression was higher than in 5 μ M ddC treated HUVECs. This therefore raised the possibility that the changes in the expression of these pro-inflammatory markers were dependent on the extent of mtDNA depletion. Higher levels of mtDNA depletion meant a greater shift towards a pro-inflammatory phenotype. In addition, since ddC only inhibits mtDNA replication, whereas ethidium bromide inhibits both replication and transcription (Piechota *et al.*, 2006), it is likely that the observations are indeed due to the extent of mtDNA depletion. The mechanism for this effect is not known.

4.5.3 Effect of depleting mtDNA on H₂O₂ production

Sections 4.4.1, 4.4.2 and 4.4.3 showed that the shift towards a pro-inflammatory phenotype when HUVECs were exposed to high glucose was associated with increased ROS and reduced mtDNA content. To investigate if HUVECs depleted of mtDNA showed an increase in ROS, H₂O₂ production was monitored in Rho0 HUVECs using the Amplex Red assay. The Amplex Red assay measures the production of the highly fluorescent resorufin upon oxidation by H₂O₂ (Rinaldi *et al.*, 2007). The advantages of the assay include its simplicity and sensitivity. It is able to measure H₂O₂ concentration down to 50nM (Reszka *et al.*, 2005). Furthermore, this assay provides more reliable and reproducible results than other assays due to the stability of the H₂O₂ molecule (Votyakova and Reynolds, 2004). However, as Amplex Red is unable to cross membranes it only measures extracellular H₂O₂ production (Wagner *et al.*, 2005). Another disadvantage of this assay is the possible interference of this assay from other peroxidase substrates such as drugs or cytotoxins which

compete with Amplex Red for the horse radish peroxidase enzyme ultimately leading to underestimating the actual level of H₂O₂ (Reszka *et al.*, 2005). However, despite these disadvantages, the Amplex Red assay has been used on a number of occasions to measure H₂O₂ production (Doughan *et al.*, 2008; Sousa *et al.*, 2008).

When H₂O₂ production was measured in Rho0 HUVECs exposed to NG, H₂O₂ production was two fold higher in Rho0 HUVECs compared to control HUVECs. The reason as to why ROS was higher in these cells is unclear. As mentioned in the introduction, studies looking at ROS show conflicting results – some Rho0 cells show an increase whereas others show a decrease. A study by Vergani *et al.*, (2004) showed that reduced glutathione content and glutathione reductase activity were reduced in Rho0 bone osteosarcoma cells and Rho0 lung carcinoma cells compared to their corresponding controls. Furthermore, they also demonstrated that manganese superoxide dismutase activity although decreased in bone osteosarcoma cells was increased in lung carcinoma cells. These effects would all lead to increased H₂O₂ concentration in Rho0 HUVECs. Alternatively, it may simply be because the electron transport chain is incomplete there is increased electron leakage from the ETC to form ROS, or that affecting mtDNA reduces the availability of co-factors required for antioxidant enzymes to function efficiently e.g. NADPH for glutathione peroxidase.

There is very little published data about how mtDNA damage/depletion can affect cofactors such as NADPH levels. Chevallet *et al.*, (2006) analysed the difference in the activity of different dehydrogenases enzymes in control and Rho0 cells. They showed great variation in the activities of different dehydrogenases but showed only slight differences in isocitrate dehydrogenase (the main enzyme responsible for NADPH synthesis) between control osteosarcoma cells and Rho0 osteosarcoma cells. However, only one cell type was analysed and because such variation was shown between the activities of the different dehydrogenases, it is possible

that the expression varies between different Rho0 cell types. Furthermore, they analysed osteosarcoma cells which show very different expression profiles to human endothelial cells. However, it is impossible to be certain either way due to the lack of published data within this area. Another reason why NADPH may be lower in Rho0 cells is because isocitrate may be present at lower concentrations. Vergani *et al.*, (2004) showed that aconitase activity is lower in Rho0 bone, Rho0 muscle and Rho0 lung cells (possibly due to inactivation of the aconitase enzyme by increased ROS). The aconitase enzyme catalyses the synthesis of isocitrate from citrate (Boquist and Ericsson, 1984). Isocitrate is then converted to α -ketoglutarate by isocitrate dehydrogenase producing NADPH in the process (Yarian *et al.*, 2006). Therefore, a decrease in aconitase activity may ultimately lead to decreased NADPH reduction (Tretter and Adam-Vizi, 2000). This may reduce the activity of the antioxidant enzymes which use NADPH as a cofactor. Lastly, the activity of another enzyme transhydrogenase which reduces NADP⁺ is dependent on the proton electrochemical potential gradient (Green *et al.*, 2004) which may be altered in mtDNA depleted cells.

When Rho0 HUVECs were exposed to HG, the increase in H₂O₂ production was not as great as for control HUVECs exposed to HG. This suggests that the mitochondria are important for increased ROS generation by HG. Similarly, the addition of menadione to Rho0 HUVECs had a much smaller effect on increasing H₂O₂ release than in control HUVECs cultured in NG medium. Wochna *et al.*, (2007) showed that ROS production in Rho0 osteosarcoma cells treated with menadione was lower than control osteosarcoma cells treated with menadione after 1 hour. Furthermore, Delsite *et al.*, (2003) have also shown similar results in control HeLa and Rho0 HeLa cells. Menadione is a quinone that generates superoxide by redox cycling (Zielonka *et al.*, 2006). Menadione is reduced by the NADPH quinone acceptor oxidoreductase and menadione is oxidised by the transfer of electrons to oxygen forming superoxide (Nutter *et al.*, 1992). This constant redox cycling of menadione generates large amounts of superoxide (Sanchez *et al.*, 2001) (Figure 84).

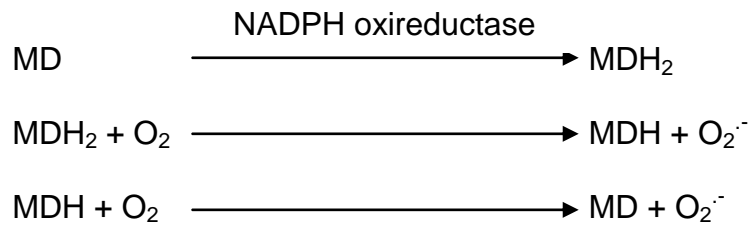


Figure 84: Menadione generates superoxide by redox cycling. MD = menadione; MDH/MDH₂ = reduced menadione; O₂^{·-} = superoxide (Nutter *et al.*, 1992).

The reaction shown in Figure 84 (menadione redox cycling) requires NADPH as a cofactor. However, as previously mentioned, in Rho0 HUVECs, NADPH levels may be lower. This may ultimately reduce the overall amount of ROS produced from menadione redox cycling in Rho0 HUVECs compared to the control HUVECs.

There is substantial evidence that increased nitric oxide production causes increased mtDNA content and mitochondrial biogenesis (Borniquel *et al.*, 2006). However, the data shown in this thesis links mtDNA depletion to decreased eNOS expression. When HUVECs were cultured in medium containing additional glucose (HG) and TFA or NAC, ROS release was lower and eNOS expression was increased compared to HUVECs cultured in HG medium. This data therefore shows a possible link between ROS release and eNOS expression. Srinivasan *et al.*, (2004) showed that increased superoxide production, induced by HG exposure in human endothelial cells, activated AP-1 and reduced eNOS expression. As the amount of ROS released in Rho0 HUVECs increased, the shift towards a pro-inflammatory phenotype in Rho0 HUVECs in part may be due to increased ROS levels. However, as the decrease in eNOS expression was so significant, increased ROS may not be the only mechanism for this decrease in eNOS. However, as more information is needed in regards to whether eNOS is affected at the transcriptional or translational level, it is impossible to speculate about the other mechanisms that may be reducing

eNOS. ICAM1 expression has also been shown to increase following exposure to increased ROS by the activation of NF- κ B (Kim *et al.*, 2008; Lee *et al.*, 2008; Kumar *et al.*, 2007). NF- κ B is a signalling pathway activated by proinflammatory cytokines TNF- α and IL-1 β (Roebuck and Finnegan, 1999). An increase in ICAM1 due to increased ROS correlates with the data obtained in this thesis in cells with depleted mtDNA content. Furthermore, as ICAM1 expression altered a number of passages after eNOS decreased, it may be possible that ICAM1 increased as a direct result of decreased eNOS. The possible mechanism for this would once again be through the activation of NF- κ B (Tripathi *et al.*, 2006; Grumbach *et al.*, 2005).

In conclusion, this chapter has demonstrated that both HG and AG reduce the mtDNA content of HUVECs and this is restored by the addition of agents that reduce ROS. It was also shown that HG and AG caused a shift towards a pro-inflammatory phenotype which was restored by the addition of agents that reduce ROS. Therefore, in both cases it suggests that these effects were mediated through increased production of ROS. Furthermore, when mtDNA was depleted, there was shift towards a pro-inflammatory phenotype and the extent of the shift appeared to be dependent on the amount of mtDNA depleted.

5 General Discussion

5.1 Hyperglycaemia and cardiovascular disease

Diabetes is a metabolic disorder that affects millions of people worldwide (Schalkwijk and Stehouwer, 2005). It is characterised by hyperglycaemia and it is associated with accelerated ageing of the vasculature and endothelial dysfunction (Ahmed, 2005; Hink *et al.*, 2001). Furthermore, diabetes is associated with cardiovascular diseases such as diabetic atherosclerosis (Libby *et al.*, 2002; Brownlee, 2001).

The high levels of glucose are proposed to mediate pathological effects in vascular cells through the production of ROS (Brownlee, 2001). Cells cultured in HG and cells from diabetic subjects have been shown to release higher levels of ROS (Giardino *et al.*, 1996 and Yu *et al.*, 2006). Several mechanisms have been proposed for this increased ROS production. The main mechanism for this increased ROS/RNS is from increased electron leakage thought to occur from damage to the mitochondrial electron transport chain (Yorek, 2003; Nishikawa *et al.*, 2000). Another mechanism for increased ROS/RNS is by PKC-dependent activation of NAD(P)H oxidase (Yorek, 2003).

Increased ROS production has been linked to endothelial ageing and endothelial dysfunction. One mechanism for this increased ageing and dysfunction is through damage to DNA. This oxidative damage is predominantly thought to occur to telomeric DNA at the guanine repeats (Oikawa and Kawanishi, 1999). Furthermore, ROS is also believed to affect mtDNA because it is closer to the site of ROS production and it is more exposed than nuclear DNA (Evans and Cooke, 2004; Genova *et al.*, 2004). Damage to DNA is hypothesised to account for ageing in both cells and whole organisms (Brandes *et al.*, 2005; Weinert and Timaras, 2003; von Zglinicki *et al.*, 2001). This thesis investigated HG-mediated changes to telomeric DNA and mtDNA as mechanisms contributing to endothelial cell ageing/dysfunction.

5.2 Summary of findings

Chapter 3 investigated the effect of HG on telomeric DNA by increased ROS production. Firstly, the uptake of glucose was increased in HUVECs cultured in HG compared with HUVECs cultured in NG medium. Furthermore, HUVECs cultured in HG medium produced increased ROS levels both over a short and long term when compared to HUVECs cultured in NG. HUVECs cultured in HG medium for 1 hour, produced two fold higher levels of H₂O₂ compared to HUVECs cultured in NG. Over 10 days of exposure to HG or AG, H₂O₂ progressively increased compared to the NG control. When the electron transport chain inhibitor TTFA was added to the HG medium, H₂O₂ production significantly decreased. This suggested that the origin of the increased ROS production was through the electron transport chain. Exposure of HUVECs to HG and AG also increased telomere attrition rates compared to HUVECs cultured in NG medium. In addition, this increased shortening was shown to be at least partly due to the increased ROS production from the electron transport chain. HUVECs cultured in HG or AG with NAC or TTFA displayed lower telomere attrition rates than HUVECs cultured in HG or AG alone.

Chapter 4 analysed whether high glucose caused a pro-inflammatory phenotype in endothelial cells and whether this shift was mediated by reduced mtDNA content and increased ROS production. It was shown that HG exposure led to decreased mtDNA content and a shift towards a pro-inflammatory phenotype with decreased expression of eNOS and increased expression of ICAM1. Expression was somewhat normalised by culturing HUVECs in HG medium containing NAC or TTFA. Different methods to deplete mtDNA and mitochondrial encoded proteins were then investigated. mtDNA was depleted by treating HUVECs with ethidium bromide or ddC and mitochondrial encoded proteins were depleted using chloramphenicol. When HUVECs were treated with ethidium bromide or ddC, there was a decrease in eNOS and an increase in ICAM1 and therefore a shift towards a pro-inflammatory phenotype.

HUVECs cultured in HG or AG showed increased telomere attrition rates (chapter 3) and increased mtDNA depletion (chapter 4) which appeared to be mediated through increased ROS production. The data suggest that telomeric DNA shortening and a reduction in mtDNA content (through damage to mtDNA) result in endothelial ageing and endothelial dysfunction which results in cardiovascular pathology. Figure 85 summarises the findings and demonstrates how the data from chapter 3 and 4 may be inter-related.

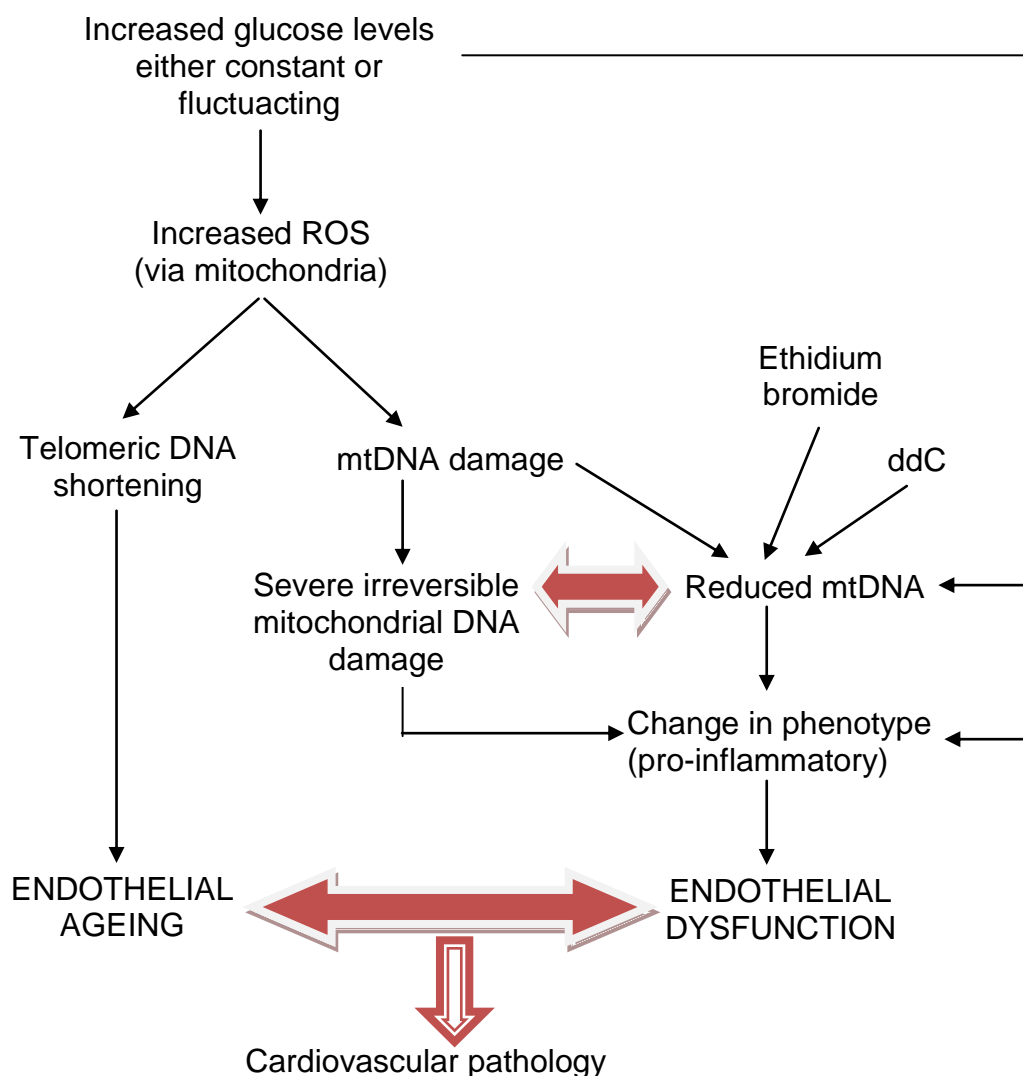


Figure 85: Hypothesis for increased glucose mediated endothelial cell ageing and/or dysfunction.

There are a number of novel findings within this thesis. Firstly, both constant levels and fluctuating glucose levels decreased telomere length more rapidly than normal glucose levels. This was shown to be at least partly mediated through a ROS related mechanism. This trend was demonstrated using a novel technique called STELA – a PCR based technique that provided more information than the regularly used technique of Southern blotting. Furthermore, this is the first study that shows such a dramatic effect on eNOS and ICAM1 expression following mtDNA depletion. Lastly, increased glucose levels mediated some of their effects on the phenotype of cells by increasing ROS levels. This therefore implicated the importance of increased ROS by damage to the mitochondrial ETC had on the pro-inflammatory phenotype. These novel findings could potentially have many implications on the future direction of high glucose research.

5.3 Clinical implications of these findings

This study investigated the effect of HG and AG (mimicking the conditions seen in diabetes) on ROS, telomeric DNA, mtDNA and endothelial dysfunction in HUVECs (*in vitro*). Both HUVECs cultured in HG and HUVECs cultured in AG were investigated. AG media has more clinical relevance than HG as these conditions imitate the fluctuations of glucose seen in patients with diabetes. Although there is a clear difference in these parameters between HUVECs cultured in NG and HG or AG, the data in this thesis generally shows that the effect on telomere length and mtDNA content observed in HUVECs cultured in AG medium is very similar to HUVECs cultured in HG. However, ROS production is clearly increased in HUVECs treated with AG when treatment is completed with HG medium. This is similar to data shown in the literature (Quagliaro *et al.*, 2003).

Studies have investigated these parameters (ROS, telomeric DNA, mtDNA and endothelial dysfunction) within cells of patients with diabetes (*in vivo*). Guzik *et al.*, (2002) measured ROS in both saphenous veins and internal mammary arteries from diabetic and non diabetic subjects using lucigenin-enhanced chemiluminescence. Superoxide production was significantly

higher in veins and arteries from diabetic subjects. Furthermore, shorter telomeres were observed in cells from patients with diabetes. Monocytes from diabetic subjects had shorter telomeres compared to telomeres in monocytes from controls (Sampson *et al.*, 2006; Adaikalakoteswari *et al.*, 2005). Furthermore, telomere length was lower in cells from patients with pre-diabetes (impaired glucose tolerance) and even shorter in patients with type II diabetes (Adaikalakoteswari *et al.*, 2007). Moreover, when mtDNA content was measured in diabetics it was found to be reduced in leukocytes (Lee *et al.*, 1998), muscle cells (Suzuki *et al.*, 1999) and peripheral blood mononuclear cells (Garcia-Ramirez *et al.*, 2008) when compared to mtDNA content in cells from 'healthy' subjects. A number of studies have investigated the effect of diabetes on the pro-inflammatory phenotype. eNOS expression was lower in HUVECs from diabetic subjects (Makino *et al.*, 2005; Bolega *et al.*, 2006) and the plasma level of soluble ICAM1 was increased in patients with diabetes (Cipollone *et al.*, 2004; Bluher *et al.*, 2002). Therefore, the effects observed in this thesis appear to correlate closely with those effects observed *in vivo*. The model cellular system and the mechanism suggested in this thesis therefore provide possible explanations for the observations made *in vivo* in patients with diabetes.

The findings from this thesis could potentially have a number of clinical implications. Diabetes is treated either through lifestyle changes or through pharmacology based interventions. Obviously, hyperglycaemia is sometimes treated by insulin and the reduction in glucose levels is vitally important. The findings from this study suggest that HG induced telomeric DNA and mtDNA damage which lead to endothelial ageing and endothelial dysfunction are mediated through increased ROS production. Therefore, this study further supports the use of antioxidants or drugs that reduce ROS levels *in vivo*. Studies have investigated treating diabetes with antioxidants such as vitamin E. However, in general they have failed to demonstrate any beneficial effects on reducing endothelial dysfunction (Marchioli *et al.*, 2001; Darko *et al.*, 2002; Bilsborough *et al.*, 2002; Liu *et al.*, 2006). Therefore studies have investigated the effect of targeted antioxidants both *in vitro* and

in vivo to the mitochondria (Dhanasekaran *et al.*, 2004; Sheu *et al.*, 2006; Green *et al.*, 2004). As mitochondrial oxidative damage is believed to play a central role in the pathophysiology of diabetes, mitochondrial targeted antioxidants are believed to have a greater effect on reducing ROS levels than general antioxidants (Green *et al.*, 2004). Compounds such as MitoVitE and MitoQ have been developed that are directed towards the mitochondria and these have been shown to reduce ROS much more effectively than untargeted antioxidants (Sheu *et al.*, 2006). Although targeted antioxidants have a more beneficial effect than untargeted antioxidants, studies are also focussing on drugs that are not conventional antioxidants but are thought to act at least in part by reducing ROS levels. L-propionyl-carnitine acts as a superoxide scavenger (Packer *et al.*, 1991; Vanella *et al.*, 2000). Furthermore, many of the beneficial effects seen after treatment with thiazolinediones, statins and ACE are believed to be due to the strong intracellular antioxidant activity of these compounds (Ceriello, 2003; Cumbie and Hermayer, 2007; Hamilton *et al.*, 2007; Johansen *et al.*, 2005). Therefore, some of the current treatments for diabetes support the findings in this thesis. Nonetheless, the treatment of diabetes by antioxidants or compounds with superoxide scavenging abilities is indicated by both the data presented here and in the literature.

5.4 Further Work

5.4.1 Do other ROS detection systems confirm the increase in ROS and do other antioxidants and mitochondrial inhibitors show similar effects seen when using Amplex Red?

To confirm the effects on ROS production seen using the Amplex Red assay, other ROS detection systems could be used. For example, superoxide could be measured using DHE (Benov *et al.*, 1998; Miller *et al.*, 1998) or ROS/RNS could be measured using DCFDA (Soh, 2006). Furthermore, to confirm that increased ROS are due to the electron

transport chain, other antioxidants or electron transport chain inhibitors such as mitoQ should be used.

5.4.2 Is there a role for telomerase?

As HG and AG both show increased telomere attrition rates and increased ROS levels, is this due to ROS inhibiting telomerase? Haendeler *et al.*, (2004) and Haendeler *et al.*, (2003) investigated the effect of antioxidants

5.4.3 Are NADPH levels affected in Rho0 HUVECs?

NADPH is lower in diabetics due to increased aldose reductase activity (Okuda *et al.*, 1997). NADPH acts as a cofactor for many antioxidant enzymes and decreased NADPH may result in increased ROS levels. Therefore NADPH levels could be monitored in HUVECs exposed to HG or AG. Moreover, the activities of NADPH-requiring antioxidant enzymes could be determined.

5.4.4 Are other markers indicating a pro-inflammatory phenotype affected in Rho0 HUVECs?

ICAM1 protein increased in Rho0 HUVECs and eNOS protein expression decreased. However, to investigate this further, other markers of a pro-inflammatory phenotype could be analysed such as VCAM1 expression. Furthermore, proteomics could be performed on these cells to investigate protein expression. To investigate changes at a transcriptional level, microarrays could be performed.

5.4.5 Are the changes in pro-inflammatory phenotype in Rho0 HUVECs due to increased ROS?

To investigate if changes in the pro-inflammatory phenotype observed in Rho0 HUVECs was mediated by increased ROS production, Rho0 HUVECs

could be treated with antioxidants or electron transport chain inhibitors that have been shown to decrease ROS production in these cells. Protein levels of eNOS and ICAM1 could then be measured using Western blotting.

5.4.6 Are the changes in pro-inflammatory phenotype in Rho0 HUVECs reverted by mtDNA reconstitution?

As depleting mtDNA levels shifted the cells towards a pro-inflammatory phenotype, it would be interesting to see if the cells would revert to their original phenotype when reconstituting mtDNA. Literature shows that the effect of ethidium bromide on mtDNA can be reversed by the removing ethidium bromide from the media (Wiseman and Attardi, 1978). Alternatively, other groups have demonstrated different methods by which the mtDNA can be re-introduced in cells (Swerdlow *et al.*, 1997; King and Attardi, 1989; Navratil *et al.*, 2008). Furthermore, it would be interesting to investigate the mechanism of how mtDNA depletion significantly reduced the amount of eNOS (see section 5.4.7).

5.4.7 Is eNOS mRNA half life decreased in Rho0 HUVECs?

First of all, is eNOS mRNA decreased in Rho0 HUVECs? This would suggest transcriptional control. Secondly, is the half life of the eNOS mRNA molecule affected? Studies have shown that eNOS mRNA content and eNOS mRNA half life are often both affected (Ramasamy *et al.*, 1998).

5.4.8 Do Rho0 HUVECs have shorter telomeres?

As Rho0 HUVECs have been shown to produce increased ROS levels, it would be interesting to investigate whether mtDNA depletion could have a direct effect on telomere attrition rates.

5.5 Presentations and publications arising from this study

5.5.1 Presentations

1. Poster and oral presentation. 'High glucose induces mitochondrial ROS and accelerates human endothelial cell ageing'. GRC conference entitled 'Oxidant Radicals' in Ventura, CA, USA January 2008.
2. Poster presentations. 'Mitochondrial DNA depletion promotes an atherogenic phenotype in human endothelial cells' AND 'High glucose accelerates biological ageing of human endothelial cells by oxidative DNA damage and subsequent loss of telomere loss of telomere DNA'. Association of physicians. 10th/11th April 2008.
3. Poster presentation. 'Does diabetes over-work the powerhouses of cells'. Festival of Postgraduate research. 26th June 2008.

5.5.2 Publications

1. Herbert, K, E., Bowers, L., Mistry, Y., Williams, B. (2007) Mitochondrial DNA depletion affects eNOS expression. *Free Radical Biology and Medicine*. **43** (Supplement 1) S151
2. Bowers, L,L, Williams, B. Herbert, K, E (In preparation for *European Journal of Circulation Research*) Mitochondrial DNA depletion promotes pro-inflammatory changes in human endothelial cells.
3. Bowers, L, L., Herbert, K, E., Patel, H., Williams, B. (In preparation for *Diabetes*) High glucose accelerates ageing of endothelial cells by oxidative telomeric damage.

6 Appendices

List of reagent and instrument suppliers:

ABCAM
330 Cambridge Science Park
Cambridge
CB4 0FL
UK

Abgene Limited
Abgene House
Blenheim Road
Epsom
KT19 9AP
UK

Amersham Pharmacia Biotech
Little Chalfont
Buckinghamshire
UK

BD Biosciences
The Danby Building
Edmund Halley Road
Oxford Science Park
OX4 4DQ Oxford
United Kingdom

Bio-Rad Laboratories Ltd.
Bio-Rad House
Maxted Road
Hemel Hempstead
Hertfordshire
HP2 7DX

BioTex Instruments Inc
Vermont
USA

Dako UK Ltd
Cambridge House
St Thomas Place, Ely
Cambridgeshire CB7 4EX

Fisher Scientific UK Ltd
Bishop Meadow Road
Loughborough
Leicestershire
LE11 5RG

GE Healthcare Life Sciences
Amersham Place
Little Chalfont
Buckinghamshire
HP7 9NA
UK

Invitrogen
3 Fountain Drive
Inchinnan Business Park
Paisley
UK
PA4 9RF

Lonza Biologics Plc
228 Bath Road
Slough
Berkshire
SL1 4DX
UK

New England Biolabs Ltd
75/77 Knowl Piece
Wilbury Way
Hitchin
Herts
SG4 0TY

PerSeptive Biosystems
500 Old Connecticut Path
Framingham
MA 01701
USA

QIAGEN Ltd
QIAGEN House
Fleming Way
Crawley
West Sussex
RH10 9NQ

Roche Applied Sciences,
Charles Avenue
Burgess Hill
RH15 9RY
UK

Sigma-Aldrich
The Old Brickyard
New Road,
Gillingham
Dorset
SP8 4XT

Stratagene
An agilent Technologies Division
Agilent Technologies UK Limited
Cheadle Royal Business Park
Stockport
Cheshire
SK8 3GR

Vector laboratories Ltd.
3 Accent Park
Bakewell Road,
Orton Southgate
Peterborough,
PE2 6XS,
United Kingdom

HG media:

16.5mM glucose:

Molecular weight: 180.1 Final concentration: 1M Volume: 10cm³

$0.01 \times 180.1 \times 1 = 1.8\text{g}$ glucose to 10cm^3 of sterilised ultrapure water.

10mls media: $1\text{M} \rightarrow 16.5\text{mM}$, a 1 in 60 dilution.

Add $166\mu\text{l}$ glucose solution.

Determining the concentration of primers:

e.g. absorbance at 260nm 0.240 so:

OD x dilution x nmol/OD (provided by Invitrogen)

Concentration of primer: $240\mu\text{M}$

Hexokinase kit:

Glucose loss for NG media:

13.9 pmoles/cell/day

T75 flask with 15mls media and a cell count of 1×10^6 .

$13.9 \times 1000000 = 13900000$ pmoles/day

$13900000 / (15/1000) = 926666666.7$ pM/day

$926666666.7 / 1000 / 1000 / 1000 = 0.927\text{mM/day}$ decrease for 1×10^6 .

$= 1.854\text{mM/day}$ decrease for 2×10^6 .

So maximum glucose loss in 2 days = 3.5mM

3-O-methylglucose:

16.5mM 3-O-methylglucose:

Molecular weight: 194.18 Final concentration: 1M Volume: 10cm^3

$0.01 \times 194.18 \times 1 = 1.94\text{g}$ glucose to 10cm^3 of sterilised ultrapure water.

10mls media: $1\text{M} \rightarrow 16.5\text{mM}$, a 1 in 60 dilution.

Add $166\mu\text{l}$ glucose solution.

Mannitol:

16.5mM mannitol:

Molecular weight: 182.2 Final concentration: 1M Volume: 10cm^3

$0.01 \times 182.2 \times 1 = 1.82\text{g}$ glucose to 10cm^3 of sterilised ultrapure water.

10mls media: $1\text{M} \rightarrow 16.5\text{mM}$, a 1 in 60 dilution.

Add $166\mu\text{l}$ glucose solution.

NAC:

3mM NAC:

Molecular weight: 163.2 Final concentration: 1M Volume: 10cm^3

$0.01 \times 163.2 \times 1 = 1.6\text{g}$ glucose to 10cm^3 of sterilised ultrapure water.

10mls media: $1\text{M} \rightarrow 3\text{mM}$, a 1 in 33.3 dilution.

Add $300\mu\text{l}$ glucose solution.

TTFA:

$25\mu\text{M}$ glucose:

Molecular weight: 222.18 Final concentration: 1M Volume: 10cm^3

$0.01 \times 222.18 \times 1 = 2.22\text{g}$ glucose to 10cm^3 of sterilised ultrapure water.

10mls media: $1\text{M} \rightarrow 25\mu\text{M}$, a 1 in 400 dilution.

Add $2.5\mu\text{l}$ glucose solution.

Amplex Red:

Stock Amplex Red (10mM):

$[(0.001/257.24)/0.01] \times 1000 \times 1000$

$389.61\mu\text{l}$ DMSO

HRP (10U/ml):

1000 units per 0.007g

100 units per 0.0007g in 10mls HBSS

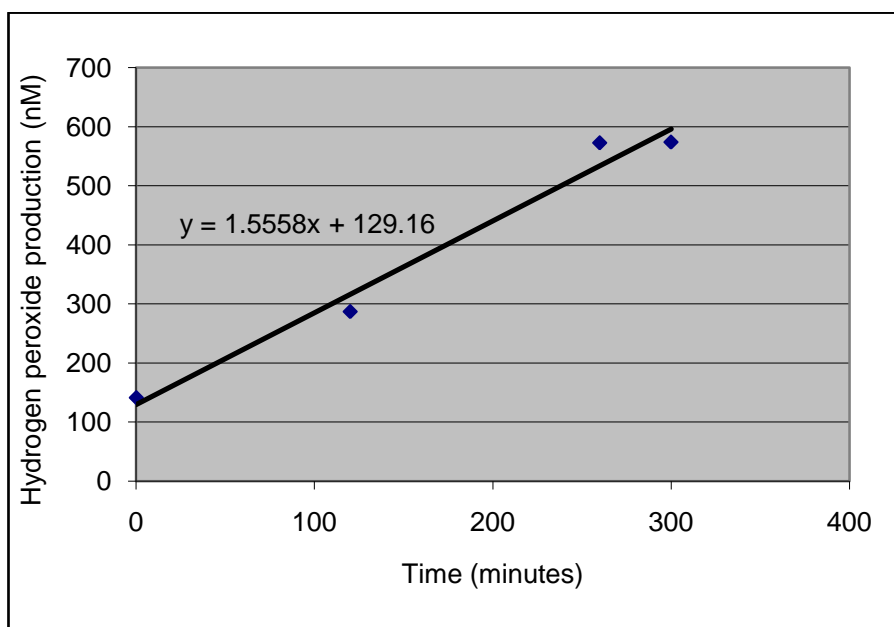
Hydrogen peroxide concentration was calculated at each timepoint using standard curve. Values were calculated in terms of nM. Rate of H_2O_2

production was then calculated by taking the gradient of the slope (nM/min). This was then converted to hydrogen peroxide production in 60µl (nmoles/min). At this point, protein concentration in each well was calculated in terms of mg/100µl. The rate was then corrected with the protein concentration (nmoles/min/mg). This was then converted to pmoles/min/mg. An example of this calculation is shown below:

Concentration of hydrogen peroxide production (nM):

0 minutes: 141.3; 120 minutes: 287.0; 260 minutes: 572.5;

300 minutes: 573.8



Rate of H₂O₂ production: 1.555 nM/min

H₂O₂ production in 60µl: $1.555/1000/1000 \times 60$
 $= 0.0000933480$ nmoles/min

Protein concentration per well: 0.00426

$0.0000933480/0.00426 = 0.0219$ nmoles/min/mg
 $= 21.91$ pmoles/min/mg

7 References

- Abdul-Ghani MA, Tripathy D, & DeFronzo RA (2006) Contributions of beta-cell dysfunction and insulin resistance to the pathogenesis of impaired glucose tolerance and impaired fasting glucose. *Diabetes Care* **29**: 1130-1139
- Abraham NG, Kushida T, McClung J, Weiss M, Quan S, Lafaro R, Darzynkiewicz Z, & Wolin M (2003) Heme oxygenase-1 attenuates glucose-mediated cell growth arrest and apoptosis in human microvessel endothelial cells. *Circ Res* **93**: 507-514
- Adaikalakoteswari A, Balasubramanyam M, & Mohan V (2005) Telomere shortening occurs in Asian Indian Type 2 diabetic patients. *Diabetic Med* **22**: 1151-1156
- Adaikalakoteswari A, Balasubramanyam M, Ravikumar R, Deepa R, & Mohan V (2007) Association of telomere shortening with impaired glucose tolerance and diabetic macroangiopathy. *Atherosclerosis* **195**: 83-89
- Afonso V, Champy R, Mitrovic D, Collin P, & Lomri A (2007) Reactive oxygen species and superoxide dismutases: role in joint diseases. *Joint Bone Spine* **74**: 324-329
- Ahmed N (2005) Advanced glycation endproducts--role in pathology of diabetic complications. [Review] [100 refs]. *Diabetes Research & Clinical Practice* **67**: 3-21
- Albrecht EW, Stegeman CA, Heeringa P, Henning RH, & van Goor H (2003) Protective role of endothelial nitric oxide synthase. *J Pathol* **199**: 8-17
- Alderton WK, Cooper CE, & Knowles RG (2001) Nitric oxide synthases: structure, function and inhibition. *Biochem J* **357**: 593-615

Ali MH, Pearlstein DP, Mathieu CE, & Schumacker PT (2004) Mitochondrial requirement for endothelial responses to cyclic strain: implications for mechanotransduction. *Am J Physiol Lung Cell Mol Physiol* **287**: L486-96

Alpert E, Gruzman A, Riahi Y, Blejter R, Aharoni P, Weisinger G, Eckel J, Kaiser N, & Sasson S (2005) Delayed autoregulation of glucose transport in vascular endothelial cells. *Diabetologia* **48**: 752-755

Alpert E, Gruzman A, Totary H, Kaiser N, Reich R, & Sasson S (2002) A natural protective mechanism against hyperglycaemia in vascular endothelial and smooth-muscle cells: role of glucose and 12-hydroxyeicosatetraenoic acid. *Biochem J* **362**: 413-422

American Diabetes Association (2009) Diagnosis and classification of diabetes mellitus. *Diabetes Care* **32 Suppl 1**: S62-7

Ames BN, Shigenaga MK, & Hagen TM (1993) Oxidants, antioxidants, and the degenerative diseases of aging. [Review] [217 refs]. *Proc Natl Acad Sci U S A* **90**: 7915-7922

Anderson PR, Kirby K, Orr WC, Hilliker AJ, & Phillips JP (2008) Hydrogen peroxide scavenging rescues frataxin deficiency in a Drosophila model of Friedreich's ataxia. *Proc Natl Acad Sci U S A* **105**: 611-616

Ashley N, Harris D, & Poulton J (2005) Detection of mitochondrial DNA depletion in living human cells using PicoGreen staining. *Exp Cell Res* **303**: 432-446

Asin-Cayuela J & Gustafsson CM (2007) Mitochondrial transcription and its regulation in mammalian cells. *Trends Biochem Sci* **32**: 111-117

Atkuri KR, Mantovani JJ, Herzenberg LA, & Herzenberg LA (2007) N-Acetylcysteine--a safe antidote for cysteine/glutathione deficiency. *Curr Opin Pharmacol* **7**: 355-359

Baird DM (2005) New developments in telomere length analysis. [Review] [52 refs]. *Exp Gerontol* **40**: 363-368

Baird DM & Kipling D (2004) The extent and significance of telomere loss with age. [Review] [10 refs]. *Ann N Y Acad Sci* **1019**: 265-268

Baird DM, Rowson J, Wynford-Thomas D, & Kipling D (2003) Extensive allelic variation and ultrashort telomeres in senescent human cells. *Nat Genet* **33**: 203-207

Balaban RS, Nemoto S, & Finkel T (2005) Mitochondria, oxidants, and aging. *Cell* **120**: 483-495

Ballinger SW, Patterson C, Knight-Lozano CA, Burow DL, Conklin CA, Hu Z, Reuf J, Horaist C, Lebovitz R, Hunter GC, McIntyre K, & Runge MS (2002) Mitochondrial integrity and function in atherogenesis. *Circulation* **106**: 544-549

Bartnik M, Norhammar A, & Ryden L (2007) Hyperglycaemia and cardiovascular disease. *J Intern Med* **262**: 145-156

Barton M, Cosentino F, Brandes RP, Moreau P, Shaw S, & Luscher TF (1997) Anatomic heterogeneity of vascular aging: role of nitric oxide and endothelin. *Hypertension* **30**: 817-824

Basta G (2008) Receptor for advanced glycation endproducts and atherosclerosis: From basic mechanisms to clinical implications. *Atherosclerosis* **196**: 9-21

Basta G, Schmidt AM, & De Caterina R (2004) Advanced glycation end products and vascular inflammation: implications for accelerated atherosclerosis in diabetes. [Review] [98 refs]. *Cardiovasc Res* **63**: 582-592

Baynes JW (2002) The Maillard hypothesis on aging: time to focus on DNA. *Ann N Y Acad Sci* **959**: 360-367

- Bayraktutan U (2002) Free radicals, diabetes and endothelial dysfunction. [Review] [159 refs]. *Diabetes Obes Metab* **4**: 224-238
- Beckman KB & Ames BN (1998) The free radical theory of aging matures. *Physiol Rev* **78**: 547-581
- Benov L, Sztejnberg L, & Fridovich I (1998) Critical evaluation of the use of hydroethidine as a measure of superoxide anion radical. *Free Radic Biol Med* **25**: 826-831
- Berrone E, Beltramo E, Solimine C, Ape AU, & Porta M (2006) Regulation of intracellular glucose and polyol pathway by thiamine and benfotiamine in vascular cells cultured in high glucose. *J Biol Chem* **281**: 9307-9313
- Bilsborough W, O'Driscoll G, Stanton K, Weerasooriya R, Dembo L, Taylor R, & Green D (2002) Effect of lowering tumour necrosis factor-alpha on vascular endothelial function in Type II diabetes. *Clin Sci (Lond)* **103**: 163-169
- Birkus G, Hitchcock MJ, & Cihlar T (2002) Assessment of mitochondrial toxicity in human cells treated with tenofovir: comparison with other nucleoside reverse transcriptase inhibitors. *Antimicrob Agents Chemother* **46**: 716-723
- Blackburn EH (2001) Switching and signaling at the telomere. [Review] [109 refs]. *Cell* **106**: 661-673
- Blasco MA (2005) Telomeres and human disease: ageing, cancer and beyond. [Review] [110 refs]. *Nature Reviews Genetics* **6**: 611-622
- Bluher M, Unger R, Rassoul F, Richter V, & Paschke R (2002) Relation between glycaemic control, hyperinsulinaemia and plasma concentrations of soluble adhesion molecules in patients with impaired glucose tolerance or Type II diabetes. *Diabetologia* **45**: 210-216

Bolego C, Buccellati C, Radaelli T, Cetin I, Puglisi L, Folco G, & Sala A (2006) eNOS, COX-2, and prostacyclin production are impaired in endothelial cells from diabetics. *Biochem Biophys Res Commun* **339**: 188-190

Boquist L & Ericsson I (1984) Inhibition by alloxan of mitochondrial aconitase and other enzymes associated with the citric acid cycle. *FEBS Lett* **178**: 245-248

Borniquel S, Valle I, Cadenas S, Lamas S, & Monsalve M (2006) Nitric oxide regulates mitochondrial oxidative stress protection via the transcriptional coactivator PGC-1alpha. *FASEB J* **20**: 1889-1891

Boukamp P (2001) Ageing mechanisms: the role of telomere loss. [Review] [15 refs]. *Clinical & Experimental Dermatology* **26**: 562-565

Brandes RP, Fleming I, & Busse R (2005) Endothelial aging. *Cardiovasc Res* **66**: 286-294

Bras ID, Colitz CM, Kusewitt DF, Chandler H, Lu P, Gemensky-Metzler AJ, & Wilkie DA (2007) Evaluation of advanced glycation end-products in diabetic and inherited canine cataracts. *Graefes Arch Clin Exp Ophthalmol* **245**: 249-257

Brevig T, Rohrmann JH, & Riemann H (2006) Oxygen reduces accumulation of type IV collagen in endothelial cell subcellular matrix via oxidative stress. *Artif Organs* **30**: 915-921

Broccoli D (2004) Function, replication and structure of the mammalian telomere. *Cytotechnology* **45**: 3-12

Brouillette S, Singh RK, Thompson JR, Goodall AH, & Samani NJ (2003) White cell telomere length and risk of premature myocardial infarction.[see comment]. *Arteriosclerosis, Thrombosis & Vascular Biology* **23**: 842-846

Brown GK (2000) Glucose transporters: structure, function and consequences of deficiency. [Review] [54 refs]. *J Inherit Metab Dis* **23**: 237-246

Brown SM, Smith DM, Alt N, Thorpe SR, & Baynes JW (2005) Tissue-specific variation in glycation of proteins in diabetes: evidence for a functional role of amadoriase enzymes. *Ann N Y Acad Sci* **1043**: 817-823

Brownlee M (2001) Biochemistry and molecular cell biology of diabetic complications. *Nature* **414**: 813-820

Burcham PC (1998) Genotoxic lipid peroxidation products: their DNA damaging properties and role in formation of endogenous DNA adducts. *Mutagenesis* **13**: 287-305

Burnett KG & Scheffler IE (1981) Integrity of mitochondria in a mammalian cell mutant defective in mitochondrial protein synthesis. *J Cell Biol* **90**: 108-115

Burns EM, Kruckeberg TW, Comerford LE, & Buschmann MT (1979) Thinning of capillary walls and declining numbers of endothelial mitochondria in the cerebral cortex of the aging primate, *Macaca nemestrina*. *J Gerontol* **34**: 642-650

Busik JV, Olson LK, Grant MB, & Henry DN (2002) Glucose-induced activation of glucose uptake in cells from the inner and outer blood-retinal barrier. *Invest Ophthalmol Vis Sci* **43**: 2356-2363

Cai H & Harrison DG (2000) Endothelial dysfunction in cardiovascular diseases - The role of oxidant stress. *Circ Res* **87**: 840-844

Ceriello A (2003) New insights on oxidative stress and diabetic complications may lead to a "causal" antioxidant therapy. *Diabetes Care* **26**: 1589-1596

- Chandel NS, Maltepe E, Goldwasser E, Mathieu CE, Simon MC, & Schumacker PT (1998) Mitochondrial reactive oxygen species trigger hypoxia-induced transcription. *Proc Natl Acad Sci U S A* **95**: 11715-11720
- Chang TS, Cho CS, Park S, Yu S, Kang SW, & Rhee SG (2004) Peroxiredoxin III, a mitochondrion-specific peroxidase, regulates apoptotic signaling by mitochondria. *J Biol Chem* **279**: 41975-41984
- Chen YH, Guh JY, Chuang TD, Chen HC, Chiou SJ, Huang JS, Yang YL, & Chuang LY (2007) High glucose decreases endothelial cell proliferation via the extracellular signal regulated kinase/p15(INK4b) pathway. *Arch Biochem Biophys* **465**: 164-171
- Cherif H, Tarry JL, Ozanne SE, & Hales CN (2003) Ageing and telomeres: a study into organ- and gender-specific telomere shortening. *Nucleic Acids Res* **31**: 1576-1583
- Cheung I, Schertzer M, Baross A, Rose AM, Lansdorp PM, & Baird DM (2004) Strain-specific telomere length revealed by single telomere length analysis in *Caenorhabditis elegans*. *Nucleic Acids Res* **32**: 3383-3391
- Chevallet M, Lescuyer P, Diemer H, van Dorsselaer A, Leize-Wagner E, & Rabilloud T (2006) Alterations of the mitochondrial proteome caused by the absence of mitochondrial DNA: A proteomic view. *Electrophoresis* **27**: 1574-1583
- Cipollone F, Chiarelli F, Davi G, Ferri C, Desideri G, Fazia M, Iezzi A, Santilli F, Pini B, Cucurullo C, Tumini S, Del Ponte A, Santucci A, Cucurullo F, & Mezzetti A (2005) Enhanced soluble CD40 ligand contributes to endothelial cell dysfunction in vitro and monocyte activation in patients with diabetes mellitus: effect of improved metabolic control. *Diabetologia* **48**: 1216-1224
- Cleaver O & Melton DA (2003) Endothelial signaling during development. [Review] [87 refs]. *Nat Med* **9**: 661-668

- Constans J & Conri C (2006) Circulating markers of endothelial function in cardiovascular disease. *Clin Chim Acta* **368**: 33-47
- Cooke MS, Evans MD, Dizdaroglu M, & Lunec J (2003) Oxidative DNA damage: mechanisms, mutation, and disease. *FASEB J* **17**: 1195-1214
- Cooke MS, Olinski R, & Evans MD (2006) Does measurement of oxidative damage to DNA have clinical significance? *Clin Chim Acta* **365**: 30-49
- Csiszar A, Ungvari Z, Edwards JG, Kaminski P, Wolin MS, Koller A, & Kaley G (2002) Aging-induced phenotypic changes and oxidative stress impair coronary arteriolar function. *Circ Res* **90**: 1159-1166
- Cumbie BC & Hermayer KL (2007) Current concepts in targeted therapies for the pathophysiology of diabetic microvascular complications. *Vasc Health Risk Manag* **3**: 823-832
- d'Adda di Fagagna F, Reaper PM, Clay-Farrace L, Fiegler H, Carr P, Von Zglinicki T, Saretzki G, Carter NP, & Jackson SP (2003) A DNA damage checkpoint response in telomere-initiated senescence. *Nature* **426**: 194-198
- Darko D, Dornhorst A, Kelly FJ, Ritter JM, & Chowienczyk PJ (2002) Lack of effect of oral vitamin C on blood pressure, oxidative stress and endothelial function in Type II diabetes. *Clin Sci (Lond)* **103**: 339-344
- Das Evcimen N & King GL (2007) The role of protein kinase C activation and the vascular complications of diabetes. *Pharmacol Res* **55**: 498-510
- Davidson SM & Duchon MR (2007) Endothelial mitochondria: contributing to vascular function and disease. *Circ Res* **100**: 1128-1141
- Davis B & Zou MH (2005) CD40 ligand-dependent tyrosine nitration of prostacyclin synthase in vivo. *Circulation* **112**: 2184-2192
- de Lange T (2005) Shelterin: the protein complex that shapes and safeguards human telomeres. [Review] [84 refs]. *Genes Dev* **19**: 2100-2110

- de Lange T (2002) Protection of mammalian telomeres. [Review] [80 refs]. *Oncogene* **21**: 532-540
- de Magalhaes JP & Church GM (2006) Cells discover fire: employing reactive oxygen species in development and consequences for aging. *Exp Gerontol* **41**: 1-10
- Delsite RL, Rasmussen LJ, Rasmussen AK, Kalen A, Goswami PC, & Singh KK (2003) Mitochondrial impairment is accompanied by impaired oxidative DNA repair in the nucleus. *Mutagenesis* **18**: 497-503
- Dhanasekaran A, Kotamraju S, Kalivendi SV, Matsunaga T, Shang T, Keszler A, Joseph J, & Kalyanaraman B (2004) Supplementation of endothelial cells with mitochondria-targeted antioxidants inhibit peroxide-induced mitochondrial iron uptake, oxidative damage, and apoptosis. *J Biol Chem* **279**: 37575-37587
- Dhindsa S, Tripathy D, Mohanty P, Ghanim H, Syed T, Aljada A, & Dandona P (2004) Differential effects of glucose and alcohol on reactive oxygen species generation and intranuclear nuclear factor-kappaB in mononuclear cells. *Metabolism* **53**: 330-334
- Dias N & Bailly C (2005) Drugs targeting mitochondrial functions to control tumor cell growth. *Biochem Pharmacol* **70**: 1-12
- Dong CK, Masutomi K, & Hahn WC (2005) Telomerase: regulation, function and transformation. [Review] [132 refs]. *Critical Reviews in Oncology-Hematology* **54**: 85-93
- Doughan AK, Harrison DG, & Dikalov SI (2008) Molecular mechanisms of angiotensin II-mediated mitochondrial dysfunction: linking mitochondrial oxidative damage and vascular endothelial dysfunction. *Circ Res* **102**: 488-496
- Drew B & Leeuwenburgh C (2002) Aging and the role of reactive nitrogen species. *Ann N Y Acad Sci* **959**: 66-81

Druzhyina NM, Wilson GL, & LeDoux SP (2008) Mitochondrial DNA repair in aging and disease. *Mech Ageing Dev* **129**: 383-390

Dudzinski DM & Michel T (2007) Life history of eNOS: partners and pathways. *Cardiovasc Res* **75**: 247-260

Dutta U, Cohenford MA, & Dain JA (2005) Nonenzymatic glycation of DNA nucleosides with reducing sugars. *Anal Biochem* **345**: 171-180

Edelstein D & Brownlee M (1992) Mechanistic studies of advanced glycosylation end product inhibition by aminoguanidine. *Diabetes* **41**: 26-29

Ehrlich M (2003) Expression of various genes is controlled by DNA methylation during mammalian development. *J Cell Biochem* **88**: 899-910

Elizalde M, Ryden M, van Harmelen V, Eneroth P, Gyllenhammar H, Holm C, Ramel S, Olund A, Arner P, & Andersson K (2000) Expression of nitric oxide synthases in subcutaneous adipose tissue of nonobese and obese humans. *J Lipid Res* **41**: 1244-1251

Elliot WH & Elliot DC (2001) *Biochemistry and Molecular Biology*. Oxford University Press: Oxford

Erusalimsky JD & Kurz DJ (2005) Cellular senescence in vivo: Its relevance in ageing and cardiovascular disease. *Exp Gerontol* **40**: 634-642

Evans JL, Goldfine ID, Maddux BA, & Grodsky GM (2002) Oxidative stress and stress-activated signaling pathways: a unifying hypothesis of type 2 diabetes. [Review] [416 refs]. *Endocr Rev* **23**: 599-622

Evans MD & Cooke MS (2004) Factors contributing to the outcome of oxidative damage to nucleic acids. [Review] [66 refs]. *Bioessays* **26**: 533-542

Falkenberg M, Larsson NG, & Gustafsson CM (2007) DNA replication and transcription in mammalian mitochondria. *Annu Rev Biochem* **76**: 679-699

Fernandez-Hernando C, Fukata M, Bernatchez PN, Fukata Y, Lin MI, Bredt DS, & Sessa WC (2006) Identification of Golgi-localized acyl transferases that palmitoylate and regulate endothelial nitric oxide synthase. *J Cell Biol* **174**: 369-377

Finkel T & Holbrook NJ (2000) Oxidants, oxidative stress and the biology of ageing. *Nature* **408**: 239-247

Foreman KE & Tang J (2003) Molecular mechanisms of replicative senescence in endothelial cells. [Review] [67 refs]. *Exp Gerontol* **38**: 1251-1257

Frey TG & Mannella CA (2000) The internal structure of mitochondria. *Trends Biochem Sci* **25**: 319-324

Furumoto K, Inoue E, Nagao N, Hiyama E, & Miwa N (1998) Age-dependent telomere shortening is slowed down by enrichment of intracellular vitamin C via suppression of oxidative stress. *Life Sci* **63**: 935-948

Fuster JJ & Andres V (2006) Telomere biology and cardiovascular disease. *Circ Res* **99**: 1167-1180

Garcia-Cao M, O'Sullivan R, Peters AH, Jenuwein T, & Blasco MA (2004) Epigenetic regulation of telomere length in mammalian cells by the Suv39h1 and Suv39h2 histone methyltransferases. *Nat Genet* **36**: 94-99

Garcia-Cardena G, Martasek P, Masters BS, Skidd PM, Couet J, Li S, Lisanti MP, & Sessa WC (1997) Dissecting the interaction between nitric oxide synthase (NOS) and caveolin. Functional significance of the nos caveolin binding domain in vivo. *J Biol Chem* **272**: 25437-25440

Garcia-Ramirez M, Francisco G, Garcia-Arumi E, Hernandez C, Martinez R, Andreu AL, & Simo R (2008) Mitochondrial DNA oxidation and manganese superoxide dismutase activity in peripheral blood mononuclear cells from type 2 diabetic patients. *Diabetes Metab* **34**: 117-124

Garesse R & Vallejo CG (2001) Animal mitochondrial biogenesis and function: a regulatory cross-talk between two genomes. *Gene* **263**: 1-16

Garrett, R. H., Grisham, C. M. (1995) *International Edition: Biochemistry*. Saunders College Publishing, USA.

Genova ML, Pich MM, Bernacchia A, Bianchi C, Biondi A, Bovina C, Falasca AI, Formiggini G, Castelli GP, & Lenaz G (2004) The mitochondrial production of reactive oxygen species in relation to aging and pathology. *Ann N Y Acad Sci* **1011**: 86-100

Genuth S, Alberti KG, Bennett P, Buse J, DeFronzo R, Kahn R, Kitzmiller J, Knowler WC, Lebovitz H, Lernmark A, Nathan D, Palmer J, Rizza R, Saudek C, Shaw J, Steffes M, Stern M, Tuomilehto J, Zimmet P, & Expert Committee on the Diagnosis and Classification of Diabetes Mellitus (2003) Follow-up report on the diagnosis of diabetes mellitus. *Diabetes Care* **26**: 3160-3167

Giardino I, Edelstein D, & Brownlee M (1996) BCL-2 expression or antioxidants prevent hyperglycemia-induced formation of intracellular advanced glycation endproducts in bovine endothelial cells. *J Clin Invest* **97**: 1422-1428

Gilkerson RW, Margineantu DH, Capaldi RA, & Selker JM (2000) Mitochondrial DNA depletion causes morphological changes in the mitochondrial reticulum of cultured human cells. *FEBS Lett* **474**: 1-4

Glass CK & Witztum JL (2001) Atherosclerosis. the road ahead. *Cell* **104**: 503-516

Glynn SL & Yazdanian M (1998) In vitro blood-brain barrier permeability of nevirapine compared to other HIV antiretroviral agents. *J Pharm Sci* **87**: 306-310

Gorgoulis VG, Zacharatos P, Kotsinas A, Kletsas D, Mariatos G, Zoumpourlis V, Ryan KM, Kittas C, & Papavassiliou AG (2003) p53

activates ICAM-1 (CD54) expression in an NF-kappaB-independent manner. *EMBO J* **22**: 1567-1578

Govers R & Rabelink TJ (2001) Cellular regulation of endothelial nitric oxide synthase. *Am J Physiol Renal Physiol* **280**: F193-206

Goytisolo FA & Blasco MA (2002) Many ways to telomere dysfunction: in vivo studies using mouse models. [Review] [105 refs]. *Oncogene* **21**: 584-591

Green K, Brand MD, & Murphy MP (2004) Prevention of mitochondrial oxidative damage as a therapeutic strategy in diabetes. [Review] [53 refs]. *Diabetes* **53**: S110-8

Greider CW (1999) Telomeres do D-loop-T-loop.[comment]. [Review] [21 refs]. *Cell* **97**: 419-422

Griendling KK & FitzGerald GA (2003) Oxidative stress and cardiovascular injury: Part I: basic mechanisms and in vivo monitoring of ROS. *Circulation* **108**: 1912-1916

Grumbach IM, Chen W, Mertens SA, & Harrison DG (2005) A negative feedback mechanism involving nitric oxide and nuclear factor kappa-B modulates endothelial nitric oxide synthase transcription. *J Mol Cell Cardiol* **39**: 595-603

Guzik TJ, Mussa S, Gastaldi D, Sadowski J, Ratnatunga C, Pillai R, & Channon KM (2002) Mechanisms of increased vascular superoxide production in human diabetes mellitus: role of NAD(P)H oxidase and endothelial nitric oxide synthase. *Circulation* **105**: 1656-1662

Gyllenhammar H (1987) Lucigenin chemiluminescence in the assessment of neutrophil superoxide production. *J Immunol Methods* **97**: 209-213

Haendeler J (2005) Nitric oxide and endothelial cell aging. *Eur J Clin Pharmacol*: 1-4

- Haendeler J, Hoffmann J, Brandes RP, Zeiher AM, & Dimmeler S (2003) Hydrogen peroxide triggers nuclear export of telomerase reverse transcriptase via Src kinase family-dependent phosphorylation of tyrosine 707. *Mol Cell Biol* **23**: 4598-4610
- Haendeler J, Hoffmann J, Diehl JF, Vasa M, Spyridopoulos I, Zeiher AM, & Dimmeler S (2004) Antioxidants inhibit nuclear export of telomerase reverse transcriptase and delay replicative senescence of endothelial cells. *Circ Res* **94**: 768-775
- Hamilton SJ, Chew GT, & Watts GF (2007) Therapeutic regulation of endothelial dysfunction in type 2 diabetes mellitus. *Diab Vasc Dis Res* **4**: 89-102
- Han D, Canali R, Garcia J, Aguilera R, Gallaher TK, & Cadenas E (2005) Sites and mechanisms of aconitase inactivation by peroxynitrite: modulation by citrate and glutathione. *Biochemistry* **44**: 11986-11996
- Hao LY, Armanios M, Strong MA, Karim B, Feldser DM, Huso D, & Greider CW (2005) Short telomeres, even in the presence of telomerase, limit tissue renewal capacity. *Cell* **123**: 1121-1131
- Harding JJ & Ganea E (2006) Protection against glycation and similar post-translational modifications of proteins. *Biochim Biophys Acta* **1764**: 1436-1446
- Harman D (2003) The free radical theory of aging. *Antioxid Redox Signal* **5**: 557-561
- Hayashi T, Matsui-Hirai H, Miyazaki-Akita A, Fukatsu A, Funami J, Ding QF, Kamalanathan S, Hattori Y, Ignarro LJ, & Iguchi A (2006) Endothelial cellular senescence is inhibited by nitric oxide: implications in atherosclerosis associated with menopause and diabetes. *Proc Natl Acad Sci U S A* **103**: 17018-17023

Hink U, Li H, Mollnau H, Oelze M, Matheis E, Hartmann M, Skatchkov M, Thaiss F, Stahl RA, Warnholtz A, Meinertz T, Griendling K, Harrison DG, Forstermann U, & Munzel T (2001) Mechanisms underlying endothelial dysfunction in diabetes mellitus. *Circ Res* **88**: E14-22

Hoffmann J, Haendeler J, Aicher A, Rossig L, Vasa M, Zeiher AM, & Dimmeler S (2001) Aging enhances the sensitivity of endothelial cells toward apoptotic stimuli: important role of nitric oxide. *Circ Res* **89**: 709-715

Hollensworth SB, Shen C, Sim JE, Spitz DR, Wilson GL, & LeDoux SP (2000) Glial cell type-specific responses to menadione-induced oxidative stress. *Free Radic Biol Med* **28**: 1161-1174

Hsueh WA & Quinones MJ (2003) Role of endothelial dysfunction in insulin resistance. *Am J Cardiol* **92**: 10J-17J

Hubbard AK & Rothlein R (2000) Intercellular adhesion molecule-1 (ICAM-1) expression and cell signaling cascades. *Free Radic Biol Med* **28**: 1379-1386

Hunt BJ, Poston L, Schachter M, & Halliday A (2002) *An Introduction to Vascular Biology - From Basic Science to Clinical Practice*. Cambridge University Press: Cambridge, United Kingdom

Jay D, Hitomi H, & Griendling KK (2006) Oxidative stress and diabetic cardiovascular complications. *Free Radic Biol Med* **40**: 183-192

Jeanclous E, Krolewski A, Skurnick J, Kimura M, Aviv H, Warram JH, & Aviv A (1998) Shortened telomere length in white blood cells of patients with IDDM. *Diabetes* **47**: 482-486

Johansen JS, Harris AK, Rychly DJ, & Ergul A (2005) Oxidative stress and the use of antioxidants in diabetes: linking basic science to clinical practice. *Cardiovasc Diabetol* **4**: 5

- Jones CM, Lawrence A, Wardman P, & Burkitt MJ (2003) Kinetics of superoxide scavenging by glutathione: an evaluation of its role in the removal of mitochondrial superoxide. *Biochem Soc Trans* **31**: 1337-1339
- Karbowski M, Kurono C, Wozniak M, Ostrowski M, Teranishi M, Soji T, & Wakabayashi T (1999) Cycloheximide and 4-OH-TEMPO suppress chloramphenicol-induced apoptosis in RL-34 cells via the suppression of the formation of megamitochondria. *Biochim Biophys Acta* **1449**: 25-40
- Karnieli E, Hissin PJ, Simpson IA, Salans LB, & Cushman SW (1981) A possible mechanism of insulin resistance in the rat adipose cell in streptozotocin-induced diabetes mellitus. Depletion of intracellular glucose transport systems. *J Clin Invest* **68**: 811-814
- Kawanishi S & Oikawa S (2004) Mechanism of telomere shortening by oxidative stress. *Ann N Y Acad Sci* **1019**: 278-284
- Kennedy ED, Maechler P, & Wollheim CB (1998) Effects of depletion of mitochondrial DNA in metabolism secretion coupling in INS-1 cells. *Diabetes* **47**: 374-380
- Kim SR, Bae YH, Bae SK, Choi KS, Yoon KH, Koo TH, Jang HO, Yun I, Kim KW, Kwon YG, Yoo MA, & Bae MK (2008) Visfatin enhances ICAM-1 and VCAM-1 expression through ROS-dependent NF-kappaB activation in endothelial cells. *Biochim Biophys Acta* **1783**: 886-895
- King MP & Attardi G (1996) Isolation of human cell lines lacking mitochondrial DNA. *Methods Enzymol* **264**: 304-313
- King MP & Attardi G (1989) Human cells lacking mtDNA: repopulation with exogenous mitochondria by complementation. *Science* **246**: 500-503
- Kleinert H, Wallerath T, Euchenhofer C, Ihrig-Biedert I, Li H, & Forstermann U (1998) Estrogens increase transcription of the human endothelial NO synthase gene: analysis of the transcription factors involved. *Hypertension* **31**: 582-588

Kumar S, Sharma A, Madan B, Singhal V, & Ghosh B (2007) Isoliquiritigenin inhibits I κ B kinase activity and ROS generation to block TNF- α induced expression of cell adhesion molecules on human endothelial cells. *Biochem Pharmacol* **73**: 1602-1612

Kurz DJ, Decary S, Hong Y, Trivier E, Akhmedov A, & Erusalimsky JD (2004) Chronic oxidative stress compromises telomere integrity and accelerates the onset of senescence in human endothelial cells. *J Cell Sci* **117**: 2417-2426

Lansdorp PM (2005) Major cutbacks at chromosome ends. [Review] [86 refs]. *Trends Biochem Sci* **30**: 388-395

Lansdorp PM (2000) Repair of telomeric DNA prior to replicative senescence. *Mech Ageing Dev* **118**: 23-34

Leary SC & Shoubridge EA (2003) Mitochondrial biogenesis: which part of "NO" do we understand? *Bioessays* **25**: 538-541

Lee CF, Liu CY, Hsieh RH, & Wei YH (2005) Oxidative stress-induced depolymerization of microtubules and alteration of mitochondrial mass in human cells. *Ann N Y Acad Sci* **1042**: 246-254

Lee HC, Yin PH, Lu CY, Chi CW, & Wei YH (2000) Increase of mitochondria and mitochondrial DNA in response to oxidative stress in human cells. *Biochem J* **348 Pt 2**: 425-432

Lee HK, Song JH, Shin CS, Park DJ, Park KS, Lee KU, & Koh CS (1998) Decreased mitochondrial DNA content in peripheral blood precedes the development of non-insulin-dependent diabetes mellitus. *Diabetes Res Clin Pract* **42**: 161-167

Lee SH & Blair IA (2001) Oxidative DNA damage and cardiovascular disease. [Review] [62 refs]. *Trends Cardiovasc Med* **11**: 148-155

- Lee YJ, Kang DG, Kim JS, & Lee HS (2008) Lycopodium inhibits high glucose-induced vascular inflammation in human umbilical vein endothelial cells. *Vascul Pharmacol* **48**: 38-46
- Li CH, Tzeng SL, Cheng YW, & Kang JJ (2005) Chloramphenicol-induced mitochondrial stress increases p21 expression and prevents cell apoptosis through a p21-dependent pathway. *J Biol Chem* **280**: 26193-26199
- Li M, Absher PM, Liang P, Russell JC, Sobel BE, & Fukagawa NK (2001) High glucose concentrations induce oxidative damage to mitochondrial DNA in explanted vascular smooth muscle cells. *Experimental Biology & Medicine* **226**: 450-457
- Li WG, Li QH, & Tan Z (2005) Detection of telomere damage as a result of strand breaks in telomeric and subtelomeric DNA. *Electrophoresis* **26**: 533-536
- Libby P (2006) Inflammation and cardiovascular disease mechanisms. *Am J Clin Nutr* **83**: 456S-460S
- Libby P, Ridker PM, & Maseri A (2002) Inflammation and atherosclerosis. *Circulation* **105**: 1135-1143
- Lin KW & Yan J (2005) The telomere length dynamic and methods of its assessment. *J Cell Mol Med* **9**: 977-989
- Lin MT & Beal MF (2006) Mitochondrial dysfunction and oxidative stress in neurodegenerative diseases. *Nature* **443**: 787-795
- Liochev SI & Fridovich I (1997) Lucigenin (bis-N-methylacridinium) as a mediator of superoxide anion production. *Arch Biochem Biophys* **337**: 115-120
- Liu S, Lee IM, Song Y, Van Denburgh M, Cook NR, Manson JE, & Buring JE (2006) Vitamin E and risk of type 2 diabetes in the women's health study randomized controlled trial. *Diabetes* **55**: 2856-2862

Louis EJ & Vershinin AV (2005) Chromosome ends: different sequences may provide conserved functions. *Bioessays* **27**: 685-697

Lund KC, Peterson LL, & Wallace KB (2007) Absence of a universal mechanism of mitochondrial toxicity by nucleoside analogs. *Antimicrob Agents Chemother* **51**: 2531-2539

Madamanchi NR & Runge MS (2007) Mitochondrial dysfunction in atherosclerosis. *Circ Res* **100**: 460-473

Maeda H (2008) Which are you watching, an individual reactive oxygen species or total oxidative stress? *Ann N Y Acad Sci* **1130**: 149-156

Makarov VL, Hirose Y, & Langmore JP (1997) Long G tails at both ends of human chromosomes suggest a C strand degradation mechanism for telomere shortening. *Cell* **88**: 657-666

Makino N, Maeda T, Sugano M, Satoh S, Watanabe R, & Abe N (2005) High serum TNF-alpha level in Type 2 diabetic patients with microangiopathy is associated with eNOS down-regulation and apoptosis in endothelial cells. *J Diabetes Complications* **19**: 347-355

Mannella CA (2006) Structure and dynamics of the mitochondrial inner membrane cristae. *Biochim Biophys Acta* **1763**: 542-548

Marchioli R, Schweiger C, Levantesi G, Tavazzi L, & Valagussa F (2001) Antioxidant vitamins and prevention of cardiovascular disease: epidemiological and clinical trial data. *Lipids* **36 Suppl**: S53-63

Maritim AC, Sanders RA, & Watkins JB,3rd (2003) Diabetes, oxidative stress, and antioxidants: a review. [Review] [112 refs]. *Journal of Biochemical & Molecular Toxicology* **17**: 24-38

Marnett LJ (2000) Oxyradicals and DNA damage. [Review] [131 refs]. *Carcinogenesis* **21**: 361-370

Matsushita H, Chang E, Glassford AJ, Cooke JP, Chiu CP, & Tsao PS (2001) eNOS activity is reduced in senescent human endothelial cells: Preservation by hTERT immortalization. *Circ Res* **89**: 793-798

Matthews C, Gorenne I, Scott S, Figg N, Kirkpatrick P, Ritchie A, Goddard M, & Bennett M (2006) Vascular smooth muscle cells undergo telomere-based senescence in human atherosclerosis: effects of telomerase and oxidative stress. *Circ Res* **99**: 156-164

Matthews CK, Holde KE, & Ahern KG (2000) *Biochemistry*. Benjamin Cummings: San Francisco

McCance DR, Hanson RL, Pettitt DJ, Bennett PH, Hadden DR, & Knowler WC (1997) Diagnosing diabetes mellitus--do we need new criteria? *Diabetologia* **40**: 247-255

McGinn S, Poronnik P, King M, Gallery ED, & Pollock CA (2003) High glucose and endothelial cell growth: novel effects independent of autocrine TGF-beta 1 and hyperosmolarity. *Am J Physiol Cell Physiol* **284**: C1374-86

McNally JS, Davis ME, Giddens DP, Saha A, Hwang J, Dikalov S, Jo H, & Harrison DG (2003) Role of xanthine oxidoreductase and NAD(P)H oxidase in endothelial superoxide production in response to oscillatory shear stress. *Am J Physiol Heart Circ Physiol* **285**: H2290-7

Meerwaldt R, Links T, Zeebregts C, Tio R, Hillebrands JL, & Smit A (2008) The clinical relevance of assessing advanced glycation endproducts accumulation in diabetes. *Cardiovasc Diabetol* **7**: 29

Messner KR & Imlay JA (2002) In vitro quantitation of biological superoxide and hydrogen peroxide generation. *Methods Enzymol* **349**: 354-361

Miller FJ, Jr, Gutterman DD, Rios CD, Heistad DD, & Davidson BL (1998) Superoxide production in vascular smooth muscle contributes to oxidative stress and impaired relaxation in atherosclerosis. *Circ Res* **82**: 1298-1305

Minamino T, Miyauchi H, Yoshida T, Tateno K, Kunieda T, & Komuro I (2004) Vascular cell senescence and vascular aging. [Review] [112 refs]. *Journal of Molecular & Cellular Cardiology* **36**: 175-183

Miranda S, Foncea R, Guerrero J, & Leighton F (1999) Oxidative stress and upregulation of mitochondrial biogenesis genes in mitochondrial DNA-depleted HeLa cells. *Biochem Biophys Res Commun* **258**: 44-49

Mohanty JG, Jaffe JS, Schulman ES, & Raible DG (1997) A highly sensitive fluorescent micro-assay of H₂O₂ release from activated human leukocytes using a dihydroxyphenoxazine derivative. *J Immunol Methods* **202**: 133-141

Molavi B & Mehta JL (2004) Oxidative stress in cardiovascular disease: molecular basis of its deleterious effects, its detection, and therapeutic considerations. *Curr Opin Cardiol* **19**: 488-493

Moreira PI, Nunomura A, Nakamura M, Takeda A, Shenk JC, Aliev G, Smith MA, & Perry G (2008) Nucleic acid oxidation in Alzheimer disease. *Free Radic Biol Med* **44**: 1493-1505

Mount PF, Kemp BE, & Power DA (2007) Regulation of endothelial and myocardial NO synthesis by multi-site eNOS phosphorylation. *J Mol Cell Cardiol* **42**: 271-279

Mueckler M (1994) Facilitative glucose transporters. *Eur J Biochem* **219**: 713-725

Muller FL, Liu Y, & Van Remmen H (2004) Complex III releases superoxide to both sides of the inner mitochondrial membrane. *J Biol Chem* **279**: 49064-49073

Munzel D, Lehle K, Haubner F, Schmid C, Birnbaum DE, & Preuner JG (2007) Impact of diabetic serum on endothelial cells: an in-vitro-analysis of endothelial dysfunction in diabetes mellitus type 2. *Biochem Biophys Res Commun* **362**: 238-244

Muzykantov VR (2001) Targeting of superoxide dismutase and catalase to vascular endothelium. *J Control Release* **71**: 1-21

Najjar SS, Scuteri A, & Lakatta EG (2005) Arterial aging - Is it an immutable cardiovascular risk factor? *Hypertension* **46**: 454-462

Naseem KM (2005) The role of nitric oxide in cardiovascular diseases. [Review] [172 refs]. *Mol Aspects Med* **26**: 33-65

Nass MM (1972) Differential effects of ethidium bromide on mitochondrial and nuclear DNA synthesis in vivo in cultured mammalian cells. *Exp Cell Res* **72**: 211-222

Navarro-Antolin J, Rey-Campos J, & Lamas S (2000) Transcriptional induction of endothelial nitric oxide gene by cyclosporine A. A role for activator protein-1. *J Biol Chem* **275**: 3075-3080

Navratil M, Terman A, & Arriaga EA (2008) Giant mitochondria do not fuse and exchange their contents with normal mitochondria. *Exp Cell Res* **314**: 164-172

Neidle S & Parkinson GN (2003) The structure of telomeric DNA. [Review] [52 refs]. *Curr Opin Struct Biol* **13**: 275-283

Nishikawa T, Edelstein D, Du XL, Yamagishi S, Matsumura T, Kaneda Y, Yorek MA, Beebe D, Oates PJ, Hammes HP, Giardino I, & Brownlee M (2000) Normalizing mitochondrial superoxide production blocks three pathways of hyperglycaemic damage. *Nature* **404**: 787-790

Nisoli E, Clementi E, Carruba MO, & Moncada S (2007) Defective mitochondrial biogenesis: a hallmark of the high cardiovascular risk in the metabolic syndrome? *Circ Res* **100**: 795-806

Nisoli E, Clementi E, Moncada S, & Carruba MO (2004) Mitochondrial biogenesis as a cellular signaling framework. *Biochem Pharmacol* **67**: 1-15

- Norbury CJ & Zhivotovsky B (2004) DNA damage-induced apoptosis. [Review] [137 refs]. *Oncogene* **23**: 2797-2808
- Nutter LM, Ngo EO, Fisher GR, & Gutierrez PL (1992) DNA strand scission and free radical production in menadione-treated cells. Correlation with cytotoxicity and role of NADPH quinone acceptor oxidoreductase. *J Biol Chem* **267**: 2474-2479
- Ohara Y, Peterson TE, & Harrison DG (1993) Hypercholesterolemia increases endothelial superoxide anion production. *J Clin Invest* **91**: 2546-2551
- Oikawa S & Kawanishi S (1999) Site-specific DNA damage at GGG sequence by oxidative stress may accelerate telomere shortening. *FEBS Lett* **453**: 365-368
- Okuda K, Khan MY, Skurnick J, Kimura M, Aviv H, & Aviv A (2000) Telomere attrition of the human abdominal aorta: relationships with age and atherosclerosis. *Atherosclerosis* **152**: 391-398
- Okuda Y, Kawashima K, Suzuki S, Asakura Y, Asano M, Tsurumaru K, Dai H, Tachi Y, Bannai C, Saitoh M, & Yamashita K (1997) Restoration of nitric oxide production by aldose reductase inhibitor in human endothelial cells cultured in high-glucose medium. *Life Sci* **60**: PL53-6
- Olgun A & Akman S (2007) Mitochondrial DNA-deficient models and aging. *Ann N Y Acad Sci* **1100**: 241-245
- Olson AL & Pessin JE (1996) Structure, function, and regulation of the mammalian facilitative glucose transporter gene family. *Annu Rev Nutr* **16**: 235-256
- Opresko PL, Fan J, Danzy S, Wilson DM,3rd, & Bohr VA (2005) Oxidative damage in telomeric DNA disrupts recognition by TRF1 and TRF2. *Nucleic Acids Res* **33**: 1230-1239

Packer L, Valenza M, Serbinova E, Starke-Reed P, Frost K, & Kagan V (1991) Free radical scavenging is involved in the protective effect of L-propionyl-carnitine against ischemia-reperfusion injury of the heart. *Arch Biochem Biophys* **288**: 533-537

Palmeira CM, Rolo AP, Berthiaume J, Bjork JA, & Wallace KB (2007) Hyperglycemia decreases mitochondrial function: the regulatory role of mitochondrial biogenesis. *Toxicol Appl Pharmacol* **225**: 214-220

Pan-Zhou XR, Cui L, Zhou XJ, Sommadossi JP, & Darley-Usmar VM (2000) Differential effects of antiretroviral nucleoside analogs on mitochondrial function in HepG2 cells. *Antimicrob Agents Chemother* **44**: 496-503

Parinandi NL, Kleinberg MA, Usatyuk PV, Cummings RJ, Pennathur A, Cardounel AJ, Zweier JL, Garcia JG, & Natarajan V (2003) Hyperoxia-induced NAD(P)H oxidase activation and regulation by MAP kinases in human lung endothelial cells. *Am J Physiol Lung Cell Mol Physiol* **284**: L26-38

Park KS, Nam KJ, Kim JW, Lee YB, Han CY, Jeong JK, Lee HK, & Pak YK (2001) Depletion of mitochondrial DNA alters glucose metabolism in SK-Hep1 cells. *Am J Physiol Endocrinol Metab* **280**: E1007-14

Passos JF, von Zglinicki T, & Kirkwood TB (2007) Mitochondria and ageing: winning and losing in the numbers game. *Bioessays* **29**: 908-917

Patti ME, Butte AJ, Crunkhorn S, Cusi K, Berria R, Kashyap S, Miyazaki Y, Kohane I, Costello M, Saccone R, Landaker EJ, Goldfine AB, Mun E, DeFronzo R, Finlayson J, Kahn CR, & Mandarino LJ (2003) Coordinated reduction of genes of oxidative metabolism in humans with insulin resistance and diabetes: Potential role of PGC1 and NRF1. *Proc Natl Acad Sci U S A* **100**: 8466-8471

Piconi L, Quagliario L, Da Ros R, Assaloni R, Giugliano D, Esposito K, Szabo C, & Ceriello A (2004) Intermittent high glucose enhances ICAM-1,

VCAM-1, E-selectin and interleukin-6 expression in human umbilical endothelial cells in culture: the role of poly(ADP-ribose) polymerase. *J Thromb Haemost* **2**: 1453-1459

Piechota J, Szczesny R, Wolanin K, Chlebowski A, & Bartnik E (2006) Nuclear and mitochondrial genome responses in HeLa cells treated with inhibitors of mitochondrial DNA expression. *Acta Biochim Pol* **53**: 485-495

Proctor CJ & Kirkwood TB (2002) Modelling telomere shortening and the role of oxidative stress. *Mechanisms of Ageing & Development* **123**: 351-363

Qi X, Guy J, Nick H, Valentine J, & Rao N (1997) Increase of manganese superoxide dismutase, but not of Cu/Zn-SOD, in experimental optic neuritis. *Invest Ophthalmol Vis Sci* **38**: 1203-1212

Quagliaro L, Piconi L, Assaloni R, Da Ros R, Szabo C, & Ceriello A (2007) Primary role of superoxide anion generation in the cascade of events leading to endothelial dysfunction and damage in high glucose treated HUVEC. *Nutr Metab Cardiovasc Dis* **17**: 257-267

Quagliaro L, Piconi L, Assaloni R, Martinelli L, Motz E, & Ceriello A (2003) Intermittent high glucose enhances apoptosis related to oxidative stress in human umbilical vein endothelial cells: the role of protein kinase C and NAD(P)H-oxidase activation. *Diabetes* **52**: 2795-2804

Raha S & Robinson BH (2000) Mitochondria, oxygen free radicals, disease and ageing. [Review] [55 refs]. *Trends Biochem Sci* **25**: 502-508

Rajagopalan S, Kurz S, Munzel T, Tarpey M, Freeman BA, Griending KK, & Harrison DG (1996) Angiotensin II-mediated hypertension in the rat increases vascular superoxide production via membrane NADH/NADPH oxidase activation. Contribution to alterations of vasomotor tone. *J Clin Invest* **97**: 1916-1923

Rajesh M, Mukhopadhyay P, Batkai S, Hasko G, Liaudet L, Drel VR, Obrosova IG, & Pacher P (2007) Cannabidiol attenuates high glucose-induced endothelial cell inflammatory response and barrier disruption. *Am J Physiol Heart Circ Physiol* **293**: H610-9

Ramachandran A, Levonen AL, Brookes PS, Ceaser E, Shiva S, Barone MC, & Darley-Usmar V (2002) Mitochondria, nitric oxide, and cardiovascular dysfunction. *Free Radic Biol Med* **33**: 1465-1474

Ramasamy S, Parthasarathy S, & Harrison DG (1998) Regulation of endothelial nitric oxide synthase gene expression by oxidized linoleic acid. *J Lipid Res* **39**: 268-276

Reardon W, Ross RJ, Sweeney MG, Luxon LM, Pembrey ME, Harding AE, & Trembath RC (1992) Diabetes mellitus associated with a pathogenic point mutation in mitochondrial DNA. *Lancet* **340**: 1376-1379

Reszka KJ, Wagner BA, Burns CP, & Britigan BE (2005) Effects of peroxidase substrates on the Amplex red/peroxidase assay: antioxidant properties of anthracyclines. *Anal Biochem* **342**: 327-337

Rhodes D, Fairall L, Simonsson T, Court R, & Chapman L (2002) Telomere architecture. [Review] [45 refs]. *EMBO Rep* **3**: 1139-1145

Rinaldi M, Moroni P, Paape MJ, & Bannerman DD (2007) Evaluation of assays for the measurement of bovine neutrophil reactive oxygen species. *Vet Immunol Immunopathol* **115**: 107-125

Risso A, Mercuri F, Quagliari L, Damante G, & Ceriello A (2001) Intermittent high glucose enhances apoptosis in human umbilical vein endothelial cells in culture. *Am J Physiol Endocrinol Metab* **281**: E924-30

Ritthaler U, Deng Y, Zhang Y, Greten J, Abel M, Sido B, Allenberg J, Otto G, Roth H, & Bierhaus A (1995) Expression of receptors for advanced glycation end products in peripheral occlusive vascular disease. *Am J Pathol* **146**: 688-694

- Roebuck KA & Finnegan A (1999) Regulation of intercellular adhesion molecule-1 (CD54) gene expression. *J Leukoc Biol* **66**: 876-888
- Ross R (1999) Atherosclerosis--an inflammatory disease. *N Engl J Med* **340**: 115-126
- Salpea KD, Nicaud V, Tiret L, Talmud PJ, Humphries SE, & EARS II group (2008) The association of telomere length with paternal history of premature myocardial infarction in the European Atherosclerosis Research Study II. *J Mol Med* **86**: 815-824
- Samani NJ, Boulby R, Butler R, Thompson JR, & Goodall AH (2001) Telomere shortening in atherosclerosis.[see comment]. *Lancet* **358**: 472-473
- Sampson MJ, Winterbone MS, Hughes JC, Dozio N, & Hughes DA (2006) Monocyte telomere shortening and oxidative DNA damage in type 2 diabetes. *Diabetes Care* **29**: 283-289
- Sanchez LB, Elmendorf H, Nash TE, & Muller M (2001) NAD(P)H:menadione oxidoreductase of the amitochondriate eukaryote *Giardia lamblia*: a simpler homologue of the vertebrate enzyme. *Microbiology* **147**: 561-570
- Saretzki G & Von Zglinicki T (2002) Replicative aging, telomeres, and oxidative stress. *Ann N Y Acad Sci* **959**: 24-29
- Satpute RM, Hariharakrishnan J, & Bhattacharya R (2008) Alpha-ketoglutarate and N-acetyl cysteine protect PC12 cells from cyanide-induced cytotoxicity and altered energy metabolism. *Neurotoxicology* **29**: 170-178
- Schalkwijk CG & Stehouwer CDA (2005) Vascular complications in diabetes mellitus: the role of endothelial dysfunction. *Clin Sci* **109**: 143-159
- Schapira AH (2006) Mitochondrial disease. *Lancet* **368**: 70-82

Schauen M, Spitkovsky D, Schubert J, Fischer JH, Hayashi J, & Wiesner RJ (2006) Respiratory chain deficiency slows down cell-cycle progression via reduced ROS generation and is associated with a reduction of p21CIP1/WAF1. *J Cell Physiol* **209**: 103-112

Schotta G, Lachner M, Sarma K, Ebert A, Sengupta R, Reuter G, Reinberg D, & Jenuwein T (2004) A silencing pathway to induce H3-K9 and H4-K20 trimethylation at constitutive heterochromatin. *Genes Dev* **18**: 1251-1262

Searles CD (2006) Transcriptional and posttranscriptional regulation of endothelial nitric oxide synthase expression. *Am J Physiol Cell Physiol* **291**: C803-16

Sell DR & Monnier VM (1989) Structure elucidation of a senescence cross-link from human extracellular matrix. Implication of pentoses in the aging process. *J Biol Chem* **264**: 21597-21602

Serrano AL & Andres V (2004) Telomeres and Cardiovascular Disease: Does Size Matter? *Circ Res* **94**: 575-584

Shaul PW (2003) Endothelial nitric oxide synthase, caveolae and the development of atherosclerosis. *J Physiol* **547**: 21-33

Sheu SS, Nauduri D, & Anders MW (2006) Targeting antioxidants to mitochondria: a new therapeutic direction. *Biochim Biophys Acta* **1762**: 256-265

Shi Q, Aida K, Vandeberg JL, & Wang XL (2004) Passage-dependent changes in baboon endothelial cells--relevance to in vitro aging. *DNA Cell Biol* **23**: 502-509

Simon DK & Johns DR (1999) Mitochondrial disorders: clinical and genetic features. *Annu Rev Med* **50**: 111-127

Singh KK, Kulawiec M, Still I, Desouki MM, Geradts J, & Matsui S (2005) Inter-genomic cross talk between mitochondria and the nucleus plays an important role in tumorigenesis. *Gene* **354**: 140-146

Skatchkov MP, Sperling D, Hink U, Mulsch A, Harrison DG, Sindermann I, Meinertz T, & Munzel T (1999) Validation of lucigenin as a chemiluminescent probe to monitor vascular superoxide as well as basal vascular nitric oxide production. *Biochem Biophys Res Commun* **254**: 319-324

Snustad DP & Simmons MJ (2000) *Principles of Genetics*. John Wiley and Sons: USA

Soh N (2006) Recent advances in fluorescent probes for the detection of reactive oxygen species. *Anal Bioanal Chem* **386**: 532-543

Sohal RS, Mockett RJ, & Orr WC (2002) Mechanisms of aging: an appraisal of the oxidative stress hypothesis. [Review] [79 refs]. *Free Radic Biol Med* **33**: 575-586

Sommer M, Gerth J, Stein G, & Wolf G (2005) Transdifferentiation of endothelial and renal tubular epithelial cells into myofibroblast-like cells under in vitro conditions: a morphological analysis. *Cells Tissues Organs* **180**: 204-214

Sousa T, Pinho D, Morato M, Marques-Lopes J, Fernandes E, Afonso J, Oliveira S, Carvalho F, & Albino-Teixeira A (2008) Role of superoxide and hydrogen peroxide in hypertension induced by an antagonist of adenosine receptors. *Eur J Pharmacol* **588**: 267-276

Spiteller G (2007) The important role of lipid peroxidation processes in aging and age dependent diseases. *Mol Biotechnol* **37**: 5-12

Srinivasan S, Hatley ME, Bolick DT, Palmer LA, Edelstein D, Brownlee M, & Hedrick CC (2004) Hyperglycaemia-induced superoxide production

decreases eNOS expression via AP-1 activation in aortic endothelial cells.

Diabetologia **47**: 1727-1734

Srivastava AK & Pandey SK (1998) Potential mechanism(s) involved in the regulation of glycogen synthesis by insulin. *Mol Cell Biochem* **182**: 135-141

Stoppa GR, Cesquini M, Roman EA, Ogo SH, & Torsoni MA (2006) Aminoguanidine prevented impairment of blood antioxidant system in insulin-dependent diabetic rats. *Life Sci* **78**: 1352-1361

Sun M, Yokoyama M, Ishiwata T, & Asano G (1998) Deposition of advanced glycation end products (AGE) and expression of the receptor for AGE in cardiovascular tissue of the diabetic rat. *Int J Exp Pathol* **79**: 207-222

Suzuki S, Hinokio Y, Komatu K, Ohtomo M, Onoda M, Hirai S, Hirai M, Hirai A, Chiba M, Kasuga S, Akai H, & Toyota T (1999) Oxidative damage to mitochondrial DNA and its relationship to diabetic complications. *Diabetes Res Clin Pract* **45**: 161-168

Swerdlow RH, Parks JK, Cassarino DS, Maguire DJ, Maguire RS, Bennett JP, Jr, Davis RE, & Parker WD, Jr (1997) Cybrids in Alzheimer's disease: a cellular model of the disease? *Neurology* **49**: 918-925

Takahashi S & Mendelsohn ME (2003) Calmodulin-dependent and -independent activation of endothelial nitric-oxide synthase by heat shock protein 90. *J Biol Chem* **278**: 9339-9344

Takahashi Y, Kuro-O M, & Ishikawa F (2000) Aging mechanisms. *Proc Natl Acad Sci U S A* **97**: 12407-12408

Takubo K, Izumiyama-Shimomura N, Honma N, Sawabe M, Arai T, Kato M, Oshimura M, & Nakamura K (2002) Telomere lengths are characteristic in each human individual. *Exp Gerontol* **37**: 523-531

Tanabe T, Maeda S, Miyauchi T, Iemitsu M, Takanashi M, Irukayama-Tomobe Y, Yokota T, Ohmori H, & Matsuda M (2003) Exercise training

improves ageing-induced decrease in eNOS expression of the aorta. *Acta Physiol Scand* **178**: 3-10

Tarrago-Litvak L, Viratelle O, Darriet D, Dalibart R, Graves PV, & Litvak S (1978) The inhibition of mitochondrial DNA polymerase gamma from animal cells by intercalating drugs. *Nucleic Acids Res* **5**: 2197-2210

Thor H, Smith MT, Hartzell P, Bellomo G, Jewell SA, & Orrenius S (1982) The metabolism of menadione (2-methyl-1,4-naphthoquinone) by isolated hepatocytes. A study of the implications of oxidative stress in intact cells. *J Biol Chem* **257**: 12419-12425

Tommerup H, Dousmanis A, & de Lange T (1994) Unusual chromatin in human telomeres. *Mol Cell Biol* **14**: 5777-5785

Toth E, Racz A, Toth J, Kaminski PM, Wolin MS, Bagi Z, & Koller A (2007) Contribution of polyol pathway to arteriolar dysfunction in hyperglycemia. Role of oxidative stress, reduced NO, and enhanced PGH(2)/TXA(2) mediation. *Am J Physiol Heart Circ Physiol* **293**: H3096-104

Tretter L & Adam-Vizi V (2000) Inhibition of Krebs cycle enzymes by hydrogen peroxide: A key role of [alpha]-ketoglutarate dehydrogenase in limiting NADH production under oxidative stress. *J Neurosci* **20**: 8972-8979

Tripathi AK, Sullivan DJ, & Stins MF (2006) Plasmodium falciparum-infected erythrocytes increase intercellular adhesion molecule 1 expression on brain endothelium through NF-kappaB. *Infect Immun* **74**: 3262-3270

Turk E, Martin MG, & Wright EM (1994) Structure of the human Na⁺/glucose cotransporter gene SGLT1. *J Biol Chem* **269**: 15204-15209

Turner RJ & Moran A (1982) Heterogeneity of sodium-dependent D-glucose transport sites along the proximal tubule: evidence from vesicle studies. *Am J Physiol* **242**: F406-14

Twigg SM, Kamp MC, Davis TM, Neylon EK, Flack JR, Australian Diabetes Society, & Australian Diabetes Educators Association (2007) Prediabetes: a position statement from the Australian Diabetes Society and Australian Diabetes Educators Association. *Med J Aust* **186**: 461-465

van der Loo B, Labugger R, Skepper JN, Bachschmid M, Kilo J, Powell JM, Palacios-Callender M, Erusalimsky JD, Quaschnig T, Malinski T, Gygi D, Ullrich V, & Luscher TF (2000) Enhanced peroxynitrite formation is associated with vascular aging. *J Exp Med* **192**: 1731-1744

Vanella A, Russo A, Acquaviva R, Campisi A, Di Giacomo C, Sorrenti V, & Barcellona ML (2000) L -propionyl-carnitine as superoxide scavenger, antioxidant, and DNA cleavage protector. *Cell Biol Toxicol* **16**: 99-104

Vanhoutte PM (2002) Ageing and endothelial dysfunction. *European Heart Journal Supplements* **4**: A8-A17

Vaux EC, Metzen E, Yeates KM, & Ratcliffe PJ (2001) Regulation of hypoxia-inducible factor is preserved in the absence of a functioning mitochondrial respiratory chain. *Blood* **98**: 296-302

Vergani L, Floreani M, Russell A, Ceccon M, Napoli E, Cabrelle A, Valente L, Bragantini F, Leger B, & Dabbeni-Sala F (2004) Antioxidant defences and homeostasis of reactive oxygen species in different human mitochondrial DNA-depleted cell lines. *Eur J Biochem* **271**: 3646-3656

Vidal F, Colome C, Martinez-Gonzalez J, & Badimon L (1998) Atherogenic concentrations of native low-density lipoproteins down-regulate nitric-oxide-synthase mRNA and protein levels in endothelial cells. *Eur J Biochem* **252**: 378-384

Vina J, Sastre J, Pallardo F, & Borras C (2003) Mitochondrial theory of aging: importance to explain why females live longer than males. *Antioxid Redox Signal* **5**: 549-556

- Vincent AM, McLean LL, Backus C, & Feldman EL (2005) Short-term hyperglycemia produces oxidative damage and apoptosis in neurons. *FASEB J* **19**: 638-640
- Vlassara H & Palace MR (2002) Diabetes and advanced glycation endproducts. *J Intern Med* **251**: 87-101
- Voghel G, Thorin-Trescases N, Farhat N, Mamarbachi AM, Villeneuve L, Fortier A, Perrault LP, Carrier M, & Thorin E (2008) Chronic treatment with N-acetyl-cystein delays cellular senescence in endothelial cells isolated from a subgroup of atherosclerotic patients. *Mech Ageing Dev* **129**: 261-270
- von Zglinicki T, Burkle A, & Kirkwood TB (2001) Stress, DNA damage and ageing -- an integrative approach. [Review] [88 refs]. *Exp Gerontol* **36**: 1049-1062
- von Zglinicki T, Pilger R, & Sittte N (2000) Accumulation of single-strand breaks is the major cause of telomere shortening in human fibroblasts. *Free Radic Biol Med* **28**: 64-74
- Votyakova TV & Reynolds IJ (2004) Detection of hydrogen peroxide with Amplex Red: interference by NADH and reduced glutathione auto-oxidation. *Arch Biochem Biophys* **431**: 138-144
- Wagner BA, Evig CB, Reszka KJ, Buettner GR, & Burns CP (2005) Doxorubicin increases intracellular hydrogen peroxide in PC3 prostate cancer cells. *Arch Biochem Biophys* **440**: 181-190
- Walford GA, Moussignac RL, Scribner AW, Loscalzo J, & Leopold JA (2004) Hypoxia potentiates nitric oxide-mediated apoptosis in endothelial cells via peroxynitrite-induced activation of mitochondria-dependent and - independent pathways. *J Biol Chem* **279**: 4425-4432
- Wang RC, Smogorzewska A, & de Lange T (2004) Homologous recombination generates T-loop-sized deletions at human telomeres. *Cell* **119**: 355-368

Wang X & Baumann P (2008) Chromosome fusions following telomere loss are mediated by single-strand annealing. *Mol Cell* **31**: 463-473

Wardman P (2007) Fluorescent and luminescent probes for measurement of oxidative and nitrosative species in cells and tissues: progress, pitfalls, and prospects. *Free Radic Biol Med* **43**: 995-1022

Watson B, Jr, Khan MA, Desmond RA, & Bergman S (2001) Mitochondrial DNA mutations in black Americans with hypertension-associated end-stage renal disease. *Am J Kidney Dis* **38**: 529-536

Watson RT & Pessin JE (2001) Intracellular organization of insulin signaling and GLUT4 translocation. [Review] [85 refs]. *Recent Prog Horm Res* **56**: 175-193

Watson RT & Pessin JE (2000) Functional cooperation of two independent targeting domains in syntaxin 6 is required for its efficient localization in the trans-golgi network of 3T3L1 adipocytes. *J Biol Chem* **275**: 1261-1268

Wautier MP, Chappey O, Corda S, Stern DM, Schmidt AM, & Wautier JL (2001) Activation of NADPH oxidase by AGE links oxidant stress to altered gene expression via RAGE. *Am J Physiol Endocrinol Metab* **280**: E685-94

Weber P, Bendich A, & Machlin LJ (1997) Vitamin E and human health: rationale for determining recommended intake levels. *Nutrition* **13**: 450-460

Weinert BT & Timiras PS (2003) Invited review: Theories of aging. *J Appl Physiol* **95**: 1706-1716

Wilson WR, Herbert KE, Mistry Y, Stevens SE, Patel HR, Hastings RA, Thompson MM, & Williams B (2008) Blood leucocyte telomere DNA content predicts vascular telomere DNA content in humans with and without vascular disease. *Eur Heart J* **29**: 2689-2694

Wiseman A & Attardi G (1978) Reversible tenfold reduction in mitochondria DNA content of human cells treated with ethidium bromide. *Mol Gen Genet* **167**: 51-63

Wochna A, Niemczyk E, Kurono C, Masaoka M, Kedzior J, Slominska E, Lipinski M, & Wakabayashi T (2007) A possible role of oxidative stress in the switch mechanism of the cell death mode from apoptosis to necrosis--studies on rho0 cells. *Mitochondrion* **7**: 119-124

Yamagishi S, Ueda S, Matsui T, Nakamura K, & Okuda S (2008) Role of advanced glycation end products (AGEs) and oxidative stress in diabetic retinopathy. *Curr Pharm Des* **14**: 962-968

Yamagishi SI, Edelstein D, Du XL, & Brownlee M (2001) Hyperglycemia potentiates collagen-induced platelet activation through mitochondrial superoxide overproduction. *Diabetes* **50**: 1491-1494

Yan SD, Schmidt AM, Anderson GM, Zhang J, Brett J, Zou YS, Pinsky D, & Stern D (1994) Enhanced cellular oxidant stress by the interaction of advanced glycation end products with their receptors/binding proteins. *J Biol Chem* **269**: 9889-9897

Yao D, Shi W, Gou Y, Zhou X, Yee Aw T, Zhou Y, & Liu Z (2005) Fatty acid-mediated intracellular iron translocation: a synergistic mechanism of oxidative injury. *Free Radic Biol Med* **39**: 1385-1398

Yarian CS, Toroser D, & Sohal RS (2006) Aconitase is the main functional target of aging in the citric acid cycle of kidney mitochondria from mice. *Mech Ageing Dev* **127**: 79-84

Yetik-Anacak G & Catravas JD (2006) Nitric oxide and the endothelium: history and impact on cardiovascular disease. *Vascul Pharmacol* **45**: 268-276

Yildiz O (2007) Vascular smooth muscle and endothelial functions in aging. *Ann N Y Acad Sci* **1100**: 353-360

Yorek MA (2003) The role of oxidative stress in diabetic vascular and neural disease. *Free Radic Res* **37**: 471-480

Yu BP & Chung HY (2001) Oxidative stress and vascular aging. *Diabetes Res Clin Pract* **54**: S73-S80

Yu T, Robotham JL, & Yoon Y (2006) Increased production of reactive oxygen species in hyperglycemic conditions requires dynamic change of mitochondrial morphology. *Proc Natl Acad Sci U S A* **103**: 2653-2658

Zafarullah M, Li WQ, Sylvester J, & Ahmad M (2003) Molecular mechanisms of N-acetylcysteine actions. *Cell Mol Life Sci* **60**: 6-20

Zhou X, Perez F, Han K, & Jurivich DA (2006) Clonal senescence alters endothelial ICAM-1 function. *Mech Ageing Dev* **127**: 779-785

Zielonka J, Sarna T, Roberts JE, Wishart JF, & Kalyanaraman B (2006) Pulse radiolysis and steady-state analyses of the reaction between hydroethidine and superoxide and other oxidants. *Arch Biochem Biophys* **456**: 39-47

Zmijewski JW, Moellering DR, Le Goffe C, Landar A, Ramachandran A, & Darley-Usmar VM (2005) Oxidized LDL induces mitochondrially associated reactive oxygen/nitrogen species formation in endothelial cells. *Am J Physiol Heart Circ Physiol* **289**: H852-61

Zou MH, Cohen R, & Ullrich V (2004) Peroxynitrite and vascular endothelial dysfunction in diabetes mellitus. [Review] [56 refs]. *Endothelium: Journal of Endothelial Cell Research* **11**: 89-97